ULTRASONIC VIBRATION - ASSISTED PELLETING AND DILUTE ACID
PRETREATMENT OF CELLULOSIC BIOMASS FOR BIOFUEL MANUFACTURING

by

XIAOXU SONG

B.S., Dalian University of Technology, 2009

AN ABSTRACT OF A DISSERTATION

submitted in partial fulfillment of the requirements for the degree

DOCTOR OF PHILOSOPHY

Department of Industrial and Manufacturing Systems Engineering
College of Engineering

KANSAS STATE UNIVERSITY
Manhattan, Kansas

2015

Abstract

In the U.S. and many other countries, the transportation sector is almost entirely dependent on petroleum-based fuels. In 2011, half of the petroleum used in the U.S. was imported. The dependence on foreign petroleum is a real threat to national energy security. Furthermore, the transportation sector is responsible for about 30% of U.S. greenhouse gas emissions and is growing faster than any other major economic sector. National energy security, economy, environment sustainability are all driving the U.S. to develop alternative liquid transportation fuels that are domestically produced and environmentally friendly. Promoting biofuel is one of the efforts to reduce the use of petroleum-based fuels in the transportation sector. Cellulosic biomass are abundant and diverse. Thus, the ability to produce biofuel from cellulosic biomass will be a key to making ethanol competitive with petroleum-based fuels. Ultrasonic vibration- assisted (UV-A) pelleting can increase not only the density of cellulosic biomass but also the sugar yield.

This PhD dissertation consists of fourteen chapters. Firstly, an introduction of the research is given in Chapter 1. Chapters 2, 3, 4, and 5 present experimental investigations on effects of input variables in UV-A pelleting on pellet quality. Chapter 6 investigates effects of input variables on energy consumption in UV-A pelleting. Chapter 7 develops a predictive model for energy consumption in UV-A pelleting using the response surface method. Chapter 8 investigates effects of input variables on energy consumption, water usage, sugar yield, and pretreatment energy efficiency in dilute acid pretreatment. Chapter 9 develops a predictive model for energy consumption in dilute acid pretreatment using the response surface method. Chapter 10 studies ultrasonic vibration-assisted (UV-A) dilute acid pretreatment of poplar wood for biofuel manufacturing. Chapter 11 compares sugar yields in terms of total sugar yield and enzymatic hydrolysis sugar yield between two kinds of materials: pellets processed by UV-A pelleting and biomass not processed by UV-A pelleting in terms of total sugar yield and enzymatic hydrolysis sugar yield. Chapter 12 develops a physics-based temperature model to predict temperature in UV-A pelleting. Chapter 13 develops a physics-based density model to predict pellet density in UV-A pelleting. Finally, conclusions and contributions of this research are summarized in Chapter 14.

ULTRASONIC VIBRATION - ASSISTED PELLETING AND DILUTE ACID
PRETREATMENT OF CELLULOSIC BIOMASS FOR BIOFUEL MANUFACTURING

by

XIAOXU SONG

B.S., Dalian University of Technology, 2009

A DISSERTATION

submitted in partial fulfillment of the requirements for the degree

DOCTOR OF PHILOSOPHY

Department of Industrial and Manufacturing Systems Engineering
College of Engineering

KANSAS STATE UNIVERSITY
Manhattan, Kansas

2015

Approved by:

Major Professor
Dr. Zhijian Pei

Co-Major Professor
Dr. Donghai Wang

Copyright

XIAOXU SONG

2015

Abstract

In the U.S. and many other countries, the transportation sector is almost entirely dependent on petroleum-based fuels. In 2011, half of the petroleum used in the U.S. was imported. The dependence on foreign petroleum is a real threat to national energy security. Furthermore, the transportation sector is responsible for about 30% of U.S. greenhouse gas emissions and is growing faster than any other major economic sector. National energy security, economy, environment sustainability are all driving the U.S. to develop alternative liquid transportation fuels that are domestically produced and environmentally friendly. Promoting biofuel is one of the efforts to reduce the use of petroleum-based fuels in the transportation sector. Cellulosic biomass are abundant and diverse. Thus, the ability to produce biofuel from cellulosic biomass will be a key to making ethanol competitive with petroleum-based fuels. Ultrasonic vibration- assisted (UV-A) pelleting can increase not only the density of cellulosic biomass but also the sugar yield.

This PhD dissertation consists of fourteen chapters. Firstly, an introduction of the research is given in Chapter 1. Chapters 2, 3, 4, and 5 present experimental investigations on effects of input variables in UV-A pelleting on pellet quality. Chapter 6 investigates effects of input variables on energy consumption in UV-A pelleting. Chapter 7 develops a predictive model for energy consumption in UV-A pelleting using the response surface method. Chapter 8 investigates effects of input variables on energy consumption, water usage, sugar yield, and pretreatment energy efficiency in dilute acid pretreatment. Chapter 9 develops a predictive model for energy consumption in dilute acid pretreatment using the response surface method. Chapter 10 studies ultrasonic vibration-assisted (UV-A) dilute acid pretreatment of poplar wood for biofuel manufacturing. Chapter 11 compares sugar yields in terms of total sugar yield and enzymatic hydrolysis sugar yield between two kinds of materials: pellets processed by UV-A pelleting and biomass not processed by UV-A pelleting in terms of total sugar yield and enzymatic hydrolysis sugar yield. Chapter 12 develops a physics-based temperature model to predict temperature in UV-A pelleting. Chapter 13 develops a physics-based density model to predict pellet density in UV-A pelleting. Finally, conclusions and contributions of this research are summarized in Chapter 14.

Table of Contents

List of Figures

List of Tables

Acknowledgements

I would like to take this opportunity to express my appreciation to many people who have been helping me during my PhD study.

Firstly, I would like to express my gratitude to my advisor Dr. Zhijian Pei, for his excellent support, guidance, and encouragement to my research. His open-minded research approaches inspired me all the time in my research. I also would like to thank Dr. Donghai Wang, my co-advisor, who supports me to conduct experiments in his lab and give me valuable advice. My sincere thanks also go to Dr. Shuting Lei, and Dr. Shing I Chang for their advice, feedback, and consent to serve on my supervisory committee. I would like to thank Dr. Hulya Dogan to serve as my outside chair.

I would like to thank the constant support from my department head Dr. Bradley A. Kramer. My thanks also go to Mr. Timothy Deines, for his excellent technical assistance in setting up the machines and instruments. I am also thankful for the kind assistance from our department staff: Mrs. Vicky Geyer, Mrs. Doris Galvan, and Ms. Michele Bradfield. I would like to thank Dr. John Wu, Dr. David Ben-Arieh, Dr. E. Stanley Lee, Dr. Jessica Heier Stamm, and all other faculty members in my department for their kindly help on my academic courses during my PhD study.

I would like to express my thanks to Mr. Clyde Trdeadwell from Sonic-Mill, Inc., for his generous help and support to my research.

I would like to acknowledge my colleagues and friends: Dr. Pengfei Zhang, Dr. Weilong Cong, Dr. Qi Zhang, Dr. Na Qin, Ms. Zhenzhen Shi, Dr. S.H. Chou, Dr. Feng Xu, Dr. Ke Zhang, Mr. Xiaoming Yu, Mrs. Nannan Liu, Dr. Xin Sun, and Dr. Daming Wei, for their generous help.

I would like to give my gratitude to the financial support from US National Science Foundation. Special acknowledge goes to China Scholarship Council for offering me financial support during my PhD program.

Lastly, I would like to thank my family for all their love and encouragement. For my parents who raised me with a love of science and supported me in all my pursuits. And most of all for my loving, supportive, encouraging, and patient husband, Meng Zhang, whose faithful support during the stages of this PhD is much appreciated. Thank you.

Chapter 1 - Introduction

1.1 Significance of cellulosic biofuel

In the U.S. and many other countries, the transportation sector is almost entirely dependent on petroleum-based fuels [1, 2]. In 2011, half of the petroleum used in the U.S. was imported [1]. The dependence on foreign petroleum is a real threat to national energy security [3]. Furthermore, the transportation sector is responsible for about 30% of U.S. greenhouse gas (GHG) emissions and is growing faster than any other major economic sector [4]. National energy security, economy, environment sustainability are all driving the U.S. to develop alternative liquid transportation fuels that are domestically produced and environmentally friendly. Promoting biofuel is one of the efforts to reduce the use of petroleum-based fuels in the transportation section.

Biofuels have the potential to reduce GHG emissions by as much as 86% compared to gasoline [5]. Because biofuels are made from renewable, plant-based feedstocks, the carbon dioxide released during fuel combustion is "recycled" by the plant as it grows [6].

At present, about 97% of the biofuels used in the U.S. is distilled from corn. The production of biofuels from corn is a mature technology and it is not likely to see "significant reductions in production costs" [7]. Moreover, corn-based biofuel causes a competition for the limited agricultural farm land and other resources with food and feed production [1, 2]. However, if cellulosic feedstocks are used instead of corn, there will be much less competition. Cellulosic feedstocks are abundant and diverse [8]. Agricultural and forestry residues, such as wheat straw and wood chips, and dedicated energy crops, such as switchgrass and poplar wood, can all be utilized to convert into biofuels.

1.2 Major process steps of cellulosic biofuel manufacturing

Major process steps of cellulosic biofuel manufacturing from cellulosic biomass are listed in Figure 1-1. Conversion of cellulosic biomass into ethanol generally consists of the following steps: size reduction to reduce the biomass particle size [9-15]; pretreatment to break the lignin seal and disrupt the crystalline structure of cellulose, to increase cellulose surface area and to make cellulose more accessible to the enzyme in the following enzymatic hydrolysis process

[16-18]; enzymatic hydrolysis of cellulose and hemicellulose to fermentable sugars and fermentation of the sugars to biofuel (ethanol) [16-18].

Currently, several technical barriers hinder large-scale and cost-effective production of cellulosic biofuels, such as the low density of cellulosic biomass feedstocks (causing high transportation and storage cost), and the lack of efficient pretreatment technologies for cellulosic biomass [8, 19].

1.3 Ultrasonic vibration-assisted pelleting of cellulosic biomass

Pelleting is generally described as "the agglomeration of small particles into firm, uniformly shaped granules by the means of a mechanical process" [20]. Pelleting of biomass can increase the overall efficiency of biofuel manufacturing by enabling the use of existing transportation infrastructure and storage systems [21]. Traditionally, biomass pellets are made by screw extruding or piston ramming ground biomass particles through round cross sectional dies [22]. Ultrasonic vibration-assisted (UV-A) pelleting is a newly developed pelleting method. UV-A pelleting can produce biomass pellet with density as high as 1000 kg/m^3, which is about a 30-time increase in density comparing with the bulk density of cellulosic biomass before pelleting [23, 24]. Moreover, biomass (switchgrass) processed with UV-A pelleting has more than 20% higher sugar yield (proportional to biofuel yield) than biomass pellets processed without ultrasonic vibration or non-pelleted biomass [25].

1.4 Objectives and scope of this research

The objectives of this research are as the following:

(1) To develop a model to predict temperature in UV-A pelleting of cellulosic biomass.

(2) To develop a model to predict pellet density in UV-A pelleting of cellulosic biomass.

(3) To investigate the mechanisms through which UV-A pelleting increases density.

(4) To study effects of ultrasonic vibration on pellet quality and sugar yield in UV-A pelleting.

(5) To evaluate effects of process variables and develop a predict model on energy consumption in UV-A pelleting.

(6)   To evaluate effects of process variables and develop a predict model on energy consumption in dilute acid pretreatment.

Figure 1-1 Major process steps of biofuel production from cellulosic biomass (after [17])

```
┌─────────────┐
│  Cellulosic │
│   Biomass   │
└─────────────┘
       ↓
┌─────────────┐
│Size Reduction│
└─────────────┘
       ↓
┌─────────────┐
│ Pretreatment│
└─────────────┘
       ↓
┌─────────────┐
│  Hydrolysis │
└─────────────┘
       ↓
┌─────────────┐
│ Fermentation│
└─────────────┘
       ↓
┌─────────────┐
│   Ethanol   │
└─────────────┘
```
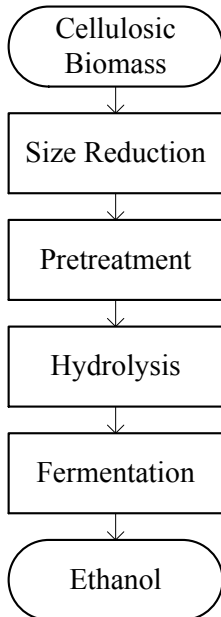
This dissertation is consisted of an introduction and a collection of twelve papers. Chapter 1 is an introduction providing the background and the objectives of this work. Chapters 2, 3, 4, and 5 present experimental investigations on effects of input variables on pellet quality in UV-A pelleting. Chapter 2 investigates effects of moisture content on pellet quality. The biomass material investigated is wheat straw. Results are obtained at three levels of moisture content while keeping all other input variables constant. Chapter 3 investigates effects of moisture content and biomass types on pellet quality. The biomass materials investigated are wheat straw, switchgrass, and sorghum. For each type of biomass, effects of moisture content are studied while keeping all other input variables constant. For each level of moisture content, effects of biomass types are studied while keeping all other input variables constant. Chapter 4 investigates effects of binder material on pellet quality. Chapter 5 studies effects of ultrasonic vibration on pellet quality and pelleting force in UV-A pelleting. Comparisons are made between pellets made by pelleting with and without ultrasonic-vibration in terms of pellet quality and pelleting force. Chapter 6 investigates effects of input variables (sieve size used in size reduction, pelleting pressure, ultrasonic power, and pellet weight) and size reduction machine type (knife milling versus hammer milling) on energy consumption in UV-A pelleting. Chapter 7 develops a

predictive model for energy consumption in UV-A pelleting using the response surface method. Chapter 8 investigates effects of process variables (pretreatment time, temperature, and acid concentration) on energy consumption, water usage, sugar yield, and pretreatment energy efficiency in dilute acid pretreatment. Chapter 9 develops a predictive model for energy consumption in dilute acid pretreatment using the response surface method. Chapter 10 studies ultrasonic vibration-assisted (UV-A) dilute acid pretreatment of poplar wood for biofuel manufacturing. Chapter 11 compares sugar yields between pellets processed by UV-A pelleting and biomass not processed by UV-A pelleting in terms of total sugar yield and enzymatic hydrolysis sugar yield. Chapter 12 develops a physics-based temperature model to predict temperature in UV-A pelleting. Chapter 13 develops a physics-based density model to predict pellet density in UV-A pelleting. Chapter 14 summarizes the conclusions and contributions of this research.

References

[1]   U. S. Energy Information Administration, 2012, "Annual Energy Review 2011," http://www.eia.gov/totalenergy/data/annual/pdf/aer.pdf.

[2]   U. S. Energy Information Administration, 2012, "Monthly Energy Review," http://www.eia.gov/totalenergy/data/monthly/pdf/mer.pdf.

[3]   Huber, G. W., 2008, Breaking the chemical and engineering barriers to lignocellulosic biofuels: next generation hydrocarbon biorefineries, Citeseer.

[4]   Environmental Protection Agency, 2011, "Inventory of U.S. Greenhouse Gas Emissions and Sinks: 1990-2009," http://www.epa.gov/climatechange/Downloads/ghgemissions/US-GHG-Inventory-2011-Complete_Report.pdf.

[5]   U. S. Department of Energy, 2010, "Environmental Benefits," http://www1.eere.energy.gov/biomass/printable_versions/environmental.html.

[6]   RFA, 2011, "Ethanol Facts: Environment," http://www.ethanolrfa.org/pages/ethanol-facts-environment.

[7]   DiPardo, J., 2000, "Outlook for biomass ethanol production and demand," US Energy Information Administration. www. eia. doe. gov/oiaf/analysis paper/pdf/biomass. pdf.

[8]   Perlack, R. D., Wright, L. L., Turhollow, A. F., Graham, R. L., Stokes, B. J., and Erbach, D. C., 2005, "Biomass for a Feedstock for Bioenergy and Bioproducts Industry: the Technical Feasibility of a Billion Ton Annual Supply," Oak Ridge National Laboratory, 2135(78).

[9]   Lynd, L. R., 1996, "Overview and evaluation of fuel ethanol from cellulosic biomass: technology, economics, the environment, and policy," Annual review of energy and the environment, 21(1), pp. 403-465.

[10]   Zhu, J. Y., Pan, X. J., Wang, G. S., and Gleisner, R., 2009, "Sulfite Pretreatment (SPORL) for Robust Enzymatic Saccharification of Spruce and Red Pine," Bioresource Technology, 100(8), pp. 2411-2418.

[11]   Zhu, J. Y., Wang, G. S., Pan, X. J., and Gleisner, R., 2009, "Specific Surface to Evaluate the Efficiencies of Milling and Pretreatment of Wood for Enzymatic Saccharification," Chemical Engineering Science, 64(3), pp. 474-485.

[12]   Zhu, W., Zhu, J. Y., Gleisner, R., and Pan, X. J., 2010, "On Energy Consumption for Size-Reduction and Yields from Subsequent Enzymatic Saccharification of Pretreated Lodgepole Pine," Bioresource Technology, 101(8), pp. 2782-2792.

[13]   Song, X. X., Zhang, M., Pei, Z. J., Deines, T., Zhang, Q., Zhang, P. F., and Wang, D. H., 2011, "Size Reduction of Poplar Wood Using a Lathe for Biofuel Manufacturing: A Preliminary Experiment," Proceedings of the ASME 2011 International Mechanical Engineering Congress & Exposition (IMECE), ASME, Denver, Colorado,USA, pp. 683-690.

[14]   Zhang, M., Song, X., Zhang, P., Pei, Z. J., Deines, T. W., and Wang, D., 2012, "Size Reduction of Cellulosic Biomass in Biofuel Manufacturing: A Study on Confounding Effects of Particle Size and Biomass Crystallinity," Journal of Manufacturing Science and Engineering, 134.

[15]   Zhang, M., Song, X. X., Deines, T. W., Pei, Z. J., and Wang, D., 2012, "Biofuel manufacturing from woody biomass: effects of sieve size used in biomass size reduction," Journal of Biomedicine and Biotechnology, 2012.

[16]   von Sivers, M., and Zacchi, G., 1996, "Ethanol from Lignocellulosics: A Review of the Economy," Bioresource Technology, 56(2-3), pp. 131-140.

[17]   Rubin, E. M., 2008, "Genomics of cellulosic biofuels," Nature, 454(7206), pp. 841-845.

[18]   Energy, U. S. D. o., 2009, "Breaking the Biological Barriers to Cellulosic Ethanol: A Joint Research Agenda," http://genomicscience.energy.gov/biofuels/b2bworkshop.shtml.

[19]   Perlack, R, D., Stokes, B. J., 2011, "U.S. billion-ton update: biomass supply for a bioenergy and bioproducts industry," ORNL/TM-2011/224, Oak Ridge National Laboratory. http://www1.eere.energy.gov/biomass/pdfs/billion_ton_update.pdf

[20]   Falk, D., 1985, Pelleting cost center, American Feed Industry Association, Arlington, VA.

[21]   Hess, J. R., Wright, C. T., and Kenney, K. L., 2007, "Cellulosic biomass feedstocks and logistics for ethanol production," Biofuels, Bioproducts and biorefining, 1(3), pp. 181-190.

[22]   Sokhansanj, S., and Turhollow, A., 2004, "Biomass densification-cubing operations and costs for corn stover," Applied Engineering in Agriculture, 20(4), pp. 495-502.

[23]   Song, X. X., Zhang, M., Pei, Z. J., and Deines, T., 2010, "Ultrasonic-Vibration-Assisted Pelleting of Cellulosic Biomass: Effects of Moisture Content," Proceedings of the ASME 2010 International Manufacturing Science and Engineering Conference (MSEC)Erie, PA, USA.

[24]   Song, X. X., Zhang, M., Pei, Z. J., and Deines, T., 2010, "Ultrasonic-Vibration-Assisted Pelleting of Cellulosic Biomass: Effects of Moisture Content," Proceedings of the IIE Annual Conference and ExpoCancun, Mexico.

[25]   Zhang P. F., Pei Z. J., Wang D., Wu, X., Cong, W., Zhang, M., and Deines, T., 2011 "Ultrasonic Vibration-Assisted Pelleting of Cellulosic Biomass for Biofuel Manufacturing," Journal of Manufacturing Science and Engineering. 133(1), pp. 0110121 − 0110127.

Chapter 2 - Effects of Moisture Content on Pellet Quality in UV-A Pelleting

Authors' names:

Xiaoxu Song, Meng Zhang, Timothy Deines, P.F. Zhang, Q. Zhang, and Z.J. Pei

Authors' affiliation:

Department of Industrial and Manufacturing Systems Engineering, Kansas State University, Manhattan KS 66506 USA

Abstract

Wheat straw can be used to make biofuels. However, there are several barriers to cost-effective manufacturing of biofuels using wheat straw. One such barrier is related to the high transportation cost due to the low density of wheat straw. Pelleting of wheat straw is one way to increase its density. This paper reports an experimental study on ultrasonic vibration-assisted pelleting of wheat straw. The study was focused on effects of moisture content on pellet density and stability. The experimental results show that low moisture content (13%) produced higher density and stability than high moisture contents (20% and 25%).

Keywords

2.1 Introduction

Transportation fuels in the U.S. today are primarily petroleum-based and require a great amount of imported crude oil [1]. Taking into account the global energy crisis, energy supply diversity, and the impact of greenhouse gas emissions on global climate, it is important to find a substitute for petroleum-based fuels [1].

Biofuels produced from cellulosic biomass are sustainable sources of liquid fuels [2]. Biofuels generate significantly less greenhouse gas emissions than petroleum-based fuels and have the potential to be greenhouse gas neutral if efficient manufacturing methods for biofuels are developed [2-6].

So far, the primary biofuels in the U.S. are ethanol from corn grains and biodiesel from soybean [1]. These accounted for less than 3 percent of U.S. transportation-fuel consumption in 2007 [1]. However, converting corn and soybean crops to biofuels brings competition between food, feed, and fuel. Furthermore, a lot of petroleum-based fuels are required to grow such crops, such as fertilizer and farm vehicles, making the reductions in greenhouse gas emissions compared with petroleum-based gasoline small at best [1].

The next generation of biofuels is expected to be made from cellulosic biomass, which are from nonfood sources, such as residues from agricultural and forestry practices, and crops grown only for conversion to fuel (i.e. dedicated energy crops). It was reported that

approximately 550 million tons of cellulosic biomass could be produced per year by 2020 without any major impact on food production or the environment [1].

However, cellulosic biomass feedstocks have low bulk density, which causes higher costs in their storage, handling and transportation [7]. One way to increase the density is to consolidate them into pellets.

There are many factors which affect the quality of pellets, such as moisture content (MC), binder content, pellet size, and particle size. Fasina and Sokhansanj studied effects of moisture content on bulk handling properties of alfalfa pellets [8]. The moisture content of biomass materials was studied over a wide range from 10% to 25% [9-14]. Research on hey showed that relaxed pellet density decreased with increasing moisture content up to 55% [9,10,13-15], and the density decrease was exponential [9]. O'dogherty and Wheeler showed that pelleting was impossible if moisture content was greater than 26% for wheat straw, barely straw and oil seed rape straw [16].

Traditional pelleting methods (for example, using a screw extruder, a briquetting press, or a rolling machine [7,17]) generally involve high-temperature steam and high pressure and often use binder materials, making it difficult to realize cost-effective pelleting on or near the field where cellulosic biomass is available. Ultrasonic-vibration-assisted (UV-A) pelleting, without using high-temperature steam, high pressure and binder materials, can produce biomass pellets whose density is comparable to that processed by conventional pelleting methods [18,19].Therefore, studying the factors (including moisture content) that affect the density and stability of the ultrasonic-vibration-assisted (UV-A) pelleting will help to produce high quality pellets.

2.2 Experiment set-up and measurement methods

2.2.1 Wheat straw materials

The biomass (wheat straw) was ground with a cutting mill (shown in Figure 2-1) (model SM 2000 from Retsch, Inc., Haan, Germany) using a sieve size of 1.5 mm. The moisture content of wheat straw was about 6.5% when it was received for this study.

The moisture content (MC) was measured using the following procedure. A sample of wheat straw was measured on a scale to get its weight. Then it was heated in an oven (Blue M Electric Co., Blue island, IL, USA) at 130°C for 2 hours to evaporate the moisture. After

heating, the weight of the sample was measured again. The original moisture content was calculated by Equation (1):

$$Original \quad MC = \left(\frac{Original \quad sample \quad weight - Weight \quad after \quad heating}{Original \quad sample \quad weight} \right) \times 100\% \tag{1}$$

Figure 2-1 Cutting mill

The wheat straw was divided into three groups for three levels of MC (13%, 20%, and 25%). The MC of each group was adjusted by the following procedure.

The total weight of each group before adjusting was 50 g. Equations (2-4) were used to calculate the weight of distilled water needed to add to each group.

$$(1 - 6.5\%) \times 50g = (1 - 13\%) \times X_1 \tag{2}$$

$$(1 - 6.5\%) \times 50g = (1 - 20\%) \times X_2 \tag{3}$$

$$(1 - 6.5\%) \times 50g = (1 - 25\%) \times X_3 \tag{4}$$

Where X_1, X_2, X_3 are the total weights of each group after adjusting. (X_1-50), (X_2-50), and (X_3-50) are the weights of distilled water that will be added into each of the three groups (with three different levels of MC), respectively.

2.2.2 Experimental conditions

A Sonic Mill series 10 rotary ultrasonic machine (shown in Figure 2-2) (Sonic-Mill, Albuquerque, NM, USA) was used for the pelleting experiments. The machine was composed of an ultrasonic spindle system and a feed system. Water was pumped through the spindle using a

refrigerated recirculator (CFT-75 Neslab Instrument Inc. Portsmouth, NH, USA) to cool the spindle. The water temperature was keep at 25°C. The ultrasonic spindle system consisted of a power supply unit, an ultrasonic vibration generation unit, and a motor with its controller. The power supply unit converted 60 Hz AC electricity into high frequency (20 kHz) AC output. The AC output was converted into high frequency mechanical vibration through an ultrasonic vibration generation unit in the ultrasonic spindle. Ultrasonic power was set at 35% for all the tests.

Figure 2-2 Rotary ultrasonic machine

The tool (shown in Figure 2-3) was custom made. The tool tuning length was 55.88 mm. The diameter of the tool was 17.4 mm. During pelleting, the tool rotation speed was 50 rpm, and the feedrate of the tool was 10 mm/min.

The aluminum mold (shown in Figure 2-4) was made in two separate parts; the upper part was a hollow cylinder which was mounted on the bottom base. These two parts were assembled together by two screws. The length and the diameter of the mold cavity were 39.37 mm and 19.05 mm respectively. The weight of wheat straw loaded into the mold for every test was 3 g.

Figure 2-3 Illustration of the tool

Figure 2-4The mold used in UV-A pelleting

2.2.3 Measurement methods

2.2.3.1 Density

Density of the pellets was calculated by Equation (5):

$$\rho = \frac{M}{V} \tag{5}$$

Where ρ: density,

M: the weight of a pellet,

V: the volume of a pellet.

The weight was measured by an electronic scale (model TAJ 602, Ohaus Corporation, Pine Brook, NJ, USA), and the volume was obtained by measuring the diameter and height of the pellet with a caliper. From each of the three groups (13%, 20%, and 25%), five pellets were randomly selected for density measurements. The measurement was carried out by the same person after pelleting every 24 hours for nine days. For all density measurements, at least four pellets were measured and their average values are reported in this paper.

2.2.3.2 Stability

Stability measures the changes in their dimensions. It is desirable that pellets maintain their initial dimensions. Thus, the less the change, the more stable the pellet [20].

Stability of a pellet was evaluated by spring-back and determined by Equation (6):

$$Spring-back = \frac{V - V_o}{V_o} \times 100\% \qquad (6)$$

Where V: Volume measured,

V_o: Original volume.

The volume of the pellets would increase (called spring-back or relaxation) with time after they were taken out from the mold. The original pellet volume was calculated by the theoretical dimensions of the pellet, determined by the diameter of the mold cavity and the stop position of the tool. Since all pellets in all groups of milled wheat straw were pelleted using the same mold and same tool stop position, their original volumes were the same.

2.3 Experimental results and discussion

2.3.1 Effects of MC on density

Effects of MC on pellet density are shown in Figure 2-5 and Table 2-1. The highest density was found with 13% MC. The lowest density was found with 25% MC. The density of the pellets processed with 13% MC (627 kg/m^3) was 30% higher than that with 25% MC (485 kg/m^3). For different levels of MC, the density did not change significantly as the number of days increased.

Figure 2-5 Results on pellet density

13
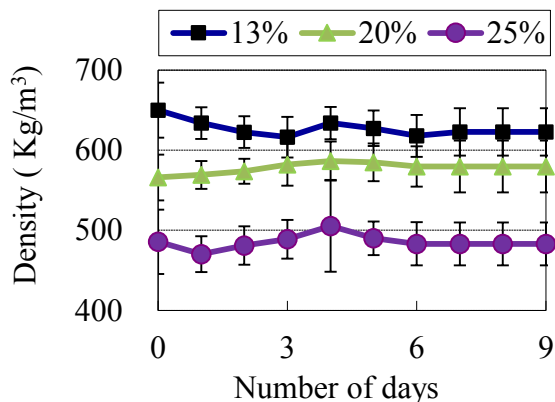
2.3.2 Effects of MC on stability

Effects of MC on spring-back are shown in Figure 2-6 and Table 2-2. Spring-back ranged from 106% to 60% with 25% MC. Spring-back reduced by 22% with 13% MC, 38% with 20% MC, and 43% with 25% MC. Therefore, it is clear that the pellets processed with a lower MC were more stable (or had smaller spring-back). The reason for the decrease in volume of the pellets was that cluster of biomass fell off from the pellets after some time.

Figure 2-6 Results on pellet spring-back
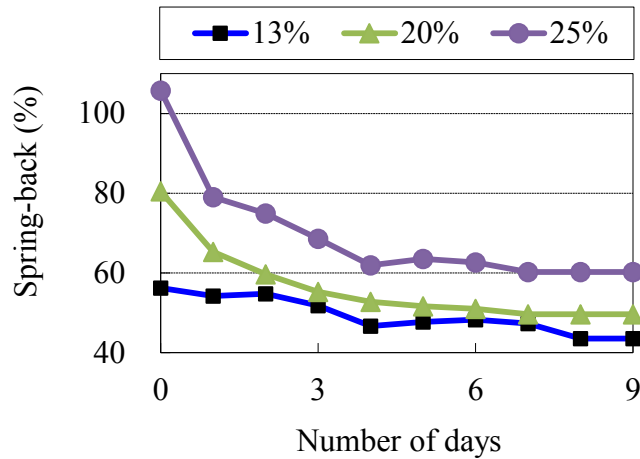
Table 2-1 Experimental results on density (kg/m^3)

Day	MC 13%	MC 20%	MC 25%
0	650	566	486
1	634	569	470
2	623	574	481
3	616	582	489
4	634	586	505
5	627	585	490
6	618	580	483
7	623	580	483
8	623	580	483
9	623	580	483
average	627	578	485

Table 2-2 Experimental results on spring-back (%)

Day	MC 13%	MC 20%	MC 25%
0	56	81	106
1	54	65	79
2	55	60	75
3	52	55	69
4	47	53	62
5	48	52	64
6	48	51	63
7	47	50	60
8	44	50	60
9	44	50	60

2.4 Conclusions

Effects of moisture content (MC) in ultrasonic-vibration assisted pelleting of wheat straw have been studied. MC had significant effects on pellet density and stability. Among the three MC levels tested, the highest density was found with 13% MC. The density of the pellets processed with 13% MC (627 kg/m^3) was 30% higher than that with 25% MC (485 kg/m^3). Furthermore, the pellets processed with a lower MC were more stable.

Acknowledgements

References

[1]   National Academy of Sciences, National Research Council, 2009, "Liquid Transportation Fuels from Coal and Biomass: Technological Status, Costs, and Environmental Impacts," National Academy Press.

[2]   Huber, G.W., Iborra, S., and Corma A., 2006, "Synthesis of Transportation Fuels from Biomass: Chemistry, Catalysts, and Engineering," Chemical Reviews, 106, 4044-4098.

[3]   Wyman, C.E., and Hinman, N.D., 1990, "Ethanol: Fundamentals of Ethanol Production from Renewable Feedstocks and Use as a Ttransportation Fuel," Applied Biochemistry and Biotechnology, 24/25, 735-753.

[4]   Wyman, C.E., 1994, "Alternative Fuels from Biomass and Their Impact on Carbon Dioxide Accumulation," Applied Biochemistry and Biotechnology, 45/46, 897-915.

[5]   Tyson, K.S., 1993, "Fuel Cycle Evaluations of Biomass-ethanol and Reformulated Gasoline," Report No. NREL/TP-263-2950, DE94000227, National Renewable Energy Laboratory: Golden, CO.

[6]   Lynd, L.R., Cushman, J.H., Nichols, R.J., and Wyman, C.E., 1991, "Fuel Ethanol from Cellulosic Biomass," Science, 251 (4999), 1318-1323.

[7]   Mani, S., Tabil, L.G., and Sokhansanj, S., 2003, "An Overview of Compaction of Biomass Grinds," Powder Handling and Processing, The International Journal of Storing, Handling, and Processing Powder, 15 (3), 160-168.

[8]   Fasina, O.O., and Sokhansanj, S., 1993, "Effect of Moisture Content on Bulk Handling Properties of Alfalfa Pellets," Canadian Agricultural Engineering, 35 (4), 269-273.

[9]   Butler, B.J., and McColly, H.F., 1959, "Factors Affecting the Pelleting of Hay," Agricultural Engineering, 40 (8), 442-446.

[10]   Gustafson, A.S., and Kjelgaard, W.L., 1963, "Hay Pellet Geometry and Stability," Agricultural Engineering, 44 (8), 442-445.

[11]   Reece, F.N., 1966, "Temperature, Pressure and Time Relationships in Forming Dense Hay Wafers," Trans. ASAE, 9 (6), 749-751.

[12]   Hall, G.E., and Hall, C.W., 1968, "Heated Die Wafer Formation of Alfalfa and Bermuda Grass," Trans. ASAE, 11 (4), 578-581.

[13]   Rehkugler, G.E., and Buchele, W.F., 1969, "Biomechanics of forage wafering," Trans. ASAE, 12 (1), 1-8.

[14]   Bruhn, H.D., Zimmerman, A., and Niedermeir, R.P., 1959, "Developments in Pelleting Forage Crops," Agricultural Engineering, 40 (4), 204-206.

[15]   Bellinger, P.L., and McColly, H.F., 1961, "Energy Requirements for Forming Hay Pellets," Agricultural Engineering, 42 (5), 244-247.

[16]   O'dogherty, M.J., and Wheeler, J.A., 1984, "Compression of Straw to High Densities in Closed Cylindrical Dies," Journal of Agricultural Engineering Research, 29 (1), 61-72.

[17]   Sokhansanj, S., Mani, S., and Zaini, P., 2005, "Binderless Pelletization of Biomass," ASABE Paper No. 056061, American Society of Agricultural and Biological Engineers, St. Joseph, MI.

[18]   Pei, Z.J., Wang, D.H., and Clark, R., 2009, "Ultrasonic Vibration-assisted Pelleting of Cellulosic Biomass: a Preliminary Experiment," Proc. of International Manufacturing Science and Engineering Conference, October 4-7, West Lafayette, IN, USA.

[19]   Cong, W.L., Zhang, P.F., Qin, N., Zhang, M., Song, X.X., Zhang, Q., Nottingham, D., Clark, R., Deines, T., Pei, Z.J., and Wang, D.H., 2009, "Ultrasonic-Vibration-assisted Pelleting of Cellulosic Biomass for Biofuel Manufacturing," Poster Presentation at the 2009 International Manufacturing Science and Engineering Conference, October 4-7, West Lafayette, IN, USA, MSEC2009-84432.

[20]   Al-Widyan, M.I., Al-Jalil, H.F., Abu-Zreig, M.M., and Abu-Hamdeh, N.H., 2002, "Physical Durability and Stability of Olive Cake Briquettes," Canadian Biosystems Engineering, 44, 341-345.

Chapter 3 - Effects of Moisture Content and Biomass Type on Pellet Quality in UV-A Pelleting

Authors' names:

Xiaoxu Song, Meng Zhang, Timothy Deines, and Z.J. Pei

Authors'affiliation:

Department of Industrial and Manufacturing Systems Engineering, Kansas State University, Manhattan KS 66506 USA

Abstract

Cellulosic biomass is an important source for making biofuels. However, there are several barriers to cost-effective manufacturing of biofuels using cellulosic biomass. One such barrier is related to the high transportation cost due to the low density of cellulosic biomass. Pelleting of cellulosic biomass is one way to increase its density. This paper reports an experimental study on ultrasonic vibration-assisted pelleting of cellulosic biomass. The study was focused on effects of moisture content (MC) on pellet density of three kinds of cellulosic biomass (wheat straw, switchgrass, and sorghum). The experimental results show that sorghum has the highest density with three levels of MC among these biomass materials. The highest density was found with sorghum of 20% MC.

3.1 Introduction

Global consumption of petroleum has tripled since 1970 [1]. Energy demand is projected to grow by more than 50% by 2025 [2]. Shifting society's dependence away from petroleum to renewable biomass resources is important to the development of a sustainable industrial society and effective management of greenhouse gas emissions [2].

The U.S. Department of Energy has made determination to replace 30% of the petroleum-based transportation fuels with biofuels and to replace 25% of industrial organic chemicals with biomass-derived chemicals by 2025 [1-3].

First generation bioethanol relies largely on the fermentation of starch from corn in the U.S. or from sugar cane in Brazil [1, 4]. The next generation of biofuels is expected to be made from cellulosic biomass from nonfood sources, such as residues from agricultural and forestry practices, and crops grown only for conversion to fuel (i.e. dedicated energy crops). It was reported that approximately 550 million tons of cellulosic biomass could be produced per year in the U.S. by 2020 without any major impact on food production or the environment [5].

Low bulk density is one characteristic that causes the high cost of transporting cellulosic biomass from field to conversion plants [6]. This characteristic demands for new biomass storage that will exceed 4.5 billion and 14.9 billion cubic ft, generating more than $3.1 billion and $10.6

billion new storage structures in 2010 and 2020, respectively [7]. Handling, storage, and transportation costs can be lowered by increasing the density via consolidating cellulosic biomass into pellets. Dense pellets require less space for storage and transport than loose biomass [8,9]. In addition to savings in transportation and storage, dense pellets lend them to easy and cost effective handling. Dense pellets have the flow ability similar to cereal grains [8,9].

While considerable research efforts have been spent on developing efficient conversion technologies, only meager research is conducted on problems associated with biomass processing and handling [8]. Loose cellulosic biomass has a low bulk density ranging from 50 to 130 kg/m^3 depending on the plant species, size and distribution of particles. The density of biomass pellets ranges from 120 to 500 kg/m^3 [10].

Traditional pelleting methods (for example, using a screw extruder, a briquetting press, or a rolling machine [11,12]) generally involve high-temperature steam and high pressure and often use binder materials, making it difficult to realize cost-effective pelleting on or near the field where cellulosic biomass is available. Ultrasonic-vibration-assisted (UV-A) pelleting, without using high-temperature steam, high pressure and binder materials, can produce biomass pellets whose density is comparable to that processed by conventional pelleting methods [13,14]. Studying the factors including moisture content (MC) that affect the density and stability in ultrasonic-vibration-assisted (UV-A) pelleting will help to produce high quality pellets.

This paper focuses on three different biomass materials with three different levels of MC during ultrasonic-vibration-assisted (UV-A) pelleting. Effects of MC and different biomass materials on density are discussed. The aim of this paper is to determine which level of moisture content and which kind of biomass material can result in the highest density.

3.2 Experiment conditions

3.2.1 Material Preparation

Three kinds of cellulosic biomass materials were used in this study, wheat straw, switchgrass, and sorghum. The biomass was ground with a cutting mill (model SM 2000 from Retsch, Inc., Haan, Germany) using a sieve size of 1.5 mm. The MC levels of these three kinds of materials were about 6.5%, 6.6% and 9% when they were received for this study.

The original MC was measured using the following procedure. An oven (Blue M Electric Co., Blue island, IL, USA) was preheated to 103°C for half an hour. The weight of a glass

20

container was measured. Then 25g biomass was put inside the container. The container without a cover was placed into the preheated oven for 24 hours. The weight of the glass container with biomass was measured again. The original MC was calculated by Equation (1):

$$Original \quad MC = \left(\frac{Original \quad sample \quad weight - Weight \quad after \quad heating}{Original \quad sample \quad weight} \right) \times 100\%$$

(1)

Each kind of biomass was divided into three groups for three levels of MC (13%, 20%, and 25%), and all groups were pelletized. The MC of each group was adjusted by the following procedure.

The total weight of each group before adjusting was 60 g. The weight after adjusting was calculated by Equation (2):

$$Weight \quad after \quad adjustment = \left(\frac{1 - Original \quad MC}{1 - Desired \quad MC} \right) \times 60g$$

(2)

Three desired MC levels were used in this study. They were 13%, 20%, and 25%. The difference between the weight after adjustment and 60 g was the weight of distilled water that needed to add to the biomass. Table 3-1 shows the data for MC adjustment. The biomass and distilled water were put in a zip-lock bag and the bag was shaked until there were no biomass clumps. The biomass after MC adjustment was kept in the refrigerator (Model #: GVS04BDWSS, General Electric Company, U.S.) for 24 hours before being pelletized.

Table 3-1 Data of MC adjustment

Materials	Original MC (%)	Desired MC (%)	Weight before adjustment (g)	Weight after adjustment (g)	Weight of distilled water (g)
Wheat straw	6.5	13	60	64.48	4.48
Wheat straw	6.5	20	60	70.13	10.13
Wheat straw	6.5	25	60	74.80	14.80
Switchgrass	6.6	13	60	64.41	4.41
Switchgrass	6.6	20	60	70.05	10.05
Switchgrass	6.6	25	60	74.72	14.72
Sorghum	9	13	60	62.76	2.76
Sorghum	9	20	60	68.25	8.25
Sorghum	9	25	60	72.80	12.80

3.2.2 Pelleting Conditions

Pelleting was performed on an ultrasonic machine (AP1000, Sonic-Mill Inc, Albuquerque, NM, USA). The experiment set up is illustrated in Figure 3-1. Ultrasonic power was set at 35% for all the tests. The tool was mounted to an ultrasonic spindle that provided high-frequency (20 kHz) ultrasonic vibration. The mold (Figure 3-2) was made in three separate parts for easy assembly and disassembly. The top two parts formed a hollow cube which could be assembled by pins and the bottom was a square-shaped base. The diameter of the tool (17.4 mm) was slightly smaller than that of the central hole in the mold (18.3 mm).

The weight of biomass loaded in the center cavity of the mold for every test was 3 g. The tool pressed the biomass inside the mold cavity, with the ultrasonic power on for 2 minutes. The tool then was retracted and the mold disassembled to unload the pellet.

Figure 3-1 Experiment set up
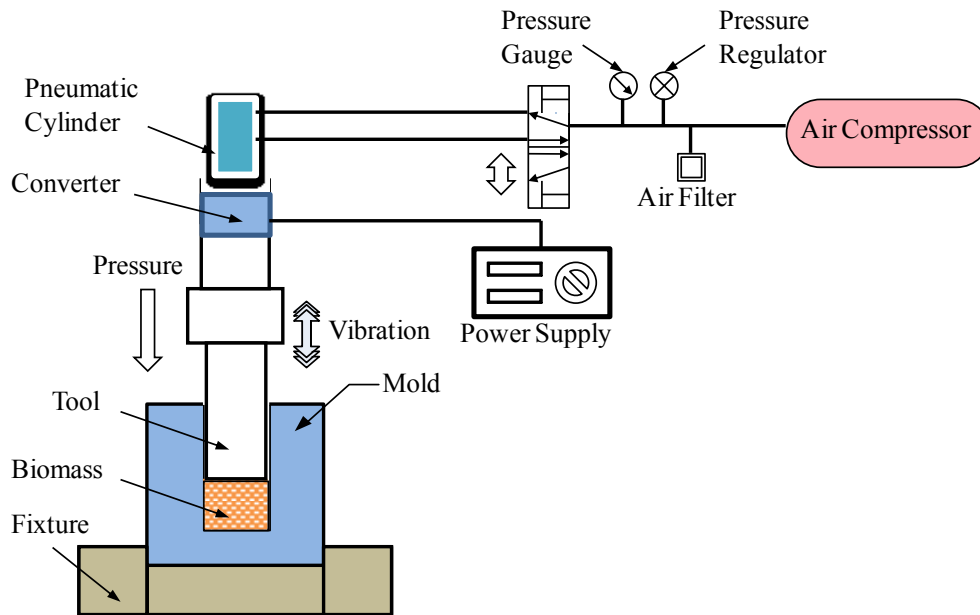
3.2.3 Measurement Procedure

Density of the pellets was calculated by dividing the weight of a pellet by its volume.

$$\rho = \frac{W}{V} \tag{3}$$

where ρ: density, W: the weight of a pellet, V: the volume of a pellet.

The weight of a pellet was measured by an electronic scale (model TAJ 602, Ohaus Corp., Pine Brook, NJ, USA), and the volume was obtained by measuring the diameter and height of the pellet with a caliper. Three measurements were taken for the diameter and height of a pellet and the average value was used. From each of the three groups (13%, 20%, and 25% MC), five pellets were randomly selected for density measurements. The measurement was carried out by the same person after pelleting every 24 hours for nine days. For all density measurements, at least four pellets were measured and their average values are reported in this paper.

Figure 3-2 the Mold Used in UV-A pelleting
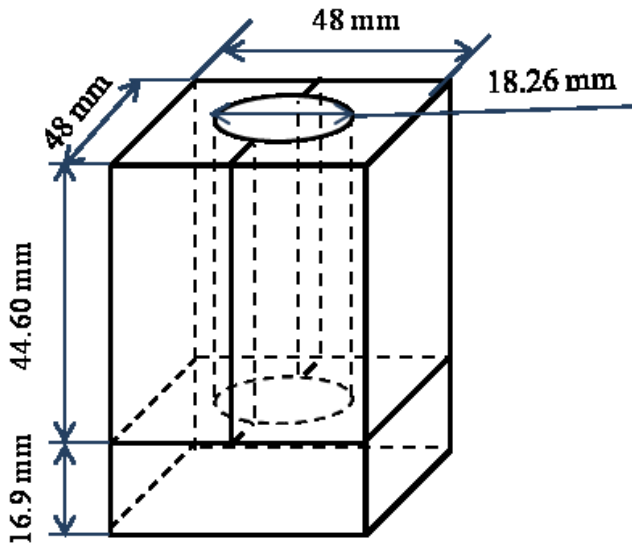
3.3 Results and discussion

3.3.1 Effects of MC on density

Effects of MC on pellet density are shown in Figures 3-3, 3-4, and 3-5. The highest density was found with sorghum of 20% MC (1043 kg/m3). The lowest density was found with wheat straw of 25% MC (446 kg/m3). For different MC levels of each kind of biomass materials, the density did not change significantly as number of days increased.

3.3.2 Effects of biomass materials on density

Sorghum has the highest density among all three kinds of biomass materials (shown in Figures 3-6, 3-7, and 3-8). The density of switchgrass was almost the same as that of wheat straw.

Figure 3-3 Effects of MC on wheat straw pellet density

Wheat Straw
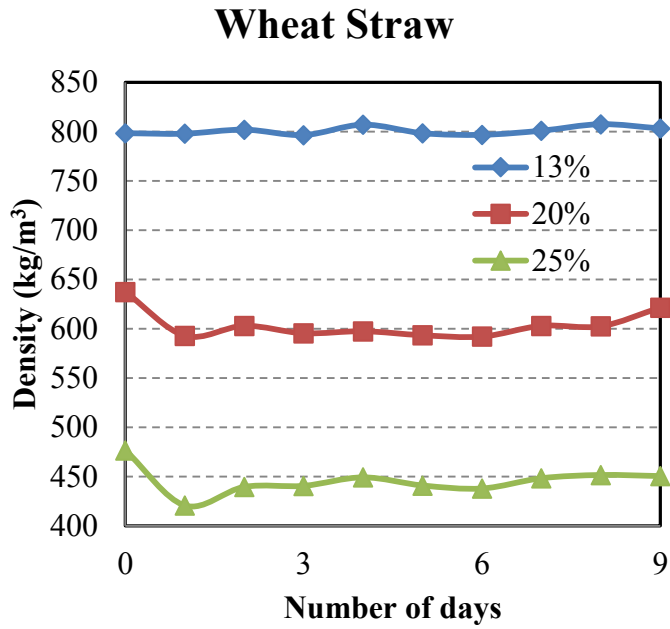
Figure 3-4 Effects of MC on switchgrass pellet density

Switchgrass
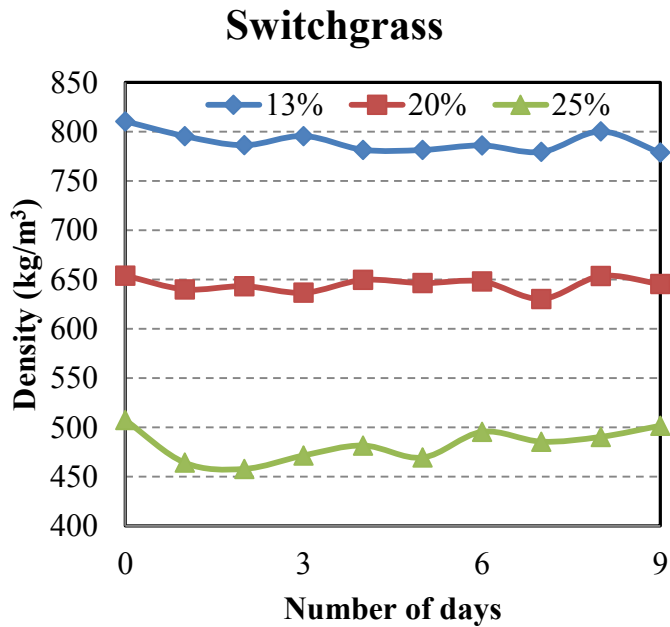
Figure 3-5 Effects of MC on sorghum pellet density

Sorghum
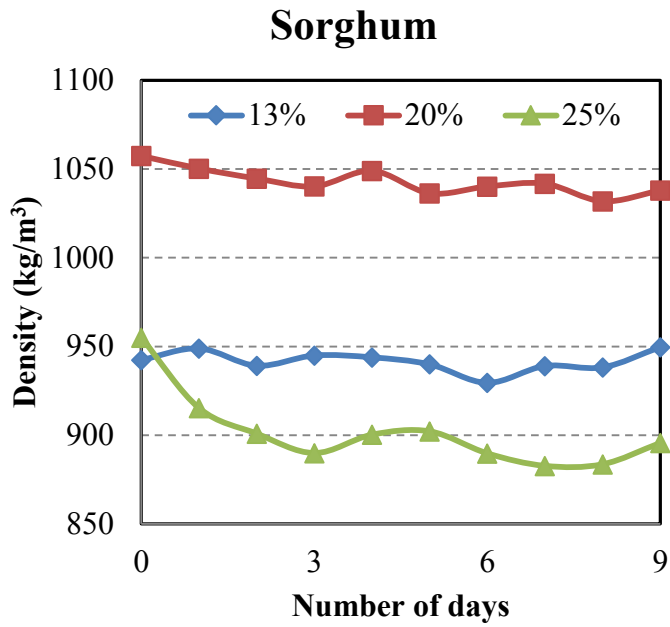
Figure 3-6 Effects of different biomass materials on density with 13% MC

MC=13%
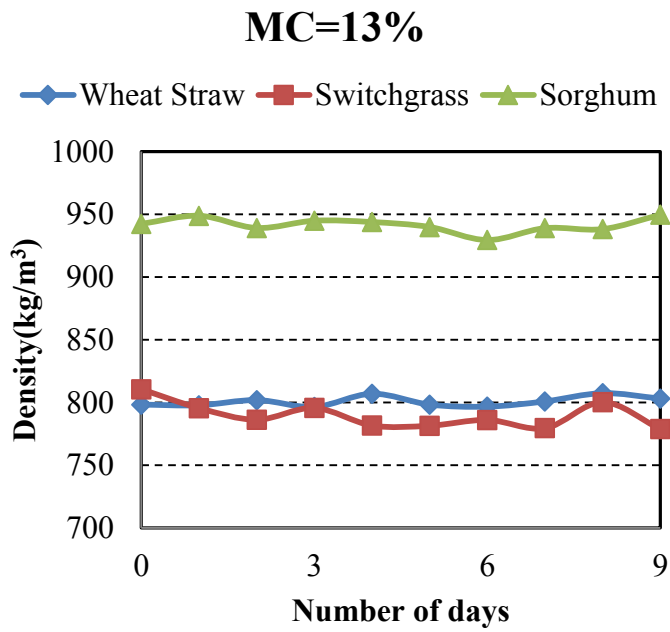
Figure 3-7 Effects of different biomass materials on density with 20% MC

MC=20%
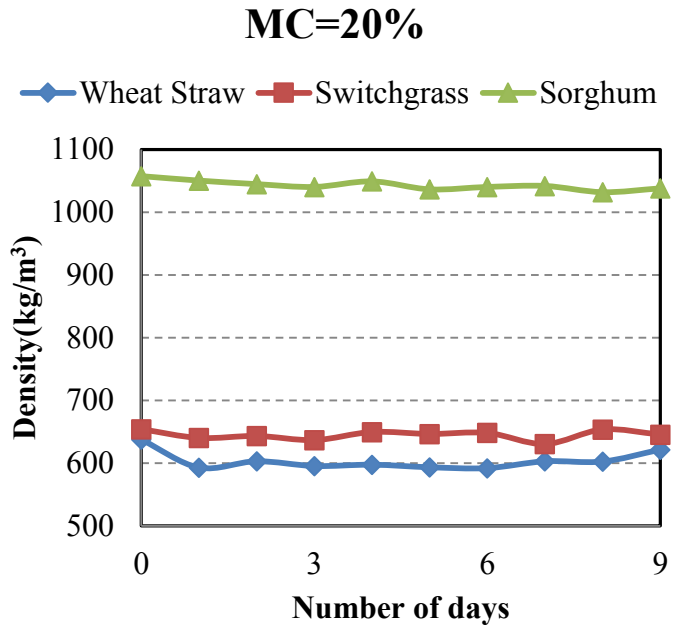
Figure 3-8 Effects of different biomass materials on density with 25% MC

MC=25%
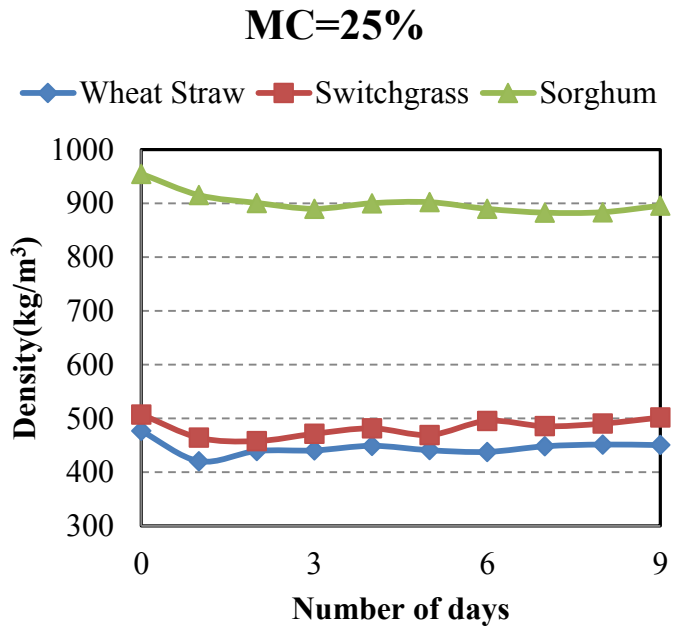
3.4 Conclusions

Effects of moisture content (MC) in ultrasonic-vibration assisted pelleting of three kinds of biomass materials have been studied. MC had significant effects on pelleting density. The highest density was found with sorghum of 20% MC (1043 kg/m^3). The lowest density was found with wheat straw of 25% MC (446 kg/m^3). Sorghum has the highest density among these three biomass materials.

Acknowledgments

References

[1] Lovins，A.B., (2004). "Winning the Oil Endgame: Innovation for Profits, Jobs, and Security." Rocky Mountain Institute, Snowmass, CO.

[2] Ragauskas, A.J., Williams, C.K., Davison, B.H., Britovsek, G., Cairney, J., Eckert, C.A., Frederick, W.J., Hallett, J.P., Leak, D.J., Liotta, C.L., Mielenz, J.R., Murphy, R., Templer, R., and Tschaplinski, T., (2006). "The Path Forward for Biofuels and Biomaterials." Science, 311 (5760), pp. 484-489.

[3] Chum, H.L., and Overend, R.P., (2004). "Biomass Conversion to Fuels and Chemical." Preprint Papers - American Chemical Society, Division of Fuel Chemistry (Prepr Pap - Am Chem Soc, Div Fuel Chem), 49 (2).

[4] Parikka, M., (2004). "Global Biomass Fuel Resources." Biomass Bioenergy, 27, pp. 613.

[5] National Academy of Sciences, (2009). "Liquid Transportation Fuels from Coal and Biomass: Technological Status, Costs, and Environmental Impacts." National Academy Press.

[6] Lindley, J.A. and Backer, L., (1994). "Agricultural Residue Harvest and Collection. Prepared for Western Regional Biomass Energy Program." in, PO#AA-PO-111671-12134. ND 58105-5626. Agricultural Engineering Department,, Fargo, North Dakota State University.

[7]   Sokhansanj, S., and Wright, L., (2002). "Impact of Future Biorefineries on Feedstock Supply Systems -Equipment and Infrastructure." ASAE Paper No. 021073. ASAE. St. Joseph, MI.

[8]   Sokhansanj, S., Cushman, J., and Wright, L., (2003). "Collection and Delivery of Biomass for Fuel and Power Production." The CIGR Journal of Scientific, 5.

[9]   Fasina, O.O., and Sokhansanj, S., (1996). "Storage and Handling Characteristics of Alfalfa Pellets." Powder Handling and Processing 8 (4), pp. 361-365.

[10]   Sokhansanj, S. and Turhollow, A.F., (2004). "Biomass Densification-Cubing Operations and Costs for Corn Stover." Applied engineering in agriculture, 20 (4), pp. 495-499.

[11]   Mani, S., Tabil, L.G., and Sokhansanj, S., (2003). "An Overview of Compaction of Biomass Grinds." Powder Handling and Processing, The International Journal of Storing, Handling, and Processing Powder, 15 (3), pp. 160-168.

[12]   Sokhansanj, S., Mani, S., and Zaini, P., (2005). "Binderless Pelletization of Biomass." ASABE Paper No.056061, in, American Society of Agricultural and Biological Engineers, St. Joseph, MI.

[13]   Pei, Z.J., Wang, D.H., and Clark, R, (2009). "Ultrasonic Vibration-Assisted Pelleting of Cellulosic Biomass: A Preliminary Experiment." in Proc. the 2009 of International Manufacturing Science and Engineering Conference, MESC2009-84205. West Lafayette, IN, USA.

[14]   Cong, W.L., Zhang, P.F., Qin, N., Zhang, M., Song, X.X., Zhang, Q., Nottingham, D., Clark, R., Deines, T., Pei, Z.J., and Wang, D.H., (2009). "Ultrasonic-Vibration-Assisted Pelleting of Cellulosic Biomass for Biofuel Manufacturing." Poster Presentation at the 2009 International Manufacturing Science and Engineering Conference, MESC2009-84432. West Lafayette, IN, USA.

Chapter 4 - Effects of Binder Material on Pellet Quality in UV-A Pelleting

Authors' names:

Xiaoxu Song, Meng Zhang, Timothy Deines, P.F. Zhang, Q. Zhang, W.L. Cong, N. Qin, and Z.J. Pei

Authors' affiliation:

Department of Industrial and Manufacturing Systems Engineering, Kansas State University, Manhattan KS 66506 USA

Abstract

Liquid biofuels produced from cellulosic biomass can significantly reduce the nation's dependence on foreign oil, create new jobs, improve rural economies, reduce greenhouse gas emissions, and improve national security. Moreover, cellulosic biomass would not bring a competition for farmland with food and feed products. Nevertheless, significant hurdles must be overcome to cost-effectively manufacture cellulosic biofuels. One of the hurdles is related to the low density of cellulosic feedstocks, which causes high costs in their transportation and storage. Pelleting can increase the density of cellulosic feedstocks; therefore, can increase the overall efficiency by utilizing existing transportation infrastructure and storage systems. This paper presents an experimental study on ultrasonic vibration assisted (UV-A) pelleting of switchgrass. This study focuses on effects of binder material. The results show that, in UV-A pelleting, the influence of the binder material on pellet density, stability, and durability is not significant. If UV-A pelleting can produce pellets without adding binder materials, the pelleting cost will be reduced.

4.1 Introduction

The increasing demand for transportation liquid fuels in the U.S. has been far beyond U.S. domestic production capacity [1]. In the near future the heavy use of petroleum (fossil fuels) for transportation fuels will not change [2]. These facts leave the nation "vulnerable to the political, economic, and national security consequences of importing foreign oil" [2]. Additionally, fossil liquid fuels are nonrenewable energy sources and use of them emits greenhouse gas. Therefore, there is an urgent need to find alternative sustainable sources for transportation liquid fuels that can be used in existing vehicles.

Biofuels (such as ethanol and biodiesel) can be used as transportation fuels [3]. They are considered to be the only sustainable source of liquid fuels [4-6]. At present, about 97% of the ethanol used in the U.S. is distilled from corn. However, corn-based ethanol causes a competition between grain products for ethanol and food and feed products for the limited agricultural farm land and other resources [7, 8].   Cellulosic biofuels are produced from renewable cellulosic

30

biomass feedstocks such as corn stover (plant matter left in the field after harvest); switchgrass, wood chips, and other plants. Feedstocks used for cellulosic biofuels are abundant and diverse. The U.S. Department of Energy said that more than 1 billion dry tons of biomass could be sustainably harvested from U.S. fields and forests, enough to displace 30 percent of the nation's annual petroleum consumption for transportation fuels [9]. Developing cellulosic biofuels will reduce reliance on imported oil and cut greenhouse gas emissions, while continue to meet the nation's transportation energy needs [10]. Moreover, by using non-edible cellulosic biomass in ethanol production would put less inflationary pressure on food supplies [11]. Also, the existing well-developed agricultural and biological technologies are strong supports to cellulosic biofuels technologies. Now development and demonstration of cellulosic biofuels technologies are encouraged by both USDA and DOE [12].

Significant hurdles must be overcome for cost-effective manufacturing of cellulosic biofuels. One of the hurdles is related to the low density of cellulosic feedstocks, which would result in high transportation and storage cost. Furthermore, due to the low bulk density of the feedstocks, very large volume flow rates are required to maintain the capacity of a moderately sized (>1500 tones day−1) biorefinery [13].

By pelleting a material, the bulk density is increased and material handling properties are improved [14]. Pelleting is generally described as "the agglomeration of small particles into larger particles by the means of a mechanical process, and in some applications, thermal processing" [15]. Therefore, pelleting can result in a cost reduction in logistics related to cellulosic biomass feedstocks transportation and storage. In traditional pelleting or briquetting, in order to achieve high pellet density and durability, high-temperature steam and high pressure are used. Moreover, binder materials would be needed to achieve high pellet quality [16]. Young and Pfost [17, 18] studied effects of binder material on pelleting of milled wheat and showed that a binder significantly improved the durability. Tabil [19] reported several kinds of binder materials on pelleting characteristics of alfalfa and found that the durability of pellets was improved by addition of binders. Nalladurai et al. studied binding mechanisms of corn stover and switchgrass in briquettes and pellets [20].

Ultrasonic-vibration-assisted (UV-A) pelleting of cellulosic biomass can significantly increase biomass density. Compared with traditional pelleting, UV-A pelleting process does not use high-temperature steam and high pressure [21].

However, no information is available about the use of binder materials in UV-A pelleting. This paper will be the first about effects of binder material in UV-A pelleting. Knowledge obtained in this work will fill a gap in the literature and provide guidance in manufacturing of cellulosic biofuels.

4.2 Experiment set-up and procedures

4.2.1 Experiment conditions

Ultrasonic-vibration-assisted (UV-A) pelleting is shown in Figure 4-1 and 4-2. Pelleting experiments were performed on a Sonic Mill Series 10 (Sonic-Mill, Albuquerque, NM, USA) rotary ultrasonic machine. The machine included an ultrasonic spindle, a power supply, and a motor with its controller. The power supply converted 60 Hz AC electricity into high frequency (20 kHz) AC output. Through a piezoelectric converter in the ultrasonic spindle, the AC output was converted into high frequency mechanical vibration.

Figure 4-1 UV-A pelleting process
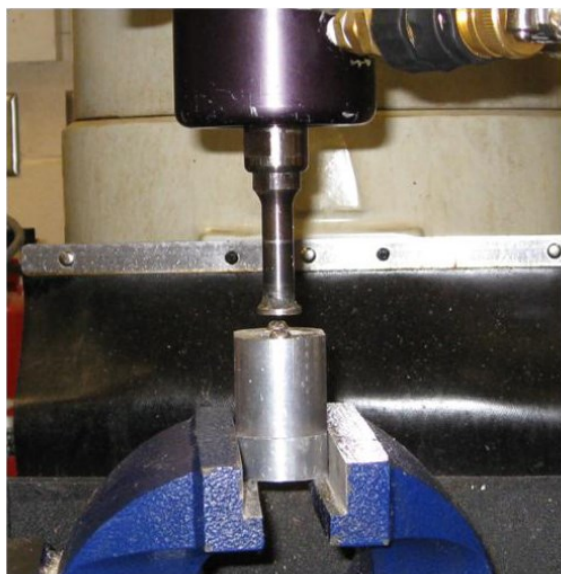
Water was pumped through the spindle using a refrigerated recirculator (CFT-75 Neslab Instrument Inc. Portsmouth, NH, USA). The water temperature was keep at 25℃ to cool down the spindle. The tool (illustrated in Figure 4-3) was custom made. The diameter of the tool was 0.685 in, and the tuning length of the tool was 2.2 in.

Figure 4-2 Illustration of UV-A pelleting of biomass
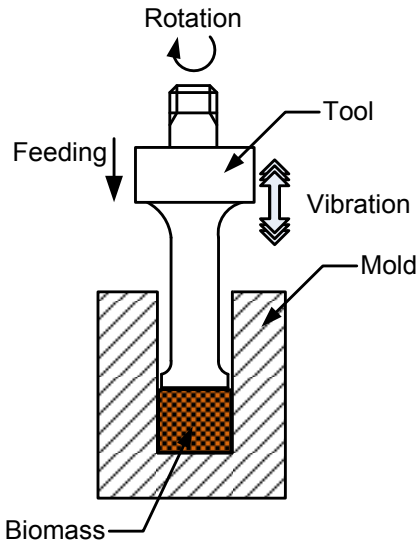
Figure 4-3 Illustration of the tool
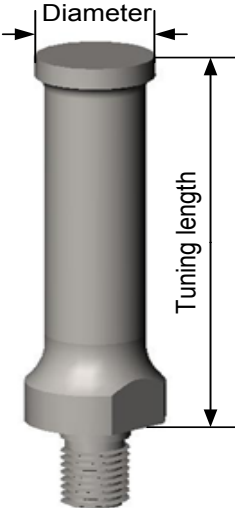
Figure 4-4 Molds in UV-A pelleting

Figure 4-5 A finished pellet

Table 4-1 Experimental parameters

Parameter	Value
Ultrasonic power	35%
Feedrate	10 mm/min
Tool rotation speed	50 rpm
Pelleting length	0.6 in

The aluminum mold (shown in Figure 4-4) had two separate pieces. The upper piece was a hollow cylinder; the inner diameter was 0.75 in, and the length was 1.55 in. The lower piece was a round plate, serving as a base. The two pieces were assembled together by two screws.

Before each pelleting, 3 grams of biomass was loaded into the mold cavity. The tool fed into the cavity at a certain feed rate. In this series of tests, the same tool stop position was set. When the tool reached at this position, it would retract. After the pelleting process, the mold was disassembled and pellet was unloaded. Figure 4-5 shows a finished pellet. Values of important experimental parameters are listed in Table 4-1. Ultrasonic power controlled the amplitude of the ultrasonic vibration. The pelleting length was the distance from the top of the mold to the tool stop position.

4.2.2 Biomass preparation

The biomass used in the UV-A pelleting experiment was switchgrass. It was prepared on a cutting mill (model SM 2000 from Retsch, Inc.) with a sieve size of 1 mm. The moisture content (MC) of the biomass after milling was adjusted to 15 %. Five samples of milled biomass (each having a weight of 3 grams) were heated in an oven for 2 hours to get rid of moisture in the biomass material. By measuring the weight lost, the original moisture content was calculated as follows:

$$Original \quad moisture \quad content = \frac{Sample \quad weight \quad lost}{Original \quad sample \quad weight} \times 100\% \tag{1}$$

In this experiment, the average original moisture content (6.5%) of the five samples represented the moisture content of the entire milled biomass. Then the weight of distilled water needed to prepare a certain weight of switchgrass having 10% moisture content was calculated as follows:

$$a \times (1 - 6.5\%) = (a + x) \times (1 - 10\%) \tag{2}$$

where, a is the weight of the initial switchgrass with MC = 6.5%; x is the amount of water needed to prepare the switchgrass with MC = 10%. To prepare the switchgrass for the experiment, distilled water was mixed with the milled switchgrass particles in a zip-lock bag, and the bag was shaken thoroughly. In this study, corn starch was used as the binder material. It was added into the biomass particles at a certain ratio by weight. For example, biomass with 10% binder content was a mixture of 1 unit of binder material and 9 units of biomass particles by weight. Four groups of tests were conducted. The binder contents of these test groups were 0%, 2%, 5%, and 10%, respectively.

4.2.3 Measurement methods

4.2.3.1 Density

The volume of the cylinder-shaped finished pellets was determined by $V = \pi d^2 h/4$. Here d is the diameter of the pellet, and h is the height of the pellet. For each test group, five finished pellets were chosen randomly, and their diameters and heights were measured using a vernier caliper (model IP-65, Mitutoyo Corp., Kawasaki, Japan.). The weight of the sample pellets was measured on a high accuracy scale (model TAJ 602, Ohaus Corp., Pine Brook, NJ, USA). Density was determined by:

$$Pellet \quad density = \frac{Weight \quad of \quad pellet}{Volume \quad of \quad pellet} \tag{3}$$

Density measurements were taken after the pellets were removed from the mold and repeated every 24 hours for the next nine days by a same person to minimize the variations in measurements.

4.2.3.2 Stability

Stability is employed to evaluate the changes in pellet's dimensions (or volume) with time. It is evaluated by spring- back defined as follows:

$$Spring-back = \frac{V - V_o}{V_o} \times 100\% \tag{4}$$

where V: Volume measured,

V$_o$: Original volume.

The original volume is calculated by the theoretical dimensions of the pellet determined by the diameter of the mold cavity and the stop position of the tool.

4.2.3.3 Durability

To evaluate the ability of the pellet to withstand impact and other forces encountered during handling and transportation, the durability index was employed. It was determined by the ASABE standard method [22]. As illustrated in Figure 4-6, 500 grams of pellets were tumbled inside a pellet durability tester (Seedburo Equipment Company, Des Plaines, IL, USA) for 10 minutes. After being tumbled for every two minutes, the pellets were taken out of the tester and sieved through a No. 6 sieve. The weight of the remaining pellets (that did not fall through the sieve) was measured. Then they were put back into the tester to be tumbled for another two minutes.

The pellet durability index was calculated as the following:

$$Durability \quad index = \frac{Weight \quad of \quad pellets \quad after \quad tumbling}{Weight \quad of \quad pellets \quad before \quad tumbling} \tag{5}$$

Figure 4-6 Illustration of durability test

500 g Biomass pellets   Durability tester   Scale

4.3 Results and discussion

4.3.1 Effects of binder content on density

The results are shown in Figure 4-7 and Table 4-2. It can be seen that, at every binder content level, the density of pellets decreased in the first day, but became stable after day 2. Compared with the test group without binder material (with 0% binder content), corn starch serving as the binder material could not significantly prevent the decrease in density. The group with 10% binder content resulted in the highest density among the four groups. The group with 5% binder content had the lowest density.

Table 4-2 Experimental results on density (10^2 kg/m^3)

Binder content	Number of days									
	0	1	2	3	4	5	6	7	8	9
0%	6.0	5.4	5.4	5.4	5.3	5.3	5.2	5.3	5.3	5.3
2%	6.3	5.9	5.8	5.7	5.8	5.9	5.9	5.7	5.7	5.7
5%	6.6	5.3	5.2	5.1	5.0	5.0	5.0	5.0	4.9	5.0
10%	7.1	6.4	6.5	6.4	6.3	6.3	6.2	6.3	6.4	6.4

Figure 4-7 Effects of binder content on pellet
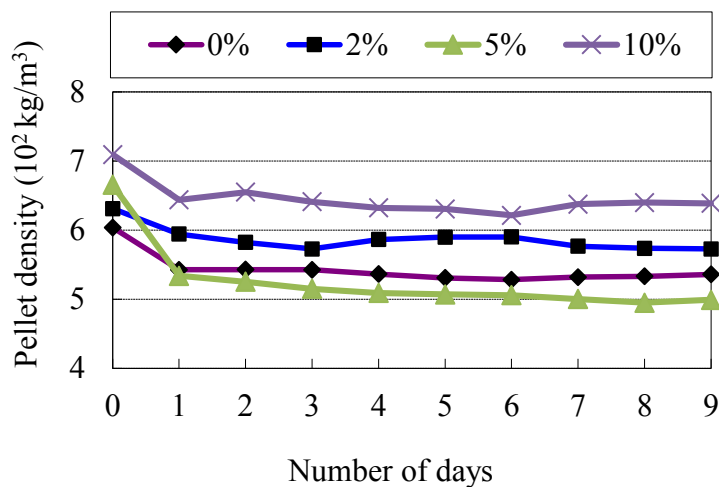
4.3.2 Effects of binder content on stability

A general trend was observed in Figure 4-8 and Table 4-3. Spring-back of the pellets increased with time after they were taken out from the mold. Especially in the first day, the

spring-back was very significant. In the following days, although the spring-back curves had some fluctuations, most of them stayed stable after day 5. The group with 2% binder content had the lowest spring-back among the four test groups, while the group with 5% binder content generated the highest spring-back.

Table 4-3 Experimental results on spring-back (%)

Binder content	Number of days									
	0	1	2	3	4	5	6	7	8	9
0%	32	43	41	39	39	38	37	37	38	37
2%	31	36	37	36	33	31	31	33	32	32
5%	20	48	49	49	50	50	47	47	47	45
10%	31	40	39	37	37	37	35	34	34	34

Figure 4-8 Effects of binder content on spring-back
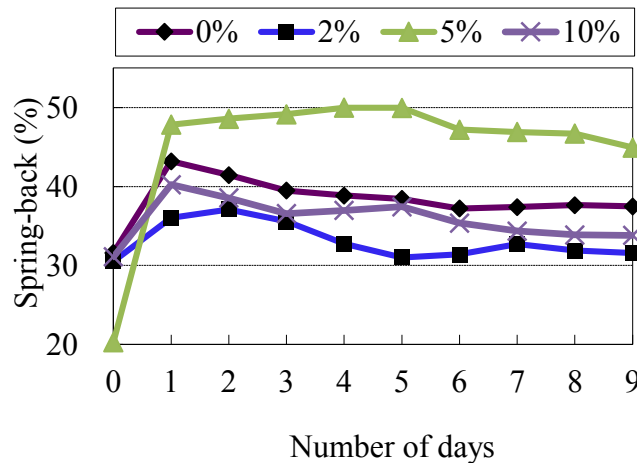
4.3.3 Effects of binder content on durability

As shown in Figure 4-9 and Table 4-4, durability index decreased as the tumbling time increased. The durability index after the first two minutes was around 60%. After tumbling for four minutes, the durability index decreased by another 10%. After that, the decreasing rate became smaller. The groups with 2% and 5% binder contents resulted in higher durability indexes, and their durability indexes after tumbling for 10 minutes reached 44% and 45%, respectively. The group with the highest binder content (10%) resulted in the lowest durability.

Therefore, higher binder content could not generate higher durability. The help of corn starch serving as binder material in improving the durability was not significant in UV-A pelleting.

4.4 Conclusions

Effects of corn starch serving as binder material in UV-A pelleting of switchgrass have been studied in this research. Pellet density, stability, and durability were evaluated. The results showed that no general trends were observed in density, stability, and durability as the binder content increased. The highest binder content (10%) could not help to improve the finished pellet quality in UV-A pelleting.

Figure 4-9 Effects of binder content on durability
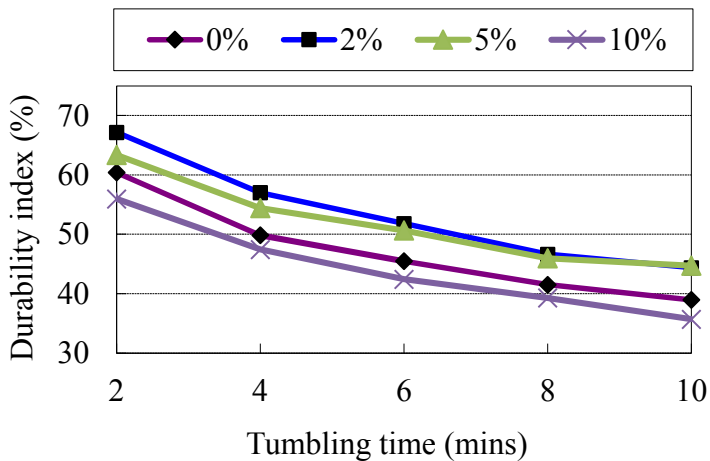
Table 4-4 Experimental results on durability index (%)

Binder content	Tumbling time (min)				
	2	4	6	8	10
0%	60	50	45	42	39
2%	57	52	47	44	44
5%	63	54	51	46	45
10%	56	47	42	39	36

Acknowledgements

References

[1]   Energy Information Administration, 2008, "U.S. Energy Consumption by Energy Source," http://www.eia.doe.gov/cneaf/alternate/page/renew_energy_consump

[2]   Huber, G.W., 2008, "Breaking the Chemical and Engineering Barriers to Lignocellulosic Biofuels: Next Generation Hydrocarbon Biorefineries," Ed. George W. Huber, University of Massachusetts Amherst, National Science Foundation, Chemical, Bioengineering, Environmental, and Transport Systems Division, Washington D.C. 180 p.

[3]   Energy Information Administration, 2009, "Biofuels: Ethanol and Biodiesel Explained," http://tonto.eia.doe.gov/energyexplained/?page=biofuel_home

[4]   Energy Information Administration, 2009, "Annual Energy Outlook 2009: With Projections to 2030," DOE/EIA-0383(2009), http://www.eia.doe.gov/oiaf/aeo/pdf/0383(2009).pdf

[5]   Plant Fuels, 2007, "Cellulosic Ethanol Background and Facts," http://www.thecesite.com/ce_faq.htm

[6]   Brown, L.R., 2008, "Why Ethanol Production Will Drive World Food Prices Even Higher in 2008," http://www.earth-policy.org/index.php?/plan_b_updates/2008/update69

[7]   Energy Information Administration, 2009, "International Energy Outlook 2009," DOE/EIA-0484(2009), http://www.eia.doe.gov/oiaf/ieo/pdf/0484(2009).pdf

[8]   Energy Information Administration, 2009, "Annual Energy Review 2008", Report No.DOE/EIA- 0384(2008), http://www.eia.doe.gov/emeu/aer/pdf/pages/sec10.pdf

[9]   Perlack, R.D., Wright, L.L., Turhollow, A.F., Graham, R.L., Stokes, B.J., and Erbach, D.C., 2005, "Biomass as Feedstocks for a Bioenergy and Byproducts Industry: the Technical Feasibility of a Billion-ton Annual Supply," DOE/ GO-102005-2135, Oak Ridge National Laboratory, http://feedstockreview.ornl.gov/pdf/billion_ton_vision.pdf.

[10]   Orbach, R.L., July 31, 2008, "DOE and USDA Announce More than $10 Million in Bioenergy Plant Feedstock Research,"

http://www.er.doe.gov/news_information/News_Room/07-08%20NewsArchive/2008NewsArchive/Jul31_FeedstockResearch.html

[11] Sutcliffe, N. and Mencin, A., 2009, "Prospecting Biofuels: Plants Matter (Energy and Earth) " , http://jrse.aip.org/01_30_09_prospecting_biofuels_plants_matter_energy_and_earth

[12] Capehart, T., 2008, "Cellulosic Biofuels: Analysis of Policy Issues for Congress," http://wikileaks.org/leak/crs/RL34738.pdf.

[13] Hess, J.R., Wright, C.T., and Kenney, K.L., 2007, "Cellulosic Biomass Feedstocks and Logistics for Ethanol Production, Biofuels, Bioproducts and Biorefining," 1(3), 181–190.

[14] Leaver, R.H., 1984, The Pelleting Process, Sprout-Waldron, Muncy, PA.

[15] Falk, D.,1985, Pelleting cost center, in: Feed Manufacturing Technology, 3rd edition, M.M. McEllhiney (ed.), American Feed Industry Association, Arlington, VA.

[16] Drzymala, Z., 1993, Industrial Briquetting: Fundamentals and Methods, Elsevier, New York.

[17] Young, L.R., and H. B., Pfost, 1962, "The Effect of Colloidal Binders and Other Factors on Pelleting," Feedstuffs, 34, 36-38.

[18] Pfost, H.B., 1964, "The Effect of Lignin Binders, Die Thickness and Temperature on the Pelleting Process," Feedstuffs, 36, 20.

[19] Tabil, L.G., 1996, "Binding and Pelleting Characteristics of Alfalfa," Ph.D. dissertation, University of Saskatchewan.

[20] Kaliyan, N., and Morey, R.V., 2008, "Binding Mechanisms of Corn Stover and Switchgrass in Briquettes and Pellets," http://asae.frymulti.com/azdez.asp?JID=5&AID=25059&CID=prov2008&T=2

[21] Pei, Z.J., Wang, D.H., and Clark, R., 2009, "Ultrasonic Vibration-assisted Pelleting of Cellulosic Biomass: A Preliminary Experiment," Proc. of the 2009 International Manufacturing Science and Engineering Conference (MSEC), October 4-7, West Lafayette, IN, USA, MSEC2009-84205.

[22] ASABE, 2002, "Cubes, Pellets, and Crumbles-definitions and Methods for Determining Density, Durability, and Moisture Content," Standard S269.4, American Society of Agricultural and Biological Engineers, St. Joseph., MI.

Chapter 5 - Effects of Ultrasonic Vibration on Pellet Quality in UV-A Pelleting

Authors'names:

Xiaoxu Song [a], Meng Zhang [a], Z.J. Pei [a], Timothy Deines [a], and C. Treadwell [b]

Authors' affiliation:

[a]Department of Industrial and Manufacturing Systems Engineering, Kansas State University, Manhattan KS 66506 USA

[b]Sonic-Mill, 7500 Bluewater Road NW, Albuquerque, NM 87121, USA

Abstract

Fossil fuels are used almost exclusively to meet the transportation needs in the United States. National energy security, economy, environment sustainability are all driving the U.S. to develop alternative liquid transportation fuels that are domestically produced and environmental friendly. Bioethanol produced from cellulosic biomass can significantly reduce the use of fossil fuels in the transportation section. Unlike corn-based ethanol, cellulosic feedstocks (forest products and residues, agricultural residues, and dedicated energy crops) would not bring a competition for farm land with food and feed production. However, significant hurdles must be overcome for cost-effective manufacturing of cellulosic bioethanol. Cellulosic feedstocks have a low bulk density, causing high costs in transportation and storage. To address this problem, this paper reports an experimental investigation on ultrasonic-vibration-assisted (UV-A) pelleting of wheat straw. Pellet density, durability, and pelleting force were evaluated and discussed. Results show that pellet density and pellet durability were greatly improved with the assistance of ultrasonic vibration.

5.1 Introduction

In the U.S. and many other countries, fuels from petroleum meet almost all transportation needs [EIA, 2008, 2009]. In 2008, 57% of the petroleum used in the U.S. was imported [EIA, 2008]. The economy can be disrupted by "unpredictable swings in supply and world crude oil price", which may also result in "unemployment and affect economic activity" [G. Santos-Leon, 2000]. This is a real threat to national energy security [Huber, G.W., 2008]. Furthermore, the transportation sector is responsible for about 30% of U.S. greenhouse gas (GHG) emissions and is growing faster than any other major economic sector [U.S. Environmental Protection Agency (EPA), 2009].

National energy security, economy, environment sustainability are all driving the U.S. to develop alternative liquid transportation fuels that are domestically produced and environmental friendly. Promoting bioethanol is one of the efforts to reduce the use of fossil fuels in the transportation section. At present, about 97% of the ethanol used in the U.S. is distilled from

corn. The production of ethanol from corn is a mature technology and it is not likely to see "significant reductions in production costs" [DiPardo, 2004]. Moreover, corn-based ethanol causes a competition for the limited agricultural farm land and other resources with food and feed production [EIA, 2009, 2008]. However, if cellulosic feedstocks (forest products and residues, agricultural residues, and dedicated energy crops) are used instead of corn, there will be no such competition. Cellulosic feedstocks are abundant and diverse [Perlack, R.D, 2005]. Thus, the ability to produce ethanol from cellulosic biomass will be a key to making ethanol competitive with gasoline [DiPardo, 2004].

Significant hurdles must be overcome for cost-effective manufacturing of cellulosic biofuels. Cellulosic feedstocks have a low bulk density ranging from 50 to 130 kg/m3 depending on the plant species, size and distribution of particles [Gao, 2000, Hess, J.R., 2007 Sokhansanj et al., 1999; Fasina and Sokhansanj, 1996]. This would result in high transportation and storage costs [Hess, J.R., 2007].

By pelleting cellulosic feedstocks, their bulk density is increased and material handling properties improved [Leaver, R.H., 1984]. Pelleting is generally described as "the agglomeration of small particles into larger particles by the means of a mechanical process, and in some applications, thermal processing [Falk, D., 1985]." Biomass pellets are usually in the form of a hardened biomass cylinder. Current biomass pellets are made by screw extruding or piston ramming finely ground biomass through round, or occasionally square, cross sectional dies [S. Sokhansanj, A. F. Turhollow, 2004]. Pellets share bulk handling properties similar to those of grains, and thus can be handled efficiently using existing grain handling equipment [S. Sokhansanj, A. F. Turhollow, 2004, 2003]. Therefore, pelleting can result in a cost reduction in logistics related to transportation and storage of cellulosic feedstocks.

"By superimposing high frequency (ultrasonic) vibration, the basic mechanical behavior of many processes and materials is seen to be transformed [V.K. Astashev, 2007]." This leads to the development of new machines and processes with advanced characteristics, such as ultrasonic vibration-assisted turing [Moriwaki, T. and Shamoto, E., 1991, Klocke, F. and Rubenach, O., 2000], milling [Chern, G.L., Chang, Y.C., 2006], drilling [Heisel, U., 2008], grinding [Spur, G. Holl, S.E., 1996], lapping [Jiao, F., 2008], and horing [Gao, G.F., 2007]. The above machining processes are all related to engineering materials like ceramics or metals. However, no research has been conducted to investigate effects of ultrasonic vibration on

pelleting of cellulosic biomass using non-rotary ultrasonic unit. This paper will be the first one on this research topic. Knowledge obtained in this work will fill a gap in the literature and broaden the application of ultrasonic technology, and provide guidance in manufacturing of biofuels from cellulosic biomass.

5.2. Experimental set-up and procedures

5.2.1 Experimental conditions

Ultrasonic vibration-assisted (UV-A) pelleting system (Figure 5-1) included the ultrasonic generation system, the pneumatic loading system, and the data acquisition system. UV-A pelleting experiments were performed on a modified Sonic Mill Model AP-1000 (Sonic-Mill, Albuquerque, NM, USA) ultrasonic machine (Figure 5-2). The original machine included a power supply (which converts 60 Hz electrical power into 20,000 Hz electrical power), a converter (which converts high frequency electrical energy into mechanical motion), and a horn (which transfers the ultrasonic vibrations from the converter to the tool). In addition, a pneumatic loading system was included to provide the pelleting force. A 101.6 mm (4 in) double acting pneumatic cylinder was mounted on the top of the converter by connecting to an aluminum protecting tube. The tube was designed to protect the converter. The pneumatic cylinder was driven by compressed air provided by a 1.6 HP, 33 Gal. air compressor (Sears, Roebuck and Co., Hoffman Estates, IL, USA), and its movement was controlled by a three-position, four-way valve. The pressure of the air pumped into the cylinder was controlled by an air regulator. In each pelleting process, the compressed air pressure used was 345 kPa (50 psi), and the pelleting time was 120 seconds. Pelleting time was chosen according to a previous study. The authors have studied effects of pelleting time on density. Results were reported in a separate paper [Nottingham et al, 2010].

The horn (shown in Figure 5-3) was custom made. The horn diameter was 17.78 mm and the length was 127 mm. Before each pelleting, 3 grams of biomass was loaded into an aluminum mold (shown in Figure 5-4). This amount was determined by the diameter and depth of the central cavity in the mold. (Effects of pellet size and shape will be investigated in the future.) The mold consisted of two main parts. The upper part was a hollow cylinder; the inner diameter was 19.05 mm, and the length was 39.37 mm. The lower part was a round plate, serving as a base. The two pieces were assembled together by two screws.

Figure 5-1 Schematic illustration of experimental setup

Pneumatic Loading System

Pressure Gauge

Pressure Regulator

Pneumatic Cylinder

Air Compressor

Converter

Protecting Tube

Air Filter

Pressure

Vibration

Power Supply

Horn

Mold

Biomass

Ultrasonic Generation System

Fixture

Amplifier

PC

Dynamometer

A/D Converter

Data Acquisition System
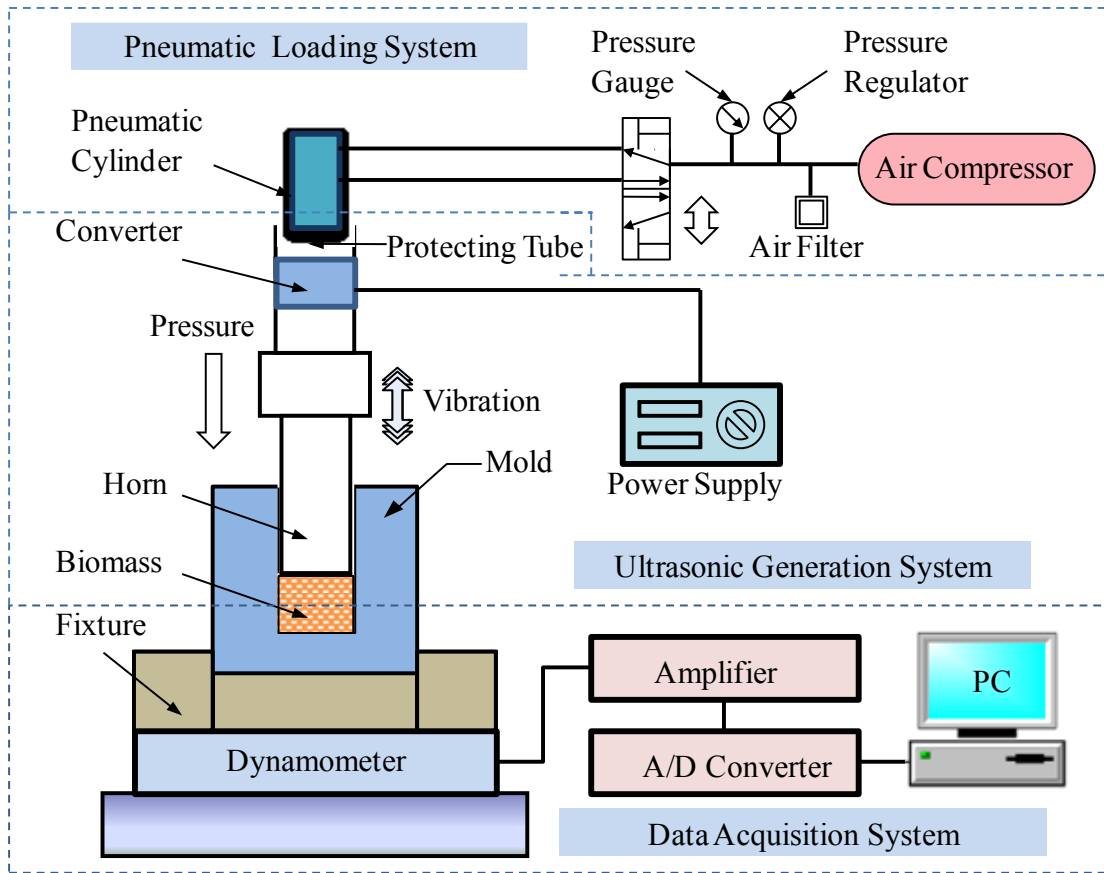
Figure 5-2 Non-rotary ultrasonic machine used for UV-A pelleting
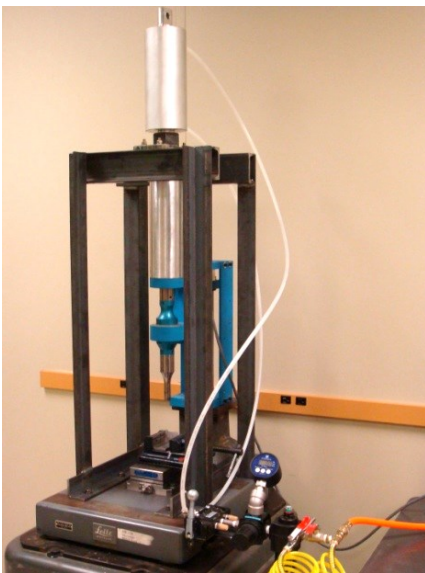
Figure 5-3 The tool used in UV-A pelleting
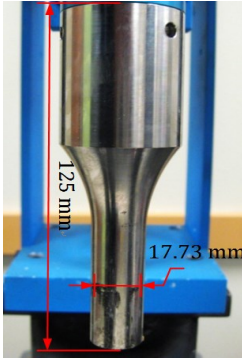
Figure 5-4 Molds used in UV-A pelleting

5.2.2 Biomass preparation

The biomass used in this investigation was wheat straw. It was prepared on a cutting mill (model SM 2000 from Retsch, Inc.) with a sieve size of 1 mm. The moisture content of the biomass after milling was adjusted to 15%. This moisture content was selected based on a previous study on effects of moisture content on pellet quality [Song et al., 2010]. That study showed that, in order to make high quality pellets, the moisture content of wheat straw should not be too high or too low. 15% was a suitable level to make good pellets. 25 grams of milled biomass was heated in an oven at 103℃ for 24 hours to get rid of moisture in the biomass material. By measuring the weight lost of the sample, the original moisture content (MC_o) was calculated as follows:

$$MC_o = \left(\frac{Sample \quad weight \quad lost}{Original \quad sample \quad weight} \right) \times 100\% \tag{1}$$

In this experiment, the original moisture content (6.3%) of 25-gram sample represented the moisture content of the entire milled biomass. Then the weight of distilled water needed to prepare a certain weight of wheat straw having 15% moisture content was calculated as follows:

47

$$a \times (1 - 6.3\%) = (a + x) \times (1 - 15\%) \tag{2}$$

where, a is the weight of the initial wheat straw with $MC_o = 6.3\%$; x is the amount of water needed to prepare the wheat straw with MC = 15%. To prepare the wheat straw for the experiment, distilled water was mixed with the milled wheat straw particles in a zip-lock bag, and the bag was shaken thoroughly.

5.2.3 Measurement procedures

5.2.3.1 Density

From each of the two test groups (pellets processed with ultrasonic vibration, and pellets without ultrasonic vibration), five pellets were randomly chosen for density measurement, and the average was used to represent the group density.

Pellet density is determined by dividing pellet weight by its volume. The weight of the sample pellets was measured on a high accuracy scale (model TAJ 602, Ohaus Corp., Pine Brook, NJ, USA). The volume of the cylinder-shaped pellets was determined by $V = \pi d^2 h/4$. Here d is the diameter of the pellet, and h is the height of the pellet. Diameters and heights of the pellets were measured using a digital caliper (model IP-65, Mitutoyo Corp., Kawasaki, Japan).

Density measurements were carried out by a same person to minimize the variations in measurements. Measurements started from Day 0 (right after pellets were made and taken out of the mold) and were conducted every 24 hours for the next nine days.

5.2.3.2 Durability

Durability test was employed to evaluate the ability of the pellet to withstand impact and abrasion encountered during transportation and storage.

To measure the durability reported in this paper, a modification of the ASABE standard method [ASABE, 2002] was used. Ten pellets from each of the two test groups were tumbled inside a pellet durability tester (Seedburo Equipment Company, Des Plaines, IL, USA) as shown in Figure 5-5. It was manufactured according to the ASABE standard [ASABE, 2002]. The rotation speed was $0.833 \text{ rev} \cdot \text{s}^{-1}$(50 rpm). The duration of each test was 10 minutes. Every two minutes, the pellets were taken out of the tester and sieved through a No. 6 sieve. The weight of the pellets that did not fall through the sieve was measured. These pellets were then put back into

the tester together with the biomass particles fell through the sieve to be tumbled for another two minutes.

The pellet durability index (DI) was calculated as the following:

$$DI = \left(\frac{Weight \quad of \quad pellets \quad after \quad tumbling}{Weight \quad of \quad pellets \quad before \quad tumbling} \right) \times 100\% \tag{3}$$

Figure 5-5 Picture of durability tester

5.2.3.3 Pelleting force

A Kistler piezoelectric dynamometer (Model 9272, Kistler Inc., Swiss) was used to measure the pelleting force. As shown in Figure 5-1, the dynamometer was mounted beneath the mold.

The charge signals from the dynamo eter were converted into voltage signals by a dual mode Kistler charge amplifier (Type 5814B1, Kistler Instrument Corp. Amherst, NY, USA). The electrical signals from the amplifier were converted into numerical signals by an A/D converter. The numerical signals to measure the pelleting force were saved on a computer with LabView software (Version 5.1, National Instruments, Austin, TX, USA). The sampling scanning rate was 20 per second. The pelleting force in this paper was the force along the direction of horn axis.

5.2.3.4 Microscope observation

The microscopic morphology of pellets was observed under an optical microscope (Model BX 51, Olympus Corp., Japan).

5.3 Results and discussion

5.3.1 Effects of ultrasonic vibration on density

Effects of ultrasonic vibration on pellet density are shown in Figure 5-6 and Table 5-1. In the test group with ultrasonic vibration, a slight increase in density was observed in the first three days. Then it stayed stable around 740 kg/m3. In the test group without ultrasonic vibration, pellet density decreased during the first 5 days. After Day 6, all the pellets without ultrasonic vibration fell apart into biomass particles; thus, measurements could not be conducted. Hence density data were not available. It is clearly shown that pellets processed with ultrasonic vibration had much higher density than those processed without ultrasonic vibration.

Figure 5-7 shows a clear contrast between the two pellets right after they were taken out of the mold. The one on the left was made with ultrasonic vibration, and it was in a solid cylindrical shape with few particles falling off. The one on the right was processed without ultrasonic vibration, which was loose with many particles falling off. The average density (during 10 days) of the five pellets with ultrasonic vibration was 740 kg/m3, which was 65% higher than the average density of the pellets without ultrasonic vibration (during the first 6 days). From the microscopic views of the pellets cylindrical surfaces (Figure 5-8 and Figure 5-9), it was obvious that wheat straw particles of the pellet processed with ultrasonic vibration were much denser than those of the pellet processed without ultrasonic vibration.

Figure 5-6 Effects of ultrasonic vibration on pellet density
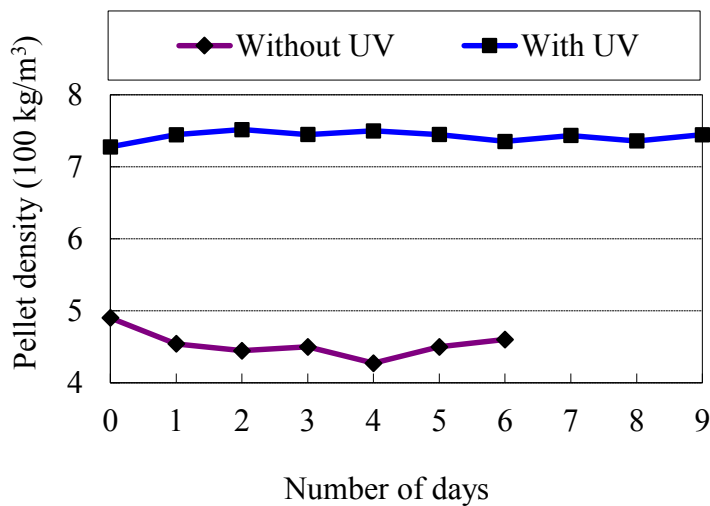
Table 5-1 Experimental results on density (kg/m³)

| | Number of days | | | | | | | | | |
	0	1	2	3	4	5	6	7	8	9
Without ultrasonic vibration	490	450	440	440	420	440	460	N/A	N/A	N/A
With ultrasonic vibration	730	740	750	740	750	740	740	740	740	740

Figure 5-7 Pellets right after being taken out of the mold

With
ultrasonic vibration

Without ultrasonic
vibration
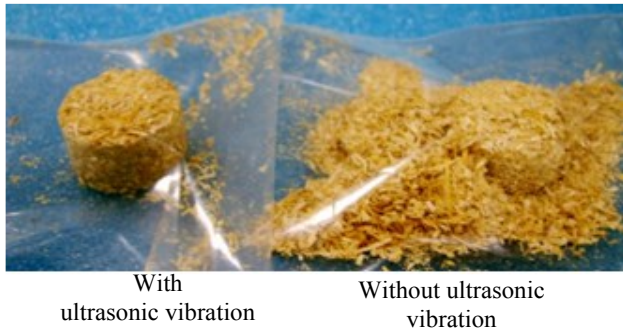
Figure 5-8 Microscopic view (×50) of pellet processed with ultrasonic vibration
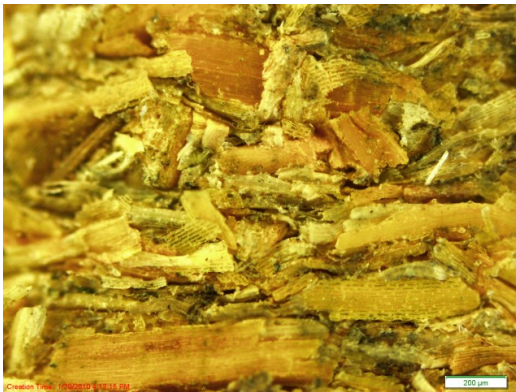
Figure 5-9 Microscopic view (×50) of pellet processed without ultrasonic vibration
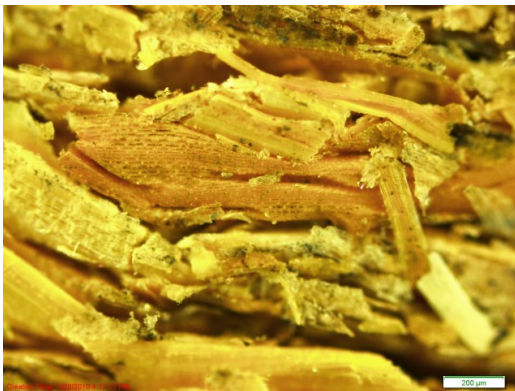
5.3.2 Effects of ultrasonic vibration on durability

For the 10 pellets processed with ultrasonic vibration, after tumbling for 2 minutes, the durability index was 80%. This means that 80% of the pellets were still in a good cylindrical shape and remained on the sieve. The durability index decreased to 68% after another 4 minutes of tumbling. After 10 minutes of tumbling, the durability index of the pellets with ultrasonic vibration stayed at 63% (Figure 5-10, and Table 5-2). Figure 5-11 shows pictures of pellets (processed with ultrasonic vibration) before and after 10 minutes of tumbling. Please note that, in Figure 5-11, there are 10 pellets in Picture (a) but 13 pellets in Picture (b). This is because one pellet broke into three pieces and another pellet broke into two pieces during the durability test, resulting in an increase in the number of pellets.

However, for the ten pellets processed without ultrasonic vibration, none of them could survive after the first 2 minutes of tumbling. They all fell into biomass particles (as shown in Figure 5-12).

Figure 5-10 Effects of ultrasonic vibration (UV) on pellet durability
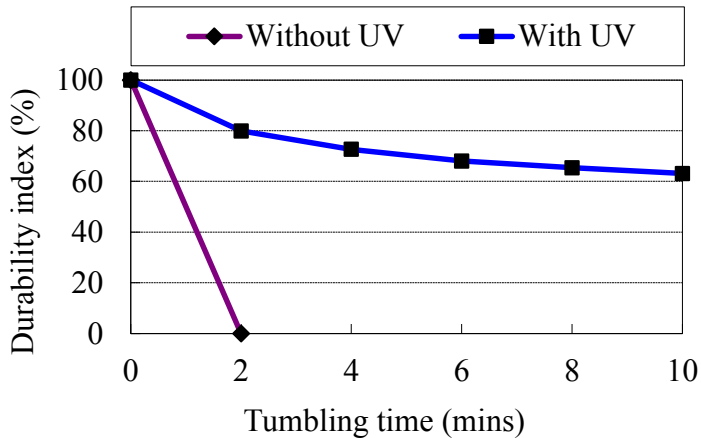
Table 5-2 Experimental result on durability index (%)

	Tumbling time (min)				
	2	4	6	8	10
Without ultrasonic vibration	0	N/A	N/A	N/A	N/A
With ultrasonic vibration	80	73	68	65	63

Figure 5-11 Pellets processed with ultrasonic vibration

(a) before durability test   (b) after durability test
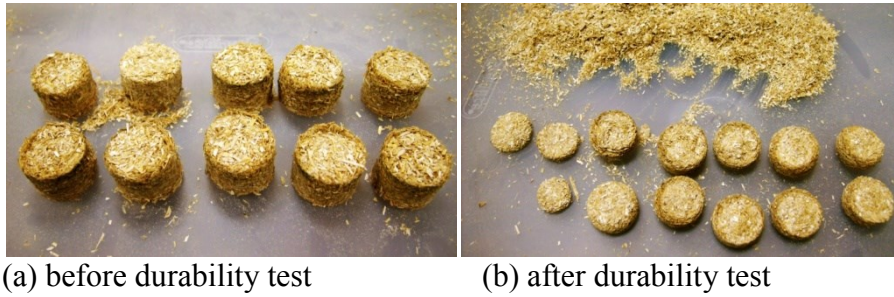
Figure 5-12 Pellets processed without ultrasonic vibration

(a) before durability test   (b) after durability test
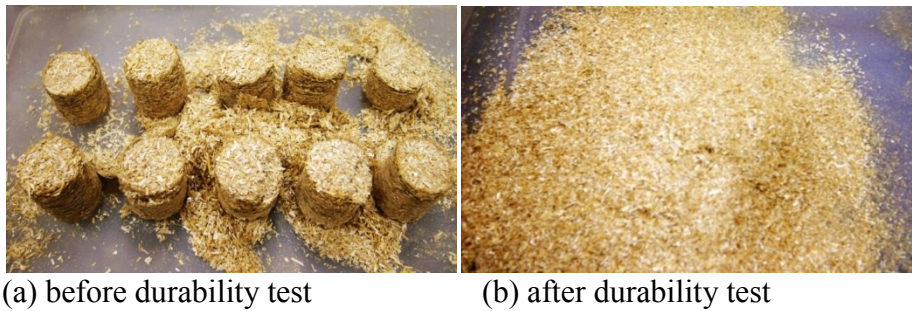
5.3.3 Effects of ultrasonic vibration on pelleting force

Pelleting force is an important parameter when designing machines as well as tools and molds for biomass pelleting. Knowledge of pelleting force will be useful for future study on UV-A pelleting.

Two sets of pelleting force data were collected under experimental conditions with and without ultrasonic vibration, respectively.

During the 120 seconds of pelleting, the maximum pelleting force was 2,835 N and the average pelleting force was 2,760 N with ultrasonic vibration (as shown in Figure 5-13). The maximum pelleting force was 2,834 N and the average pelleting force was 2,758 N without ultrasonic vibration (as shown in Figure 5-14). In Figure 5-13, a certain degree of variations can be observed on the pelleting force curve with ultrasonic vibration. In contrast, the pelleting force curve without ultrasonic vibration was smooth, as shown in Figure 5-14.

Figure 5-13 A curve of pelleting force with ultrasonic vibration
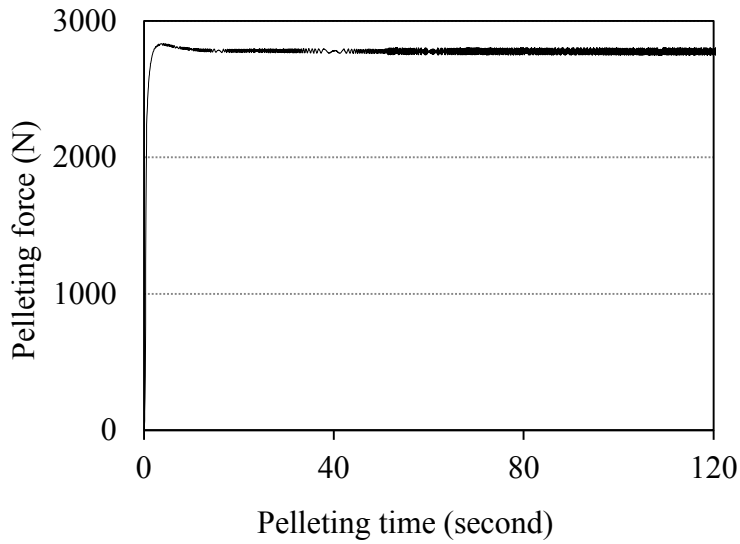
Figure 5-14 A curve of pelleting force without ultrasonic vibration
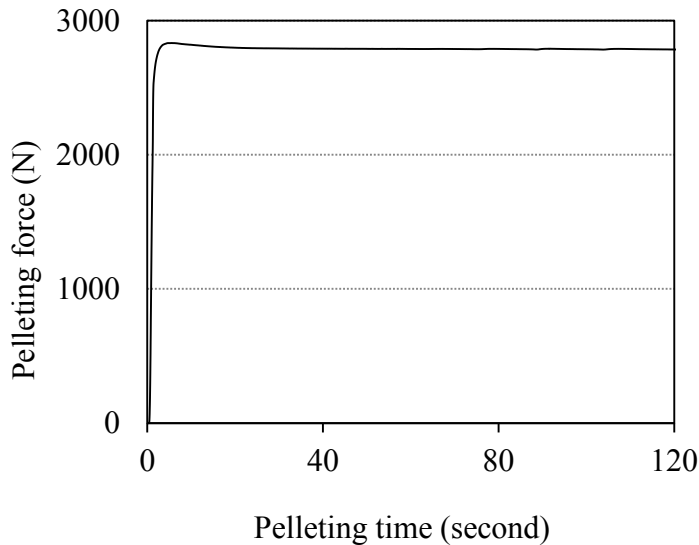
5.4 Conclusions and future work

Effects of ultrasonic vibration on pelleting of wheat straw have been studied in this paper. Pellet density, durability, and pelleting force were evaluated. The average density of the pellets processed with ultrasonic vibration was 65% higher than that of the pellets processed without ultrasonic vibration. Durability was also increased with the assistance of ultrasonic vibration. The pelleting forces under the same compressed air pressure with ultrasonic vibration and

without ultrasonic vibration were very close (2,760 N and 2,758 N). However, due to the high frequency mechanical vibration of the tool in UV-A pelleting, a certain degree of variations can be observed when pelleting with ultrasonic vibration.

This paper presents an experimental investigation on ultrasonic-vibration pelleting of wheat straw. The future work planned includes the following:

(1) Studying the energy consumption of UV-A pelleting in comparison with conventional pelleting methods;

(2) Conducting cost analysis of UV-A pelleting considering both added costs of UV-A pelleting and resulted savings in transportation and storage; and

(3) Understanding the fundamental mechanisms for experimentally observed effects of UV-A pelleting on density and durability.

Acknowledgements

References

Astashev, V.K. and Babisky, V.I. (2007) 'Ultrasonic Processes and Machines Dynamics, Control and Applications', Springer, Berlin.

Chern, G.L. and Chang, Y.C. (2006) 'Using two-dimensional vibration cutting for micro-milling', International Journal of Machine Tools and Manufacture, Vol. 46, No.6, pp. 659–666.

DiPardo, J. (2004) 'Outlook for biomass ethanol production and demand',

http://tonto.eia.doe.gov/ftproot/features/biomass.pdf

Energy Information Administration (2008) 'Oil: crude and petroleum products explained: oil imports and exports', http://tonto.eia.doe.gov/energyexplained/index.cfm?page=oil_imports

Energy Information Administration (2008) 'U.S. energy consumption by energy source', http://www.eia.doe.gov/cneaf/alternate/page/renew_energy_consump

Energy Information Administration (2009) 'Annual energy review 2008, report No.DOE/EIA-0384(2008)', http://www.eia.doe.gov/emeu/aer/pdf/pages/sec10.pdf

Energy Information Administration (2009) 'International energy outlook 2009, DOE/EIA-0484(2009)', http://www.eia.doe.gov/oiaf/ieo/pdf/0484(2009).pdf

Falk, D. (1985) 'Pelleting cost center, Feed Manufacturing Technology, 3rd edition, McEllhiney, M.M. (ed.)', American Feed Industry Association, Arlington, VA.

Fasina, O.O., and Sokhansanj, S. (1996) 'Storage and handling characteristics of alfalfa pellets', Powder Handling and Processing, Vol. 8, No. 4, pp. 361−365.

Gao, G.F., Zhao, B., Kong, Q.H. and Liu, C.S. (2007) 'Surface features in honing zirconia ceramics using fine grains with ultrasonic assistance', Materials Science Forum, Vol. 561–565, No. 2, pp. 933–936.

D. Nottingham, Z.J. Pei, M. Zhang, T. Deines (2010) 'The Effects of Pelleting Time and Ultrasonic Power during Ultrasonic Vibration-assisted Pelleting of Switchgrass', Proceedings of the 2010 Industrial Engineering Research Conference, Cancun, Mexico, June 5-9.

Song, X.X., Zhang, M., Pei, Z.J., and Deines, T. (2010) 'Ultrasonic Vibration-Assisted Pelleting of Cellulosic Biomass: Effects of Moisture Content', ASME 2010 International Manufacturing Science and Engineering Conference, Erie, PA, October 12-15, MSEC2010-34172.

Gao, X.S. (2000) 'How to convert the resource superiority of biomass into energy's in developing countries' Proc. of 1st World Conference on Biomass for Energy and Industry, Sevilla, Spain, June 5-9, pp. 1264-1268.

Heisel, U., Wallaschek, J., Eisseler and R., Potthast, C. (2008) 'Ultrasonic deep hole drilling in electrolytic copper ECu 57', Annals of CIRP, Vol. 57, No. 1, pp. 53–56.

Hess, J.R., Wright, C.T. and Kenney, K.L. (2007) 'Cellulosic biomass feedstocks and logistics for ethanol production', Biofuels, Bioproducts and Biorefining, Vol. 1, No. 3, pp. 181–190.

Huber, G.W. (2008) 'Breaking the chemical and engineering barriers to lignocellulosic biofuels: next generation hydrocarbon biorefineries', http://www.ecs.umass.edu/biofuels/Images/Roadmap2-08.pdf

Jiao, F., Zhao, B., Liu, C. and Zhu, X. (2008) 'Influences of ultrasonic assistance in high speed lapping of nano ZTA engineering ceramic on the surface machining quality', Key Engineering Materials, Vol. 359, pp. 355–359.

Klocke, F. and Rubenach, O. (2000) 'Ultrasonic-assisted diamond turning of glass and steel', Industrial Diamond Review, Vol. 60, No. 586, pp. 229–239.

Leaver, R.H. (1984) The Pelleting Process, Sprout-Waldron, Muncy, PA.

Moriwaki, T. and Shamoto, E. (1991) 'Ultraprecision turning of stainless steel by applying ultrasonic vibration', Annals of CIRP, Vol. 40, No. 1, pp. 559–562.

Novelline, R. (1997) Squire's Fundamentals of Radiology (5th ed.), Harvard University Press, MA.

Perlack, R.D., Wright, L.L., Turhollow, A.F., Graham, R.L., Stokes, B.J., and Erbach, D.C. (2005) 'Biomass as feedstocks for a bioenergy and byproducts industry: the technical feasibility of a billion-ton annual supply', http://feedstockreview.ornl.gov/pdf/billion_ton_vision.pdf.

Santos-Leon, G. and Zukor, S. (2000) 'Status of bioethanol in the United States and greenhouse gas benefits of worldwide development', Proc. of 1st World Conference on Biomass for Energy and Industry, Sevilla, Spain, 5-9 June 2000, pp. 1238-1243.

Sokhansanj, S. and Turhollow A. F. (2005) 'Biomass supply system and logistics', http://feedstockreview.ornl.gov/pdf/sokhansanj/biomass_supply_systems_logistics.pdf

Sokhansanj, S. and Turhollow, A. F. (2004) 'Biomass densification — cubing operations and costs for corn stover', Applied Engineering in Agriculture, Vol. 20, No. 4, pp. 495-499.

Sokhansanj, S., Tabil, Jr. L., and Yang,W. (1999) 'Characteristics of plant tissue to form pellets: powder handling and processing', The International Journal of Storing, Handling, and Processing Powder, Vol. 11, No. 12, pp. 149−159.

Spur, G. and Holl, S.E. (1996) 'Ultrasonic assisted grinding of ceramics', Journal of Materials Processing Technology, Vol. 62, No. 4, pp. 287–293.

Stouffer, M.R. (2001) 'Carbon: optimized activated carbons for MTBE removal in POU/POE systems—coconut vs. coal', Water Conditioning & Purification, January, pp. 34-36.

Suslick, K.S. (1988) 'Ultrasound, Its Chemical, Physical, and Biological Effects', VCH Publishers, Inc., New York.

U.S. Environmental Protection Agency (EPA) (2009) 'Inventory of U.S. greenhouse gas emissions and sinks: 1990-2007', http://www.epa.gov/climatechange/emissions/usinventoryreport.html

Yeh, S., Lutsey, N.P. and Parker, N.C. (2009) 'Assessment of technologies to meet a low carbon fuel standard', Environmental Science & Technology, Vol. 43, No. 18, pp. 6907-6914.

ASABE Standard S269.4 (2002) 'Cubes, Pellets, and Crumbles-Definitions and Methods for Determining Density, Durability, and Moisture Content', American Society of Agricultural and Biological Engineers, St. Joseph, US.

Chapter 6 - Effects of Process Variables on Energy Consumption in UV-A Pelleting

Authors' names:

Xiaoxu Song, Meng Zhang, Timothy Deines, Pengfei Zhang, and Z.J. Pei

Authors' affiliation:

Department of Industrial and Manufacturing Systems Engineering, Kansas State University, Manhattan KS 66506 USA

Abstract

Cellulosic biofuels are an alternative to petroleum-based transportation fuels. Ultrasonic vibration-assisted (UV-A) pelleting can increase density of cellulosic feedstocks, reduce transportation and storage costs, and increase sugar yield. However, energy consumption in UV-A pelleting has not been fully investigated. This paper presents an experimental study on energy consumption in UV-A pelleting of wheat straw. Effects of pelleting input variables (sieve size used in size reduction, pelleting pressure, ultrasonic power, and pellet weight) and size reduction machine type (knife milling versus hammer milling) are investigated. Results show that energy consumption in UV-A pelleting increased as sieve size, ultrasonic power, and pellet weight increased, and as pelleting pressure decreased. Energy consumption in UV-A pelleting of wheat straw particles processed by knife milling was higher than that in UV-A pelleting of those processed by hammer milling.

6.1 Introduction

Liquid transportation fuels currently used in the U.S. are mainly petroleum-based [1-3]. In 2011, the U.S. transportation sector consumed about 18.95 million barrels of petroleum per day and half of it was imported [4-5]. This creates the issue for the nation's energy security. Another issue of using petroleum-based transportation fuels is greenhouse gas (GHG) emissions. One-third of the total carbon dioxide emissions in the U.S. are from the use of petroleum-based transportation fuels [6-8].

Biofuels - particularly cellulosic biofuels – can help addressing these issues. Cellulosic biofuels are produced from cellulosic biomass, including wood, agricultural residues, and herbaceous energy crops. Unlike other type of feedstocks (e.g. corn, sugar cane, and soybean) for biofuels, cellulosic biomass does not compete with food production for the limited agriculture land [9-10].

Biofuels have the potential to reduce GHG emissions by as much as 86% compared to gasoline [11]. Because biofuels are made from renewable, plant-based feedstocks, the carbon dioxide released during fuel combustion is 'recycled' by the plant as it grows [12].

However, cellulosic biomass materials have low density, resulting in high costs in their transportation and storage. Densification of cellulosic biomass into pellets [13] can increase the density from 40 - 250 kg/m^3 for raw cellulosic materials to as high as 1200 kg/m^3 [14].

Traditional pelleting methods (for example, extruding, briquetting, and rolling) [15] generally involve high-temperature steam, high pressure, and binder materials. Ultrasonic vibration-assisted (UV-A) pelleting is a new pelleting method [16]. UV-A pelleting, without using binder materials or high-temperature steam, can produce biomass pellets whose density is comparable to that processed by traditional pelleting methods [17]. Moreover, biomass (switchgrass) processed with UV-A pelleting has more than 20% higher sugar yield (proportional to biofuel yield) than biomass pellets processed without ultrasonic vibration or non-pelleted biomass [18].

The literature on UV-A pelleting includes experimental investigations on pellet quality, sugar yield, pelleting temperature, charring, and power consumption. Table 6-1 summarized the input variables and output variables in UV-A pelleting that have already been studied. Clearly, there is a lack of comprehensive study on energy consumption in UV-A pelleting. Energy consumption in UV-A pelleting not only contributes to the manufacturing costs of biofuels, but also affects the energy balance of biofuel manufacturing. Effects of biomass type, sieve size, pelleting pressure, and ultrasonic power on energy consumption in UV-A pelleting have been investigated by Zhang et al., [27]. However, in their study, pelleting time was not kept same when other input variables changed. In other words, effects of pelleting time were confounded with effects of biomass type, sieve size, pelleting pressure, and ultrasonic power. Therefore, it is not clear how each of these input variables affects energy consumption in UV-A pelleting. The objective of this paper is to fill this research gap on energy consumption in UV-A pelleting. Effects of pelleting input variables (sieve size used in size reduction, pelleting pressure, ultrasonic power, and pellet weight) and size reduction machine type (knife milling versus hammer milling) on energy consumption in UV-A pelleting were studied while keeping pelleting time the same.

Table 6-1 Input variables and output variables in UV-A pelleting that have been studied

Output variable	Input variable							Reference
	Biomass type	Sieve size	Moisture content	Pelleting pressure	Pelleting time	Ultrasonic Power	Pellet weight	
Pellet Quality	√	√	√	√	√	√	√	[17-24]
Sugar yield		√		√		√	√	[20, 22-23]
Pelleting temperature	√		√		√	√	√	[20, 25]
Charring	√		√					[26]
Power consumption	√	√		√		√		[27]

6.2 Experimental conditions and procedures

6.2.1 Preparation of biomass materials

The cellulosic biomass used in this investigation was wheat straw. Wheat straw was harvested by Deines Farm in Northwest Kansas. The wheat straw had been run through a John Deere 9600 combine. The combine removed the grains from the straw and chaff. Wheat straw and chaff exited through the back of the combine. The average length of the wheat straw was 250 mm. After being collected, wheat straw was stored indoors until this study.

Wheat straw was processed by two types of size reduction machines: a knife mill (Model SM 2000 from Retsch, Inc., Haan, Germany) (shown in Figure 6-1) and a hammer mill (Model 5 from Meadows Mill Inc., N. Wickeabord, NC, USA) (shown in Figure 6-2). The knife mill used a 240-volt, 3 horsepower electric motor with a fixed rotation speed (1720 rpm). Three cutting blades (95 mm long and 35 mm wide) were mounted on the rotor. Four shear bars were mounted on the inside wall of the milling chamber. There was a 3 mm gap between a cutting blade and a shear bar. Biomass was cut between the cutting blades and the shear bars. The sieves used in the knife mill were of 0.45, 1, 2, 4, and 8 mm in the size of the openings. As illustrated in Figure 6-1, only one sieve was installed at a time.

The hammer mill used a 240-volt, 5 horsepower electric motor with fixed a rotation speed (3600 rpm). There were 24 hammers. The size of these hammers was $101.6 \times 25.4 \times 4.8$

mm. The sieves used in the hammer mill were 1, 2, 4, and 8 mm in the size of the openings. As illustrated in Figure 6-2, only one sieve was installed at a time.

Figure 6-1 Knife mill
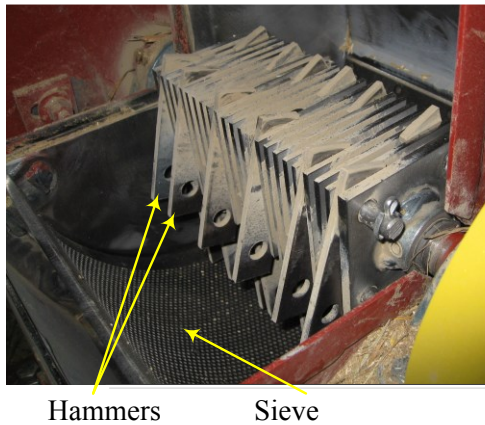
Shear bars   Cutting blades   Sieve

Figure 6-2 Hammer mill

Hammers   Sieve

Moisture content (MC) of biomass represents the amount of moisture (water) contained in a certain amount of biomass. The MC of wheat straw before milling was 1.2% measured by following the NREL LAP [28]. A sample of wheat straw (25 g) was heated in an oven (Blue M Electric Co., Blue island, IL, USA) at 105°C for 24 hours to get rid of moisture in wheat straw. By measuring the weight loss of the sample, the MC was calculated as follows:

$$MC = \left(\frac{Sample \quad weight \quad loss}{Original \quad sample \quad weight} \right) \times 100\%$$

Figure 6-3 Illustration of experimental set-up for UV-A pelleting
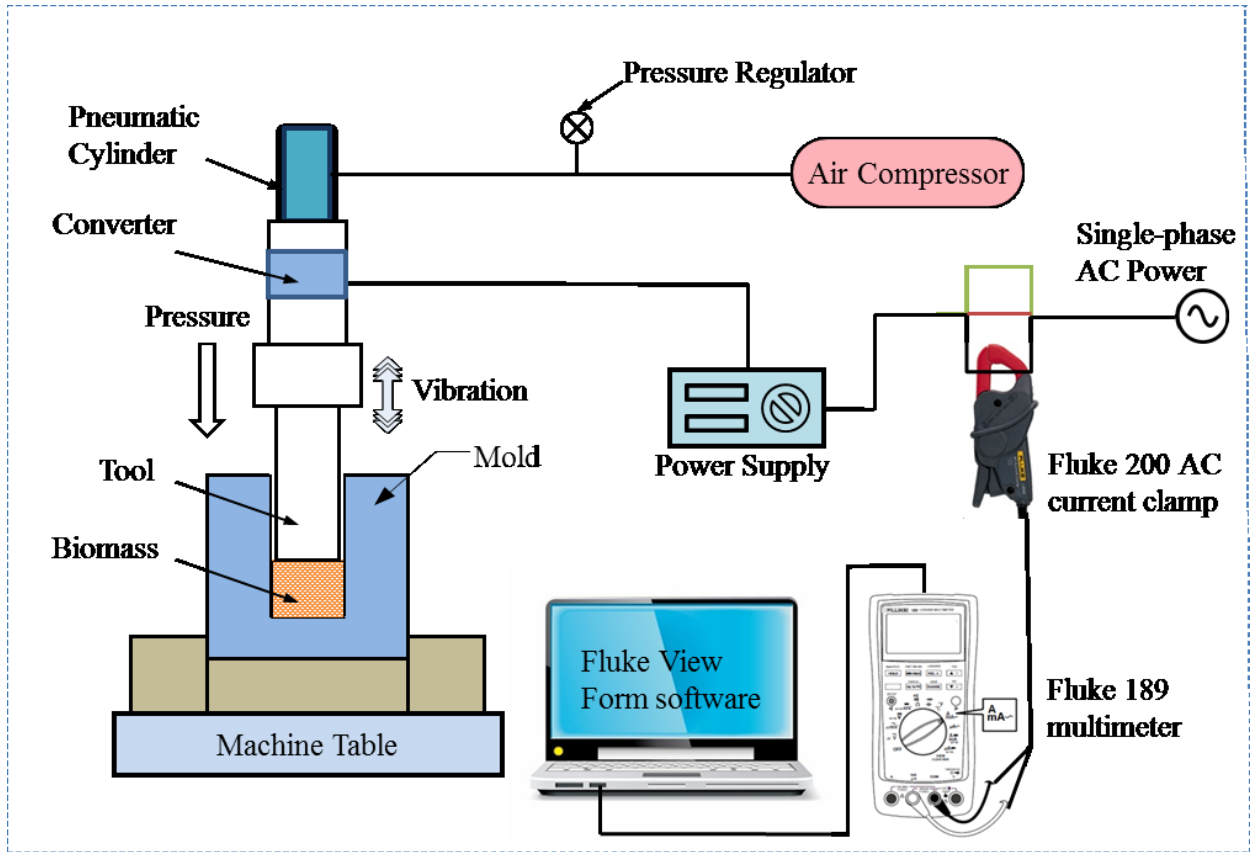
6.2.2 UV-A pelleting

Figure 6-3 is a schematic illustration of the experimental set-up for UV-A pelleting. UV-A pelleting experiments were performed on a modified ultrasonic machine Sonic Mill Model AP-1000 (Sonic-Mill, Albuquerque, NM, USA). The machine included a power supply (which converts 60 Hz electrical power into 20,000 Hz electrical power), a converter (which converts high frequency electrical energy into mechanical motion), and a tool. The tip of the tool was a solid cylinder with a flat end (17.4 mm in diameter).

Before each pelleting test, the weight of wheat straw particles loaded into an aluminum mold was measured by a scale. This weight was referred to as pellet weight. The mold was consisted of three parts. The upper two parts formed a cylindrical cavity (18.6 mm in diameter) and the bottom part was a square plate, serving as a base. They were assembled together with pins.

The pneumatic cylinder was driven by compressed air provided by a 1.6 HP, 33 Gal. air compressor (Sears, Roebuck and Co., Hoffman Estates, IL, USA). The air pressure in the pneumatic cylinder was controlled by a pressure regulator. A higher air pressure in the cylinder meant a higher pressure applied on the biomass in the mold by the tool.

In each pelleting test, the pelleting time was 120 s. After 120 s, the tool was retracted and the mold was disassembled to unload the pellet. Table 6-2 shows experimental parameters and their values. Three replicates were obtained under each experimental condition. A finished UV-A pellet is shown in Figure 6-4.

Table 6-2 Input variables and their values

Input variable	Value
Sieve size used in size reduction (mm)	0.45, 1, 2, 4, 8
Wheat straw moisture content (%)	1.2
Pelleting pressure (psi)	30, 40, 50
Pelleting time (s)	120
Ultrasonic power (%)	20, 30, 40
Pellet weight (g)	0.5,1, 1.5, 2, 2.5, 3

Figure 6-4 Picture of a pellet produced by UV-A pelleting

6.2.3 Measurement procedure for energy consumption

Energy consumption in this paper was referred to electrical energy consumed by the power supply. A Fluke 189 multimeter and a Fluke 200 AC current clamp were used to measure the electric current, as shown in Figure 6-3. The power line to the power supply has three wires: black, red, and green wires. The current clamp was clamped on the black wire to measure the current. The data was collected using Fluke View Forms software. The sampling rate was 2 per

second. After the tool touched the biomass in the mold, the power supply was switched on and Fluke View Forms software started collecting data. After 120 s, Fluke View Forms software stopped collecting data and power supply was switched off.

The software recorded the average current (I_{AVE}) in each experiment run. The voltage (V) was 120 V. The total energy consumed during 120 s can be calculated using the following equation [29]:

$$E = \frac{V \times I_{AVE} \times 120}{3600} (Wh)$$

6.3 Experimental results

Every data point and its error bars (in Figures 6.5 - 6.9) represent the calculated energy consumption average (mean) of the three replicates and 95% confidence intervals, respectively, under each test condition. If the 95% confidence intervals for two test conditions represented by the error bars do not overlap, the difference in the two means was considered significantly different at the significance level of 0.05 [30-32].

6.3.1 Effects of sieve size

Effects of sieve size (used in knife milling) on energy consumption in UV-A pelleting are shown in Figure 6-5. Energy consumption in UV-A pelleting increased as sieve size increased. This was true for all three levels of pelleting pressure (30, 40, and 50 psi). There was no significant difference in energy consumption when sieve size was 0.45, 1, and 2 mm at the significance level of 0.05. The difference in energy consumption was significant at the significance level of 0.05 when sieve size was 2, 4, and 8 mm.

Effects of sieve size (used in knife milling) on pellet quality (density, durability, and spring-back) in UV-A pelleting have been studied previously. Pellet durability measures the ability of pellets to withstand impact and other forces during transportation and storage. Spring-back measures the expansion of a pellet. Zhang et al. [22] studied pellet quality in UV-A pelleting of wheat straw particles processed by knife milling using the 2^4 full factorial design with two levels of sieve size (1 and 2 mm). The wheat straw particles milled with the smaller sieve size produced higher density and durability, and smaller spring-back. Zhang et al. [24] also studied effects of sieve size (with four levels: 0.25, 1, 2, 1.5 and 8 mm) in knife milling on pellet quality in UV-A pelleting of wheat straw. Results showed that wheat straw particles milled with

the smallest sieve size (0.25 mm) had higher density and smaller spring-back than those milled with larger sieve sizes.

Figure 6-5 Effects of sieve size used in size reduction on energy consumption in UV-A pelleting
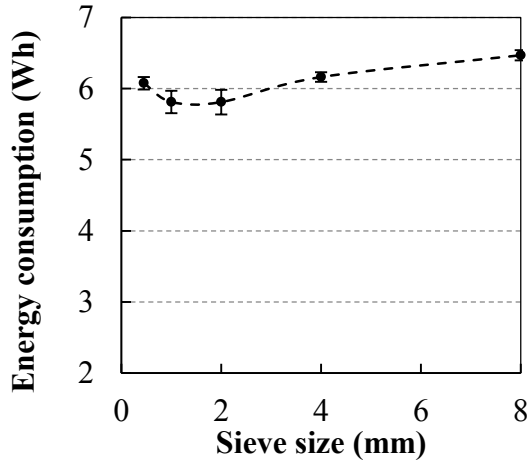
(a) Pelleting pressure = 30 psi
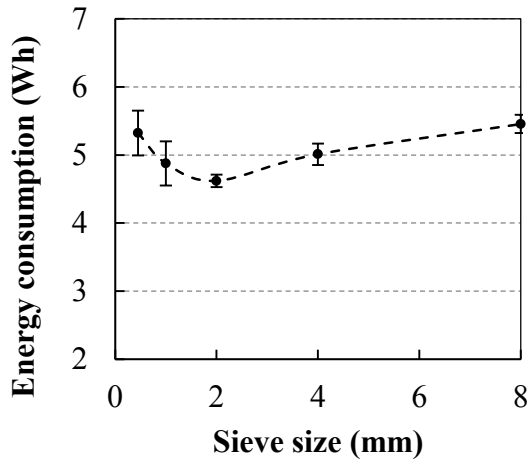
(b) Pelleting pressure = 40 psi
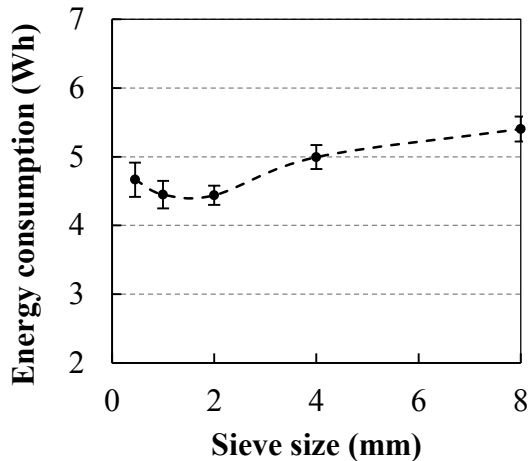
(c) Pelleting pressure = 50 psi
Ultrasonic power = 40%, Pellet weight = 2 g, Machine type = knife milling

Theerarattananoon et al. [33] studied pellet quality in ring-die pelleting of wheat straw, corn stover, big bluestem, and sorghum particles processed by hammer milling with two levels of sieve size (3.2 and 6.5 mm). Results showed that the sieve size of hammer mill did not have significant effects on pellet density and durability. Tabil and Sokhansanj [34] also studied effects of sieve size in hammer milling on durability in ring-die pelleting of alfalfa. They found that the increase of sieve size from 3.2 to 6.5 mm resulted in no significant change of pellet durability.

Effects of sieve size on energy consumption in size reduction have also been studied. Deines et al. [35-36] reported that energy consumption in knife milling increased as sieve size decreased from 8 to 0.25 mm for four types of biomass materials (sorghum stalks, switchgrass, wheat straw, and kochia). Effects of sieve size (used in size reduction) on sugar yields of cellulosic biomass were also reported. Zhang et al. [22] found that wheat straw particles milled by knife milling with 2 mm sieve produced 50% higher sugar yield than those milled with 1 mm sieve. Theerarattananoon et al. [33] reported that the use of a larger sieve size (6.5 mm) in hammer milling resulted in higher sugar yield than using smaller sieve size (3.2 mm) for wheat straw, corn stover, bluestem, and sorghum.

6.3.2 Effects of pelleting pressure

As shown in Figure 6-6, energy consumption decreased as pelleting pressure increased. This was true for all five levels of sieve size (0.45, 1, 2, 4, and 8 mm), although only the data for

68

sieve size of 2 mm are shown in the figure. The difference in energy consumption when pelleting pressure was 30 and 40 psi was significant at the significance level of 0.05. There was no significant difference in energy consumption when pelleting pressure was 40 and 50 psi.

Figure 6-6 Effects of pelleting pressure on energy consumption
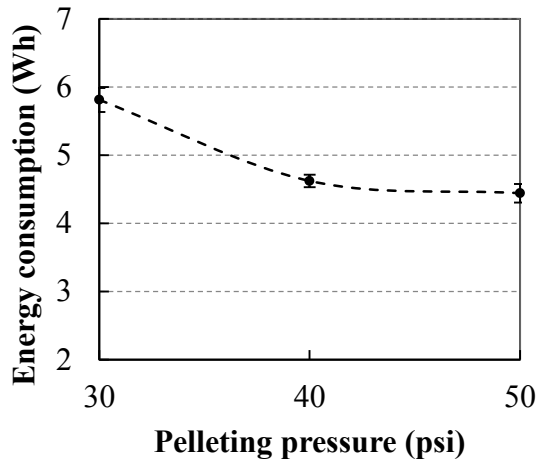
Sieve size = 2 mm, Ultrasonic power = 40%,
Pellet weight = 2 g, Machine type = knife milling

Effects of pelleting pressure on pellet quality (density, durability, and spring-back) in UV-A pelleting have been previously studied. Zhang et al. [22] reported that wheat straw pellet density increased from 625 to 663 kg/m^3 as pelleting pressure increased from 30 to 40 psi. Zhang et al. [23] reported that there was a dramatic increase in sorghum stalk pellet density as pelleting pressure increased from 20 to 40 psi. However, pellet density was approximately the same when pelleting pressure was 40 and 50 psi. As pelleting pressure increased from 20 to 40 psi, pellet durability increased. However, pellet durability had a dramatic drop when pelleting pressure increased to 50 psi. Pellet spring-back did not change much as pelleting pressure increased from 20 to 50 psi.

Zhang et al. [23] studied effects of pelleting pressure in UV-A pelleting on sugar yield in hydrolysis. As pelleting pressure increased from 20 to 50 psi, sugar yield decreased first and then increased. The lowest sugar yield was obtained when pelleting pressure was 40 psi. There were not significant differences between sugar yields when pelleting pressure was 20 and 50 psi.

6.3.3 Effects of ultrasonic power

Ultrasonic power (%) determines the amplitude of ultrasonic vibration. A higher ultrasonic power causes a larger amplitude. Effects of ultrasonic power on energy consumption in UV-A pelleting of wheat straw milled by knife milling are shown in Figure 6-7. The difference in energy consumption was significant at the significance level of 0.05. Energy consumption increased as ultrasonic power increased.

Zhang et al. [23] studied effects of ultrasonic power in UV-A pelleting on sorghum stalk pellet quality. The results showed that, as ultrasonic power increased from 30% to 50%, pellet density and durability increased but spring back decreased. Zhang et al. [22] reported that, as ultrasonic power increased from 30% to 40%, wheat straw pellet density and durability increased but spring back decreased.

Zhang et al. [23] studied effects of ultrasonic power in UV-A pelleting on sugar yield. Sugar yield increased as the ultrasonic power increased from 30% to 55%. Similar results were also reported by Zhang et al. [22].

Figure 6-7 Effects of ultrasonic power on energy consumption
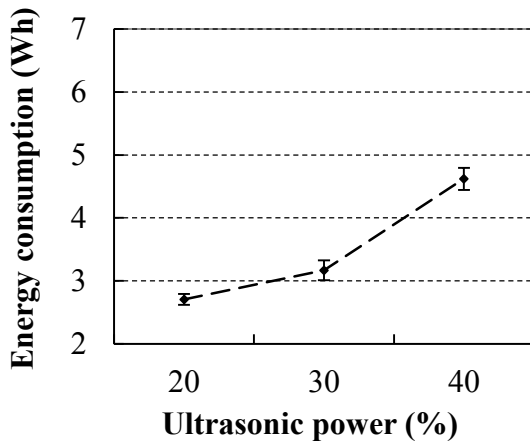
Sieve size = 2 mm, Pelleting pressure = 40 psi,

Pellet weight = 2 g, Machine type = knife milling

6.3.4 Effects of pellet weight

Effects of pellet weight on energy consumption in UV-A pelleting of wheat straw milled by knife mill were studied. As shown in Figure 6-8, energy consumption increased linearly as the increasing of pellet weight from 0.5 to 3 g.

Tang et al. [20] studied effects of pellet weight on pellet density, durability, pelleting temperature in UV-A pelleting, and sugar yield in hydrolysis. As pellet weight varied from 0.5, 1, 1.5, 2, 2.5, to 3 g, pellet density, durability, pelleting temperature, and sugar yield first increased and then decreased. The highest density, durability, pelleting temperature, and sugar yield were all obtained with pellet weight of 1.5 g.

Figure 6-8 Effects of pellet weight on energy consumption
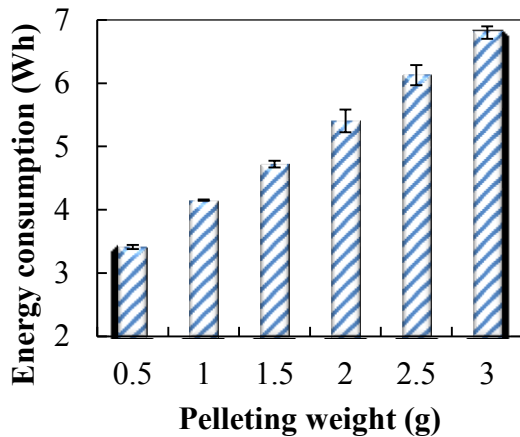
Sieve size = 8 mm, Pelleting pressure = 50 psi,
Ultrasonic power = 40%, Machine type = knife milling

6.3.5 Effects of size reduction machine type

Figure 6-9 shows effects of size reduction machine type (knife milling versus hammer milling) on energy consumption in UV-A pelleting. Energy consumption in UV-A pelleting of wheat straw particles milled by knife milling was roughly 12% higher than that in UV-A pelleting of wheat straw particles milled by hammer milling. This was true for all levels of sieve size. This result indicates that machine type used in the size reduction process has a significant effect on energy consumption in UV-A pelleting.

Figure 6-9 Effects of size reduction machine type on energy consumption in UV-A pelleting
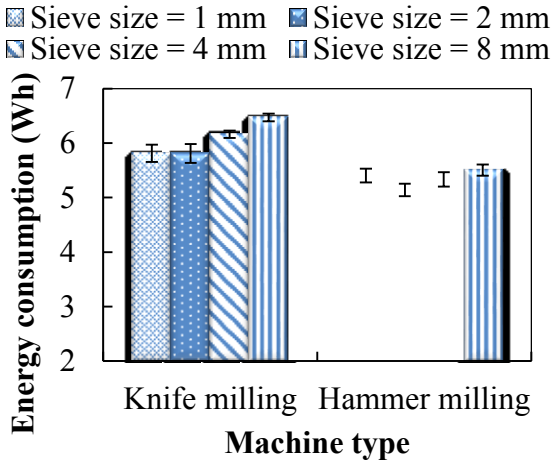
Pelleting pressure = 30 psi, Ultrasonic power = 40%, Pellet weight = 2 g,

Effects of size reduction machine type on sugar yield in hydrolysis (not processed in UV-A pelleting) have been investigated [37]. There were no significant differences in sugar yield between switchgrass particles produced by knife milling versus hammer milling [37].

6.4 Conclusions and future research

This paper studied effects of input parameters (sieve size used in size reduction, pelleting pressure, ultrasonic power, and pellet weight) in UV-A pelleting and size reduction machine type on energy consumption in UV-A pelleting of wheat straw. Major conclusions are as follows.

1. Energy consumption in UV-A pelleting increased as sieve size, ultrasonic power, and pellet weight increased, and as pelleting pressure decreased.

2. Machine type used in the size reduction process had a significant effect on energy consumption in UV-A pelleting of wheat straw. Energy consumption in UV-A pelleting of wheat straw particles milled by knife milling was roughly 12% higher than that in UV-A pelleting of wheat straw particles milled by hammer milling.

The UV-A pelleting machine used in this study is a lab scale machine. Only one pellet can be made each time. In the future, it is important to design UV-A pelleting machines that can make multiple pellets simultaneously for further reduction of energy consumption in UV-A pelleting.

In this study, effects of input variables were studied one at a time (while keeping other variables unchanged). It is important to know the interaction effects of input variables. The

response surface method will be used in the future to study the interaction effects of input variables and to find the optimal experimental conditions to minimize the energy consumption in UV-A pelleting.

In this study, energy consumption E was only calculated by voltage, current, and time. It is not clear how much percentage of E is converted to the mechanical energy and how much is converted to the heat. A model will be developed to simulate the UV-A pelleting process from the energy perspective. The energy conversion (from electric energy to mechanical energy and heat) will be studied.

Acknowledgements

References

[1]   U.S. Energy Information Administration, 2011b, Monthly Energy Review, http://www.eia.gov/totalenergy/data/monthly/pdf/mer.pdf

[2]   U.S. Energy Information Administration, 2011d, Transportation Sector Energy Consumption Estimates 1949-2010, http://205.254.135.24/totalenergy/data/annual/showtext.cfm?t=Ptb0201e

[3]   U.S. Energy Information Administration, 2011e, U.S. Energy Consumption by Sector of 1949-2010, http://www.eia.gov/totalenergy/data/annual/txt/ptb0201a.html

[4]   U.S. Energy Information Administration, 2011a, How dependent are we on foreign oil? http://www.eia.gov/energy_in_brief/foreign_oil_dependence.cfm

[5]   U.S. Energy Information Administration, 2011c, Short-Term Energy Outlook, http://205.254.135.24/steo/steo_full.pdf

[6]   Conti, J., Chase, N., and Maples, J., 2010, "US Greenhouse Gas Emissions in the Transportation Sector," Climate and Transportation Solutions, 5000 (6000), pp. 24.

[7]   Environmental Protection Agency, 2011, Inventory of U.S. Greenhouse Gas Emissions and Sinks: 1990-2009, http://www.epa.gov/climatechange/emissions/downloads11/US-GHG-Inventory-2011-Executive-Summary.pdf

[8]   National Academy of Sciences, National Academy of Engineering, and National Research Council of The National Academies, 2009, Liquid Transportation Fuels from Coal and Biomass, The National Academy, Washington, DC.

[9]   Gray, K.A., Zhao, L., and Emptage, M., 2006, "Bioethanol," Current Opinion in Chemical Biology, 10, pp. 141-146.

[10]   Brown, L.R., 2008, "Why Ethanol Production Will Drive World Food Prices Even Higher in 2008," http://www.earth-policy.org/index.php?/plan_b_updates/2008/update69

[11]   U.S. Department of Energy, 2008, "Environmental Benefits of Biofuels,"

[12]   RFA, 2011, "Ethanol Facts: Environment," Renewable Fuels Association, http://www.ethanolrfa.org/pages/ethanol-facts-environment

[13]   Leaver, R.H., 1984, The Pelleting Process, Sprout-Waldron, Muncy, PA, USA.

[14]   Mani, S., Sokhansanj, S., Bi, X., and Turhollow, A., 2006, "Economics of Producing Fuel Pellets from Biomass," Applied Engineering in Agriculture, 22(3), pp. 421-426.

[15]   Sokhansanj, S., Mani, S. and Zaini, P., 2005, "Binderless Pelletization of Biomass," ASABE Paper No. 056061, American Society of Agricultural and Biological Engineers.

[16]   Pei, Z.J., Wang, D.H., and Clark, R., 2009, "Ultrasonic vibration assisted pelleting of cellulosic biomass: a preliminary experiment," Proceedings of the ASME 2009 International Manufacturing Science & Engineering Conference (MSEC), MSEC 2009, October 4-7, 2009, West Lafayette, IN, USA.

[17]   Song, X.X., Zhang, M., Pei, Z.J., and Deines, T., 2010b, "Ultrasonic Vibration-Assisted Pelleting of Cellulosic Biomass: Effects of Moisture Content," Proceedings of the 2010 ASME International Manufacturing Science and Engineering Conference (MSEC), Erie, PA, October 12-15, 2010, MSEC 2010-34172.

[18]   Zhang, P.F., Pei, Z.J., Wang, D.H., Wu, X.R., Cong, W.L., Zhang, M., and Deines, T., 2011a, "Ultrasonic Vibration-assisted Pelleting of Cellulosic Biomass for Biofuel Manufacturing," Journal of Manufacturing Science and Engineering, 133 (1), pp. 011012-1 – 011012-7.

[19]   Song, X.X., Zhang, M., Deines, T.W., Zhang, P.F., Zhang, Q., and Pei, Z.J., 2010a, "Ultrasonic-vibration-assisted Pelleting of Wheat Straw: Effects of Moisture Content," Proceedings of the IIE Annual Conference and Expo 2010 – Cancun, Mexico, June 5 – 9, 2010.

[20]   Tang, Y.J., Zhang, P.F., Liu, D.F., and Pei, Z.J., 2011, "Effects of Pellet Weight in Ultrasonic Vibration-Assisted Pelleting for Cellulosic Biofuel Manufacturing," accepted to appear in International Journal of Manufacturing Research.

[21]   Zhang, P.F., Deines, T.W., Cong, W.L., Qin, N., Pei, Z.J., and Nottingham, D., 2010a, "Ultrasonic vibration-assisted pelleting of switchgrass: effects of moisture content on pellet density, spring-back, and durability," Proceedings of the 20th International Conference on Flexible Automation and Intelligent Manufacturing (FAIM 2010), California State University, CA, July 12-14, 2010.

[22]   Zhang, P.F., Deines, T.W., Nottingham, D., Pei, Z.J., Wang, D.H., and Wu, X.R., 2010b, "Ultrasonic Vibration-Assisted Pelleting of Biomass: A Designed Experimental Investigation on Pellet Quality and Sugar Yield," Proceedings of the 2010 ASME International Manufacturing Science and Engineering Conference (MSEC), Erie, PA, October 12-15, 2010, MSEC 2010-34179.

[23]   Zhang, Q., Zhang, P.F., Deines, T.W., Pei, Z.J., Wang, D.H., Wu, X.R., and Pritchett, G., 2010c, "Ultrasonic Vibration-Assisted Pelleting of Sorghum: Effects of Pressure and Ultrasonic Power Level," Proceedings of the 2010 ASME International Manufacturing Science and Engineering Conference (MSEC), Erie, PA, October 12-15, 2010, MSEC 2010-34173.

[24]   Zhang, Q., Zhang, P.F., Deines, T.W., Zhang, M., Song, X.X., and Pei, Z.J., 2010d, "Ultrasonic Vibration-Assisted Pelleting of Wheat Straw: Effects of Particle Size," Proceedings of the 20th Int. Conference on Flexible Automation and Intelligent Manufacturing, Oakland, CA, July 12-14, 2010.

[25]   Feng, Q., Cong, W.L., Zhang, M., Pei, Z.J., and Ren, C.Z., 2010, "An Experimental Study on Temperature in Ultrasonic Vibration-Assisted Pelleting of Cellulosic Biomass," Proceedings of the 2010 ASME International Manufacturing Science and Engineering Conference (MSEC), Erie, PA, October 12-15, 2010, MSEC 2010-34122.

[26]   Feng, Q., Cong, W.L., Zhang, M., Pei, Z.J., and Ren, C.Z., 2011a, "An Experimental Study on Charring of Cellulosic Biomass in Ultrasonic Vibration-assisted Pelleting," International Journal of Manufacturing Research, 6 (1), pp. 77-86.

[27]   Zhang, Q., Zhang, P.F., Pei, Z.J., Wilson, J., McKinney, L., and Pritchett, G., 2011c, "Ultrasonic-vibration assisted pelleting for cellulosic ethanol manufacturing: an experimental investigation of power consumption," Proceedings of the ASME 2011 International Mechanical Engineering Congress and Exposition, Denver, Colorado, November 11-17, 2011, IMECE 2011-64307.

[28]   NREL, 2008, Determination of Total Solids in Biomass and Total Dissolved Solids in Liquid Process Samples, Technical Report NREL/TP-510-42621.

[29]   Herman, S.L., 2009, Electrial Studies for Trades, 4th Edition, Delmar Cengage Learning, NY, USA.

[30]   Bernhaupt, R., 2010, Evaluating User Experience in Games: Concepts and Methods, Springer.

[31]   Healey, J.F., and Prus, S.G., 2009, Statistics: A Tool for Social Research, Cengage Learning, Belmont, CA, USA.

[32]   Peat, J.K., and Barton, B., 2005, Medical Statistics: A Guide to Data Analysis and Critical Appraisal, Wiley-Blackwell, Malden, MA, USA.

[33]   Theerarattananoon, K., Xu, F., Wilson, J., Staggenborg, S., Mckinney, L., Vadlani, P., Pei, Z.J., and Wang. D.H., 2011, "Effects of the pelleting conditions on chemical composition and sugar yield of corn stover, big bluestem, wheat straw, and sorghum stalk pellets," Bioprocess and Biosystems Engineering, DOI 10.1007/s00449-011-0642-8.

[34]   Tabil, L., and Sokhansanj, S., 1996, "Process Conditions Affecting the Physical Quality of Alfalfa Pellets," Applied Engineering in Agriculture, 12 (3), pp. 345–350.

[35]   Deines, T.W., and Pei, Z.J., 2010, "Power Consumption Study in Knife Milling of Wheat Straw," Transactions of the North American Manufacturing Research Institution of SME, 38, pp. 191–196.

[36]   Deines, T.W., Nottingham, D., and Pei, Z.J., 2010, "Effects of Biomass Type and Sieve Size on Power Consumption in Knife Milling," Proceedings of the IIE Annual Conference and Expo 2010 – Cancun, Mexico, June 5 – 9, 2010.

[37]   Zhang, Q., Zhang, P.F., Pei, Z.J., and Pei, L., 2011b, "An Experimental Investigation on Cellulosic Biofuel Manufacturing: Effects of Biomass Particle Size on Sugar Yield," Proceedings of the 2011 ASME Int. Mechanical Engineering Congress and Exposition, Denver, CO, November 11-17, 2011, IMECE 2011-62721.

Chapter 7 - A Predictive Model for Energy Consumption in UV-A Pelleting

Authors' names:

Xiaoxu Song[a], Meng Zhang[a], Z.J. Pei[a], and Donghai Wang[b]

Authors' affiliation:

[a]Department of Industrial and Manufacturing Systems Engineering, Kansas State University, Manhattan KS 66506 USA

[b]Department of Biological and Agricultural Engineering, Kansas State University, Manhattan, KS 66506, USA

Abstract

Cellulosic biomass can be used as the feedstock for biofuel manufacturing. UV-A pelleting without using binder materials or high-temperature steam can produce biomass pellets whose densities are comparable to that processed by traditional pelleting methods. This article reports the development of a predictive model, using response surface methodology, for energy consumption in ultrasonic vibration-assisted pelleting of wheat straw. The results show that energy consumption decreased as ultrasonic power, sieve size, and pellet weight decreased. Effects of pelleting pressure had no significant effects on energy consumption in UV-A pelleting. This model can predict effects of process parameters on energy consumption in ultrasonic vibration-assisted pelleting.

7.1 Introduction

Liquid transportation fuels currently used in the U.S. are mainly petroleum-based [1–3]. In 2011, the U.S. transportation sector consumed about 18.95 million barrels of petroleum per day and half of it was imported [4,5]. This creates the issue for the nation's energy security. Another issue of using petroleum-based transportation fuels is greenhouse gas (GHG) emissions. One-third of the total carbon dioxide emissions in the U.S. are from the use of petroleum-based transportation fuels [6–8].

Biofuels - particularly cellulosic biofuels – can help addressing these issues. Cellulosic biofuels are produced from cellulosic biomass, including wood, agricultural residues, and herbaceous energy crops. Unlike other type of feedstocks (e.g. corn, sugar cane, and soybean) for biofuels, cellulosic biomass does not compete with food production for the limited agriculture land [9,10].

Biofuels have the potential to reduce GHG emissions by as much as 86% compared with gasoline [11]. Because biofuels are made from renewable, plant-based feedstocks, the carbon dioxide released during fuel combustion is 'recycled' by the plant as it grows [12].

However, cellulosic biomass materials have low density, resulting in high costs in their transportation and storage. Densification of cellulosic biomass into pellets [13] can increase the density from 40 - 250 kg/m^3 for raw cellulosic materials to as high as 1200 kg/m^3 [14].

Traditional pelleting methods (for example, extruding, briquetting, and rolling) [15] generally involve high-temperature steam, high pressure, and binder materials. Ultrasonic vibration-assisted (UV-A) pelleting is a new pelleting method [16]. UV-A pelleting, without using binder materials or high-temperature steam, can produce biomass pellets whose densities are comparable to those processed by traditional pelleting methods [17] Moreover, biomass (switchgrass) processed with UV-A pelleting has more than 20% higher sugar yield (proportional to biofuel yield) than biomass pellets processed without ultrasonic vibration or non-pelleted biomass [18].

The literature on UV-A pelleting includes experimental investigations on pellet quality, sugar yield, pelleting temperature, charring, and energy consumption. Energy consumption in UV-A pelleting not only contributes to the manufacturing costs of biofuels, but also affects the energy balance of biofuel manufacturing. Effects of biomass type, sieve size, pelleting pressure, and ultrasonic power on energy consumption in UV-A pelleting have been investigated by Zhang et al. [19]. However, in their study, pelleting time was not kept same when other input variables changed. In other words, effects of pelleting time were confounded with effects of biomass type, sieve size, pelleting pressure, and ultrasonic power. Therefore, it is not clear how each of these input variables affects energy consumption in UV-A pelleting.

Although some experimental studies [19,20] have been published concerning energy consumption in UV-A pelleting of biomass, no model has been reported in the literature to predict effects of process variables on energy consumption in UV-A pelleting. This paper, for the first time, develops a predictive model, using the response surface methodology (RSM), for energy consumption in UV-A pelleting. The develop model is used to predict the main effects and the interaction effects of process variables on energy consumption in UV-A pelleting.

7.2 Experimental procedure and conditions

7.2.1 Cellulosic biomass preparation

The cellulosic biomass used in this investigation was wheat straw. Wheat straw was harvested by Deines Farm in Northwest Kansas. The wheat straw had been run through a John

Deere 9600 combine. The combine removed the grains from the straw and chaff. Wheat straw and chaff exited through the back of the combine. The average length of the wheat straw was 250 mm. After being collected, wheat straw was stored indoors until this study.

Wheat straw was processed by a knife mill (Model SM 2000 from Retsch, Inc., Haan, Germany) (shown in Figure 7-1). The knife mill used a 240-volt, 3 horsepower electric motor with a fixed rotation speed (1720 rpm). Three cutting blades (95 mm long and 35 mm wide) were mounted on the rotor. Four shear bars were mounted on the inside wall of the milling chamber. There was a 3 mm gap between a cutting blade and a shear bar. Biomass was cut between the cutting blades and the shear bars. The sieves used in the knife mill were of 2, 4, and 8 mm in the size of the openings. As illustrated in Figure 7-1, only one sieve was installed at a time.

Figure 7-1 Knife mill

Shear bars   Cutting blades   Sieve
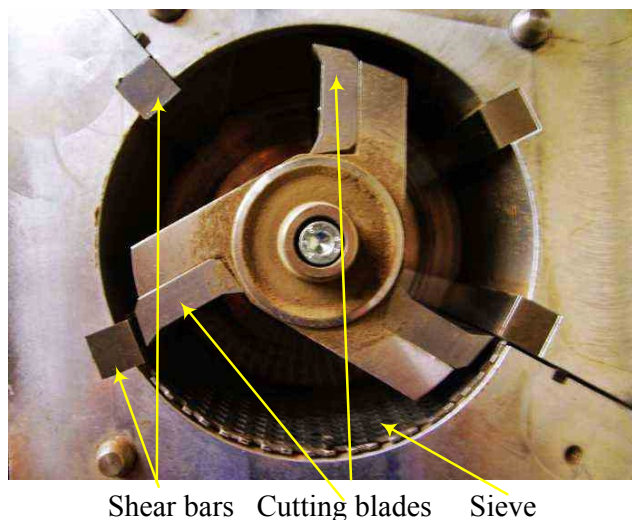
7.2.2 Experimental setup and procedure

Figure 7-2 is a schematic illustration of the experimental set-up for UV-A pelleting. UV-A pelleting experiments were performed on a modified ultrasonic machine (Model AP-1000, Sonic-Mill, Albuquerque, NM, USA). The machine included a power supply (which converts 60 Hz electrical power into 20,000 Hz electrical power), a converter (which converts high frequency electrical energy into mechanical motion), and a tool. The tip of the tool was a solid cylinder with a flat end (17.4 mm in diameter).

Before each pelleting test, the weight of wheat straw particles loaded into an aluminum mold was measured by a scale. This weight was referred to as pellet weight. The mold was

consisted of three parts. The upper two parts formed a cylindrical cavity (18.6 mm in diameter) and the bottom part was a square plate, serving as a base. They were assembled together with pins.

Figure 7-2 Illustration of experimental set-up for UV-A pelleting
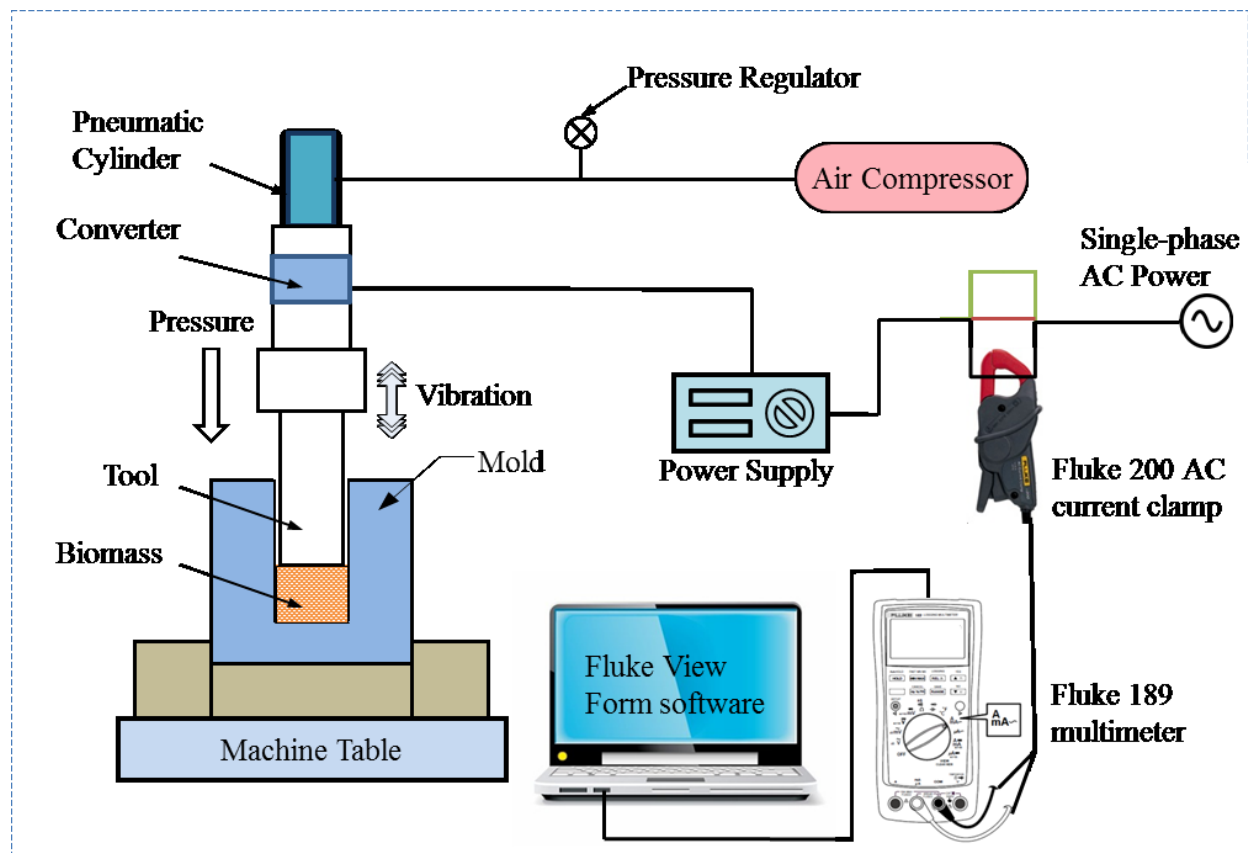
The pneumatic cylinder was driven by compressed air provided by a 1.6 HP, 33 Gal. air compressor (Sears, Roebuck and Co., Hoffman Estates, IL, USA). The air pressure in the pneumatic cylinder was controlled by a pressure regulator. A higher air pressure in the cylinder meant a higher pressure applied on the biomass in the mold by the tool. In each pelleting test, the pelleting time was 120 s. After 120 s, the tool was retracted and the mold was disassembled to unload the pellet. A finished UV-A pellet is shown in Figure 7-3.

Figure 7-3 Picture of a pellet produced by UV-A pelleting

7.2.3 Measurement of energy consumption

Energy consumption in this paper was referred to electrical energy consumed by the power supply. A Fluke 189 multimeter and a Fluke 200 AC current clamp were used to measure the electric current, as shown in Figure 7-2. The power line to the power supply has three wires: black, red, and green wires. The current clamp was clamped on the black wire to measure the current. The data was collected using Fluke View Forms software. The sampling rate was 2 per second. After the tool touched the biomass in the mold, the power supply was switched on and Fluke View Forms software started collecting data. After 120 s, Fluke View Forms software stopped collecting data and power supply was switched off.

The software recorded the average current (I_{AVE}) in each experiment run. The voltage (V) was 120 V. The total energy consumed during 120 s can be calculated using the following equation [21]:

$$E = \frac{V \times I_{AVE} \times 120}{3600}(Wh) \tag{1}$$

7.2.4 Design of experiments using RSM

According to the results of previous experiments, the appropriate conditions for obtaining a stable pellet were selected. The Box-Behnken design was employed to obtain the response surface model. Three coded levels were used for the process parameters, as shown in Table 7-1. In this study, a random order of 27 conditions was generated by Minitab 16 (Minitab, Inc., State College, PA, U.S.)

7.3 Response surface model

Energy consumptions for 27 conditions are shown in Table 7-1. Through analysis in Minitab 16, a response surface model for energy consumption was obtained. The model can be described by

$$
\begin{aligned}
E = {}& 4.47441 - 0.0434494 \times A - 0.0332448 \times B - 0.278111 \times C - 0.446989 \times D \\
& + 0.000338333 \times A^2 + 0.000998333 \times B^2 + 0.0151597 \times C^2 + 0.0278333 \times D^2 \\
& + 0.00015 \times A \times B + 0.00263448 \times A \times C + 0.001 \times A \times D \\
& - 8.96552E - 05 \times B \times C + 0.0106 \times B \times D + 0.0306897 \times C \times D
\end{aligned}
\tag{2}
$$

Where E, A, B, C, and D represent energy consumption, pelleting pressure, ultrasonic power, sieve size, and pellet weight, respectively. Analysis of variance (ANOVA) was then performed to remove the insignificant terms (p-value > 0.05), resulting in the following model:

$$
\begin{aligned}
E = {}& 3.0342 - 0.0183833 \times B - 0.15615 \times C - 0.295655 \times D \\
& + 0.000844167 \times B^2 + 0.0132326 \times C^2 + 0.0106 \times B \times D + 0.0306897 \times C \times D
\end{aligned}
\tag{3}
$$

The ANOVA showed that the model is highly significant (p-value < 0.0001). The coefficient of determination $R^2 = 0.9672$, which was defined as the ratio of the explained variation to the total variation. This suggests that the response surface model could provide good predictions. The lack-of-fit test showed that the lack-of-fit was insignificant, indicating that the model fitted well the experimental data.

The response surface model explicitly relates the energy consumption to the process parameters. The energy consumption can be predicted from the response surface model as long as the process parameters varied within the ranges tested in this study.

7.4 Predicted effects of process parameters

The ANOVA showed that ultrasonic power, sieve size, and pellet weight had significant effects on energy consumption.

7.4.1 Effects of ultrasonic power

Effects of ultrasonic power on energy consumption, predicted by Eq. (3), are shown in Figure 7-4. Energy consumption decreased as ultrasonic power decreased for different levels of pellet weight. A similar trend was reported by Song et al. [20], who studied effects of ultrasonic power on energy consumption in UV-A pelleting of wheat straw. They found that energy

consumption decreased as ultrasonic power decreased from 40% to 20%. A similar trend was also reported by Zhang et al. [19].

Table 7-1 Experimental design with response surface methodology

RunOrder	Pelleting pressure (psi)	Ultrasonic power (%)	Sieve size (mm)	Pellet weight (g)	Energy consumption (Wh)
1	40	40	4	1	3.468
2	40	30	4	2	3.068
3	40	20	4	1	2.544
4	40	40	8	2	3.98
5	50	30	8	2	3.576
6	40	30	4	2	3.04
7	30	30	8	2	3.296
8	50	40	4	2	3.728
9	40	30	2	3	3.168
10	50	30	4	1	2.952
11	40	40	4	3	4.144
12	30	20	4	2	2.688
13	40	30	8	3	3.556
14	40	30	2	1	3.16
15	30	30	4	3	3.284
16	50	30	2	2	3.18
17	30	40	4	2	3.66
18	40	30	8	1	3.1
19	40	20	4	3	2.796
20	40	20	2	2	2.664
21	40	40	2	2	3.74
22	40	30	4	2	3.128
23	30	30	2	2	3.16
24	30	30	4	1	3.068
25	50	30	4	3	3.208
26	50	20	4	2	2.696
27	40	20	8	2	2.916

Zhang et al. [21] studied effects of ultrasonic power in UV-A pelleting on sorghum stalk pellet quality. The results showed that, as ultrasonic power increased from 30% to 50%, pellet density and durability increased but spring back decreased. Zhang et al. [22] reported that, as ultrasonic power increased from 30% to 40%, wheat straw pellet density and durability increased but spring back decreased.

Zhang et al. [21] studied effects of ultrasonic power in UV-A pelleting on sugar yield. Sugar yield increased as the ultrasonic power increased from 30% to 55%. Similar results were also reported by Zhang et al. [22].

Figure 7-4 Effects of ultrasonic power on energy consumption
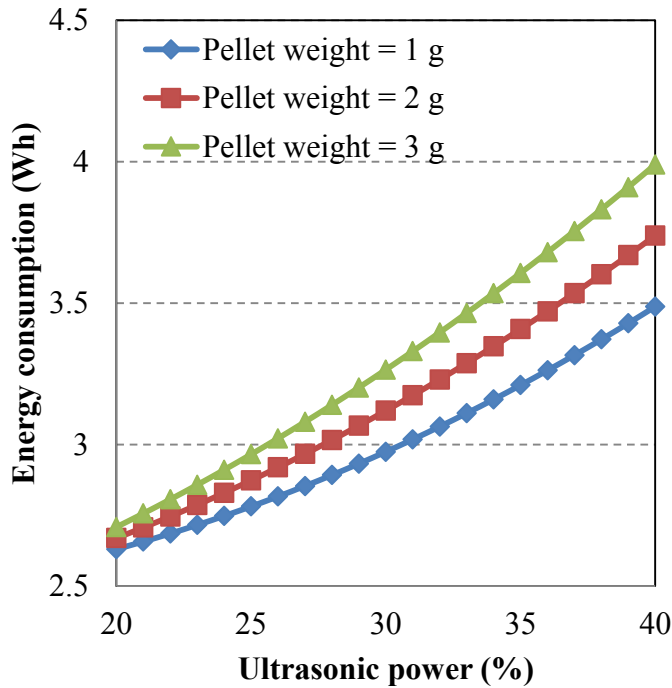
Sieve size = 4 mm, pelleting pressure = 40 psi

7.4.2 Effects of sieve size

Effects of sieve size on energy consumption, predicted by Eq. (3), are shown in Figure 7-5. Energy consumption decreased as sieve size decreased for different levels of ultrasonic power.

Effects of sieve size on energy consumption in size reduction have also been studied. Deines et al. [23] reported that energy consumption in knife milling increased as sieve size decreased from 8 to 0.25 mm for four types of biomass materials (sorghum stalks, switchgrass, wheat straw, and kochia).

Effects of sieve size (used in knife milling) on pellet quality (density, durability, and spring-back) in UV-A pelleting have been studied previously. Pellet durability measures the ability of pellets to withstand impact and other forces during transportation and storage. Spring-

back measures the expansion of a pellet. Zhang et al. [22] studied pellet quality in UV-A pelleting of wheat straw particles processed by knife milling using the 2^4 full factorial design with two levels of sieve size (1 and 2 mm). The wheat straw particles milled with the smaller sieve size produced higher density and durability, and smaller spring-back. Zhang et al. [24] also studied effects of sieve size (with four levels: 0.25, 1, 2, 1.5 and 8 mm) in knife milling on pellet quality in UV-A pelleting of wheat straw. Results showed that wheat straw particles milled with the smallest sieve size (0.25 mm) had higher density and smaller spring-back.

Figure 7-5 Effects of sieve size on energy consumption
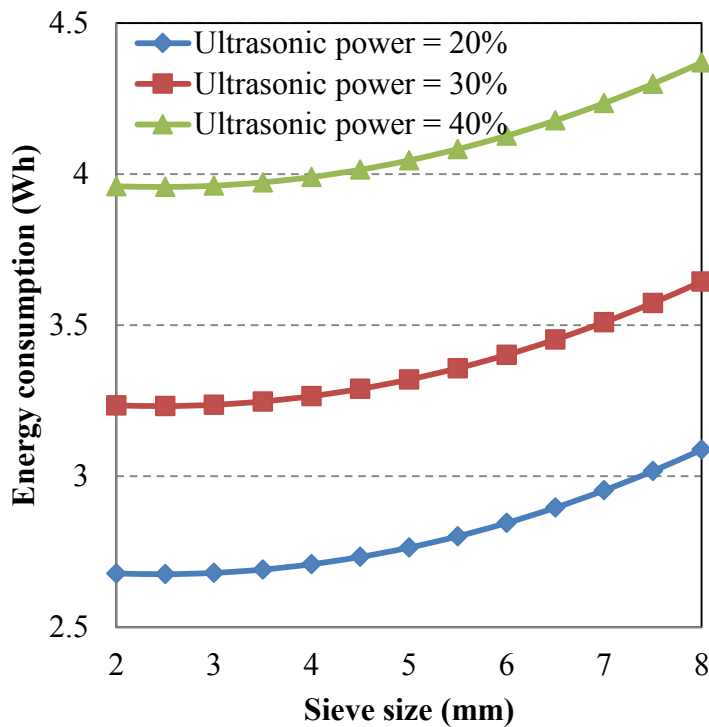
Pellet weight = 3 g, pelleting pressure = 40 psi

Theerarattananoon et al. [25] studied pellet quality in ring-die pelleting of wheat straw, corn stover, big bluestem, and sorghum particles processed by hammer milling with two levels of sieve size (3.2 and 6.5 mm). Results showed that the sieve size of hammer mill did not have significant effects on pellet density and durability. Tabil and Sokhansanj [26] also studied effects of sieve size in hammer milling on durability in ring-die pelleting of alfalfa. They found that the increase of sieve size from 3.2 to 6.5 mm resulted in no significant change of pellet durability.

Effects of sieve size (used in size reduction) on sugar yield of cellulosic biomass were also reported. Zhang et al. [22] found that wheat straw particles milled by knife milling with 2 mm sieve produced 50% higher sugar yield than those milled with 1 mm sieve. Theerarattananoon et al. [25] reported that the use of a larger sieve size (6.5 mm) in hammer milling resulted in higher sugar yield than using smaller sieve size (3.2 mm) for wheat straw, corn stover, bluestem, and sorghum.

7.4.3 Effects of pellet weight

Effects of pellet weight on energy consumption, predicted by Eq. (2), are shown in Figure 7-6. Energy consumption decreased linearly as pellet weight decreased for different levels of sieve size.

Figure 7-6 Effects of pellet weight on energy consumption
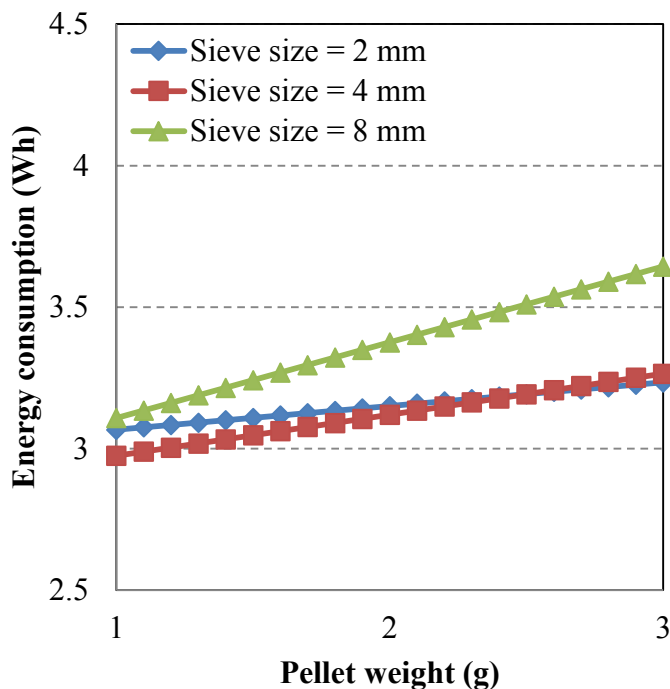
Ultrasonic power = 30%, pelleting pressure = 40 psi

Effects of pellet weight on energy consumption in UV-A pelleting of wheat straw milled by knife mill were also studied by Song et al. [20]. They reported that energy consumption increased linearly as the increasing of pellet weight from 0.5 to 3 g.

Tang et al. [27] studied effects of pellet weight on pellet density, durability, pelleting temperature in UV-A pelleting, and sugar yield in hydrolysis. As pellet weight varied from 0.5, 1, 1.5, 2, 2.5, to 3 g, pellet density, durability, pelleting temperature, and sugar yield first increased and then decreased. The highest density, durability, pelleting temperature, and sugar yield were all obtained with pellet weight of 1.5 g.

7.4.4 Interaction effects

Two of the two- factor interaction effects (between ultrasonic power and pellet weight, and between sieve size and pellet weight), predicted by Eq. (3), were significant, as shown in Figure 7-7 and Figure 7-8, respectively. For the interaction effects between ultrasonic power and pellet weight, energy consumption decreased from 3.99 to 3.49 Wh (decreased by 0.5 Wh) at a higher ultrasonic power level (40%), and decreased from 2.70 to 2.63 Wh (decreased by 0.07 Wh) at a lower ultrasonic power level (20%) when pellet weights decreased from 3 to 1 g, as shown in Figure 7-7. This showed that effects of pellet weight on energy consumption were stronger at the higher level of ultrasonic power.

For the interaction effects between sieve size and pellet weight, energy consumption decreased from 3.64 to 3.10 Wh (decreased by 0.54 Wh) at a higher sieve size level (8 mm), and decreased from 3.23 to 3.07 Wh (decreased by 0.16 Wh) at a lower sieve size level (2 mm) when pellet weights decreased from 3 to 1 g, as shown in Figure 7-8. This showed that effects of pellet weight on energy consumption were stronger at the higher level of sieve size.

7.5 Conclusions

This paper reports the development of a predictive model, using response surface methodology, for energy consumption in UV-A pelleting of wheat straw. The model can predict effects of ultrasonic power, sieve size, and pellet weight on energy consumption in UV-A pelleting of wheat straw. It was found that all these three parameters significantly affected the energy consumption in UV-A pelleting. Under the experimental conditions applied here, energy consumption decreased with a decrease in ultrasonic power, sieve size, and pellet weight. Effects of pelleting pressure had no significant effects on energy consumption in UV-A pelleting. In addition, two of the predicted two-factor interaction effects (between ultrasonic power and pellet weight, and between sieve size and pellet weight) were significant. Effects of pellet weight on

energy consumption were stronger at the higher level of ultrasonic power and at the higher level of sieve size.

The results obtained in this study can be used to optimize pelleting process to achieve the minimum energy consumption in UV-A pelleting. Pellet durability and sugar yield are other important measurements in UV-A pelleting. Investigation of pellet durability and sugar yield will be part of the future work. In addition, the temperature of biomass increased significantly in UV-A pelleting [28]. A systematic study on effects of process parameters on temperature of biomass in UV-A pelleting is underway.

Figure 7-7 3-D response surface of energy consumption in relation to ultrasonic power and pellet weight (sieve size = 4 mm, pelleting pressure = 40 psi)
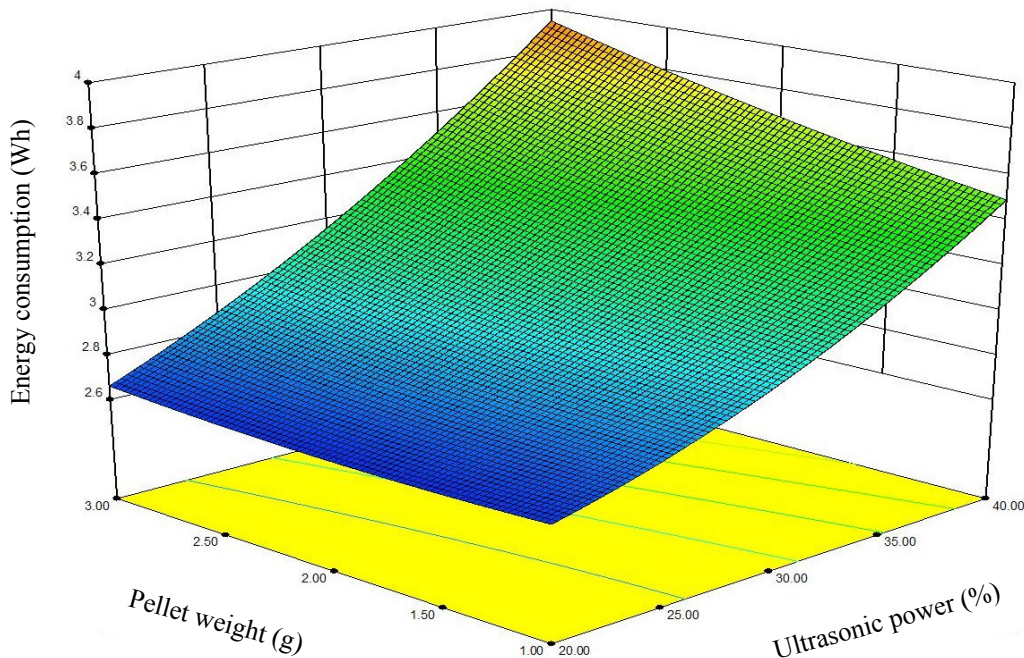
Figure 7-8 3-D response surface of energy consumption in relation to sieve size and pellet weight (ultrasonic power = 30%, pelleting pressure = 40 psi)
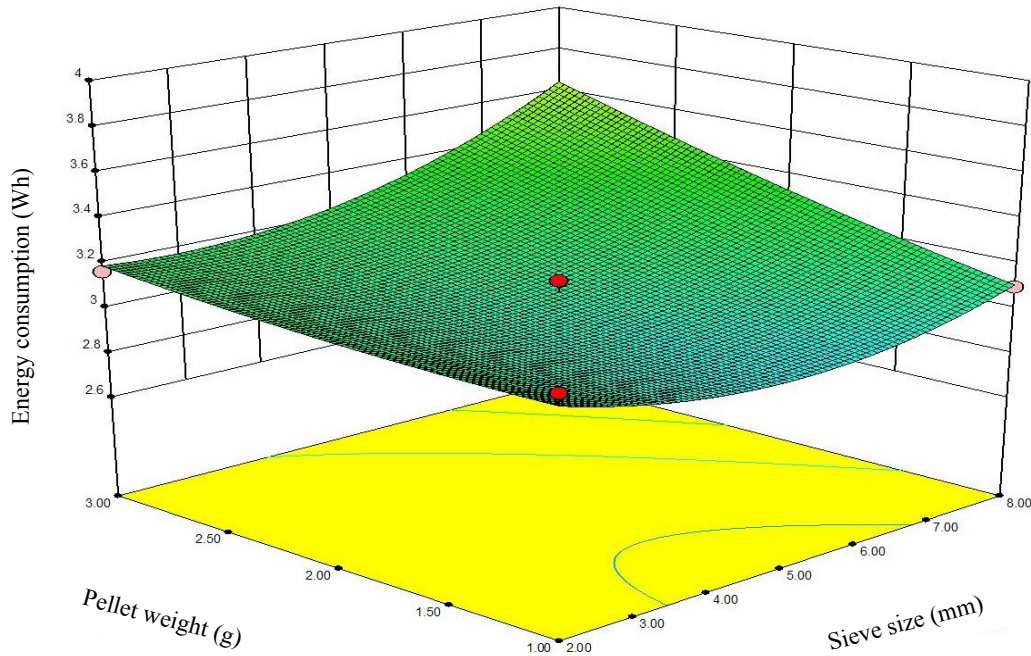
References

[1]   U.S. Energy Information Administration, 2011. "Monthly Energy Review," http://www.eia.gov/totalenergy/data/monthly/pdf/mer.pdf.

[2]   U.S. Energy Information Administration, 2011. "Transportation Sector Energy Consumption Estimates 1949-2010," http://205.254.135.24/totalenergy/data/annual/showtext.cfm?t=Ptb0201e.

[3]   U.S. Energy Information Administration, 2011. "U.S. Energy Consumption by Sector of 1949-2010," http://www.eia.gov/totalenergy/data/annual/txt/ptb0201a.html.

[4]   U.S. Energy Information Administration, "EIAs Energy in Brief: How dependent are we on foreign oil?," http://ethanolrfa.3cdn.net/5b9bd0152522901e81_jtm6bhwh7.pdf.

[5]   U.S. Energy Information Administration, 2011. "Short-Term Energy Outlook," http://205.254.135.24/steo/steo_full.pdf.

[6]   Conti, J., Chase, N., and Maples, J., 2010. "US Greenhouse Gas Emissions in the Transportation Sector," Climate and Transportation Solutions, **5000**(6000), p. 24.

[7]   Environmental Protection Agency, 2011. "Inventory of U.S. Greenhouse Gas Emissions and Sinks: 1990-2009," http://www.eia.gov/totalenergy/data/monthly/pdf/mer.pdf.

[8]   National Academy of Sciences, National Academy of Engineering, and National Academy of Sciences, 2009. Liquid Transportation Fuels from Coal and Biomass.

[9]   Gray, K.A., Zhao, L., and Emptage, M., 2006. "Bioethanol," Current Opinion in Chemical Biology, **10**(2), pp. 141–146.

[10]   Brown, L.R., 2008. "Why Ethanol Production Will Drive World Food Prices Even Higher in 2008."

[11]   U.S. Department of Energy, 2008. "Environmental Benefits of Biofuels."

[12]   RFA, 2011. "Ethanol Facts: Environment," http://www.ethanolrfa.org/pages/ethanol-facts-environment.

[13]   Leaver, R.H., 1984. The Pelleting Process, Sprout-Waldron, Muncy, PA, USA.

[14]   Mani, S., Sokhansanj, S., Bi, X., and Turhollow, A., 2006. "Economics of Producing Fuel Pellets from Biomass," Applied Engineering in Agriculture, **22**(3), pp. 421–426.

[15]   Sokhansanj, S., Mani, S., Bi, X., Zaini, P., and Tabil, L., 2005. "Binderless pelletization of biomass," ASAE Annual International Meeting, Tampa Convention Centre, Tampa, Florida, pp. 17–20.

[16]   Pei, Z., Wang, D., and Clark, R., 2009. "Ultrasonic Vibration Assisted Pelleting of Cellulosic Biomass: A Preliminary Experiment," Proceedings of the ASME 2009 International Manufacturing Science & Engineering Conference (MSEC), MSEC 2009, October 4-7, 2009, West Lafayette, IN, USA.

[17]   Song, X., Zhang, M., Pei, Z., and Deines, T., 2010. "Ultrasonic-Vibration-Assisted Pelleting of Cellulosic Biomass: Effects of Moisture Content," Proceedings of the IIE Annual Conference and Expo 2010 – Cancun, Mexico, June 5 – 9, 2010.

[18]   Zhang, P., Pei, Z., Wang, D., Wu, X., Cong, W., Zhang, M., and Deines, T., 2011. "Ultrasonic Vibration-Assisted Pelleting of Cellulosic Biomass for Biofuel Manufacturing," Journal of manufacturing science and engineering, **133**(1).

[19]   Zhang, Q., Zhang, P.F., Pei, Z.J., Wilson, J., McKinney, L., and Pritchett, G., "Ultrasonic-Vibration Assisted Pelleting for Cellulosic Ethanol Manufacturing: An Experimental Investigation of Power Consumption," Proceedings of the ASME 2011 International Mechanical Engineering Congress and Exposition, Denver, Colorado, November 11-17, 2011, IMECE 2011-64307.

[20]   Song, X.X., Zhang, M., Deines, T.W., Zhang, P.F., and Pei, Z.J., 2012. "Energy Consumption Study in Ultrasonic Vibration-Assisted Pelleting of Wheat Straw for Cellulosic Biofuel Manufacturing," accepted to appear in International Journal of Manufacturing Research.

[21]   Zhang, Q., Zhang, P., Deines, T., Pei, Z., Wang, D., Wu, X., and Pritchett, G., 2010. "Ultrasonic Vibration-Assisted Pelleting of Sorghum Stalks: Effects of Pressure and Ultrasonic Power," Proceedings of the ASME 2010 International Manufacturing Science and Engineering Conference (MSEC), Erie, PA, October 12-15, 2010, MSEC 2010-34173.

[22]   Zhang, P., Deines, T., Nottingham, D., Pei, Z., Wang, D., and Wu, X., 2010. "Ultrasonic Vibration-Assisted Pelleting of Biomass: A Designed Experimental Investigation on Pellet Quality and Sugar Yield," Proceedings of the ASME 2010 International Manufacturing Science and Engineering Conference (MSEC), Erie, PA, October 12-15, 2010.

[23]   Deines, T.W., Nottingham, D., and Pei, Z.J., "Effects of Biomass Type and Sieve Size on Power Consumption in Knife Milling," Proceedings of the IIE Annual Conference and Expo 2010 – Cancun, Mexico, June 5 – 9, 2010.

[24]   Zhang, Q., Zhang, P.F., Deines, T.W., Zhang, M., Song, X.X., and Pei, Z.J., 2010. "Ultrasonic vibration assisted pelleting of wheat straw: effects of particle size," Proceedings of the 20th International Conference on Flexible Automation and Intelligent Manufacturing (FAIM 2010), California State University, CA.

[25]   Theerarattananoon, K., Xu, F., Wilson, J., Staggenborg, S., McKinney, L., Vadlani, P., Pei, Z., and Wang, D., 2011. "Effects of the Pelleting Conditions on Chemical Composition and Sugar Yield of Corn Stover, Big Bluestem, Wheat Straw, and Sorghum Stalk Pellets," Bioprocess and Biosystems Engineering.

[26]   Tabil, L., and Sokhansanj, S., 1996. "Process Conditions Affecting the Physical Quality of Alfalfa Pellets," Applied Engineering in Agriculture, **12**(3), pp. 345–350.

[27]   Tang, Y.J., Zhang, P.F., Liu, D.F., and Pei, Z.J., 2012. "Effects of pellet weight in ultrasonic vibration-assisted pelleting for cellulosic biofuel manufacturing," accepted to appear in International Journal of Manufacturing Research.

[28]   Feng, Q., Cong, W., Zhang, M., Pei, Z., and Ren, C., 2010. "An Experimental Study on Temperature in Ultrasonic Vibration-Assisted Pelleting of Cellulosic Biomass," Proceedings of the ASME 2010 International Manufacturing Science and Engineering Conference (MSEC), Erie, PA, October 12-15, 2010, MSEC 2010-34148.

Chapter 8 - Dilute Acid Pretreatment of poplar wood for biofuel production

Authors' names:

Xiaoxu Song[a], Meng Zhang[a], Z.J. Pei[a], and Donghai Wang[b]

Authors' affiliation:

[a]Department of Industrial and Manufacturing Systems Engineering, Kansas State University, Manhattan KS 66506 USA

[b]Department of Biological and Agricultural Engineering, Kansas State University, Manhattan, KS 66506, USA

Abstract

Background: The literature does not contain any systematic study on effects of operating variables in dilute acid pretreatment of poplar wood. **Results & discussion:** This paper reports experimental determined effects of operating variables on energy consumption, water usage, sugar yield, and pretreatment energy efficiency (PEE) in dilute acid pretreatment of poplar wood. **Conclusions:** As pretreatment time increased, energy consumption, water usage, and sugar yield increased; PEE first increased and then decreased. As pretreatment temperature increased, energy consumption and water usage increased; sugar yield and PPE first increased and then became constant or decreased. As acid concentration increased, energy consumption and water usage did not change noticeably; sugar yield and PEE first increased and then decreased.

Keywords

Cellulosic biofuel; Energy consumption; Enzymatic hydrolysis; Poplar wood; Pretreatment; Sugar yield.

8.1 Introduction

Ninety four percent of the transportation fuels consumed in the U.S. in 2010 are petroleum based [101]. About half of the petroleum used in the U.S. is imported [102]. The major issue of using these fuels is greenhouse gas (GHG) emissions and natural resource limitation. In order to reduce GHG emissions and the nation's dependence on foreign resources, it is imperative to produce and use fuels from domestic and renewable resources. One such example is cellulosic biofuels [101,102,1,2].

Biofuels have the potential to reduce GHG emissions by as much as 86% [103] (although CO_2 from biofuel combustion can also accumulate in the atmosphere). Because biofuels are made from renewable, plant-based feedstocks, CO_2 released during fuel combustion is "recycled" by plants as they grow [104]. Cellulosic biofuels are made from cellulosic biomass (including wood, agricultural residues, and herbaceous energy crops). Unlike other type of feedstocks (e.g. corn, sugar cane, and soybean) for biofuels, cellulosic biomass can grow on non-agricultural land and, therefore, does not have to compete with food production for limited agricultural land [1,2].

Poplar wood has a higher glucan content (about 50%) [3] than other types of biomass such as switchgrass (about 31%) [4] and corn stover (about 40%) [5]. Since the final ethanol yield is highly related to biomass cellulose content [6], poplar wood has the potential for high ethanol yield.

Major process steps of biofuel manufacturing from poplar wood are listed in Figure 8-1. To produce biofuels from poplar wood, its size needs to be reduced first [7-10]. Pretreatment makes cellulose more accessible to the enzyme in the following hydrolysis step [11,12]. Hydrolysis breaks down cellulose into sugars (glucose) that are converted to ethanol by fermentation [11,13,105].

Dilute acid pretreatment has been applied to various types of cellulosic biomass including softwood, hardwood, agricultural residues, and herbaceous energy crops [14-18]. However, the literature does not contain any systematic study on effects of operating variables (pretreatment time, temperature, and acid concentration) on energy consumption, water usage, sugar yield, and pretreatment energy efficiency in dilute acid pretreatment of poplar wood. This paper presents the experimentally determined effects to fill the gap in the literature.

Figure 8-1 Major process steps of biofuel manufacturing from poplar wood (after [16])
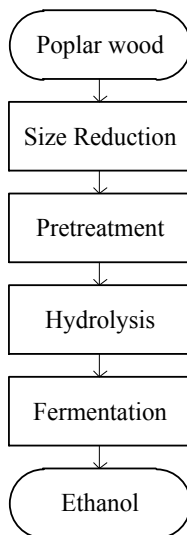
8.2 Experimental methods

8.2.1 Substrate

The poplar wood materials used in this study were poplar wood chips purchased from Petco (Manhattan, KS). The wood chips contained about 41% of cellulose, 22% of hemicellulose, 24% of lignin, and 3% of ash in dry weight basis.

Moisture content (MC) of wood chips was 1.6%, measured by following the NREL Laboratory Analytical Procedure [19]. A sample of wood chips (25 g) was dried in an oven (Blue M Electric Co., Blue island, IL) at 105°C for 24 hours to get rid of the moisture in these wood chips. After measuring the weight of the sample after the heating by a scale (Denver instrument Corp. Denver, CO, USA), MC was calculated using the following equation:

$$MC = \left(\frac{\text{Sample weight after heating} - \text{Original sample weight}}{\text{Original sample weight}} \right) \times 100\% \qquad (1)$$

The wood chips were milled into particles using a knife mill (SM2000, Retsch GmbH, Haan, Germany). The mill had a three-phase, 240-volt, and 3-horsepower electric motor with fixed rotation speed (1720 rpm). Three cutting blades were mounted on the rotor. Four shear bars were mounted on the inside wall of the milling chamber. There was a 3-mm gap between a cutting blade and a shear bar. The wood chips were cut into particles between the cutting blades and the shear bars. The sieve size used in this study was 5-mesh sieve (4 mm). Particles smaller than the sieve size would fall through the sieve. Particles larger than the sieve size were recirculated and milled further. Poplar wood particles after milling were kept in Ziploc bags and stored in a refrigerator at 4°C until being used for pretreatment experiments.

8.2.2 Pretreatment setup and conditions

The pretreatment was carried out in the 600-mL reaction vessel of a Parr pressure reactor (Parr Instrument Company, Moline, IL) (Figures 8-2 and 8-3). The poplar particles were mixed with diluted sulfuric acid (0.8% to 2%) to obtained biomass slurry with 5% solid content (10 g of poplar particles in 200 mL of diluted sulfuric acid solution). The slurry was loaded into the reaction vessel. When the pretreatment started, the heater was manually switched on to begin heating the reaction vessel. The valve was manually turned on to let the reactor controller to allow tap water to enter into the cooling loop as needed. It is noted that, for the equipment used

in this study, cooling water was used to maintain temperature in the reaction vessel. For different type of equipment, other means may be used to maintain the pretreatment temperature.

Figure 8-2 Illustration of pretreatment reactor
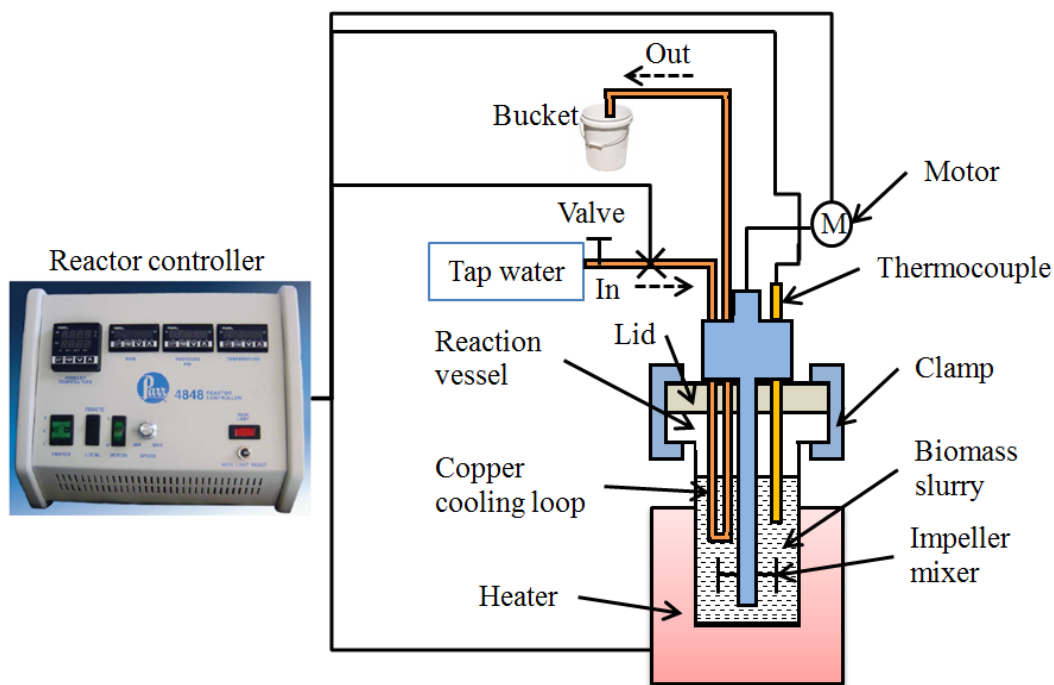
Pretreatment temperature was the reaction temperature in the reaction vessel and can be set on the reactor controller. A thermocouple in the reaction vessel connected to the reactor controller.

When the temperature measured by the thermocouple reached the pre-set pretreatment temperature, a timer was used to record the pretreatment time. (Depending on the pretreatment temperature, the time it took for the reactor to reach the pretreatment temperature could be different. For example, it took about 20 min when pretreatment temperature = 140°C.) Pretreatment time was the period of time when the biomass slurry was treated at the pretreatment temperature in the reaction vessel.

When the temperature measured by the thermocouple was above the pre-set pretreatment temperature, the heater stopped heating the vessel and tap water started entering into the cooling loop (controlled by the reactor controller) till the temperature became equal to the pre-set pretreatment temperature.

Figure 8-3 Experimental setup for pretreatment and energy consumption measurement
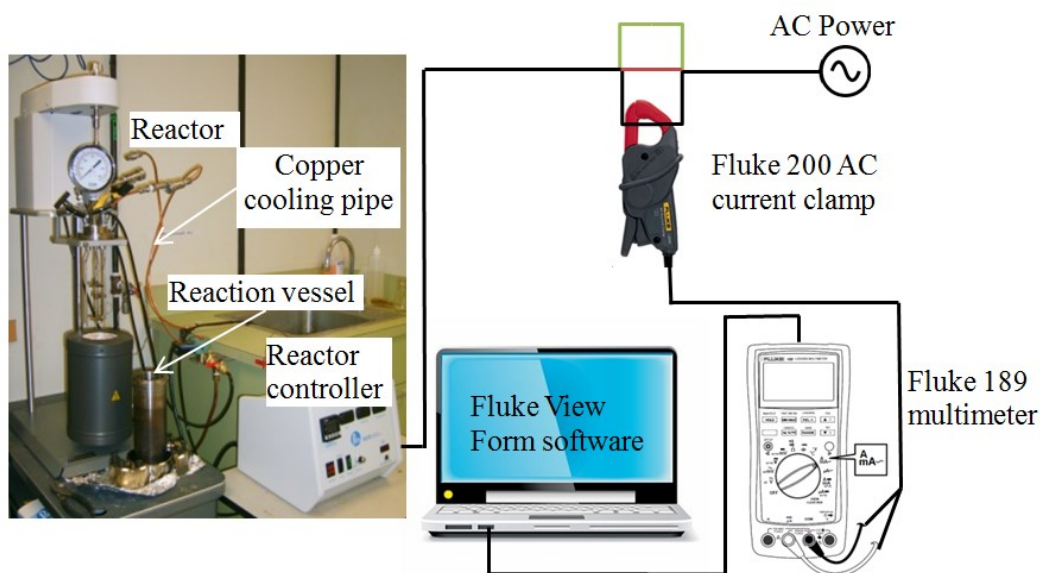
When the temperature was measured by the thermocouple below the pre-set pretreatment temperature, tap water stopped entering into the cooling loop (controlled by the reactor controller) and the heater started heating the vessel till the temperature became equal to the pre-set pretreatment temperature.

When the pretreatment was finished, the heater was manually switched off. Then, the temperature on the reactor controller was set to 60°C to decrease the temperature in the reaction vessel. The time between the heater was manually switched on and off was recorded by a timer and is referred to as heating time. The period of time during which the temperature increased to the pre-set pretreatment temperature or decreased to 60°C was not included in the pretreatment time.

The impeller mixer was connected to the motor and the rotation speed of the impeller mixer was 120 rpm. Experimental conditions are listed in Table 8-1. Important concepts used in this paper are illustrated in Figure 8-4.

Table 8-1 Experimental conditions

Process variable	Unit	Value
Pretreatment time	min	10; 20; 30
Pretreatment temperature	°C	100; 120; 140; 160; 180
Acid concentration	% (w/v)	0.8, 1; 1.5; 2

% (w/v) referred to as gram of acid in 100 mL of solution.

8.3 Measurement procedures for output variables

8.3.1 Energy consumption

Energy consumption in this paper is the electrical energy consumed by the reactor. A Fluke 189 multimeter and Fluke 200 AC current clamp were used to measure the electric current, as shown in Figure 8-3. The data was collected using Fluke View Forms software. The sampling rate was 2 per second. Fluke View Forms software started collecting data when the heater was manually switched on, and stopped collecting data when the heater was manually switched off.

The software also recorded the average current (I_{AVE}) for each test. The voltage (V) was 120 V. The total energy consumed during heating time can be calculated using the following equation [20]:

$$E\,(Wh) = V\,(V) \times I_{AVE}\,(A) \times heating\ time\,(h) \tag{2}$$

Figure 8-4 Illustration of important concepts in this study
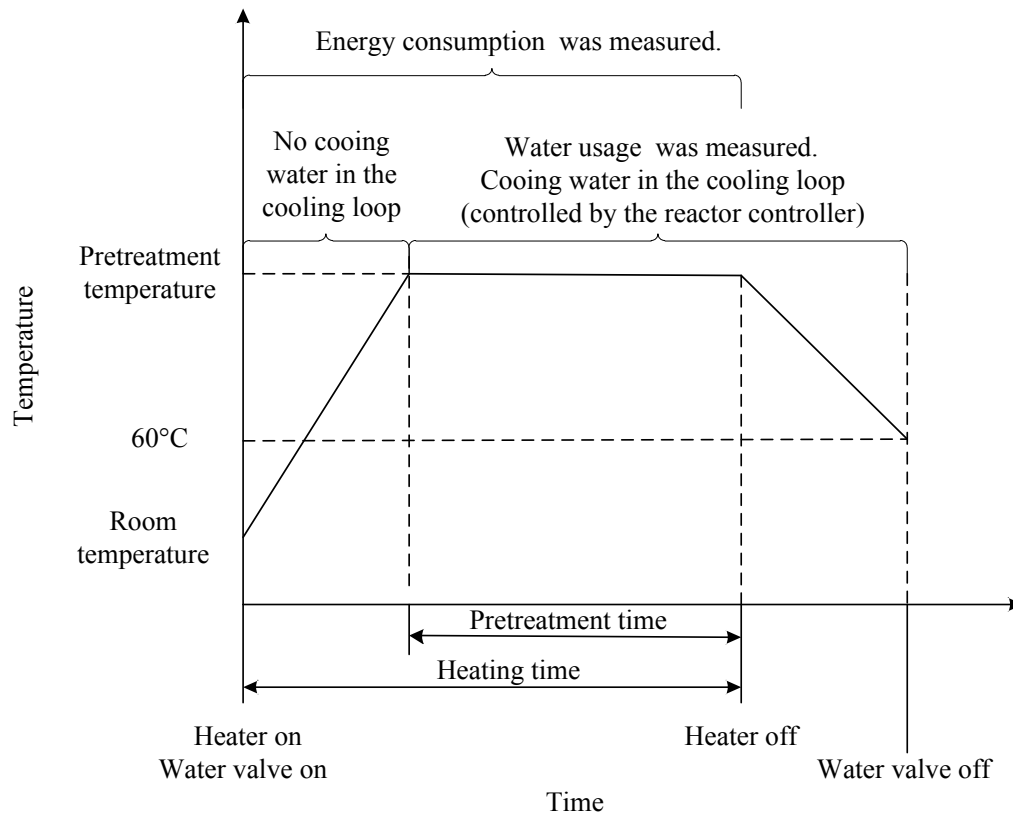
8.3.2 Water usage

Water usage in this paper is the amount of water used in the copper cooling loop (Figure 8-2) of the reactor (controlled by the reactor controller). Cooling water was measured by two 16-L buckets. One 16-L bucket was placed in the outlet of the cooling loop to collect the cooling water. When the bucket was full, the other empty bucket replaced it and continued collecting water. In the meanwhile the full bucket was emptied. The total water usage in a test was the amount of water collected during the period of time between the valve was manually turned on and off (Figure 8-4).

8.3.3 Sugar yield in enzymatic hydrolysis

The pretreated biomass samples were enzymatically hydrolyzed, following the NREL Laboratory Analytical Procedure [21]. Enzymatic hydrolysis was conducted in 125-mL flasks in a water bath at 50°C with agitation speed of 110 rpm. The pretreated wet biomass samples (2.5 g dry weight) were loaded into 50-mL solution with sodium acetate buffer (100 milliMoles, pH 4.8). Then 2.5 mL of enzyme (Accellerase^{TM} 1500 from Genencor, Rochester, NY) was loaded into the 50-mL solution based on 1 ml of enzyme/g dry biomass.

After 72 hours of enzymatic hydrolysis, the hydrolysis slurries were sampled by withdrawing 0.1 mL of slurry from each flask. Sample slurries were then mixed with 0.9 mL of double-distilled water in 1.5-mL vials. The vials were placed into boiling water for 15 min to deactivate the enzyme. After the enzyme was deactivated, samples were centrifuged in a centrifuge (RS-102, REVSCI Company, Lindstrom, MN, USA) at 10,000 rpm for 15 min. The supernatants were filtered into 2-mL autosampler vials through 0.2-μm syringe filters (Millipore, Billerica, MA, USA). Filtered samples in the autosampler vials were analyzed for sugars with an HPLC (Shimadzu, Kyoto, Japan) equipped with an RCM-monosaccharide column (300 9 7.8 mm; Phenomenex, Torrence, Cal., USA) and a refractive index detector (RID-10A, Shimadzu, Kyoto, Japan). Themobile phase was 0.6 mL/min of double-distilled water, and oven temperature was 80°C.

In this paper, sugar yield represents the amount of glucose produced from cellulosic biomass in enzymatic hydrolysis. A higher sugar yield means that more glucose is obtained. In this paper, sugar yield was determined by the following equation:

$$\text{Sugar yield} = \frac{G_{EH} \times V}{M_{EH}} \times 100\% \qquad (3)$$

where G_{EH} is the glucose concentration (g/L) of slurry in the flask after hydrolysis, M_{EH} is the dry weight (g) of cellulosic biomass in enzymatic hydrolysis, V is the total volume (L) of slurry in the flask in enzymatic hydrolysis.

8.3.4 Pretreatment energy efficiency

Pretreatment energy efficiency in this paper was defined as the amount of obtained glucose from hydrolyzing the pretreated biomass divided by the energy consumption in pretreating the biomass.

$$\eta_{pretreatment}(mg/Wh) = \frac{G_{EH} \times V \times 10 \times (1\text{-}1.6\%) \times 1000}{M_{EH} \times E} \qquad (4)$$

Since, in this study, 10 g of biomass with 1.6% MC was pretreated, the amount of obtained glucose from hydrolyzing the pretreated biomass was equal to $\frac{G_{EH} \times V}{M_{EH}} \times 10 \times (1\text{-}1.6\%) \times 1000$ (mg). E is the energy consumption (Wh) in pretreating the biomass.

8.4 Results and discussion

8.4.1 Effects of pretreatment time

Figure 8-5 shows effects of pretreatment time on energy consumption. Energy consumption increased as pretreatment time increased from 10 to 30 min. It is noted that this study was conducted on lab-scale equipment. If different equipment is used, the results might be different but the methodology employed here should still be applicable.

Water usage increased as pretreatment time increased, as shown in Figure 8-6. As illustrated in Figure 8-4, water usage was measured during the duration of pretreatment time. When pretreatment time increased, more water would be needed to maintain the pretreatment temperature.

Figure 8-5 Effects of pretreatment time on energy consumption
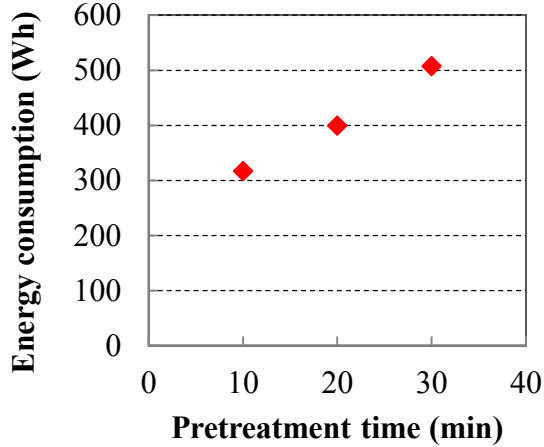
Pretreatment temperature = 140°C, Acid concentration = 2%

Figure 8-6 Effects of pretreatment time on water usage
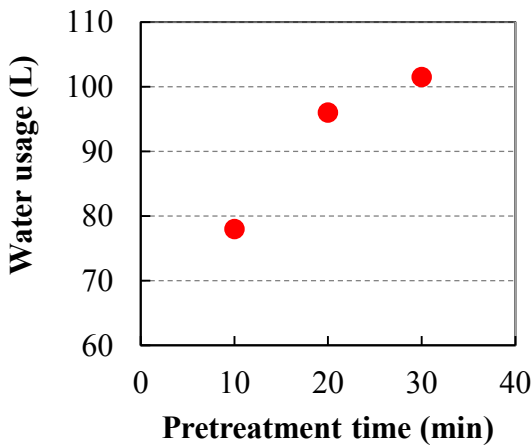
Pretreatment temperature = 140°C, Acid concentration = 2%

Effects of pretreatment time on sugar yield are shown in Figure 8-7. Sugar yield increased as pretreatment time increased from 10 to 30 min. Please note that the values of sugar yield in this figure were low. There are two reasons. (1) In this paper, sugar yield is defined as the amount of glucose produced from cellulosic biomass in enzymatic hydrolysis divided by the dry weight (g) of cellulosic biomass in enzymatic hydrolysis. The values can be higher if different definitions are used. (2) In this study, sugar yield was measured after 72 hours of hydrolysis. The values of sugar yield will be higher if sugar yield is measured after more than 72 hours of hydrolysis. Please also note that heating time consisted of ramping-up time and

pretreatment time (as illustrated in Figure 8-4). In this study, only effects of pretreatment time were considered. Effects of heating time and ramping-up time will be studied in the future.

Figure 8-8 shows effects of pretreatment time on pretreatment energy efficiency. Pretreatment energy efficiency increased when pretreatment time increased from 10 to 20 min, but decreased slightly when pretreatment time increased from 20 to 30 min.

Figure 8-7 Effects of pretreatment time on sugar yield
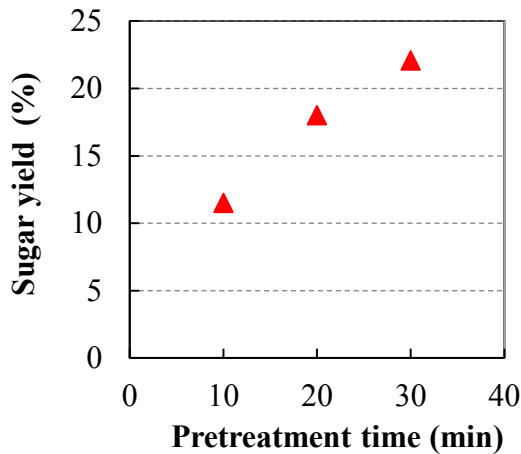
Pretreatment temperature = 140°C, Acid concentration = 2%

Figure 8-8 Effects of pretreatment time on pretreatment energy efficiency
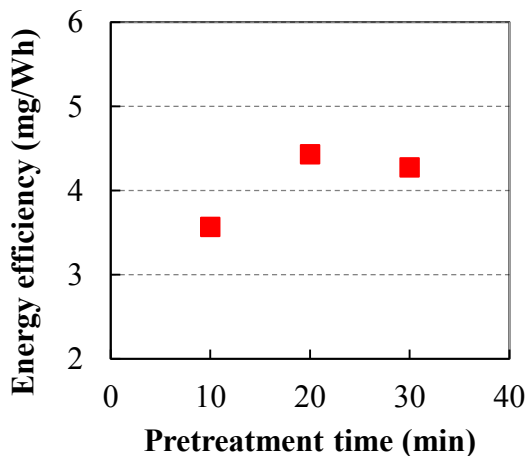
Pretreatment temperature = 140°C, Acid concentration = 2%

There are no reports in the literature on effects of pretreatment time on energy consumption, water usage, and pretreatment energy efficiency in dilute acid pretreatment of poplar wood. Saha et al. [14] and Baboukani et al. [15] studied effects of pretreatment time on

sugar yield in enzymatic hydrolysis of dilute acid pretreated wheat straw. Both studies showed that sugar yield (glucose yield) increased when pretreatment time increased.

8.4.2 Effects of pretreatment temperature

Figure 8-9 and Figure 8-10 show effects of pretreatment temperature on energy consumption and water usage. There was an increasing trend in energy consumption and water usage when pretreatment temperature increased from 100°C to 180°C.

Effects of pretreatment temperature on sugar yield and pretreatment energy efficiency are shown in Figure 8-11 and Figure 8-12. Both sugar yield and pretreatment energy efficiency had an increasing trend when pretreatment temperature increased.

There are no reports in the literature about effects of pretreatment temperature on energy consumption, water usage, and pretreatment energy efficiency in dilute acid pretreatment of poplar wood. Saha et al. [16] studied effects of pretreatment temperature on sugar yield in enzymatic hydrolysis of dilute acid pretreated rice hulls. Their results showed that sugar yield increased as pretreatment temperature increased. Baboukani et al. [15] studied effects of pretreatment temperature on sugar yield in enzymatic hydrolysis of dilute acid pretreated wheat straw. They found that sugar yield (glucose yield) increased when pretreatment temperature increased from 120°C to 160°C.

Figure 8-9 Effects of pretreatment temperature on energy consumption
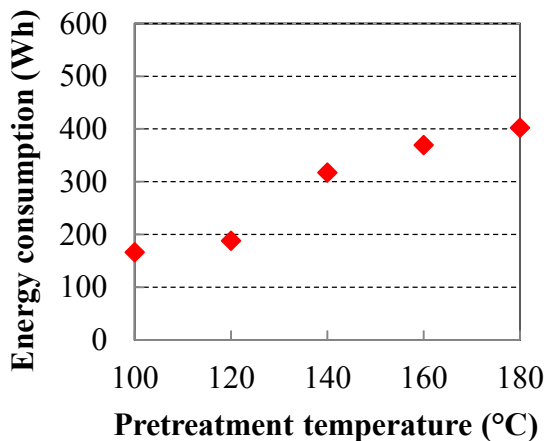
Pretreatment time = 10 min, Acid concentration = 2%

Figure 8-10 Effects of pretreatment temperature on water usage
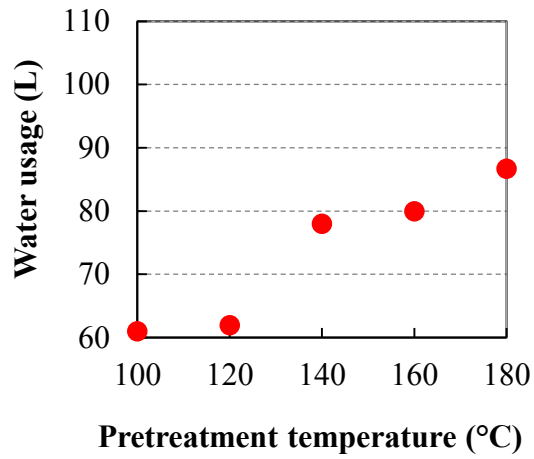
Pretreatment time = 10 min, Acid concentration = 2%

Figure 8-11 Effects of pretreatment temperature on sugar yield
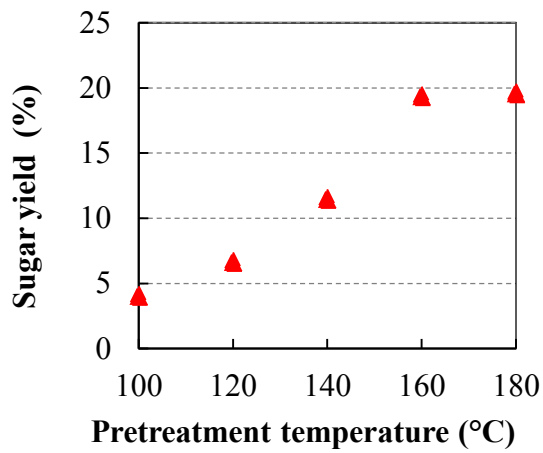
Pretreatment time = 10 min, Acid concentration = 2%

Figure 8-12 Effects of pretreatment temperature on pretreatment energy efficiency
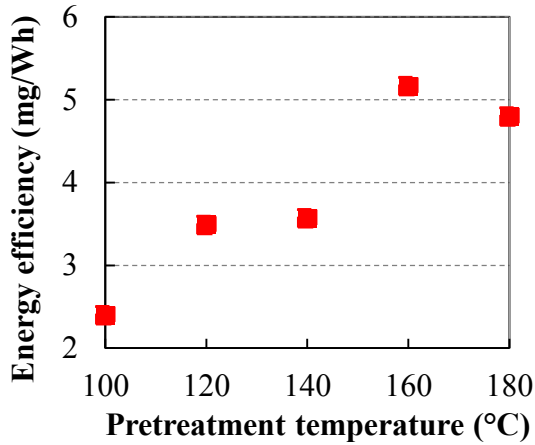
Pretreatment time = 10 min, Acid concentration = 2%

8.4.3 Effects of acid concentration

Figure 8-13 shows effects of acid concentration on energy consumption. Energy consumption changed little when acid concentration changed form 0.8% to 2%. As shown in Figure 8-14, water usage was constant as acid concentration increased from 0.8% to 2%. Effects of acid concentration on sugar yield are shown in Figure 8-15. Sugar yield first increased as acid concentration increased from 0.8% to 1.5%, and then decreased as acid concentration increased from 1.5% to 2%. Figure 8-16 shows effects of acid concentration on pretreatment energy efficiency. Pretreatment energy efficiency first increased as acid concentration increased from 0.8% to 1.5%, and then decreased as acid concentration increased from 1.5% to 2%.

Figure 8-13 Effects of acid concentration on energy consumption
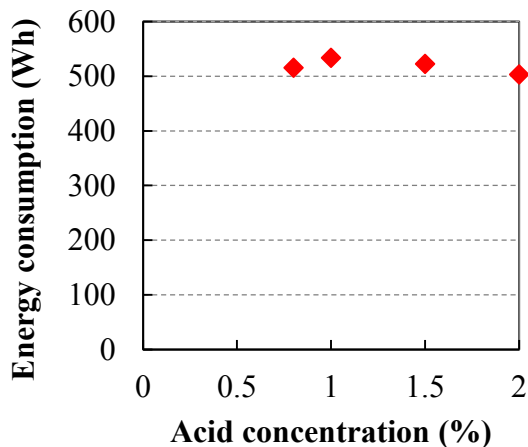
Pretreatment temperature = 140°C, Pretreatment time = 30 min

Figure 8-14 Effects of acid concentration on water usage
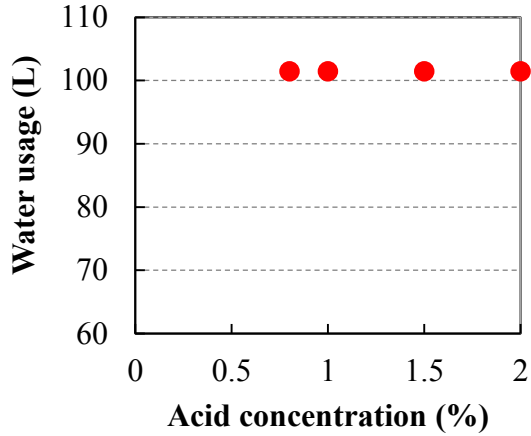
Pretreatment temperature = 140°C, Pretreatment time = 30 min

Figure 8-15 Effects of acid concentration on sugar yield
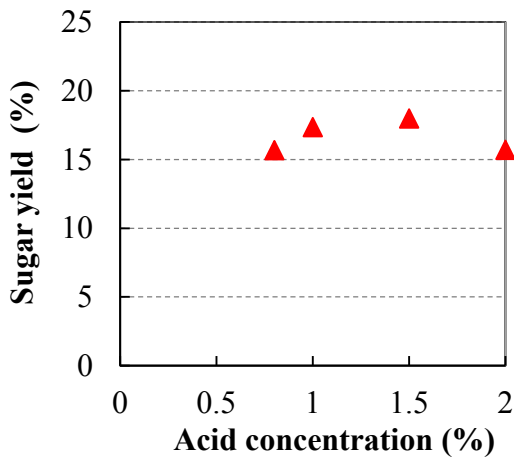
Pretreatment temperature = 140°C, Pretreatment time = 30 min

There are no reports in the literature about effects of acid concentration on energy consumption, water usage, and pretreatment energy efficiency in dilute acid pretreatment of poplar wood. Saha et al. [14] and Baboukani et al. [15] studied effects of acid concentration on sugar yield in enzymatic hydrolysis of dilute acid pretreated wheat straw. Saha et al.'s study showed that sugar yield increased when acid concentration increased from 0.25% to 0.75%, but decreased when acid concentration further increased to 1%. Baboukani et al.'s results showed that sugar yield (glucose yield) increased when acid concentration increased from 0.75% to 2.25%.

Figure 8-16 Effects of acid concentration on pretreatment energy efficiency
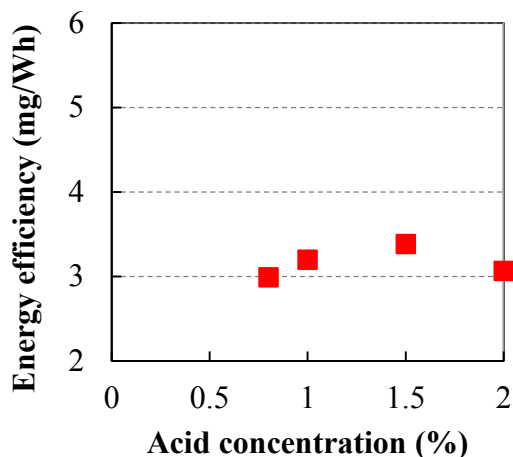
Pretreatment temperature = 140°C, Pretreatment time = 30 min

8.5 Conclusions

In this paper, effects of operating variables (pretreatment time, pretreatment temperature, and acid concentration) in dilute acid pretreatment of poplar wood on energy consumption, water usage, sugar yield, and pretreatment energy efficiency were experimentally studied. The major findings are as follows:

1. As pretreatment time increased from 10 to 30 min, energy consumption, water usage, and sugar yield increased; but pretreatment energy efficiency first increased (when pretreatment time increased from 10 to 20 min) and then decreased slightly.

2. As pretreatment temperature increased from 100°C to 180°C , energy consumption and water usage increased; sugar yield and pretreatment energy efficiency first increased (when pretreatment temperature increased from 100°C to 160°C) and then became constant or decreased slightly.

3. As acid concentration increased (from 0.8% to 2%), energy consumption and water usage did not change noticeably; sugar yield and pretreatment energy efficiency first increased (when acid concentration first increased from 0.8% to 1.5%) and then decreased.

In this study, operating variables were changed one at a time. Their interaction effects could not be revealed and, therefore, the optimized conditions could not be obtained. In the

future, the authors plan to study the interaction effects of operating variables and optimize pretreatment conditions.

Acknowledgements

References

[1]   U.S. Energy Information Administration. Annual Energy Review 2010. http://www.eia.gov/totalenergy/data/annual/ (2011).

[2]   U.S. Energy Information Administration. Short-Term Energy Outlook. http://205.254.135.24/steo/steo_full.pdf (2011).

[3]   U.S. Department of Energy. Environmental Benefits of Biofuels. http://alternativeenergy.procon.org/view.answers.php?questionID=001177 (2008).

[4]   Renewable Fuels Association. Ethanol Facts: Environment. http://www.ethanolrfa.org/pages/ethanol-facts-environment (2011).

[5]   Zhang PF, Pei ZJ, Wang D, et al. Ultrasonic Vibration-Assisted Pelleting of Cellulosic Biomass for Biofuel Manufacturing. *Journal of Manufacturing Science and Engineering*. 133(1), 0110121 − 0110127 (2011).

[6]   Gray KA, Zhao L, Emptage M. Bioethanol. *Current Opinion in Chemical Biology*. 10(2), 141-146 (2006).

[7]   Balatinecz JJ, Kretschmann, DE. Properties and Utilization of Poplar Wood, In: *Poplar Culture in North America*, Canadian Science Publishing (NRC Research Press), Ontario, Canada, (2001).

[8]   Wiselogel A, Tyson S, Johnson D. *Biomass Feedstock Resources and Composition*, Taylor & Francis, Washington, DC, (1996).

[9]   Mosier N, Wyman C, Dale B, et al. Features of Promising Technologies for Pretreatment of Lignocellulosic Biomass. *Bioresource Technology*. 96(6), 673-686 (2005).

[10] Ayhan D. Progress and Recent Trends in Biofuels. *Progress in Energy and Combustion Science*. 33(1), 1–18 (2007).

[11] Lynd LR. Overview and Evaluation of Fuel Ethanol from Cellulosic Biomass: Technology, Economics, the Environment, and Policy. *Annual Review of Energy and the Environment*. 21(1), 403-465 (1996).

[12] Zhu JY, Wang GS, Pan XJ, Gleisner R. Specific Surface to Evaluate the Efficiencies of Milling and Pretreatment of Wood for Enzymatic Saccharification. *Chemical Engineering Science*. 64(3), 474-485 (2009).

[13] Zhu JY, Pan XJ, Wang GS, Gleisner R. Sulfite Pretreatment (SPORL) for Robust Enzymatic Saccharification of Spruce and Red Pine. *Bioresource Technology*. 100(8), 2411-2418 (2009).

[14] Zhu W, Zhu JY, Gleisner R, Pan XJ. On Energy Consumption for Size-Reduction and Yields from Subsequent Enzymatic Saccharification of Pretreated Lodgepole Pine. *Bioresource Technology*. 101(8), 2782-2792 (2010).

[15] von Sivers M, Zacchi G. Ethanol from Lignocellulosics: A Review of the Economy. *Bioresource Technology*. 56(2-3), 131-140 (1996).

[16] Rubin EM. Genomics of Cellulosic Biofuels. *Nature*. 454(7206), 841-845 (2008).

[17] Houghton J, Weatherwax S, Ferrell J. Breaking the Biological Barriers to Cellulosic Ethanol: A Joint Research Agenda. U.S. Department of Energy. http://genomicscience.energy.gov/biofuels/2005workshop/2005low_bioprocess.pdf (2005)

[18] Sluiter A, Hames B, Hyman D, et al. Determination of Total Solids in Biomass and Total Dissolved Solids in Liquid Process Samples. Laboratory Analytical Procedure (LAP), *NREL*, Golden, CO, (2008).

[19] Herman S. *Electrical Studies for Trades*. Cengage Learning. Baytown, Texas (2009).

[20] Selig M, Weiss N, Ji Y. Enzymatic Saccharification of Lignocellulosic Biomass. Laboratory Analytical Procedure (LAP), *NREL*, Golden, CO, (2008).

[21] Saha BC, Iten LB, Cotta MA, Wu YV. Dilute Acid Pretreatment, Enzymatic Saccharification, and Fermentation of Wheat Straw to Ethanol. *Process Biochemistry*. 40(12), 3693-3700 (2005).

[22]   Baboukani BS, Vossoughi M, Alemzadeh I. Optimisation of Dilute-acid Pretreatment Conditions for Enhancement Sugar Recovery and Enzymatic Hydrolysis of Wheat Straw. *Biosystems Engineering*. 111(2), 166-174 (2012).

[23]   Saha BC, Iten LB, Cotta MA, Wu YV. Dilute Acid Pretreatment, Enzymatic Saccharification, and Fermentation of Rice Hulls to Ethanol. *Biotechnology Progress*. 21(3), 816-822 (2005).

Chapter 9 - A Predictive Model for Energy Consumption in Dilute Acid Pretreatment

Authors' names:

Xiaoxu Song, Meng Zhang, Z.J. Pei, A.J. Nottingham, and Pengfei Zhang

Authors' affiliation:

Department of Industrial and Manufacturing Systems Engineering, Kansas State University, Manhattan KS 66506 USA

Abstract

Response surface methodology was used to study effects of parameters namely, time, temperature, and solid content and to optimize the process conditions for the minimum energy consumption in dilute acid pretreatment. Box-Behnken design using response surface methodology was employed. Effects of time and temperature are significant at the significance level of $\alpha=0.05$. Longer time and higher temperature result in higher power energy consumption. The optimal values of the process conditions are times 14-21 min and temperatures 129-139 °C.

9.1 Introduction

Ninety three percent of the transportation fuels consumed in the U.S. in 2011 are petroleum based [1]. About half of the petroleum used in the U.S. is imported [2]. One big issue of using petroleum-based transportation fuels is greenhouse gas (GHG) emissions. In order to reduce the dependence on foreign petroleum and GHG emissions, it is imperative to produce and use non petroleum-based fuels made from domestic resources. One such example is cellulosic biofuels.

Biofuels have the potential to reduce GHG emissions by as much as 86% [3]. Because biofuels are made from renewable, plant-based feedstocks, the carbon dioxide released during fuel combustion is "recycled" by plants as they grow [4].

Cellulosic biofuels are made from cellulosic biomass (including wood, agricultural residues, and herbaceous energy crops). Unlike other type of feedstocks (e.g. corn, sugar cane, and soybean) for biofuels, cellulosic biomass does not compete with food production for limited agricultural land [5,6].

Major processes of biofuel manufacturing from cellulosic biomass are listed in Figure 9-1. To produce biofuels from cellulosic biomass, its size needs to be reduced first [7–10]. Pretreatment makes cellulose more accessible to the enzyme in the following hydrolysis step [11]. Hydrolysis breaks down cellulose into sugars (glucose) that are converted to ethanol by fermentation [11–13].

114

Figure 9-1 Major processes of biofuel production from cellulosic biomass (after [7])
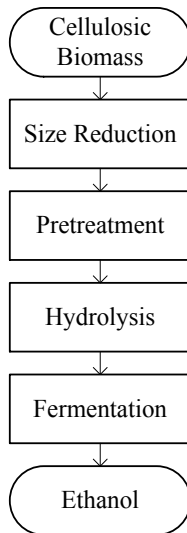
```
   ( Cellulosic )
   (  Biomass   )
        |
        v
 [ Size Reduction ]
        |
        v
 [  Pretreatment  ]
        |
        v
 [   Hydrolysis   ]
        |
        v
 [  Fermentation  ]
        |
        v
   (   Ethanol   )
```

Dilute acid pretreatment has been applied to various types of cellulosic biomass including softwood, hardwood, agricultural residues, and herbaceous energy crops. However, no model has been reported in the literature to predict the optimum values of process parameters to achieve minimum energy consumption in pretreatment of wheat straw. This paper develops a predictive model, using the response surface methodology (RSM), for energy consumption in dilute acid pretreatment. The experimental data obtained were used for the optimization of the process conditions by means of response surface methodology (RSM) under Box-Behnken design. RSM is an effective statistical technique for optimizing multifactor experiments, building models, evaluating effects of several factors for desirable responses. The eventual objective of RSM is to determine the optimum operating conditions for the system, or to determine the region which satisfies the operating specifications [14]. RSM was also reported to optimize the process of biofuel production [15], but this was the first time that RSM was adopted to optimize energy consumption in dilute acid pretreatment.

9.2 Experimental procedure and conditions

9.2.1 Material preparation

The cellulosic biomass used in this study was wheat straw. Wheat straw was harvested by Deines Farm in Northwest Kansas. The wheat straw had been run through a John Deere 9600 combine. The combine removed grains from the straw and chaff. Wheat straw and chaff exited

through the back of the combine. The average length of the wheat straw was 250 mm. After being collected, wheat straw was stored indoors until this study.

Wheat straw was processed by a knife mill (Model SM 2000 from Retsch, Inc., Haan, Germany) (shown in Figure 9-2). The knife mill used a 240-volt, 3-horsepower electric motor with a fixed rotation speed (1720 rpm). Three cutting blades (95 mm long and 35 mm wide) were mounted on the rotor. Four shear bars were mounted on the inside wall of the milling chamber. There was a 3-mm gap between a cutting blade and a shear bar. Biomass was cut between the cutting blades and the shear bars. The sieves used in the knife mill were of 1 mm in the size of the openings.

Figure 9-2 Knife mill

Shear bars   Cutting blades   Sieve
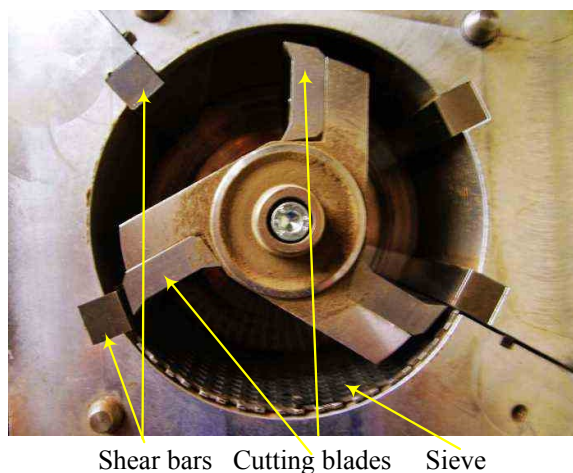
9.2.2 Experimental setup and procedure

Pretreatment was carried out in the 600-mL reaction vessel of a Parr pressure reactor (Parr Instrument Company, Moline, IL) (Figure 9-3). Wheat straw was mixed with diluted sulfuric acid (2%) to obtained biomass slurry with 5% solid content (10 g of wheat straw in 200 mL of diluted sulfuric acid). The slurry was loaded into the reaction vessel. When pretreatment started, the heater was manually switched on to begin heating the reaction vessel. The valve was manually turned on to let the reactor controller to allow tap water to enter into the cooling loop as needed.

Pretreatment temperature was the reaction temperature in the reaction vessel and can be set on the reactor controller. A thermocouple in the reaction vessel was connected to the reactor controller.

When the temperature measured by the thermocouple reached the pre-set pretreatment temperature, a timer was used to record the pretreatment time. Pretreatment time was the period of time when the biomass slurry was treated at the pretreatment temperature in the reaction vessel.

Figure 9-3 Illustration of pretreatment reactor
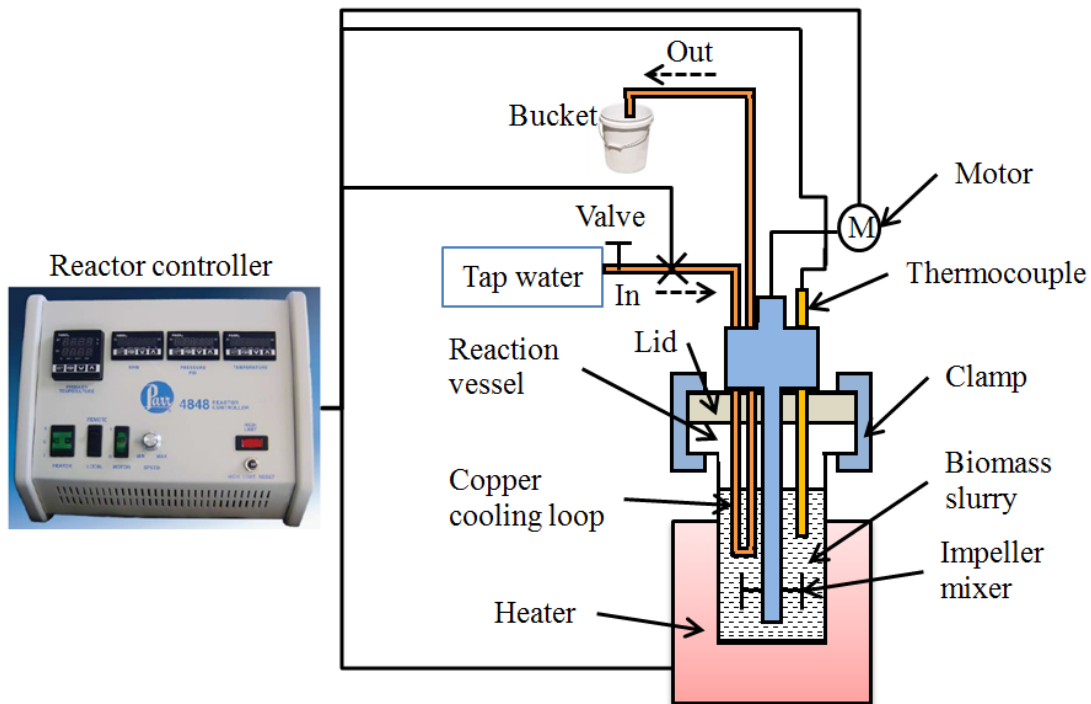
When the temperature measured by the thermocouple was above the pre-set pretreatment temperature, the heater stopped heating the vessel and tap water started entering into the cooling loop (controlled by the reactor controller) till the temperature became equal to the pre-set pretreatment temperature.

When the temperature measured by the thermocouple was below the pre-set pretreatment temperature, tap water stopped entering into the cooling loop (controlled by the reactor controller) and the heater started heating the vessel till the temperature became equal to the pre-set pretreatment temperature.

When the pretreatment was finished, the heater was manually switched off. Then, the temperature on the reactor controller was set to 60°C to decrease the temperature in the reaction vessel. The time between the heater was manually switched on and off was recorded by a timer and is referred to as heating time (Figure 9-4). The period of time during which the temperature

increased to the pre-set pretreatment temperature or decreased to 60°C was not included in the pretreatment time.

The impeller mixer was connected to the motor and the rotation speed of the impeller mixer was 120 rpm. Important concepts used in this paper are illustrated in Figure 9-4.

Figure 9-4 Illustration of important concepts in this study
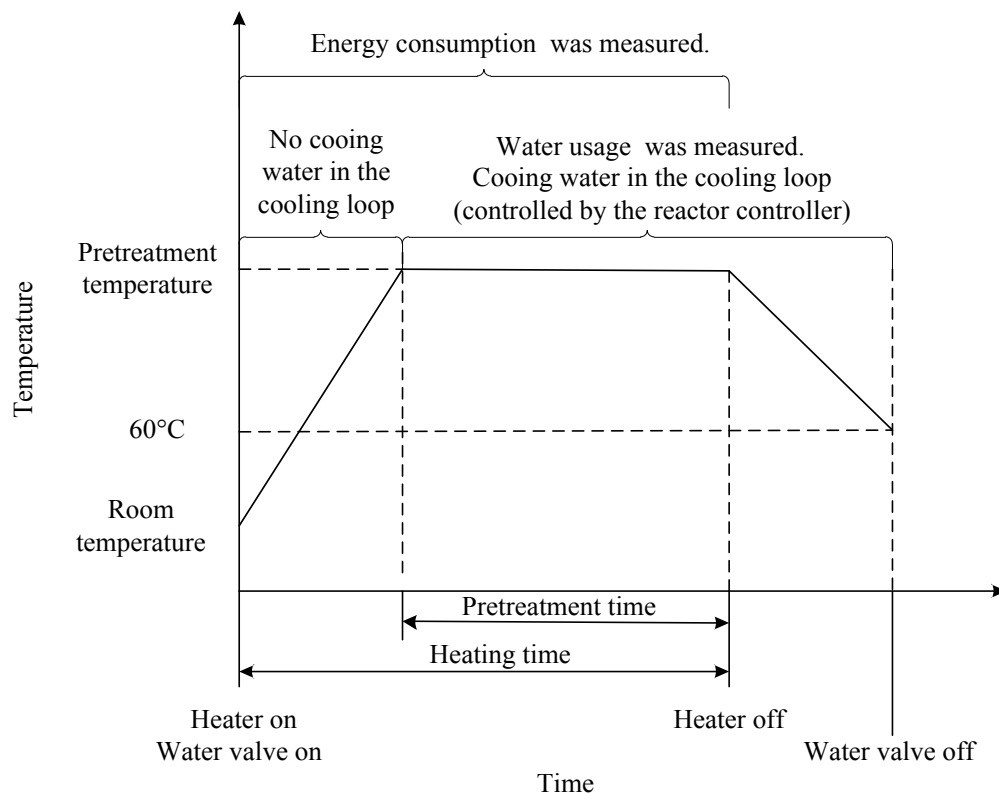
9.2.3 Measurement of energy consumption

Energy consumption in this paper is the electrical energy consumed by the reactor during heating time. A Fluke 189 multimeter and Fluke 200 AC current clamp were used to measure the electric current, as shown in Figure 9-5. The power line to the reactor had three wires: black, red, and green wires. The current clamp was clamped on the black wire to measure the current. The data was collected using Fluke View Forms software. The sampling rate was 2 per second. Fluke View Forms software started collecting data when the heater was manually switched on, and stopped collecting data when the heater was manually switched off.

118

Figure 9-5 Experimental setup for pretreatment and energy consumption measurement
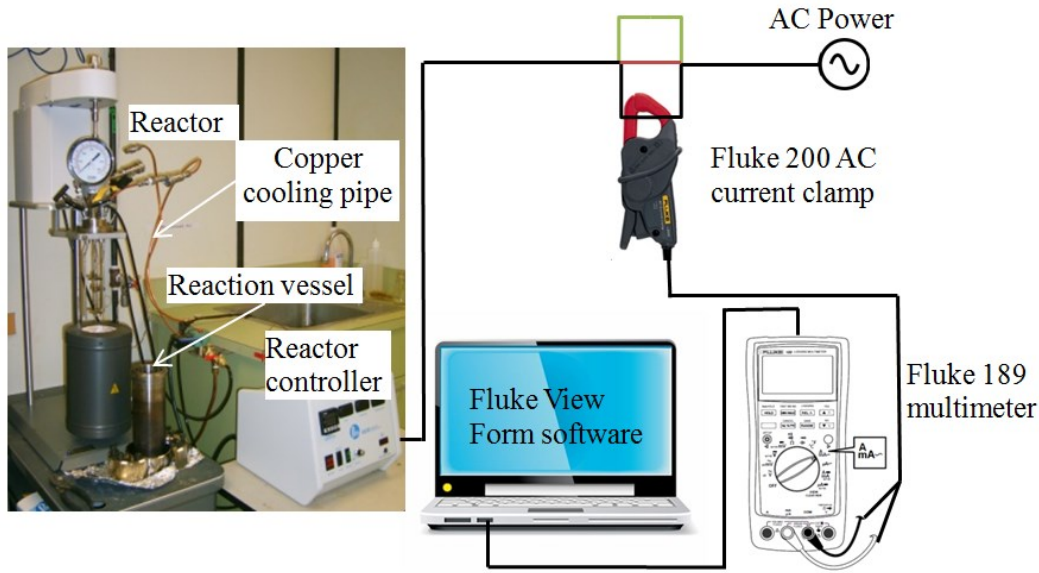
The software also recorded the average current (I_{AVE}) for each test. The voltage (V) was 120 V. The total energy consumed during heating time can be calculated using the following equation [16]:

$$E(Wh) = V(V) \times I_{AVE}(A) \times heatingtime\ (h) \tag{1}$$

9.2.4 Response surface methodology

The Box-Behnken design was employed to optimize the processing conditions of pretreatment. Three coded levels were used for the process parameters, as shown in Table 9-1. In this study, a random order of 15 conditions was generated by Minitab 16 (Minitab, Inc., State College, PA, U.S.). The behavior of the system was explained by the following equation:

$$E = \beta_0 + \sum \beta_i X_i + \sum \beta_{ij} X_i X_j + \sum \beta_{ij} X_i^2 \tag{2}$$

where β represents the coefficient for each term and X represents condition parameter.

9.3 Response surface model

Through analysis in Minitab 16, a response surface model for energy consumption was obtained. Analysis of variance (ANOVA) (Table 9-2) was then performed to remove the insignificant terms (p-value > 0.05), resulting in the following model:

$$E = 2584.18 + 4.27554 \times X_1 - 36.5565 \times X_2 + 0.14229 \times X_2^2 \tag{3}$$

where E, X_1, and X_2 represent energy consumption, time, and temperature, respectively.

Table 9-1 Experimental design and results

Run order	Time (min)	Temperature (°C)	Solid content (g)	Energy consumption (Wh)
1	10	140	20	345
2	10	160	15	358
3	20	120	10	356
4	20	140	15	261
5	30	120	15	349
6	30	160	15	524
7	20	160	20	456
8	30	140	10	350
9	20	160	10	516
10	30	140	20	432
11	10	120	15	266
12	20	140	15	276
13	10	140	10	345
14	20	140	15	276
15	20	120	20	356

Table 9-2 Significance of regression coefficients for the energy consumption using Minitab 16

Term	Coefficients	T	p-value
Constant	304.407	11.618	0.000
Time	42.755	2.665	0.045
Temperature	65.707	4.095	0.009
Solid content	2.714	0.169	0.872
Time × Time	8.358	0.354	0.738
Temperature × Temperature	61.455	2.602	0.048
Solid content × Solid content	55.178	2.336	0.067
Time × Temperature	20.604	0.908	0.406
Time × Solid content	20.391	0.899	0.410
Temperature × Solid content	−14.964	−0.659	0.539

The coefficient of determination $R^2 = 0.7027$, which was defined as the ratio of the explained variation to the total variation. This suggests that the response surface model could provide good predictions. The lack-of-fit test showed that the lack-of-fit was insignificant, indicating that the model fit well the experimental data.

The response surface model explicitly relates the energy consumption to the process parameters. The energy consumption can be predicted from the response surface model as long as the process parameters varied within the ranges tested in this study.

9.4 Predicted effects of process parameters

The ANOVA showed that time (p-value = 0.045), and temperature (p-value = 0.009) had significant effects on energy consumption at the significance level of $\alpha = 0.05$.

9.4.1 Effects of time

Effects of time on energy consumption, predicted by Eq. (3), are shown in Figure 9-6. Energy consumption increased as pretreatment time increased from 10 min to 30 min for different levels of temperature.

9.4.2 Effects of temperature

Effects of temperature on energy consumption, predicted by Eq. (3), are shown in Figure 9-7. Energy consumption decreased as temperature increased from 120 °C to 130 °C and increased as temperature increased from 130 °C to 160 °C for different levels of time.

9.4.3 Interaction effects

The response surface contour plots of energy consumption versus the interaction effects between temperature and time are shown in Figure 9-8. The minimum energy consumption is indicated by the surface confined in the smallest curve (elliptical) of the contour plot. The studies of the contour plot also reveal the best optimal values of the process conditions and are given below: times 14-21 min and temperatures 129-139 °C, and times 10-13 min and temperatures 120-128 °C. A small square region in the left corner in Figure 9-8 is also the minimum values of energy consumption. However, considering other outputs in the following process (e.g. enzymatic hydrolysis), process conditions in pretreatment is the longer time and the higher

temperature the better [17]. So the compromised best optimal values of the process conditions are time 14-21 min and temperature 129-139 °C.

Figure 9-6 Effects of time on energy consumption
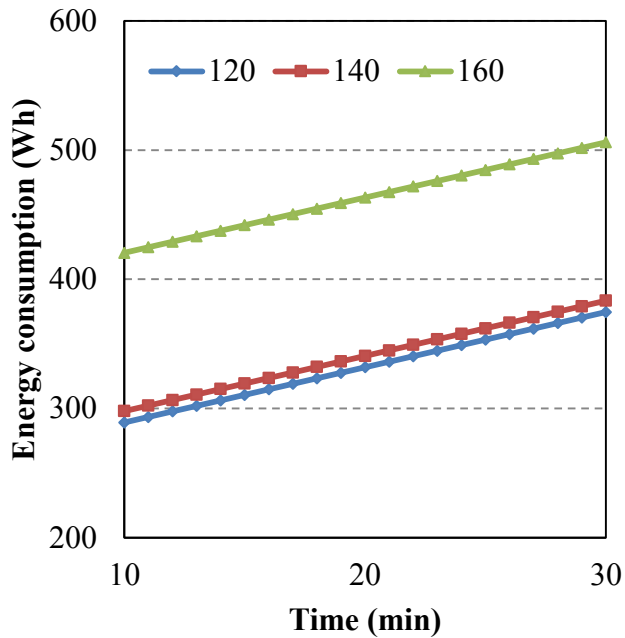
Figure 9-7 Effects of temperature on energy consumption
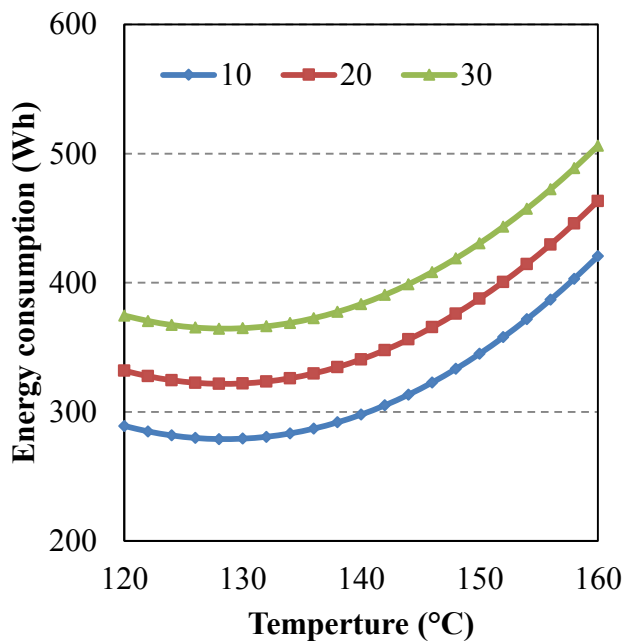
Figure 9-8 Response surface contour plots showing interactive effect of temperature and time on energy consumption

Contour Plot of E vs Temperture, Time
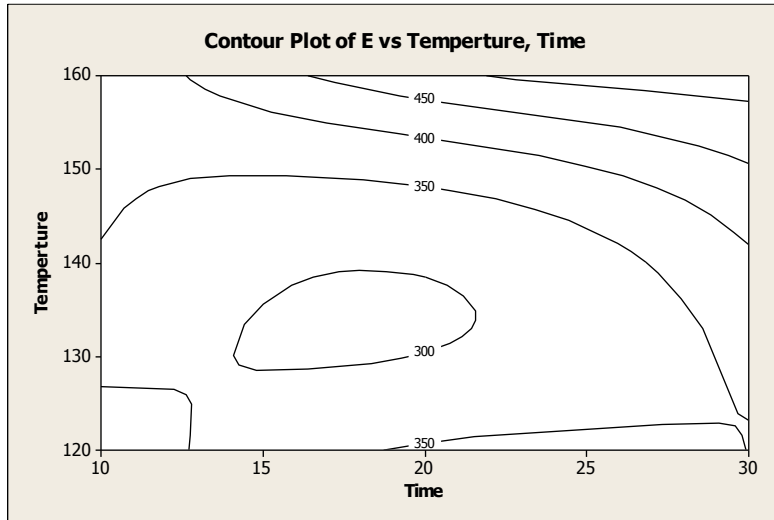
9.5 Conclusions

This paper presents the use of Box-Behnken design to determine the optimum process conditions leading to the minimum energy consumption in pretreatment. Using this experimental design, the parameters (namely, time, temperature, and solid content) were studied and optimized with a smaller number of experiments. This methodology could also be successfully employed to study the importance of individual and interaction effects of the test variables in enzymatic hydrolysis and other processes.

The following conclusions can be drawn from this study:

(1) Main effects of time and temperature are significant at the significance level of $\alpha = 0.05$. Longer time and higher temperature result in higher power energy consumption.

(2) The best optimal values of the process conditions are times 14-21 min and temperatures 129-139 °C.

Acknowledgments

References

[1]   U.S. Energy Information Administration, 2012, "Annual Energy Review 2011," http://www.eia.gov/totalenergy/data/annual/pdf/aer.pdf.

[2]   U.S. Energy Information Administration, 2011, "Short-Term Energy Outlook," http://205.254.135.24/steo/steo_full.pdf.

[3]   U.S. Department of Energy, 2008, "Environmental Benefits of Biofuels."

[4]   RFA, 2011, "Ethanol Facts: Environment," http://www.ethanolrfa.org/pages/ethanol-facts-environment.

[5]   Zhang P., Pei Z., Wang D., Wu X., Cong W., Zhang M., and Deines T., 2011, "Ultrasonic Vibration-Assisted Pelleting of Cellulosic Biomass for Biofuel Manufacturing," Journal of manufacturing science and engineering, **133**(1).

[6]   Gray K. A., Zhao L., and Emptage M., 2006, "Bioethanol," Current Opinion in Chemical Biology, **10**(2), pp. 141–146.

[7]   Lynd L. R., 1996, "Overview and Evaluation of Fuel Ethanol from Cellulosic Biomass: Technology, Economics, the Environment, and Policy," Annual review of energy and the environment, **21**(1), pp. 403–465.

[8]   Zhu J. Y., Wang G. S., Pan X. J., and Gleisner R., 2009, "Specific Surface to Evaluate the Efficiencies of Milling and Pretreatment of Wood for Enzymatic Saccharification," Chemical Engineering Science, **64**(3), pp. 474–485.

[9]   Zhu J. Y., Pan X. J., Wang G. S., and Gleisner R., 2009, "Sulfite Pretreatment (SPORL) for Robust Enzymatic Saccharification of Spruce and Red Pine," Bioresource Technology, **100**(8), pp. 2411–2418.

[10]   Zhu W., Zhu J. Y., Gleisner R., and Pan X. J., 2010, "On Energy Consumption for Size-Reduction and Yields from Subsequent Enzymatic Saccharification of Pretreated Lodgepole Pine," Bioresource Technology, **101**(8), pp. 2782–2792.

[11]   von Sivers M., and Zacchi G., 1996, "Ethanol from Lignocellulosics: A Review of the Economy," Bioresource Technology, **56**(2-3), pp. 131–140.

[12]   Rubin E. M., 2008, "Genomics of Cellulosic Biofuels," Nature, **454**(7206), pp. 841–845.

[13]   U.S. Department of Energy, 2009, "Breaking the Biological Barriers to Cellulosic Ethanol: A Joint Research Agenda" [Online]. Available: http://genomicscience.energy.gov/biofuels/b2bworkshop.shtml.

[14]   Salamatinia B., Mootabadi H., Bhatia S., and Abdullah A. Z., 2010, "Optimization of ultrasonic-assisted heterogeneous biodiesel production from palm oil: A response surface methodology approach," Fuel Processing Technology, **91**(5), pp. 441–448.

[15]   Xu F., Theerarattananoon K., Wu X., Pena L., Shi Y.-C., Staggenborg S., and Wang D., 2011, "Process optimization for ethanol production from photoperiod-sensitive sorghum: Focus on cellulose conversion," Industrial Crops and Products, **34**(1), pp. 1212–1218.

[16]   Herman S., 2009, Electrical Studies for Trades, Cengage Learning, Baytown, Texas.

[17]   Song X. X., Zhang M., Pei Z. J., and Wang D. H., 2012, "Preliminary study on pretreatment of poplar wood for biofuel production," Biofuels, **3**(5), pp. 525–533.

Chapter 10 - Ultrasonic-assisted dilute acid pretreatment of poplar wood for biofuel manufacturing

Authors' names:

Xiaoxu Song[a], Meng Zhang[a], Z.J. Pei[a], and Donghai Wang[b]

Authors' affiliation:

[a]Department of Industrial and Manufacturing Systems Engineering, Kansas State University, Manhattan KS 66506 USA

[b]Department of Biological and Agricultural Engineering, Kansas State University, Manhattan, KS 66506, USA

Abstract

For the first time, this study demonstrated that the efficiency of enzymatic hydrolysis of poplar wood biomass was drastically enhanced after being pretreated with ultrasonic-assisted dilute acid pretreatment comparing to dilute acid pretreatment only. Three levels of ultrasonic power (0%, 30%, and 70%) were used in pretreatment. Approximately 10-40% improvement in the sugar yield was attained by using ultrasound-assisted dilute acid pretreatment for 15 min. XRD analysis revealed that poplar wood biomass pretreated ultrasonically had lower biomass crystallinity than that pretreated with dilute acid only. The combination of ultrasound irradiation and dilute acid can be a key factor in the disruption of rigid cellulose structures and contribute to the improvement of cellulose saccharification in enzymatic hydrolysis.

Keywords

Cellulosic biomass, Biofuel, Hydrolysis, Poplar wood, Pretreatment, Ultrasound

10.1 Introduction

Cellulosic biomass (including agricultural and forestry residues and dedicated energy crops) has been widely used as renewable resources of fermentable sugars for bioconversion into ethanol biofuel [1-4]. Bioconversion of cellulosic biomass into ethanol biofuel generally consists of the following steps: (i) size reduction of cellulosic biomass to reduce the biomass particle size [5-11]; (ii) pretreatment of cellulosic biomass to break the lignin seal, disrupt the crystalline structure of cellulose making cellulose more accessible to enzymes in the subsequent enzymatic hydrolysis [12]; (iii) enzymatic hydrolysis of cellulose to fermentable sugars; and (iv) fermentation of the sugars to ethanol biofuel [13, 14]. Among these steps, pretreatment of cellulosic biomass can be the most expensive process, but it has great potential for improvement in efficiency and lowering of costs [15, 16].

Various pretreatment methods for cellulosic biomass have been attempted to break the lignin seal, disrupt the crystalline structure of cellulose. These pretreatments can be classified into physical pretreatment methods (e.g. size reduction [10, 11, 17-20] and gamma ray pretreatment [21]), physicochemical pretreatment methods (e.g. steam explosion [22] and ammonia fiber explosion [23]), chemical pretreatment methods (e.g. dilute acid pretreatment [24], alkaline pretreatment [25], organic solvent pretreatment [26] and oxidative delignification

[27]), and biological pretreatment methods (e.g. lignin degradation by fungi [28]). Among these methods, dilute acid pretreatment is a practical and effective method of breaking the lignin seal and disrupting the crystalline structure of cellulose [29]. However, high temperature, high pressure, and long pretreatment time are needed for dilute acid pretreatment. These severe pretreatment conditions may result in the formation of polysaccharide degradation products that may lower the overall sugar yield and inhibit microbes during fermentation [29, 30]. The use of ultrasound irradiation in dilute acid pretreatment may provide a practical solution to improve biomass sugar yield in the subsequent enzymatic hydrolysis and may cut down the cost by gentling the conditions of dilute acid pretreatment.

Ultrasound is a sound wave with frequency greater than the upper limit of the human hearing range. When ultrasound is applied to a medium such as a liquid or slurry, it produces cavitation bubbles [31] and acoustic streaming [32]. The implosion of cavitation bubbles generates powerful hydro-mechanical shear forces, high temperature, and pressure in the liquid [33], which disintegrates nearby particles. The main benefit of streaming in slurry processing is mixing, which facilitates the uniform distribution of ultrasound irradiation energy within the slurry mass, convection of the liquid and dissipation of any heating that occurs [34].

Ultrasound irradiation has been applied widely to various biological and chemical processes. It has been reported that ultrasound irradiation could increase the porosity of cellulose fiber and the cleavage of linkages in lignin [35-37]. The use of ultrasound could reduce cellulosic biomass particle size [38], decrease crystallinity [39], increase its available surface area [38], and improve the efficiency of enzymatic hydrolysis of cellulosic biomass [38, 39]. Velmurugan et al. [40] also reported that ultrasound-assisted alkaline pretreatment could improve process efficiency by reducing pretreatment time and temperature. Table 10-1 summarizes reported investigations in ultrasonic-assisted pretreatment of cellulosic biomass.

However, there was no report in the literature about applying ultrasound irradiation to dilute acid pretreatment of cellulosic biomass to enhance the efficiency of subsequent enzymatic hydrolysis. This study was aimed to do the preliminary test of ultrasonic-assisted dilute acid pretreatment. Effects of this pretreatment method on sugar yield of pretreated poplar wood biomass were investigated. The crystallinity of poplar wood biomass pretreated ultrasonically in dilute sulfuric acid was also analyzed.

Table 10-1 Summary of the reported investigations in ultrasonic-assisted pretreatment of cellulosic biomass

Reference	Biomass material	Solution	Sugar yield
Toma et al. [38]	Microcrystalline cellulose	Water	(%)
Ninomiya et al. [39]	Kenaf	Ionic liquids (ILs)	(%)
Velmurugan et al. [40]	Sugarcane bagasse	NaOH	(%)
Sasmal et al. [50]	Areca nut husk, bon bogori, and moj	Lime	(%)
Marx-Figini [51]	Cotton cellulose	Ethyl acetate	N.A.
Xiong et al. [52]	Cotton cellulose	Methyl alxohol	N.A.
Tang et al. [53]	Eucalyptus pulp	Sodium periodate	N.A.
Wang et al. [46, 54]	Microcrystalline cellulose	Water	N.A.
Wong et al. [47]	Bacterial cellulose	Cuprammonium hydroxide solution	N.A.

10.2 Experimental setup and measurement procedure

10.2.1 Material

Cellulosic biomass used in this investigation was poplar wood chips purchased from Petco Animal Supplies, Inc. (Manhattan, KS, USA). Poplar wood chips were milled into particles using a knife mill (Model SM 2000, Retsch, Inc., Haan, Germany). The knife mill was equipped with a 240-V, 3-HP electric motor with a fixed rotation speed (1,720 rpm). Three cutting blades (95 mm long and 35 mm wide) were mounted on the rotor. Four shear bars were mounted on the inside wall of the milling chamber. The gap between one cutting blade and one shear bar was 3 mm. Poplar wood chips were cut between the cutting blades and the shear bars. The sieve size used in the knife mill was 1 mm. Poplar wood chips remained in the milling chamber until they were small enough to pass through the openings on the sieve. After knife milling, particles were collected from the receiving container. They were kept in sealed Ziploc® bags and stored in a refrigerator at 4°C until further processing.

The moisture content of poplar wood chips (the amount of moisture (water) contained in the poplar wood chips) was 1.6%. It was measured by following the National Renewable Energy Laboratory (NREL) analytical procedure [41]. 25 g biomass sample was dried in an oven (Blue M Electric Co., Blue Island, IL, USA) at 105°C for 24 h to get rid of the moisture in the biomass

completely. The weight loss of the biomass sample was measured as moisture. Moisture content was calculated as follows:

$$Moisture\ content = \left(\frac{Sample\quad weight\quad loss}{Original\quad sample\quad weight} \right) \times 100\% \qquad Eq\ (5)$$

The chemical composition of poplar wood chips was measured by following the NREL analytical procedure [42]. Duplicate samples were employed. Structural carbohydrates in poplar wood chips were reported as the percentages of cellulose and hemicellulose. Lignin, the major non-carbohydrate component, was reported as the percentage of the sum of acid-insoluble and acid-soluble lignin. The percentage of ash content was also reported. Table 10-2 lists the chemical composition of the poplar wood chips.

Table 10-2 Chemical composition of poplar wood chips

Component	Percentage on dry weight basis
Cellulose	41.1 ± 0.4
Hemicellulose	22.9 ± 0.3
Lignin	24.0 ± 0.7
Ash	2.9 ± 0.1

10.2.2 Ultrasonic-assisted dilute acid pretreatment

Figure 10-1 is a schematic illustration of the experimental set-up for ultrasonic-assisted dilute acid pretreatment. Pretreatment experiments were performed on a modified ultrasonic machine (Model AP-1000, Sonic-Mill Inc., Albuquerque, NM, USA) with a heated water bath. The water bath was a 30 cm * 40 cm stainless steel basin. Pretreatment temperature was measured using a straight needle probe inserted into the water in the water bath as shown in Figure 10-1. The straight needle probe was connected to a thermometer (HH147U, OMEGA Engineering, Inc., Stamford, CT, USA). The machine included a power supply (which converts 60 Hz electrical power into 20 kHz electrical power), a converter (which converts high frequency electrical power into mechanical vibration), and a horn (which amplifies and transfers the vibration). The tip of the horn was a solid cylinder with a flat end with a diameter of 17.4 mm. The frequency of the ultrasonic irradiation generated by this ultrasonic machine is 20 kHz.

Figure 10-1 Schematic illustration of the experimental set-up for ultrasonic-assisted dilute acid pretreatment
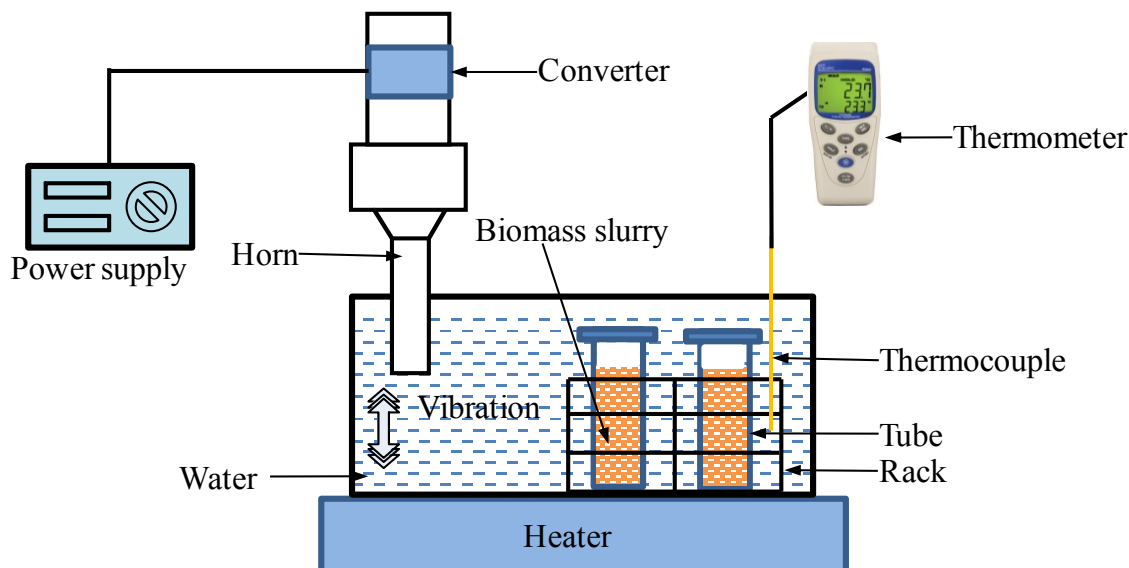
Poplar wood particles were mixed with 2% (w/v) diluted sulfuric acid to obtain biomass slurry with 4% solid content (2 g of biomass in 50 mL of diluted sulfuric acid). The biomass slurry was loaded into a 50-ml centrifuge tube (Corning Incorporated, Tewksbury, MA, USA) and sealed with cap. For each pretreatment condition, four tubes with the same content were held by a rack and immersed in the water bath. The horn of the ultrasonic machine extended into the water bath and maintained at a position where its end was 30 mm under the water level. Pretreatment time was the period when the tubes containing biomass slurry were treated at the pretreatment temperature in the water bath. Pretreatment conditions are listed in Table 10-3. Ultrasonic-assisted dilute acid pretreatment was conducted three times under each pretreatment condition.

Table 10-3 Value of ultrasonic-assisted dilute acid pretreatment variables

Variable	Unit	Value
Ultrasonic power	%	0, 30, 70
Pretreatment time	min	15, 30
Pretreatment temperature	°C	60
Acid concentration	% (w/v)	2

% (w/v) referred to as gram of acid in 100 mL of solution

After pretreatment, pretreated poplar wood biomass was washed with 50-60°C distilled water using a suction filtration system with P4 grade filter paper (Fisher Scientific Inc.,

Waltham, MA, USA) to conduct solid-liquid separation. The solid biomass after filtration was carefully collected from the filter paper using a stainless steel micro spatula. The dry weight of the collected solid biomass was measured.

10.2.3 Enzymatic hydrolysis

Enzymatic hydrolysis was carried out in 125-mL flasks in a water bath shaker (Model C76, New Brunswick Scientific, Edison, NJ, USA) with agitation speed of 110 rpm at 50°C for 72 h. Each flask contained 50 mL of hydrolysis slurry. The slurry consisted of 5% (w/v) ultrasonic-assisted dilute acid pretreated poplar wood biomass on dry weight base, sodium acetate buffer (50 mM, pH = 4.8), and 0.02% (w/v) sodium azide to prevent microbial growth during hydrolysis. Accellerase 1500^{TM} enzyme complex (Danisco USA, Inc., Rochester, NY, USA) was used. The enzyme loaded was 1 mL for each gram of dry biomass.

After hydrolysis for 72 h, 0.1 mL of slurry was withdrawn from each flask, and mixed with 0.9 mL of double distilled water in a 1.5-mL micro-centrifuge tube. The caped tubes were placed into boiling water for 15 min to deactivate the enzyme. Afterwards, the tubes were centrifuged at 10,000 rpm for 15 min to separate supernatant liquid from solid biomass residues using a micro-centrifuge (Model RS-102, Revolutionary Science, Shafer, MN, USA). Supernatant liquid from each tube was filtered through a 0.2-μm hydrophilic PTFE syringe filter (EMD Millipore, Billerica, MA, USA). Filtered supernatant liquid was kept in 1.5-mL autosampler vials at 4°C in a refrigerator before glucose concentration measurement.

10.2.4 Measurement of sugar yield

Glucose concentration was measured using high performance liquid chromatography (HPLC). The HPLC (Shimadzu, Kyoto, Japan) system was equipped with an RPM-monosaccharide column (300 × 7.8 mm; Phenomenex, Torrence, CA, USA) and a refractive index detector (RID-10A, Shimadzu, Kyoto, Japan). The mobile phase was 0.6 mL/min of degassed double-distilled water, and the column oven temperature was 80°C.

As shown in Eqs (2) and (3), hydrolysis sugar yield (Y_h) (g glucose/g dry biomass) was calculated as the glucose yield (g) per unit dry weight (1 g) of biomass loaded into enzymatic hydrolysis. Total sugar yield (Y_t) (g glucose/g dry biomass) was calculated as the glucose yield (g) per unit dry weight (1 g) of biomass loaded into ultrasonic-assisted dilute acid pretreatment.

$$Y_h = \frac{G \times V}{M_h}$$
Eq (2)

$$Y_t = \frac{M_{pret} \times G \times V}{M_{or} \times M_h}$$
Eq (3)

where M_{pret} is the dry weight (g) of biomass after pretreatment, M_{or} is the dry weight (g) of biomass loaded into pretreatment, M_{pret} was always smaller than M_{or}. This is due to the biomass weight loss in pretreatment. M_h is the dry weight (g) of biomass loaded in enzymatic hydrolysis (2.5 g for all the samples processed in different pretreatment conditions). G is the glucose concentration (g/L) measured by HPLC, V is the total volume (L) of the hydrolysis slurry, and is kept at 0.05 L for all the hydrolysis samples.

10.2.5 Measurement of crystallinity

Cellulose in cellulosic biomass consists of crystalline regions and amorphous regions. Crystallinity is determined as the percentage of crystalline material in cellulose, and it is expressed as crystallinity index (CI) [43]. Higher CI means that cellulose has a higher percentage of crystalline regions. It has been suggested that amorphous regions degrade more easily than crystalline regions [44, 45]. Therefore, a higher CI is usually associated with lower enzyme accessibility and, thus, lower sugar yield in hydrolysis. In this study, crystallinity was measured by an X-ray diffractometer (XRD) (Model MiniFlex II, Rigaku Americas Corp., The Woodlands, TX, USA), and CI was calculated using analysis software Rigaku PDXL (Version 1.6.0.0, Rigaku Americas Corp., The Woodlands, TX, USA).

10.3 Results and discussion

To examine effects of ultrasonic power used in ultrasonic-assisted dilute acid pretreatment on poplar wood biomass sugar yield, the pretreated biomass particles were subjected to enzymatic hydrolysis. Sugar yield results were presented using both hydrolysis sugar yield (Y_h) and total sugar yield (Y_t). Y_h reflects mainly the efficiency of enzymatic hydrolysis; while Y_t represents the combined effects of the pretreatment and enzymatic hydrolysis by taking into account both the biomass weight loss in pretreatment and glucose yield in enzymatic hydrolysis.

As shown in Figure 10-2, poplar wood biomass pretreated with the assistance of ultrasonic irradiation (ultrasonic power level at 30% or 70%) in dilute acid had significant higher hydrolysis sugar yield (Y_h) than that pretreated without ultrasonic irradiation (ultrasonic power level at 0%) at the significant level of 0.05. Pretreatment time for these three levels of ultrasonic power was set at 15 min. Pretreatment temperature was 60 °C. When ultrasonic power was set at 30%, Y_h was increased by 10% compared to that pretreated without ultrasonic irradiation (0%). When ultrasonic power increased to 70%, Y_h was increased by 40% compared to that pretreated without ultrasonic irradiation (0%).

Figure 10-2 Effects of ultrasonic power on hydrolysis sugar yield (Y_h)
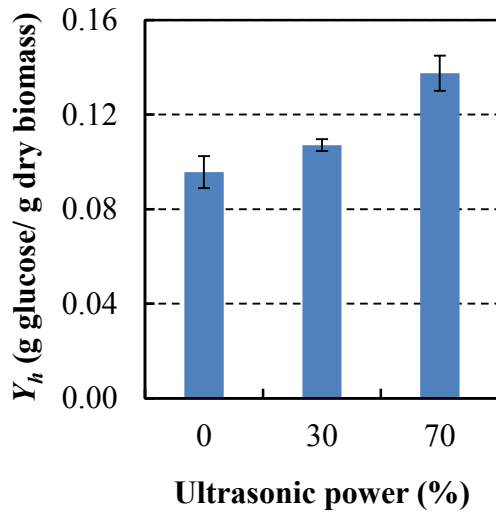
The error bars used in this paper represents the 95% confidence interval.

Effects of ultrasonic power used in pretreatment on total sugar yield (Y_t) are presented in Figure 10-3. The same trend as effects on hydrolysis sugar yield (Y_h) was observed. Y_t increased as ultrasonic power was increaed. When ultrasonic power was set at 30%, Y_t was increased by 12.5%, and when ultrasonic power increased to 70%, Y_t was 37.5% higher than poplar wood biomass pretreated without ultrasonic irradiation. There was no report in the literature regarding applying ultrasonic irradiation to assist dilute acid pretreatment of cellulosic biomass in order to enhance its sugar yield in enzymatic hydrolysis. The application of ultrasonic irradiation in other cellulosic biomass pretreatment methods was available. Velmurugan et al. [40] carried out an ultrasonic-assisted alkaline pretreatment of sugarcane bagasse for fermentable sugar production.

Ultrasonic irradiation was applied by a titanium probe-type ultrasonic processor (UP 400S, Hielscher Ultrasonics GmbH, Teltow, Germany). The ultrasonic frequency was 24 kHz, and ultrasonic power was fixed as 400 W. It was found that sugarcane bagasse pretreated with ultrasonic-assisted alkaline pretreatment showed better sugar yield than that pretreated with alkaline pretreatment alone.

Figure 10-3 Effects of ultrasonic power on total sugar yield (Y_t)
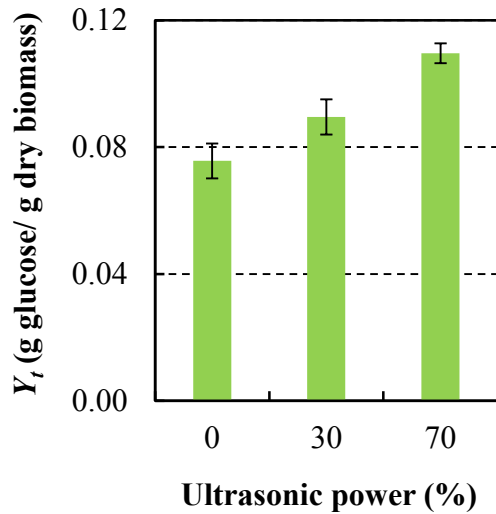
Figure 10-4 Effects of ultrasonic power on crystallinity
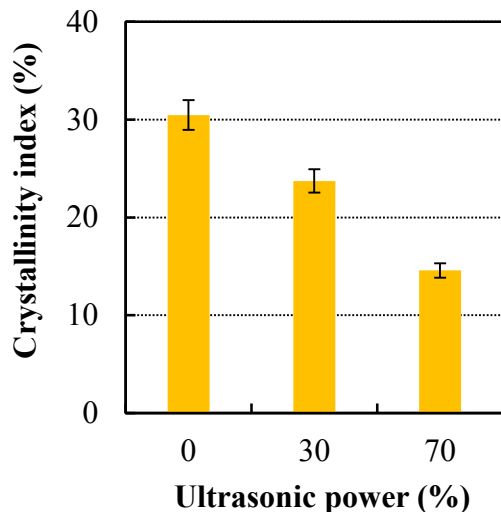
Effects of ultrasonic power used in pretreatment on crystallinity are shown in Figure 10-4. Crystallinity index decreased from 30% to 15% as ultrasonic power increased from 0% (no ultrasonic irradiation) to 70%. This indicated that ultrasonic irradiation could help to reduce

crystallinity. Crystallinity is regarded as a key characteristic of cellulosic biomass substrates because amorphous cellulose can be hydrolyzed enzymatically much more rapidly than crystalline cellulose. Ninomiya et al. [39] pretreated kenaf fiber biomass with ultrasonic irradiation generated by an ultrasonic processor (UP 201S, Hielscher Ultrasonics GmbH, Teltow, Germany) at a frequency of 24 kHz and ultrasonic power of 35 W. Crystallinity index of kenaf fiber biomass pretreated with ultrasonic irradiation decreased 36% comparing with that of untreated biomass. This decrease in crystallinity was associated with the improvement in the cellulose saccharification of the biomass pretreated ultrasonically over that pretreated by conventional thermal pretreatment. Wang et al. [46] also reported that crystallinity decreased as the ultrasonic power increased.

Effects of pretreatment time on hydrolysis sugar yield (Y_h) and total sugar yield (Y_t) are shown in Figures 10-5 and 10-6. Both Y_h and Y_t increased as pretreatment time lengthened from 15 to 30 min. Y_h was increased by 14%, and Y_t was increased by 18%. As shown in Figure 10-7, poplar wood biomass crystallinity decreased slightly as pretreatment time increased. This slight decrease in crystallinity was also reported by Wong et al. [47] when studied effects of ultrasonic treatment time on crystallinity of plant cellulose.

Figure 10-5 Effects of pretreatment time on hydrolysis sugar yield (Y_h)

(Ultrasonic power = 70%)
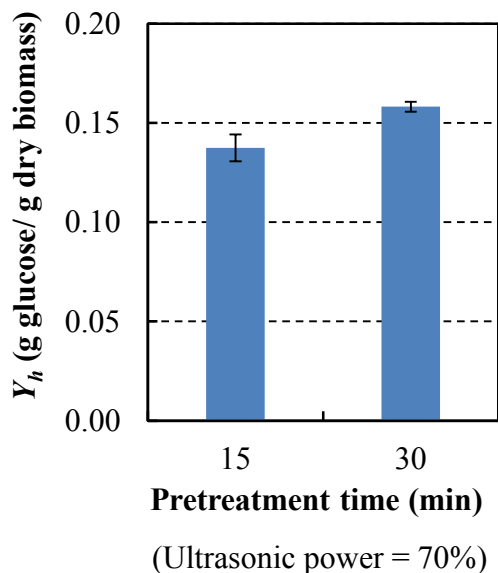
Figure 10-6 Effects of pretreatment time on total sugar yield (Y_t)

(Ultrasonic power = 70%)
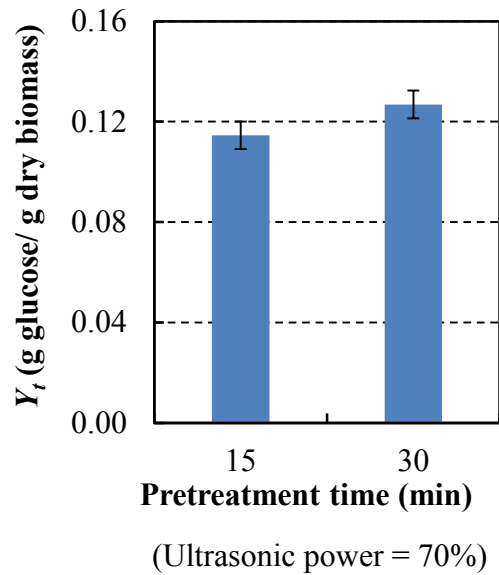
Figure 10-7 Effects of pretreatment time on crystallinity

(Ultrasonic power = 70%)
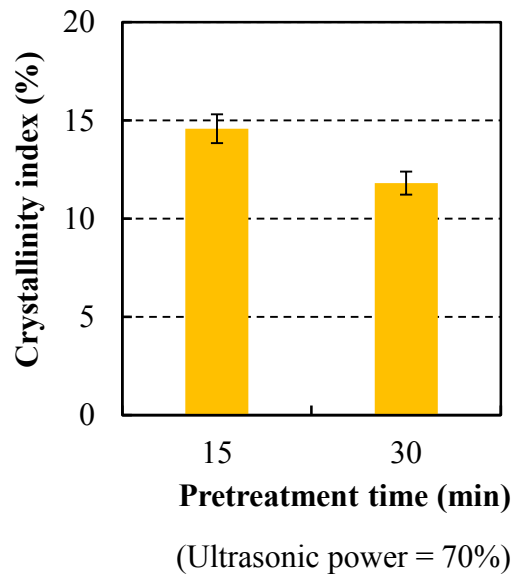
Based on these results, pretreatment using a combination of dilute acid and ultrasound irradiation could significantly enhance the enzymatic hydrolysis of poplar wood biomass. In liquid-solid ultrasonic irradiation (e.g. biomass particles in ultrasonic-assisted dilute acid pretreatment), the mechanism for the induced sonochemical effect is acoustic cavitation, which is the formation, growth, and collapse of bubbles [48]. Bubble collapse near a solid surface

(biomass) becomes non-spherical. It drives high-speed jets of liquid into biomass and creates shockwave to damage and alter biomass structure features [49]. Hypothetically, reasons associated with the improvement in the sugar yield of biomass pretreated ultrasonically can be the fact that ultrasonic irradiation can reduce crystallinity, which was observed in this study, decrease the degree of polymerization of cellulose [49], reduce particle size [38], increase the porosity of cellulose [38], and increase biomass available surface area [38]. These aforementioned changes in cellulosic biomass structural features can make cellulosic biomass substrate more amenable to enzymatic hydrolysis and eventually increase its sugar yield.

10.4 Concluding remarks

Poplar wood biomass pretreated with ultrasound-assisted dilute acid pretreatment showed better hydrolysis sugar yield (Y_h) and total sugar yield (Y_t) than that pretreated with dilute acid only. Sugar yield increased as ultrasonic power and pretreatment time increased. Approximately 10-40% improvement in the sugar yield was attained by using ultrasound-assisted dilute acid pretreatment for 15 min. XRD analysis revealed that poplar wood biomass pretreated ultrasonically had lower crystallinity than that pretreated with dilute acid only. The combination of ultrasound irradiation and dilute acid can be a key factor in the disruption of rigid cellulose structures that contribute to the improvement of cellulose saccharification in enzymatic hydrolysis. However, further research is necessary to investigate the synergetic effects of ultrasound irradiation and dilute acid on the alteration of cellulosic biomass physical and chemical features. The potential of reducing pretreatment time and temperature with improved efficiency is the most attractive feature of the ultrasound-assisted dilute acid pretreatment. However, to implement this process at a larger scale, research such as reactor design and energy consumption optimization need to be done.

Acknowledgements

References

[1]   Q.A. Nguyen, M.P. Tucker, B.L. Boynton, F.A. Keller, D.J. Schell, Dilute Acid Pretreatment of Softwoods, Applied Biochemistry and Biotechnology, 70-72 (1998) 77-87.

[2]   D.J. Schell, J. Farmer, M. Newman, J.D. McMillan, Dilute-sulfuric Acid Pretreatment of Corn Stover in Pilot-scale Reactor, Applied Biochemistry and Biotechnology, 105 (2003) 69-85.

[3]   J.R. Jensen, J.E. Morinelly, K.R. Gossen, M.J. Brodeur-Campbell, D.R. Shonnard, Effects of Dilute Acid Pretreatment Conditions on Enzymatic Hydrolysis Monomer and Oligomer Sugar Yields for Aspen, Balsam, and Switchgrass, Bioresource Technology, 101 (2010) 2317-2325.

[4]   B.C. Saha, L.B. Iten, M.A. Cotta, Y.V. Wu, Dilute Acid Pretreatment, Enzymatic Saccharification, and Fermentation of Rice Hulls to Ethanol, Biotechnology Progress, 21 (2005) 816-822.

[5]   L.R. Lynd, Overview and Evaluation of Fuel Ethanol from Cellulosic Biomass: Technology, Economics, the Environment, and Policy, Annual Review of Energy and the Environment, 21 (1996) 403-465.

[6]   X. Song, M. Zhang, Z. Pei, Effects of Ultrasonic Vibration-assisted Pelleting of Cellulosic Biomass on Sugar Yield for Biofuel Manufacturing, Biomass Conversion and Biorefinery, 3 (2013) 231-238.

[7]   X. Song, M. Zhang, Z. Pei, D. Wang, Ultrasonic Vibration-assisted Pelleting of Wheat Straw: A Predictive Model for Energy Consumption Using Response Surface Methodology, Ultrasonics, 54 (2014) 305-311.

[8]   X.X. Song, M. Zhang, T.W. Deines, P.F. Zhang, Z.J. Pei, Energy Consumption Study in Ultrasonic Vibration-Assisted Pelleting of Wheat Straw for Cellulosic Biofuel Manufacturing, International Journal of Manufacturing Research, 8 (2012) 135-149.

[9]   X.X. Song, M. Zhang, Z.J. Pei, T. Deines, Q. Zhang, P.F. Zhang, D.H. Wang, Size Reduction of Poplar Wood Using a Lathe for Biofuel Manufacturing: A Preliminary Experiment, in: Proceedings of the ASME 2011 International Mechanical Engineering Congress & Exposition (IMECE), ASME, Denver, Colorado,USA, 2011, pp. 683-690.

[10]   M. Zhang, X.X. Song, P.F. Zhang, Z.J. Pei, T.W. Deines, D.H. Wang, Size Reduction of Cellulosic Biomass in Biofuel Manufacturing: Separating the Confounding Effects of Particle Size and Biomass Crystallinity, Journal of Manufacturing Science and Engineering, 135 (2013).

[11]   M. Zhang, X.X. Song, T.W. Deines, Z.J. Pei, D. Wang, Biofuel manufacturing from woody biomass: effects of sieve size used in biomass size reduction, Journal of Biomedicine and Biotechnology, 2012 (2012).

[12]   X.X. Song, M. Zhang, Z.J. Pei, D.H. Wang, Preliminary study on pretreatment of poplar wood for biofuel production, Biofuels, 3 (2012) 525-533.

[13]   E.M. Rubin, Genomics of Cellulosic Biofuels, Nature, 454 (2008) 841-845.

[14]   U. S. Department of Energy, Breaking the Biological Barriers to Cellulosic Ethanol: A Joint Research Agenda, in, 2009.

[15]   N. Mosier, C. Wyman, B. Dale, R. Elander, Y.Y. Lee, M. Holtzapple, M. Ladisch, Features of Promising Technologies for Pretreatment of Lignocellulosic Biomass, Bioresource Technology, 96 (2005) 673-686.

[16]   M. Galbe, G. Zacchi, Pretreatment of lignocellulosic materials for efficient bioethanol production, Biofuels, (2007) 41-65.

[17]   M. Zhang, X.X. Song, Z.J. Pei, D.H. Wang, Effects of Mechanical Comminution on Enzymatic Conversion of Cellulosic Biomass in Biofuel Manufacturing: A Review, in: Proceedings of the ASME 2010 International Manufacturing Science and Engineering Conference (MSEC), Erie, PA, USA, 2010, pp. 497-504.

[18]   M. Zhang, X. Song, P.F. Zhang, Q. Zhang, Z.J. Pei, T. Deines, D.H. Wang, Size Reduction of Cellulosic Biomass in Biofuel Manufacturing: Effects of Milling Orientation on Sugar Yield, in: Proceedings of the ASME 2011 International Manufacturing Science and Engineering Conference (MSEC), ASME, Corvallis, OR, USA, 2011, pp. 653-653.

[19]   M. Zhang, X.X. Song, P.F. Zhang, Z.J. Pei, T. Deines, Size Reduction of Cellulosic Biomass in Biofuel Manufacturing: Effects of Biomass Crystallinity and Particle Size, in: Proceedings of the ASME 2011 International Mechanical Engineering Congress & Exposition (IMECE), ASME, Denver, Colorado,USA, 2011.

[20]   M. Zhang, X. Song, P. Zhang, Z.J. Pei, T.W. Deines, D. Wang, Size Reduction of Cellulosic Biomass in Biofuel Manufacturing: A Study on Confounding Effects of Particle Size and Biomass Crystallinity, Journal of Manufacturing Science and Engineering, 134 (2012).

[21]   F. Shafizadeh, A.G.W. Bradbury, Thermal degradation of cellulose in air and nitrogen at low temperatures, Journal of Applied Polymer Science, 23 (1979) 1431-1442.

[22]   R.P. Overend, E. Chornet, J.A. Gascoigne, Fractionation of Lignocellulosics by Steam-Aqueous Pretreatments and Discussion, Philosophical Transactions of the Royal Society of London. Series A, Mathematical and Physical Sciences, 321 (1987).

[23]   H. Alizadeh, F. Teymouri, T.I. Gilbert, B.E. Dale, Pretreatment of switchgrass by ammonia fiber explosion (AFEX), Applied biochemistry and biotechnology, 124 (2005) 1133-1141.

[24] Y. Sun, J.J. Cheng, Dilute Acid Pretreatment of Rye Straw And Bermudagrass for Ethanol Production, Bioresource Technology, 96 (2005) 1599-1606.

[25] R. Sierra, C. Granda, M.T. Holtzapple, Short Term Lime Pretreatment of Poplar Wood, Biotechnology progress, 25 (2009) 323-332.

[26] H.L. Chum, D.K. Johnson, S.K. Black, Organosolv Pretreatment for Enzymic Hydrolysis of Poplars. 2. Catalyst Effects and the Combined Severity Parameter, Industrial Engineering Chemistry Research, 29 (1990) 156-162.

[27] A.M. Azzam, Pretreatment of cane bagasse with alkaline hydrogen peroxide for enzymatic hydrolysis of cellulose and ethanol fermentation, Journal of Environmental Science & Health Part B, 24 (1989) 421-433.

[28] A.I. Hatakka, Pretreatment of wheat straw by white-rot fungi for enzymatic saccharification of cellulose, Applied Microbiology and Biotechnology, 18 (1983) 350-357.

[29] P. Kumar, D.M. Barrett, M.J. Delwiche, P. Stroeve, Methods for pretreatment of lignocellulosic biomass for efficient hydrolysis and biofuel production, Industrial & Engineering Chemistry Research, 48 (2009) 3713-3729.

[30] P. Alvira, E. Tomás-Pejó, M. Ballesteros, M.J. Negro, Pretreatment technologies for an efficient bioethanol production process based on enzymatic hydrolysis: A review, Bioresource Technology, 101 (2010) 4851-4861.

[31] K.S. Suslick, W.B. McNamara Iii, Y. Didenko, Hot spot conditions during multi-bubble cavitation, 1999.

[32] M. Faraday, On a Peculiar Class of Acoustical Figures; and on Certain Forms Assumed by Groups of Particles upon Vibrating Elastic Surfaces, Royal Society of London, 1831.

[33] H. Kuttruff, Ultrasonics fundamentals and applications, Elsevier Applied Science, 1991.

[34] S.K. Khanal, M. Montalbo, J. van Leeuwen, G. Srinivasan, D. Grewell, Ultrasound enhanced glucose release from corn in ethanol plants, Biotechnology and Bioengineering, 98 (2007) 978-985.

[35] T. Seino, A. Yoshioka, M. Fujiwara, K.L. Chen, T. Erata, M. Tabata, M. Takai, ESR studies of radicals generated by ultrasonic irradiation of lignin solution. An application of the spin trapping method, Wood Science and Technology, 35 (2001) 97-106.

[36] D. Chuanyun, W. Bochu, Z. Huan, H. Conglin, D. Chuanren, L. Wangqian, Y. Toyama, A. Sakanishi, Effect of low frequency ultrasonic stimulation on the secretion of siboflavin produced by Ecemothecium Ashbyii, Colloids and Surfaces B: Biointerfaces, 34 (2004) 7-11.

[37]   M. Yaldagard, S.A. Mortazavi, F. Tabatabaie, The effect of ultrasound in combination with thermal treatment on the germinated barley's alpha-amylase activity, Korean Journal of Chemical Engineering, 25 (2008) 517-523.

[38]   M. Toma, H. Bandow, M. Vinatoru, Y. Maeda, Ultrasonically assisted conversion of lignocellulosic biomass to ethanol, in, 2006.

[39]   K. Ninomiya, K. Kamide, K. Takahashi, N. Shimizu, Enhanced enzymatic saccharification of kenaf powder after ultrasonic pretreatment in ionic liquids at room temperature, Bioresource Technology, 103 (2012) 259-265.

[40]   R. Velmurugan, K. Muthukumar, Ultrasound-assisted alkaline pretreatment of sugarcane bagasse for fermentable sugar production: Optimization through response surface methodology, Bioresource Technology, 112 (2012) 293-299.

[41]   A. Sluiter, B. Hames, D. Hyman, C. Payne, R. Ruiz, Determination of Total Solids in Biomass and Total Dissolved Solids in Liquid Process Samples, NREL Laboratory Analytical Procedure Technical Report No. NREL/TP-510–42621, (2008).

[42]   A. Sluiter, B. Hames, R. Ruiz, C. Scarlata, J. Sluiter, D. Templeton, D. Crocker, Determination of structural carbohydrates and lignin in biomass, NREL Laboratory Analytical Procedure Technical Report No. NREL/TP-510–42618, (2008).

[43]   P. Sunkyu, H. Michael, P. Philip, J. David, Cellulose Crystallinity Index: Measurement Techniques and Their Impact on Interpreting Cellulase Performance, Biotechnology for Biofuels, 3 (2010).

[44]   V.P. Puri, Effect of Crystallinity and Degree of Polymerization of Cellulose on Enzymatic Saccharification, Biotechnology and Bioengineering, 26 (1984) 1219-1222.

[45]   L.T. Fan, Y.H. Lee, D.H. Beardmore, Mechanism of the Enzymatic Hydrolysis of Cellulose: Effects of Major Structural Features of Cellulose on Enzymatic Hydrolysis, Biotechnology and Bioengineering, 22 (1980) 177-199.

[46]   X. Wang, G. Fang, C. Hu, T. Du, Application of ultrasonic waves in activation of microcrystalline cellulose, Journal of Applied Polymer Science, 109 (2008) 2762-2767.

[47]   S.S. Wong, S. Kasapis, Y.M. Tan, Bacterial and plant cellulose modification using ultrasound irradiation, Carbohydrate Polymers, 77 (2009) 280-287.

[48]   T.G. Leighton, The Acoustic Bubble, Academic Press, 1994.

[49]   K.S. Suslick, G.J. Price, Applications of ultrasound to materials chemistry, in: Annual Review of Material Science, 1999, pp. 295-326.

[50]   S. Sasmal, V.V. Goud, K. Mohanty, Ultrasound Assisted Lime Pretreatment of Lignocellulosic Biomass toward Bioethanol Production, Energy Fuels, 26 (2012) 3777-3784.

[51]   M. Marx-Figini, Studies on the ultrasonic degradation of cellulose macromolecular properties, Die Angewandte Makromolekulare Chemie, 250 (1997) 85-92.

[52]   J. Xiong, Y.E. Jun, L. Wenzhi, The Influence of Ultrasonic Wave on Supermolecular Structure of Cellulose, Acta Acustica, 24 (1999) 66-69.

[53]   A. Tang, H. Zhang, G. Chen, G. Xie, W. Liang, Influence of ultrasound treatment on accessibility and regioselective oxidation reactivity of cellulose, Ultrasonics Sonochemistry, 12 (2005) 467-472.

[54]   N. Wang, E. Ding, R. Cheng, Thermal degradation behaviors of spherical cellulose nanocrystals with sulfate groups, Polymer, 48 (2007) 3486-3493.

Chapter 11 - Effects of Ultrasonic Vibration-assisted Pelleting of Cellulosic Biomass on Sugar Yield for Biofuel Manufacturing

Authors' names:

Xiaoxu Song[a], Meng Zhang[a], Z.J. Pei[a], and Donghai Wang[b]

Authors' affiliation:

[a]Department of Industrial and Manufacturing Systems Engineering, Kansas State University, Manhattan KS 66506 USA

[b]Department of Biological and Agricultural Engineering, Kansas State University, Manhattan, KS 66506, USA

Abstract

Ultrasonic vibration-assisted (UV-A) pelleting can increase the bulk density of cellulosic biomass, thus reduce the feedstock transportation cost in cellulosic biofuel manufacturing. UV-A pelleting can also increase the biomass sugar yield in enzymatic hydrolysis. There are two major processes in the sugar conversion of cellulosic biomass: pretreatment and enzymatic hydrolysis. Sugar yield definition used in reported UV-A pelleting studies is enzymatic hydrolysis sugar yield. This definition is based on enzymatic hydrolysis this single process without considering the pretreatment process. In fact, converting cellulosic biomass into fermentable sugar (glucose) is the combined effort of pretreatment and enzymatic hydrolysis. There are no papers in the literature investigating whether UV-A pelleting could increase the total sugar yield when both pretreatment and enzymatic hydrolysis are considered. This paper reports the first study using total sugar yield to investigate effects UV-A pelleting on biomass sugar yield. Experimental results show that, for all the four types of cellulosic biomass (wheat straw, corn stover, switchgrass, and sorghum stalk) used in this study, total sugar yield of biomass processed with UV-A pelleting was 30% to 43% higher than that of biomass not processed with UV-A pelleting.

11.1 Introduction

Ninety-three percent of the transportation fuels consumed in the U.S. in 2011 are petroleum based [1]. About half of the petroleum used in the U.S. is imported [2]. One big issue of using petroleum-based transportation fuels is greenhouse gas (GHG) emissions. The transportation sector accounts for one-third of carbon dioxide emissions of all U.S. end-use sectors (including industry, residential, commercial, transportation, and agriculture) [3]. In order to reduce GHG emissions and the nation's dependence on foreign petroleum, it is imperative to produce and use fuels made from renewable and domestic resources. One example is biofuels made from cellulosic biomass (bioethanol). Cellulosic biofuels have the potential to reduce GHG emissions by as much as 86% in best cases [4]. Because cellulosic biofuels are made from

renewable, plant-based feedstocks, the carbon dioxide released during fuel combustion is 'recycled' by plants as they grow [5].

Major processes of cellulosic biofuel manufacturing are listed in Figure 11-1. First, size reduction reduces bulky cellulosic biomass into small particles [6–9]. Pretreatment makes cellulose (inside cellulosic biomass) more accessible to enzymes used in enzymatic hydrolysis [10]. Enzymatic hydrolysis breaks down cellulose into fermentable sugar (glucose). Afterwards, fermentable sugar is converted to ethanol by fermentation [10–12].

Figure 11-1 Major processes of cellulosic biofuel manufacturing (after [13])
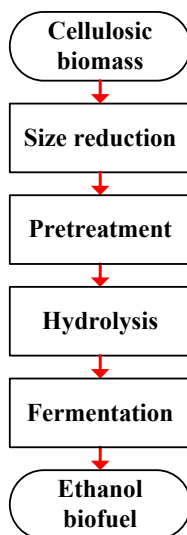
One major barrier with current cellulosic biofuel manufacturing is related to the low bulk density of cellulosic biomass feedstocks, which causes their transportation and handling to be very expensive [13]. One of the strategies to overcoming this limitation is the densification of the cellulosic biomass feedstocks. Improvement in feedstock bulk density and flowability will improve handling efficiencies and reduce transportation and handling costs. Pelleting is generally described as "the agglomeration of small particles into firm, uniformly shaped granules by the means of a mechanical process" [14]. Pelleting of the biomass can increase the overall efficiency of biofuel manufacturing by enabling the use of existing transportation infrastructure and storage systems [15]. Traditionally, biomass pellets are made by screw extruding or piston ramming ground biomass particles through round cross sectional dies [16]. Ultrasonic vibration-assisted (UV-A) pelleting is a newly developed pelleting method by the authors. Previous studies show

that UV-A pelleting can produce biomass pellet with density as high as 1000 kg/m^3, which is about a 30-time increase in density comparing with cellulosic biomass before pelleting [17–19].

For the first time, UV-A pelleting combines biomass ultrasonication and densification into one process. Ultrasonication has been applied to biomass pretreatment [20-25]. It has been reported that ultrasonication increased the porosity of cellulose fiber and the cleavage of linkages in lignin [20-22]. The use of ultrasound in pretreatment has been reported to improve subsequent enzymatic hydrolysis sugar yield [23,24].

UV-A pelleting can also increase enzymatic hydrolysis sugar yield [26]. "Sugar yield" used in reported studies on UV-A pelleting, as listed in Table 11-1, is either defined as sugar (glucose) concentration in the enzymatic hydrolysis slurry (g/L) or percentage of cellulose converted to glucose in enzymatic hydrolysis (g glucose/g glucose). These two sugar yield definitions are based on enzymatic hydrolysis this single process without considering the pretreatment process. In fact, converting cellulosic biomass into fermentable sugar (glucose) is the combined effort of pretreatment and enzymatic hydrolysis. There are no papers in the literature investigating whether UV-A pelleting could increase the total sugar yield when both pretreatment and enzymatic hydrolysis are considered.

This paper reports the first study using total sugar yield to investigate effects UV-A pelleting on biomass sugar yield. Four types of biomass materials were used in this investigation: wheat straw, corn stover, switchgrass, and sorghum stalk. For each type of biomass, besides total sugar yield, enzymatic hydrolysis sugar yield was also reported for comparison purpose.

Table 11-1 Summary of sugar yield definitions used in reported studies on UV-A pelleting of biomass

Sugar yield definition	Unit of sugar yield	Biomass material	Reference
Sugar (glucose) concentration in hydrolysis	g/L	Wheat straw	[19,27]
Sugar (glucose) concentration in hydrolysis	g/L	Sorghum stalk	[28]
Sugar (glucose) concentration in hydrolysis	g/L	Switchgrass	[29]
Percentage of cellulose enzymatically converted to glucose in hydrolysis	g glucose/g glucose	Switchgrass	[26]
Percentage of cellulose enzymatically converted to glucose in hydrolysis	g glucose/g glucose	Wheat straw, corn stover, bluestem, and sorghum	[30]

11.2 Experiment conditions

11.2.1 Biomass materials

Biomass materials were milled into small particles by a knife mill (Model SM 2000, Retsch, Inc., Haan, Germany). The knife mill used a 240-V, 2.2-kW electric motor with a fixed rotation speed (1720 rpm). Three cutting blades (95 mm long and 35 mm wide) were mounted on the rotor. Four shear bars were mounted on the inside wall of the milling chamber, as shown in Figure 11-2. There was a 3-mm gap between a cutting blade and a shear bar. Biomass was cut between the cutting blades and the shear bars. The sieve used in the knife mill had sieve size of 0.25 mm. Particles smaller than the sieve size would fall through the sieve. Particles larger than the sieve size would be recirculated and further milled. Biomass particles after milling were kept in Ziploc® bags and stored in a refrigerator at 4°C until being used for further experiments.

Figure 11-2 Milling chamber of the knife mill
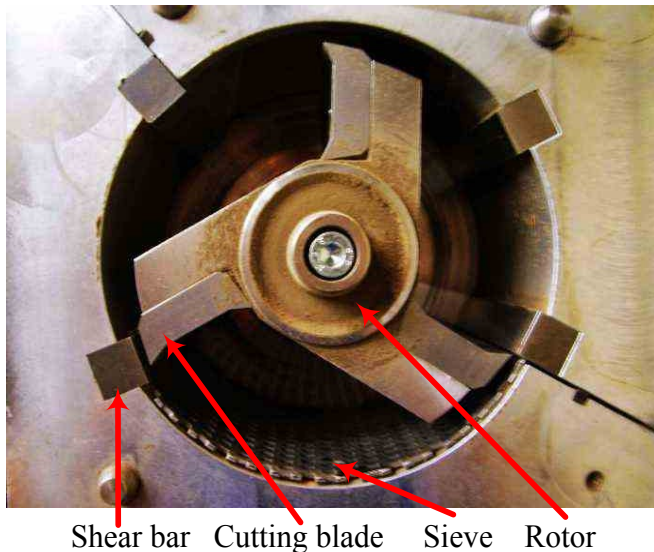
Shear bar   Cutting blade   Sieve   Rotor

Moisture content (*MC*) of biomass represents the amount of moisture (water) contained in a certain amount of biomass. The moisture content of biomass after milling was measured by following the NREL Laboratory Analytical Procedure [31]. A sample of biomass (25 g) was heated in an oven (Blue M Electric Co., Blue island, IL, USA) at 105°C for 24 hours to get rid of moisture in biomass. Moisture content was calculated as follows:

$$Moisture\ content(MC)\ (\%)\ =\frac{W_b\text{-}W_a}{W_b}\times100\%$$ (3)

where W_b is weight of biomass before drying; W_a is weight of biomass after drying.

Table 11-2 summarizes the moisture content of the four types of biomass after milling. After knowing the moisture content, biomass dry weight could be calculated by Eq (4). Biomass weight reported in this paper is dry weight.

$$Dry\ weight\ =(1-MC/100\%)\times W_b$$ (4)

Each type of biomass after milling was divided into two groups: one was processed with UV-A pelleting, followed by pretreatment and enzymatic hydrolysis; the other was treated by pretreatment and enzymatic hydrolysis without processed with UV-A pelleting.

Table 11-2 Moisture content of biomass after milling

Biomass type	Moisture content (%)
Wheat straw	11
Corn stover	6
Switchgrass	6
Sorghum stalk	7

11.2.2 UV-A pelleting

Figure 11-3 is a schematic illustration of the experimental set-up for UV-A pelleting. UV-A pelleting experiments were performed on a modified ultrasonic machine (Model AP-1000, Sonic-Mill, Albuquerque, NM, USA). The machine included a power supply (which converts 60 Hz electrical power into 20,000 Hz electrical power), a converter (which converts high frequency electrical energy into mechanical motion), and a titanium tool. The tip of the tool was a solid cylinder with a flat end (17.4 mm in diameter).

For each pelleting test, 3 g of biomass was loaded into an aluminum mold. The upper two parts formed a cylindrical cavity (18.6 mm in diameter, 46.3 mm in height) and the bottom part was a square plate, serving as a base. They were assembled together with pins.

The pneumatic cylinder was driven by compressed air provided by a 1.6-horsepower, 33-gallon air compressor (Sears, Roebuck and Co., Hoffman Estates, IL, USA). The air pressure in the pneumatic cylinder was controlled by a pressure regulator. A higher air pressure in the pneumatic cylinder meant a higher pressure applied on the biomass in the mold by the tool.

Pelleting duration is the period of time during which ultrasonic power was on. In every pelleting test, pelleting duration was 120-second. After 120-second, the tool was retracted and the mold was disassembled to unload the pellet. Table 11-3 shows experimental parameters and their values.

Besides increasing the bulk density of cellulosic biomass, Ultrasonic vibration also generated heat during the pelleting process. To better understand the impact on cellulosic biomass material by applying UV-A pelleting, pelleting temperature was measured using thermocouples (K-type, Model SC-GG-K-30-36, OMEGA Engineering, Inc, Stamford, CT, USA) inserted into the pellet through the slot on the wall of the mold as shown in Figure 11-3. The thermocouples were connected to a thermometer (HH147U, OMEGA Engineering, Inc., Stamford, CT, USA). Measurement data of temperatures at two locations (T1 and T2 as shown in Figure 11-3) of a pellet were recorded. T1 was the temperature in the middle on the bottom surface of the pellet. T2 was the temperature at the pellet center.

Figure 11-3 Schematic illustration of the experimental set-up for UV-A pelleting
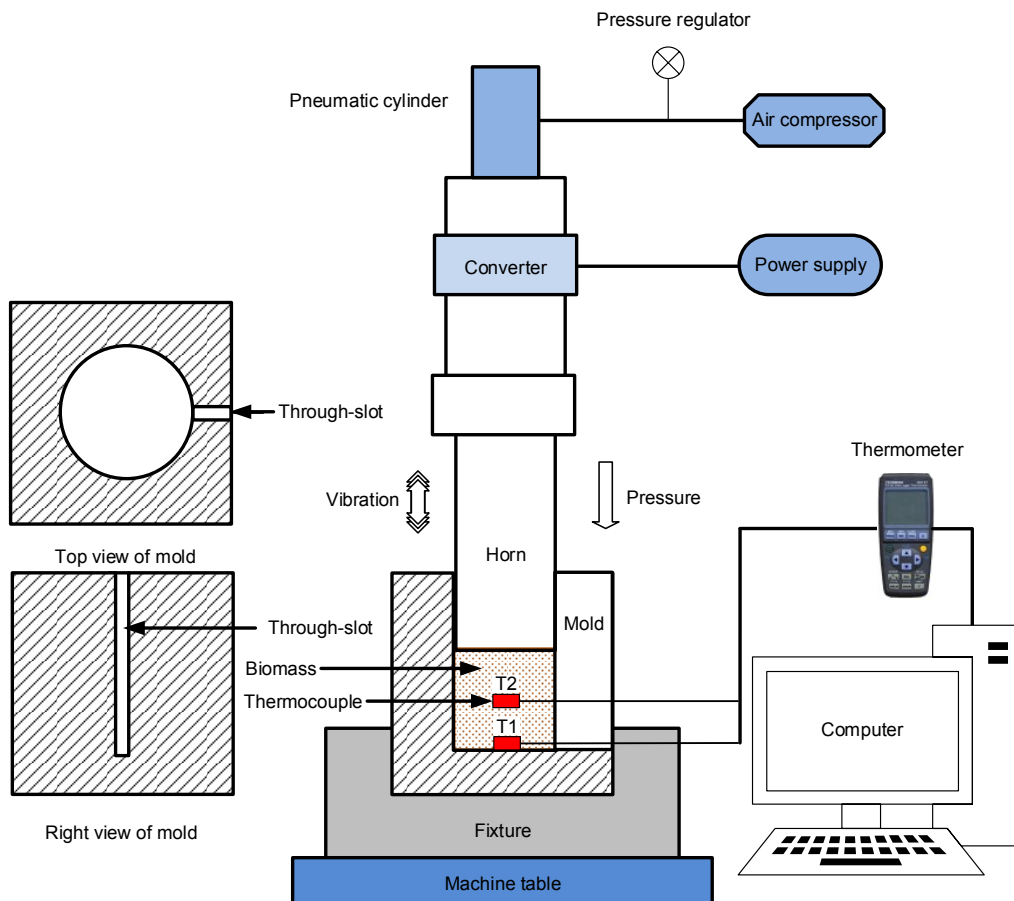
Table 11-3 UV-A pelleting experimental parameters and their values

Parameters	Unit	Value
Pelleting pressure	psi	30
Ultrasonic power	%	40
Pelleting duration	second	120
Pellet weight	gram	3

11.2.3 Pretreatment

Dilute acid pretreatment was carried out in a 600-mL reaction vessel of a Parr pressure reactor (Series 4560, Parr Instrument Company, Moline, IL, USA). The biomass was mixed with 2% diluted sulfuric acid to obtain biomass slurry with 5% solid content (10 g of biomass in 200 mL of diluted sulfuric acid). The slurry was loaded into the reaction vessel. Pretreatment temperature was the reaction temperature in the reaction vessel. Pretreatment time was the period of time during which the slurry was treated at the pretreatment temperature in the reaction vessel. The period of time during which the temperature increased to pretreatment temperature or decreased to room temperature was not included in the pretreatment time. Pretreatment parameters are listed in Table 11-4. After pretreatment, the weight and the moisture content of biomass were measured to calculate the dry weight of biomass after pretreatment.

Table 11-4 Pretreatment parameters and their values

Parameter	Unit	Value
Pretreatment time	minute	30
Pretreatment temperature	°C	140
Acid concentration	% (w/v)	2

% (w/v) referred to as gram of acid in 100 mL of solution.

11.2.4 Enzymatic hydrolysis

Enzymatic hydrolysis was carried out in 125-mL flasks in a water bath shaker (Model C76, New Brunswick Scientific, Edison, NJ, USA) with agitation speed of 110 rpm at 50°C for 72 h. Each flask contained 50 mL of hydrolysis slurry. The slurry consisted of 5% (w/v) biomass on dry weight base, sodium acetate buffer (50 mM, pH = 4.8), and 0.02% (w/v) sodium azide to prevent microbial growth during hydrolysis. Accellerase 1500™ enzyme complex (Danisco USA, Inc., Rochester, NY, USA) was used. The enzyme loaded was 0.5 mL for each gram of dry biomass.

After 72 hours of enzymatic hydrolysis, hydrolysis slurries were sampled by withdrawing 0.1 mL of slurry from each flask. Sample slurries were then mixed with 0.9 mL of double-distilled water in 1.5-mL vials. The vials were placed into boiling water for 15 minute to deactivate the enzyme. Then, the sample slurries were centrifuged in a centrifuge (RS-102, Revolutionary Science, Shafer, MN, USA) at 10,000 rpm for 15 minutes. The supernatants were filtered into 2-mL autosampler vials through 0.2-μm syringe filters (Millipore, Billerica, MA, USA). The glucose concentration of filtered samples in the autosampler vials were measured by a high performance liquid chromatography (HPLC) system (Shimadzu, Kyoto, Japan) with a Rezex RPM-monosaccharide column (300 × 7.8 mm; Phenomenex, CA, USA) and a refractive index detector (RID-10 A, Shimadzu, MD, USA). The column was eluted with double-distilled water at a flow rate of 0.6 mL/minute. The temperature of the chromatography column was maintained at 80 °C.

As shown in Eq (1) and Eq (2), total sugar yield (Y_t) (g glucose/g dry biomass) was calculated as the glucose yield (g) per unit dry weight of biomass loaded into pretreatment. Enzymatic hydrolysis sugar yield (Y_h) (g glucose/g dry biomass) was calculated as the glucose yield (g) per unit dry weight of biomass loaded into enzymatic hydrolysis:

$$Y_t = \frac{M_{pret} \times G_{EH} \times V}{M_{OR} \times M_{EH}} \tag{1}$$

$$Y_h = \frac{G_{EH} \times V}{M_{EH}} \tag{2}$$

where M_{pret} is the dry weight (g) of biomass after pretreatment, M_{OR} is the dry weight (g) of biomass loaded in pretreatment, M_{EH} is the dry weight (g) of biomass loaded in enzymatic hydrolysis (equals to 2.5 g for all the experimental conditions). G_{EH} is the glucose concentration (g/L) of slurry in the flask after enzymatic hydrolysis, V is the total volume (L) of slurry in the flask in enzymatic hydrolysis, and is kept at 0.05 L.

M_{pret} was always smaller than M_{OR}. This is due to the biomass weight loss happened in dilute acid pretreatment. Pretreatment weight recovery (R) can be expressed as follows:

$$R\ (\%) = \frac{M_{pret}}{M_{OR}} \times 100\% \tag{3}$$

This pretreatment weight recovery (R) will be taken into account if total sugar yield (Y_t) is used. On the other hand, if enzymatic hydrolysis sugar yield (Y_h) is used, pretreatment weight recovery (R) will be overlooked.

11.3 Results and discussion

Figures 11-4 – 11-7 compare sugar yield results of wheat straw, corn stover, switchgrass, and sorghum stalk biomass processed with or without UV-A pelleting. Sugar yields are reported using both total sugar yield (Y_t) and enzymatic hydrolysis sugar yield (Y_h) definitions.

Considering effects of UV-A pelleting on both pretreatment and enzymatic hydrolysis by using total sugar yield (Y_t), wheat straw processed with UV-A pelleting was 30% higher in Y_t than that of wheat straw not processed with UV-A pelleting. This advantage in Y_t of biomass processed UV-A pelleting was observed in all the other three types of biomass used in this study: 36% for corn stover, 43% for switchgrass, and 39% for sorghum stalk.

Considering effects of UV-A pelleting on enzymatic hydrolysis only by using enzymatic hydrolysis sugar yield (Y_h), the sugar yield of biomass processed with UV-A pelleting was higher than that without UV-A pelleting in all the four types of biomass used in this study. Results of the percentage higher are listed as 22% for wheat straw, 9% for corn stover, 12% for switchgrass, and 9% for sorghum stalk.

Figure 11-4 Effects of UV-A pelleting on sugar yield of wheat straw
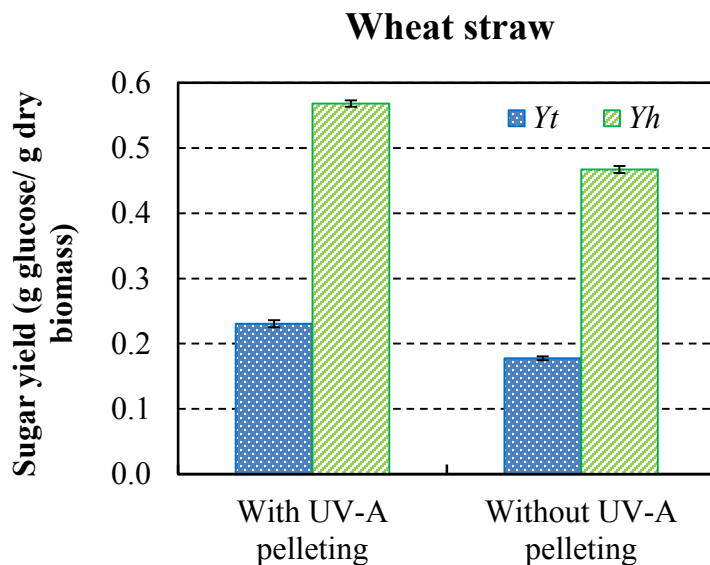
Figure 11-5 Effects of UV-A pelleting on sugar yield of corn stover

Corn stover
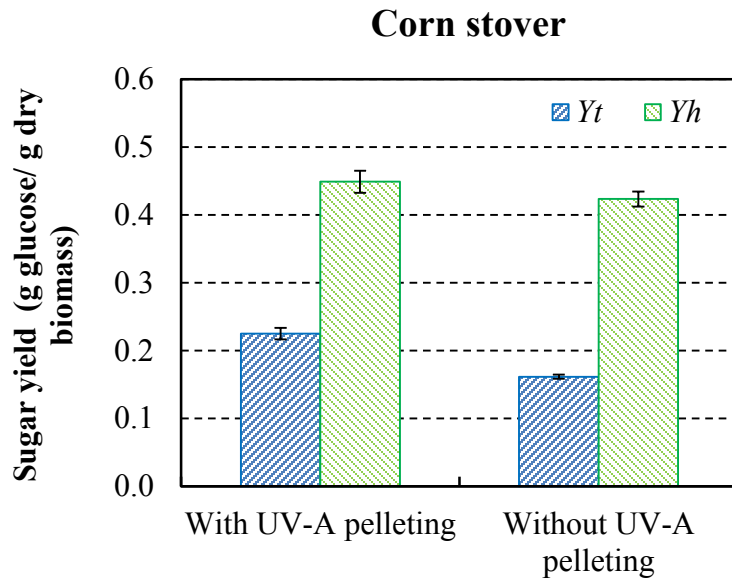
Figure 11-6 Effects of UV-A pelleting on sugar yield of switchgrass

Switchgrass
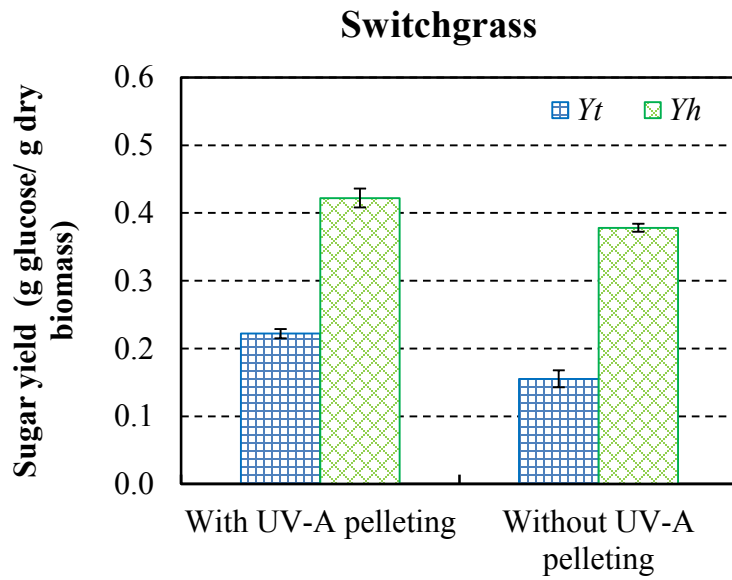
Figure 11-7 Effects of UV-A pelleting on sugar yield of sorghum stalk
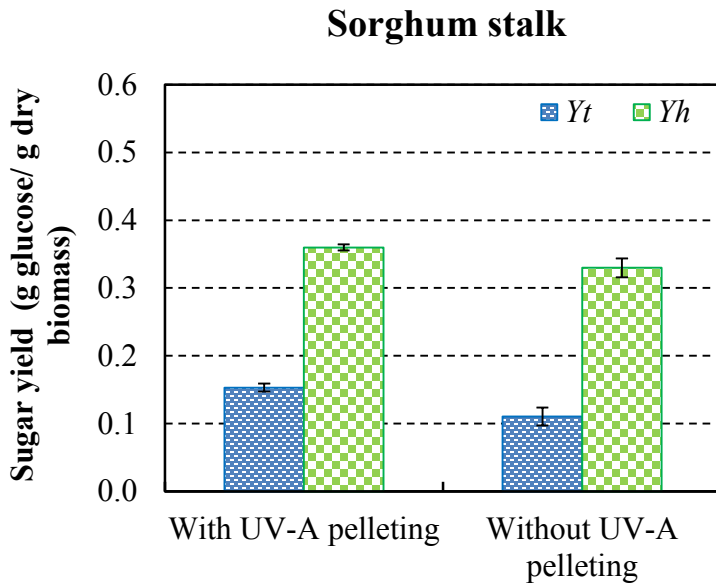
Figure 11-8 Effects of UV-A pelleting on pretreatment weight recovery (*R*)
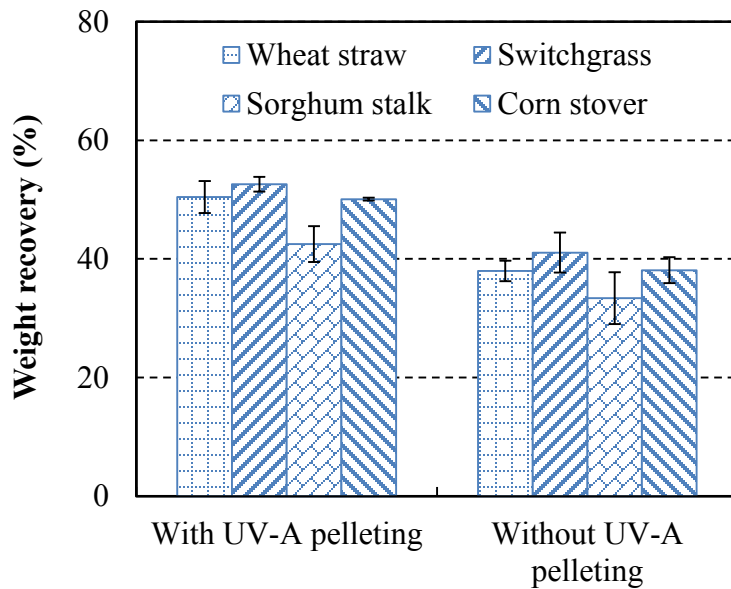
Figure 11-8 shows effects of UV-A pelleting on pretreatment weight recovery (*R*). It was observed that, for all the four types of biomass, UV-A pelleting helped to increase the pretreatment weight recovery (*R*). The major weight loss in pretreatment is the decomposing of hemicellulose. The primary objective of dilute sulfuric acid pretreatment is to break down the shield formed by highly associated lignin and hemicellulose by decomposing hemicellulose to

acid soluble products (i.e. xylose), so that cellulose can be released and become more accessible to enzymes in enzymatic hydrolysis [32]. However, a side effect is that a small amount of cellulose may be degraded to hydroxymethyl-furfural (HMF) [32]. HMF is soluble in the pretreatment liquid and will be separated from the solid biomass after pretreatment. Only the solid biomass collected after pretreatment goes into enzymatic hydrolysis. The degradation of cellulose to HMF results in a potential sugar (cellulose) loss and leads to decreasing total sugar yield [33].

Zhang et al. [26] have studied effects of UV-A pelleting on enzymatic hydrolysis sugar yield (Y_h). Switchgrass was treated at 180°C for 15-minute with 2% dilute sulfuric acid. Results shown that Y_h of switchgrass processed with UV-A pelleting is 23% higher than that of switchgrass not processed with UV-A pelleting.

In order to understand the mechanism of increasing biomass sugar yield by applying UV-A pelleting, temperature was measured during the pelleting process. Effects of UV-A pelleting on temperature of wheat straw is shown in Figure 11-9. The temperature profile was a function of time at the different locations of pellet. At 120 s, the temperature at the bottom of the pellet T1 was 55°C, increased 28°C from room temperature (27°C). The temperature at the pellet center T2 was 256°C, which increased 229°C from room temperature. Figure 11-10 shows effects of UV-A pelleting on temperature at the pellet center T2 at 120s of four types of biomass. Temperatures at the pellet center T2 with UV-A pelleting were higher than those of without UV-A pelleting for all four types of biomass. Temperatures without UV-A pelleting were about 27°C (room temperature) for all four types of biomass. There was no temperature increase from room temperature. Temperatures at the pellet center T2 with UV-A pelleting increased from 27°C to 257°C for wheat straw, 225°C for switchgrass, 267°C for sorghum stalks, and 222°C for corn stover, respectively. The significant increase in biomass temperature during UV-A pelleting is a possible aspect to understand why UV-A pelleting increased biomass sugar yield. Lignin in cellulosic biomass is less thermostable than cellulose. Mostly what happens to lignin during pretreatment is that the bonding to the hemicelluloses breaks when the temperature of pretreatment is higher than the glass transition temperature of lignin, making it possible to melt lignin and make it become mobile within the cell wall matrix [34]. Since lignin serves as a protecting shield over cellulose, the melt and move of lignin through the matrix may help to

release more cellulose and make cellulose biomass material more amenable to enzymatic hydrolysis.

Other than the studies on effects of UV-A pelleting on biomass sugar yield, Cong et al. [18] studied effects of UV-A pelleting of switchgrass on pellet quality (pellet density, pellet durability and spring-back) and pelleting force. Pellet durability measures the ability of pellets to withstand impact and other forces during transportation and storage [17]. Spring-back measures the expansion of a pellet [17]. The density of pellets processed with UV-A pelleting was higher than that of pellets processed without UV-A pelleting. The durability of pellets processed with UV-A pelleting was much higher than that of pellets processed without UV-A pelleting. Pellets processed with UV-A pelleting were more stable. As the days passed, the pellets without UV-A pelleting expanded more than the pellets processed with UV-A pelleting. To achieve the same pellet quality, UV-A pelleting required lower pelleting force and shorter pelleting time than pelleting without UV-A.

Figure 11-9 Temperature profile at the wheat straw pellet bottom (T1) and pellet center (T2)
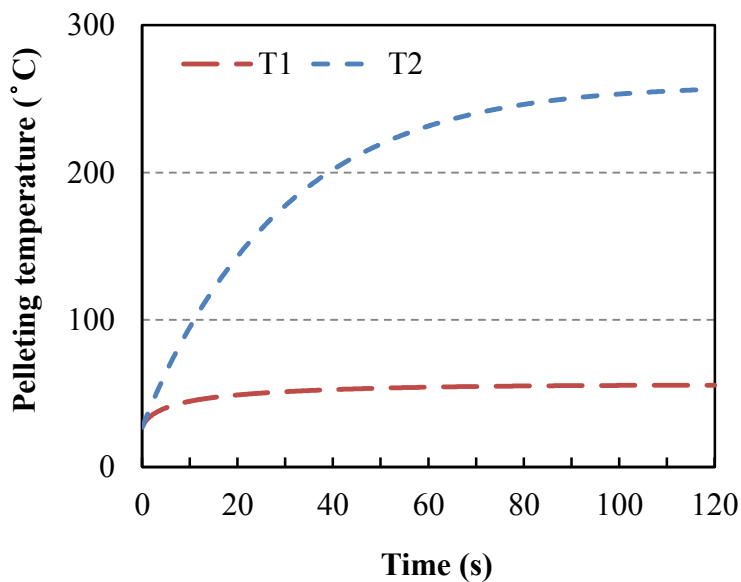
Figure 11-10 Effects of UV-A pelleting on temperature at the pellet center
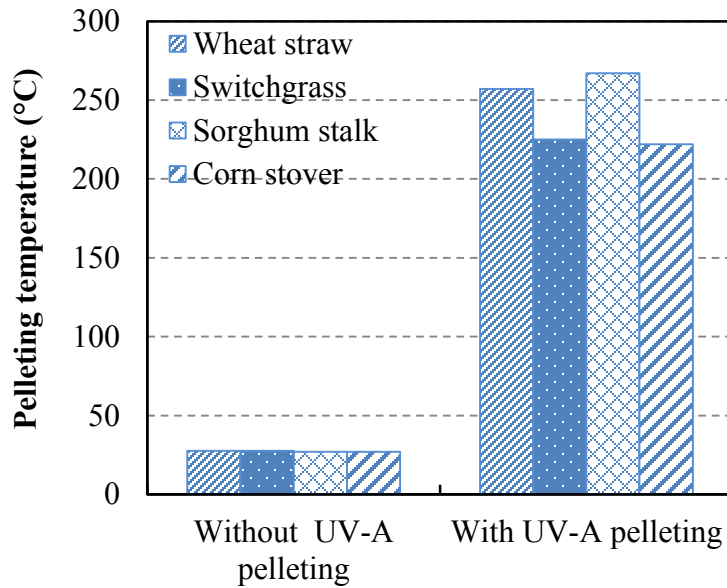
11.4 Conclusions

This paper reports an experimental investigation on effects of ultrasonic vibration-assisted (UV-A) pelleting on biomass sugar yield using two sugar yield definitions. It is the first study to use total sugar yield (considering both pretreatment and enzymatic hydrolysis) to investigate effects of UV-A pelleting on biomass sugar yield. Four types of cellulosic biomass (wheat straw, corn stover, switchgrass, and sorghum stalk) were used. Major conclusions are:

1. Considering both pretreatment and enzymatic hydrolysis processes, the total sugar yield (Y_p) of biomass processed with UV-A pelleting were 30% to 43% higher than that of biomass not processed with UV-A pelleting.

2. Considering enzymatic hydrolysis process alone, enzymatic hydrolysis sugar yield (Y_h) of biomass processed with UV-A pelleting were 6% to 22% higher than that of biomass not processed with UV-A pelleting.

3. With UV-A pelleting, pretreatment weight recovery (R) was increased for all four types of biomass.

Based on this experimental investigation, two hypotheses about the mechanism that UV-A pelleting increased biomass total sugar yield were proposed. (1): UV-A pelleting can help to increase biomass pretreatment weight recovery comparing with that of the biomass without UV-

A pelleting. In this way, more cellulose from biomass with UV-A pelleting could be recovered after pretreatment, which could increase the potential sugar content in the biomass goes to the subsequent enzymatic hydrolysis. (2): The high temperature generated during the UV-A pelleting process can melt down and decompose lignin, which serves as a protecting shield over cellulose. This effect may help to release more cellulose and make cellulose biomass material more amenable to enzymatic hydrolysis. Biomass compositional analysis and mass balance calculation will be used to assist the test of these two hypotheses in the future study.

Acknowledgements

References

[1]   U.S. Energy Information Administration (2012) Annual Energy Review 2011. http://www.eia.gov/totalenergy/data/annual/pdf/aer.pdf. Accessed 3 Jan 2013

[2]   U.S. Energy Information Administration (2011) Short-Term Energy Outlook. http://www.eia.gov/forecasts/steo/pdf/steo_full.pdf. Accessed 3 Jan 2013

[3]   Greene DL, Schafer A (2011) Reducing Greenhouse Gas Emissions from U.S. Transportation. Center for Climate and Energy Solutions. http://www.c2es.org/docUploads/reducing-transportation-ghg.pdf. Accessed 3 Jan 2013

[4]   U.S. Department of Energy (2010) Environmental Benefits. http://www1.eere.energy.gov/biomass/printable_versions/environmental.html. Accessed 3 Jan 2013

[5]   RFA (2011) Ethanol Facts: Environment. http://www.ethanolrfa.org/pages/ethanol-facts-environment. Accessed 20 Dec 2012

[6]   Lynd LR (1996) Overview and Evaluation of Fuel Ethanol from Cellulosic Biomass: Technology, Economics, the Environment, and Policy. Annual review of energy and the environment 21:403–465

[7]   Zhu JY, Wang GS, Pan XJ, Gleisner R (2009) Specific Surface to Evaluate the Efficiencies of Milling and Pretreatment of Wood for Enzymatic Saccharification. Chemical Engineering Science 64:474–485

[8]   Zhu JY, Pan XJ, Wang GS, Gleisner R (2009) Sulfite Pretreatment (SPORL) for Robust Enzymatic Saccharification of Spruce and Red Pine. Bioresource Technology 100:2411–2418

[9]   Zhu W, Zhu JY, Gleisner R, Pan XJ (2010) On Energy Consumption for Size-Reduction and Yields from Subsequent Enzymatic Saccharification of Pretreated Lodgepole Pine. Bioresource Technology 101:2782–2792

[10]   Von Sivers M, Zacchi G (1996) Ethanol from Lignocellulosics: A Review of the Economy. Bioresource Technology 56:131–140

[11]   Rubin EM (2008) Genomics of Cellulosic Biofuels. Nature 454:841–845

[12]   U.S. Department of Energy (2005) Breaking the Biological Barriers to Cellulosic Ethanol: A Joint Research Agenda. http://genomicscience.energy.gov/biofuels/b2bworkshop.shtml. Accessed 20 Dec 2012

[13]   Huber GW (2008) Breaking the Chemical and Engineering Barriers to Lignocellulosic Biofuels: Next Generation Hydrocarbon Biorefineries, Ed. George W. Huber, University of Massachusetts Amherst, National Science Foundation, Chemical, Bioengineering, Environmental, and Transport Systems Division, Washington D.C.

[14]   Falk D (1985) Pelleting cost center, Feed Manufacturing Technology, 3rd edition, McEllhiney, M.M. (ed.), American Feed Industry Association, Arlington, VA

[15]   Hess JR, Wright CT, Kenney KL (2007) Cellulosic biomass feedstocks and logistics for ethanol production, Biofuels, Bioproducts and Biorefining, 1(3): 181–190

[16]   Sokhansanj S, Turhollow AF (2004) Biomass densification — cubing operations and costs for corn stover, Applied Engineering in Agriculture, 20(4) 495-499

[17]   Song XX, Zhang M, Pei ZJ, Deines T (2010) Ultrasonic-Vibration-Assisted Pelleting of Cellulosic Biomass: Effects of Moisture Content. Proceedings of the ASME 2010 International Manufacturing Science and Engineering Conference (MSEC)

[18]   Cong W, Pei Z, Zhang P, Qin N, Deines T, Lin B (2011) Ultrasonic-vibration-assisted pelleting of switchgrass: Effects of ultrasonic vibration. Transactions of Tianjin University 17:313–319

[19]   Zhang PF, Deines TW, Nottingham D, Pei ZJ, Wang D, Wu X (2010) Ultrasonic Vibration-Assisted Pelleting of Biomass: A Designed Experimental Investigation on Pellet Quality and Sugar Yield. Proceedings of the ASME 2010 International Manufacturing Science and Engineering Conference (MSEC)

[20]   Seino T, Yoshioka A, Fujiwara M, Chen KL, Erata T, Tabata M, Takai M (2001) ESR studies of radicals generated by ultrasonic irradiation of lignin solution. An application of the spin trapping method, Wood Science and Technology, 35(1):97–106

[21]   Chuanyun D., Bochu W, Huan Z, Conglin H, Chuanren D, Wangqian L, Toyama Y, Sakanishi A (2004) Effect of low frequency ultrasonic stimulation on the secretion of siboflavin produced by Ecemothecium Ashbyii, Colloids and Surfaces B: Biointerfaces, 34(1): 7–11

[22]   Yaldagard M, Mortazavi SA, Tabatabaie F (2008) The effect of ultrasound in combination with thermal treatment on the germinated barley's alpha-amylase activity, Korean Journal of Chemical Engineering, 25(3): 517–523

[23]   Toma M, Bandow H, Vinatoru M, Maeda Y (2006) Ultrasonically assisted conversion of lignocellulosic biomass to ethanol, Proceeding of the AIChE annual meeting. http://www.nt.ntnu.no/users/skoge/prost/proceedings/aiche-2006/data/papers/P70141.pdf Accessed 22 Feb 2013

[24]   Ninomiya K, Kamide K, Takahashi K, Shimizu N (2012) Enhanced enzymatic saccharification of kenaf powder after ultrasonic pretreatment in ionic liquids at room temperature, Bioresource Technology, 103(1): 259–265

[25]   Velmurugan R, Muthukumar K (2012) Ultrasound-assisted alkaline pretreatment of sugarcane bagasse for fermentable sugar production: Optimization through response surface methodology, Bioresource Technology, 112: 293–299

[26]   Zhang PF, Pei ZJ, Wang D, Wu X, Cong WL, Zhang M, Deines TW (2011) Ultrasonic Vibration-Assisted Pelleting of Cellulosic Biomass for Biofuel Manufacturing. Journal of manufacturing science and engineering 133:011012–1 – 011012–7

[27]   Tang YJ, Zhang PF, Liu DF, Pei ZJ (2012) Effects of Pellet Weight in Ultrasonic Vibration-Assisted Pelleting for Cellulosic Biofuel Manufacturing. International Journal of Manufacturing Research 7:397–408

[28] Zhang Q, Zhang PF, Deines T, Pei ZJ, Wang D, Wu X, Pritchett G (2010) Ultrasonic Vibration-Assisted Pelleting of Sorghum Stalks: Effects of Pressure and Ultrasonic Power. Proceedings of the ASME 2010 International Manufacturing Science and Engineering Conference (MSEC)

[29] Zhang PF, Zhang Q, Pei ZJ, Pei L (2011) An experimental investigation on cellulosic biofuel manufacturing: effects of biomass particle size on sugar yield. Proceedings of the ASME 2011 International Mechanical Engineering Congress and Exposition (IMECE)

[30] Theerarattananoon K, Xu F, Wilson J, Staggenborg S, McKinney L, Vadlani P, Pei Z, Wang D (2012) Effects of the Pelleting Conditions on Chemical Composition and Sugar Yield of Corn Stover, Big Bluestem, Wheat Straw, and Sorghum Stalk Pellets. Bioprocess and Biosystems Engineering 35:615–623

[31] Sluiter A, Hames B, Hyman D, Payne C, Ruiz R (2008) Determination of Total Solids in Biomass and Total Dissolved Solids in Liquid Process Samples. NREL Laboratory Analytical Procedure Technical Report No. NREL/TP-510–42621

[32] Hu G, Heitmann JA, Rojas OJ (2008) Feedstock Pretreatment Strategies for Producing Ethanol from Wood, Bark, and Forest Residues, Bioresources, 3(1): 270-294

[33] Xu F, Theerarattananoona K, Wu X, Pena L, Shi Y, Staggenborg S, Wang D (2011) Process Optimization for Ethanol Production from Photoperiod-sensitive Sorghum: Focus on Cellulose Conversion, Industrial Crops and Products, 34(1): 1212-1218

[34] Donohoe BS, Decker SR, Tucker MP, Himmel, ME, Vinzant TB (2008) Visualizing lignin coalescence and migration through maize cell walls following thermochemical pretreatment. Biotechnology Bioengineering, 101(5): 913–925

Chapter 12 - A Physics-based Temperature Model For Ultrasonic Vibration-Assisted Pelleting for Cellulosic Biomass

Authors' names:

Xiaoxu Song[a], Xiaoming Yu[a], Meng Zhang[a], Z.J. Pei[a], and Donghai Wang[b]

Authors' affiliation:

[a]Department of Industrial and Manufacturing Systems Engineering, Kansas State University, Manhattan KS 66506 USA

[b]Department of Biological and Agricultural Engineering, Kansas State University, Manhattan, KS 66506, USA

Abstract

Temperature in ultrasonic vibration-assisted (UV-A) pelleting of cellulosic biomass has a significant impact on pellet quality. However, there are no reports on temperature models for UV-A pelleting of cellulosic biomass. The development of a physics-based temperature model can help to explain experimentally determined relations between UV-A pelleting process variables and temperature, and provide guidelines to optimize these process variables in order to produce pellets of good quality. This paper presents such a model for UV-A pelleting of cellulosic biomass. Development of the model is described first. Then, using the model, temperature distribution is investigated and temperature difference between the top and the bottom surfaces of a pellet is explained. Based on this model, relations between process variables (ultrasonic power and pelleting duration) and temperature are predicted. Experiments were conducted for model verification, and the experimental results agreed well with model predictions.

Keywords

Nomenclature

c: specific heat capacity of cellulosic biomass (J/kg K)

k: thermal conductivity of cellulosic biomass (W/m K)

m: mass of cellulosic biomass pellet (kg)

ρ: density of cellulosic biomass pellet (kg/m^3)

T: temperature of cellulosic biomass pellet (K)

h: height of cellulosic biomass pellet (m)

α: absorption coefficient of cellulosic biomass (m^{-1})

I: ultrasound intensity (W/m^2)

I_0: ultrasound intensity at the top surface of a pellet (W/m^2)

Q: volumetric heat generation rate (W/m^3)

t: pelleting time (s)

t_d: pelleting duration (s)

T_0: room temperature (300 K)

k_{Ti}: thermal conductivity of Ti (W/m K)

k_{Al}: thermal conductivity of Al (W/m K)

12.1 Introduction

Long-term economic and environmental concerns have presented incentives for research in renewable alternatives to replace petroleum-based transportation fuels [1]. Conversion of cellulosic biomass to biofuels is a viable option to improve national energy security and to reduce greenhouse gas emissions [2]. The United States government has established a goal that cellulosic biomass will supply 20% of the nation's transportation fuels by 2030 [3]. A consistent supply of high quality, low cost cellulosic biomass feedstocks are important to achieve this goal. One major barrier with current cellulosic biomass supply system is related to the low bulk density of cellulosic feedstocks, which causes their transportation and handling be very expensive [4]. One of the strategies to overcoming this barrier is the densification of cellulosic biomass feedstocks. Improvements in feedstock bulk density and flowability will reduce transportation and handling costs.

Pelleting is generally described as "the agglomeration of small particles into firm, uniformly shaped granules by the means of a mechanical process" [5]. Pelleting can increase the

overall efficiency of transportation and handling of cellulosic biomass feedstock by enabling the use of the existing grain transportation infrastructure and storage systems [6]. Traditionally, biomass pellets are made by screw extruding or piston ramming ground biomass particles through round cross sectional dies [7]. Ultrasonic vibration-assisted (UV-A) pelleting is a newly developed pelleting method. UV-A pelleting can produce biomass pellets with density as high as 1,000 kg/m^3, about 30-time higher than the bulk density of cellulosic biomass before pelleting [8, 9]. In UV-A pelleting, the pelleting pressure provides the force to agglomerate the particles and remove the voids. Ultrasonic vibration causes the increases of temperature.

Temperature of biomass during pelleting has significant impacts on pellet density and durability (the ability of one pellet to withstand impact and abrasion encountered during transportation and storage). Reported studies reveal that, with high-temperature steam or other forms of additional heat being applied to the pelleting process, pellet density and durability were improved [10-14]. This benefit has been interpreted as follows. When biomass was heated, lignin (polymers that fill the cell walls in a plant matter) would become soft and melted, exhibiting thermosetting property. This property would make lignin become permanently rigid and likely to bond together with other polymers (cellulose and hemicellulose) in the biomass [15]. Experimental studies on temperature in UV-A pelleting have been reported in the literature [16, 17]. UV-A pelleting can also induce an increase in temperature of biomass due to the high frequency ultrasonic vibration being applied to the biomass. Ultrasonic vibration causes biomass particles to vibrate at high frequency and result in absorption of the ultrasound energy mainly in form of heat generation. It was found that during the UV-A pelleting of wheat straw, temperature of the biomass could rise as high as 300°C, and the highest temperature was found at the pellet center [16]. It has been hypothesized that the generation of heat during the pelleting process may affect the biofuel yield in the downstream bioconversion process [18].

Currently, no publications are available on developing a temperature model for UV-A pelleting of cellulosic biomass. It is necessary to develop such a model to help explaining experimentally determined relations between UV-A pelleting variables (such as ultrasonic power and pelleting duration) and temperature. To fill this gap in the literature, this paper presents the first temperature model for UV-A pelleting of cellulosic biomass.

12.2 Development of the temperature model

12.2.1 Model assumptions

Development of the temperature model in this section is based on the following assumptions:

(1) Biomass uniformly fills the mold;

(2) Thermal conductivity of biomass is not a function of temperature [19-21];

(3) The ultrasound energy absorbed by the biomass all results in heat generation[22];

(4) Heat transfer takes place within the biomass by conduction only;

(5) The temperatures at the boundaries are fixed as room temperature [23, 24].

12.2.2 Derivation of model equations

According to conservation of energy, the thermal energy balance equation on a differential volume element [25] as illustrated in Figure 12-1 is given as:

{Rate of thermal energy in} - {Rate of thermal energy out} + {Net rate of thermal energy generation} = {Rate of accumulation of thermal energy}

The rate at which thermal energy enters the volume element across the face at x is given by the product of the heat flux $q_x|_x$ and the cross-sectional area A. Similarly, the rate at which

Figure 12-1 Differential volume element
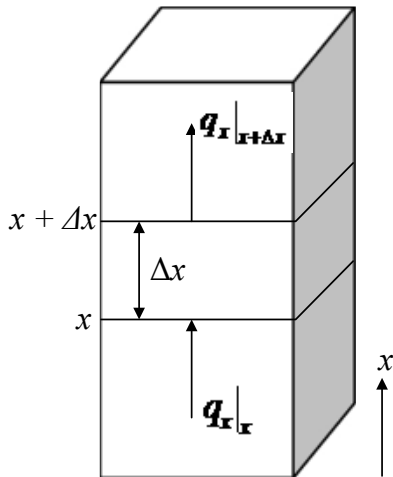
thermal energy leaves the volume element across the face at $x + \Delta x$ is $q_x\big|_{x+\Delta x}$. The net rate of generation is $QA\Delta x$. Finally, the rate of accumulation is given by the time derivative of the thermal energy content of the volume element. Thus, the balance equation becomes:

$$\left(q_x\big|_x - q_x\big|_{x+\Delta x}\right)A + QA\Delta x = \rho c \frac{\partial T}{\partial t} A \Delta x \qquad (1)$$

Dividing by $A\Delta x$ and taking the limit as $\Delta x \to 0$ yields:

$$-\frac{\partial q_x}{\partial x} + Q = \rho c \frac{\partial T}{\partial t} \qquad (2)$$

Using Fourier's law [26, 27], which is $q_x = -k\frac{\partial T}{\partial x}$, the balance equation becomes:

$$\frac{\partial}{\partial x}\left(k\frac{\partial T}{\partial x}\right) + Q = \rho c \frac{\partial T}{\partial t} \qquad (3)$$

According to the assumption, thermal conductivity of biomass k is not a function of temperature, the heat conduction differential equation becomes:

$$k\frac{\partial^2 T}{\partial r^2} + \frac{k}{r}\frac{\partial T}{\partial r} + k\frac{\partial^2 T}{\partial z^2} + Q - \rho c \frac{\partial T}{\partial t} = 0 \qquad (4)$$

The above equation is based on the following boundary and initial conditions:

- Initial condition

$$T(0,r,z) = T_0 \qquad (5)$$

- Boundary conditions

$$T(t,r,z_0) = T_0 \qquad (6)$$

$$T(t,r,z_M) = T_0 \qquad (7)$$

$$T(t,r_N,z) = T_0 \qquad (8)$$

$$\frac{\partial T}{\partial r}\bigg|_{r=0} = 0 \qquad (9)$$

When an ultrasonic wave passes through a medium, attenuation occurs due to reflection, scattering, and absorption [28]. This model only considers effects of absorption, which is the

conversion of ultrasound energy to heat. As the wave travels through the medium, energy is irreversibly lost to the medium in form of heat generation at a rate given by [28]:

$$Q = 2\alpha I \tag{10}$$

$$I = I_0 e^{-2\alpha z} \tag{11}$$

Introducing Eq. (10) and Eq. (11) in Eq. (4) results in the following heat transfer equation

$$k\frac{\partial^2 T}{\partial r^2} + \frac{k}{r}\frac{\partial T}{\partial r} + k\frac{\partial^2 T}{\partial z^2} + 2\alpha I_0 e^{-2\alpha z} - \rho c\frac{\partial T}{\partial t} = 0 \tag{12}$$

Now, it is essential to solve the above equation based on the initial and boundary conditions given by Eqs. (5) - (9).

12.2.3 Numerical scheme

Equations (5) - (9) and (12) were converted to finite difference equations where subscripts denote location and superscripts denote time ($T(x_i, t_j) = T_i^j$). Considering a cylindrical shaped pellet (shown in Figure 12-2) of radius r and height h. $i = 1$ represents the pellet bottom surface, and $i = M$ locates the pellet top surface. Then the approximation for the equation at $T(x_i, t_j)$ is

$$T_i^{j+1} = \left[\frac{k(T_{i+1}^j - 2T_i^j + T_{i-1}^j)}{\Delta x^2} + Q\right]\frac{\Delta t}{\rho c} + T_i^j \tag{13}$$

The above equation utilizes an explicit finite difference method scheme. Briefly, the unknown temperatures of locations ($i = 1, 2, \ldots, M$) at time $j = 2$ are calculated based on the known temperatures given by the initial condition. After this, the temperature at time $j = 2$ are used to calculated the temperature at time $j = 3$. This calculation could be continued iteratively further to solve temperatures at all the locations within one pellet.

Figure 12-2 Pellet explicit scheme

169
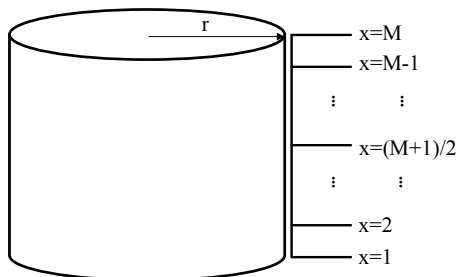
12.3 Obtaining absorption coefficient of cellulosic biomass α

12.3.1 Biomass material

The cellulosic biomass used in this investigation was wheat straw. Wheat straw was harvested by the Deines Farm in Northwest Kansas. The wheat straw had been run through a John Deere 9600 combine. The combine removed grains from straw and chaff. Wheat straw and chaff exited through the back of the combine, and had an average length 250 mm. After being collected, wheat straw was stored indoors until this study.

Wheat straw was processed by a knife mill (Model SM 2000 from Retsch, Inc., Haan, Germany). The knife mill used a 240-V, 2.2-kW electric motor with a fixed rotation speed (1720 rpm). Three cutting blades (95 mm long and 35 mm wide) were mounted on the rotor. Four shear bars were mounted on the inside wall of the milling chamber. There was a 3-mm gap between a cutting blade and a shear bar. Biomass was cut between the cutting blades and the shear bars. The sieve used in the knife mill had a sieve size of 0.25 mm. Particles smaller than the sieve size would fall through the sieve. Particles larger than the sieve size would be recirculated and further milled. Biomass particles after milling were kept in Ziploc® bags until being further used for UV-A pelleting.

Moisture content of biomass is defined as the amount of moisture (water) contained in a certain amount of biomass and is expressed as a percentage of the biomass weight. The moisture content of biomass after milling was measured by following NREL Laboratory Analytical Procedure [19]. Moisture content of the wheat straw used in this study was 7%.

12.3.2 Experimental setup

Figure 12-3 is a schematic illustration of the experimental set-up for UV-A pelleting. UV-A pelleting experiments were performed on a modified ultrasonic machine (Model AP-1000, Sonic-Mill, Albuquerque, NM, USA). The machine included a power supply (which converts 60 Hz electrical power into 20,000 Hz electrical power), a converter (which converts high frequency electrical energy into mechanical motion), and a titanium horn. The tip of the horn was a solid cylinder with a flat end (17.4 mm in diameter).

The pneumatic cylinder was driven by compressed air provided by a 1.25-kW, 125-L air compressor (Sears, Roebuck and Co., Hoffman Estates, IL, USA). The air pressure in the

pneumatic cylinder was controlled by a pressure regulator. A higher air pressure in the pneumatic cylinder produced a higher pressure applied to the biomass in the aluminum mold.

Total pelleting duration (t_d) was the entire period of a pelleting test, during which the horn was in contact with wheat straw particles inside the mold. Pelleting time (t) referred to the time between the beginning of a pelleting test till a point in time of interest. Pelleting time could have any value between 0 and the total pelleting duration (t_d).

Figure 12-3 A schematic illustration of the experimental set-up for UV-A pelleting.
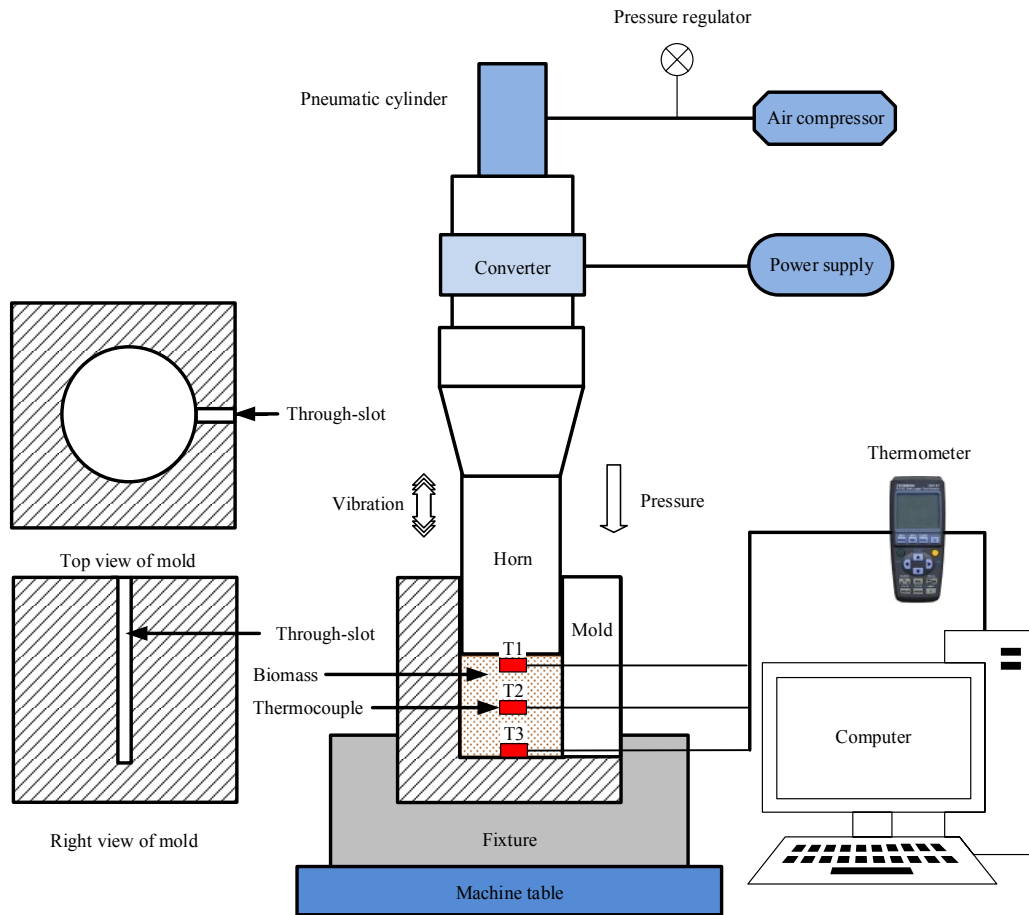
The vibration amplitude of the horn was controlled by the percentage of ultrasonic power. A higher ultrasonic power would cause the horn vibrate at a larger amplitude. Pellet weight was the weight of biomass loaded into the mold before each test.

12.3.3 Measurement procedure for pelleting temperature

Figure 12-3 illustrates the temperature measurement method during a pelleting test. Metal wire-type (K-type, Model SC-GG-K-30-36, Omega Engineering, Inc., Stamford, CT, USA) thermocouples were used to measure the temperature. They were inserted inside the biomass. The thermocouples were connected to a digital thermometer (HH147U, Omega Engineering, Inc., Stamford, CT, USA). Temperature measurement data were displayed and recorded on a computer.

Temperatures at three locations (T1, T2, and T3 as shown in Figure 12-3) of a pellet were measured. T1 was the temperature at the center on the pellet top surface. T2 was the temperature at the pellet center. T3 was the temperatures at the center on the pellet bottom surface. All of the thermocouples were inserted into the mold through a slot (the width of the slots was 2 mm) on the mold wall, so the thermocouple wires could move down as the biomass in the mold was compressed.

12.3.4 Experimental design

If α is independent of input variables, as assumed in the model development, then theoretically only one experiment is needed to get its value. However, to verify whether it is indeed independent of input variables, a number of different experiments for various combinations of input variables are necessary. The experimental conditions are shown in Table 12-1. The experiments involve two groups of input variables (ultrasonic power and biomass weight). The following variables are held constant during all test runs:

- Pelleting duration: 200 s
- Pressure: 40 psi

Table 12-1 Experimental conditions for obtaining α.

Experiment	Ultrasonic power (%)	Pellet weight (g)
1st group	20, 40, 60	1.2
2nd group	60	1.2, 1.8, 2.4

12.3.5 Analysis of experimental results

The purpose of this section is to estimate the value of α for a given biomass material using the data obtained from experiments. For each test, one value of α is obtained using

temperature measurement data by using Eq.(12). The value of α for the all data is 3.13 m^{-1}. Figure 12-4 shows the values of α estimated for each experimental group. It is seen that there are not strong correlations between the values of α and input variables. Though there are some deviations among these data, one can state that the assumption of α being constant for a particular material is reasonable and the value can be applied to evaluate the temperature for a given material over a range of input variables.

12.4 Predicted effects of input variables on temperature

In the previous section, a physics-based model for temperature in UV-A pelleting of cellulosic biomass has been developed. In this section, effects of ultrasonic power on temperature in UV-A pelleting of cellulosic biomass will be predicted using this model. In order to implement the computation numerically, values of the variables in the model are given in Table 12-2. Cellulosic biomass used in the implementation is wheat straw.

Table 12-2 Values of variables in the model.

Variable	Value
c	1243 J/kg K
k	0.34 W/m K
m	0.002 kg
h	0.008 m
α	3.13 m^{-1}
t_d	400 s

Table 12-3 Relationship between ultrasonic power and ultrasound intensity.

Ultrasonic power (%)	Ultrasonic power (W)	Ultrasonic intensity I (W/m^2)
10	50	210379
20	100	420757
30	150	631136
40	200	841515
50	250	1051894
60	300	1262272
70	350	1472651
80	400	1683030
90	450	1893409
100	500	2103787

Figure 12-4 Influences of input variables on absorption coefficient of cellulosic biomass α.
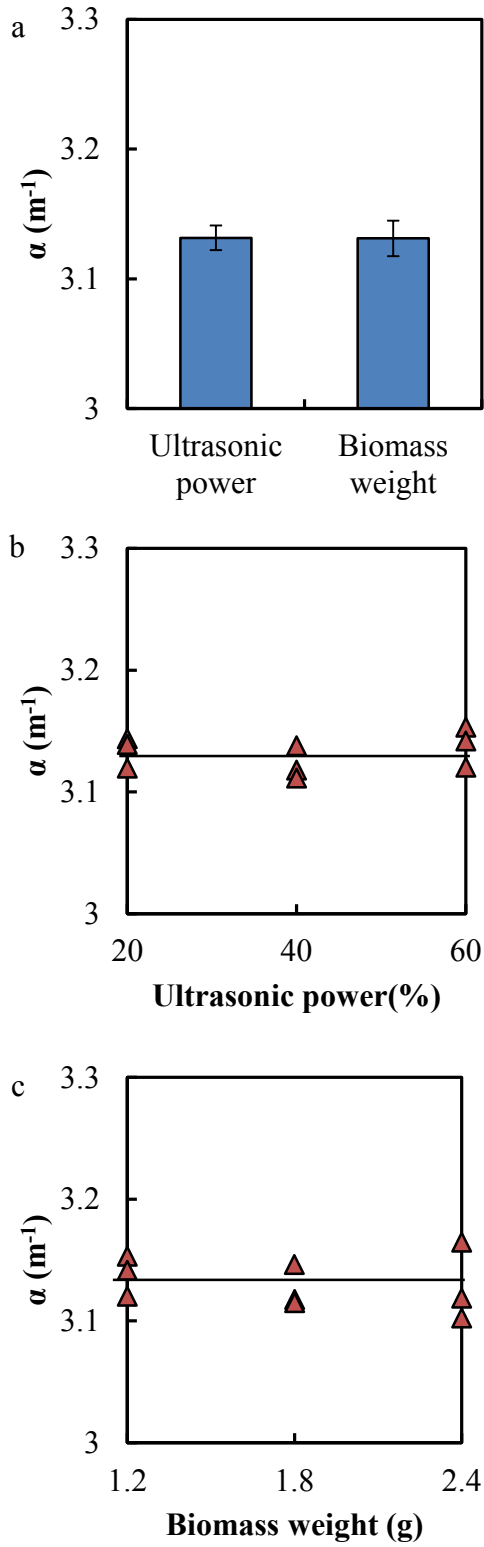
The variation of c is given as 1243 J/kg K according to Koufopanos et al. [29]. In the literature, it was found that values of k for different cellulosic biomass varied from 0.053 W/mK [30] to 1.130 W/mK [29]. The value of k for wheat straw was taken as 0.34 W/mK based on the range of similar materials given in the literature. The value of α is taken as 3.13 m^{-1}, which was determined in Section 3. Values of ultrasonic power are obtained from a specific ultrasonic machine (Model AP-1000, Sonic-Mill, Albuquerque, NM, USA). On the ultrasonic machine, the setting of ultrasonic power is calibrated as percentage (10% - 100%). Necessary conversions of this percentage into ultrasonic power (W) and ultrasonic intensity (W/m^2) are listed in Table 12-3.

Figure 12-5 shows the predicted temperature distribution of a pellet. The temperature distribution is symmetrical to the pellet center. For one pellet, the equilibrium temperatures (temperature changes with time is less than 0.01 K/s) at different locations are different. As the distance to the pellet center increases, the equilibrium temperature becomes lower. The highest equilibrium temperature locates at the pellet center as expected, because the distances from the pellet center to the mold is the longest. The heat exchange is the lowest in the pellet center. The equilibrium temperature at the pellet center is 412 K, while this temperature decreases to 328 K at the pellet top surface.

Figure 12-5 Predicted temperature distribution at pelleting time 400 s. (Ultrasonic power = 40%)
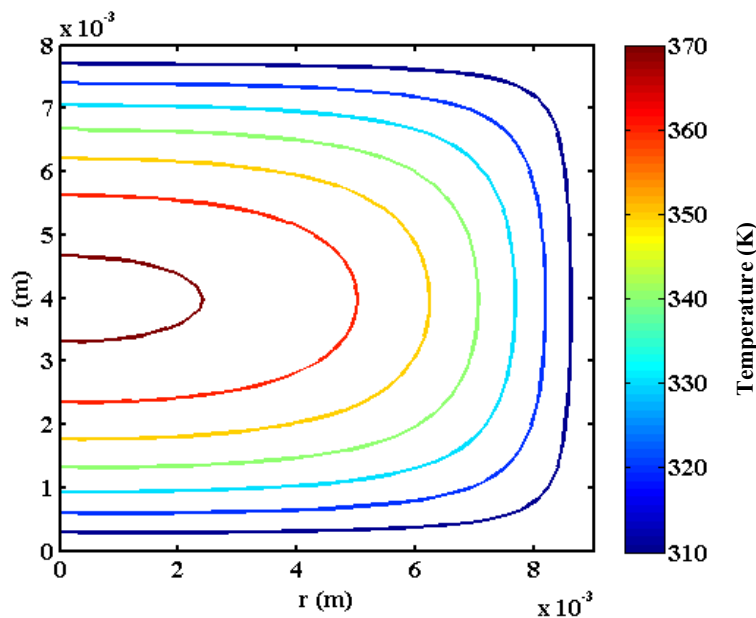
Figure 12-6 Temperature vs. pelleting duration for three locations. (Ultrasonic power = 40%)
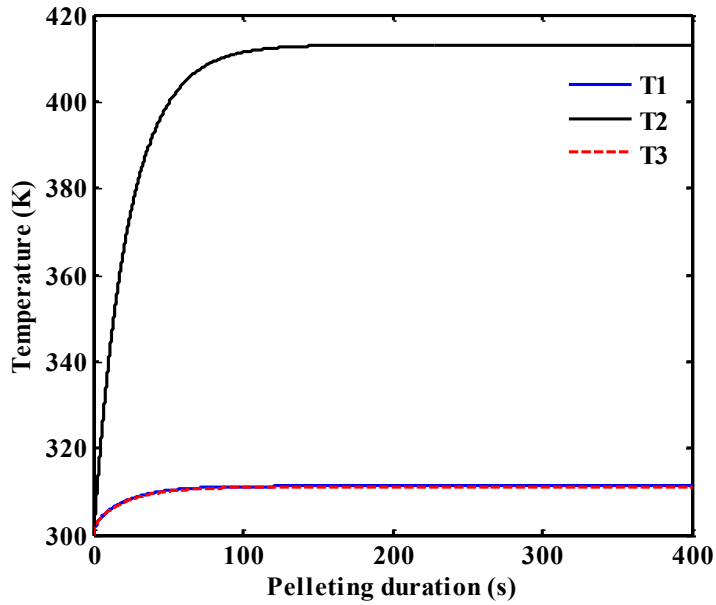
Figure 12-7 Temperature vs. pelleting duration for different ultrasonic power at the pellet center.
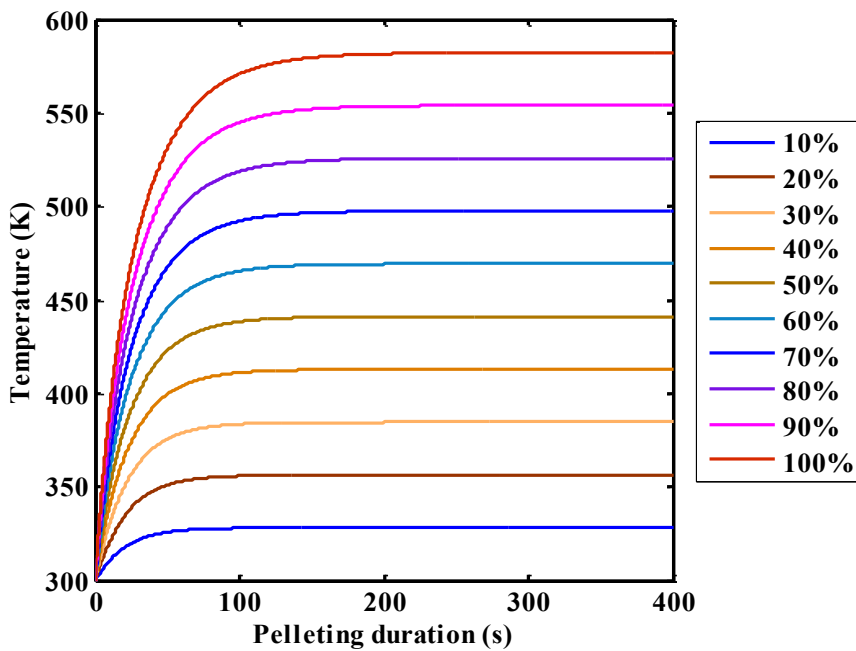
As shown in Figure 12-6, at different locations of a pellet, the time needed to reach the equilibrium temperature is different. As the distance to the pellet center increases, the time

176

needed to reach the equilibrium temperature becomes shorter. The time needed to reach the equilibrium temperature is 131 s at the pellet top surface. This time increases greatly to 149 s at the pellet center.

The predicted relation between temperature at the pellet center and ultrasonic power is shown in Figure 12-7. It can be seen that temperature increases noticeably as ultrasonic power and pelleting duration increase. The equilibrium temperatures are 356 K, 412 K, 470 K, 525 K, and 582 K, when ultrasonic powers are set at 20%, 40%, 60%, 80%, and 100%, respectively.

However, as ultrasonic power increases, the time needed to reach the equilibrium temperature becomes longer. The relation is plotted in Figure 12-8. The time needed to reach the equilibrium temperature increases linearly as ultrasonic power increases. The time needed to reach the equilibrium temperature is 120 s, when ultrasonic power is set at 20%. This time increases greatly to 221 s, when ultrasonic power is set at 100%.

The relation between ultrasonic power and equilibrium temperature can be explained that, on an ultrasonic machine, ultrasonic intensity (I) increases as ultrasonic power increases. Since $Q = 2\alpha I$, the volumetric heat generation rate (Q) increases as ultrasonic intensity (I) increases. Higher volumetric heat generation rate (Q) results in higher temperature rise.

Figure 12-8 Relation between ultrasonic power and the time needed to reach the equilibrium temperature at the pellet center.
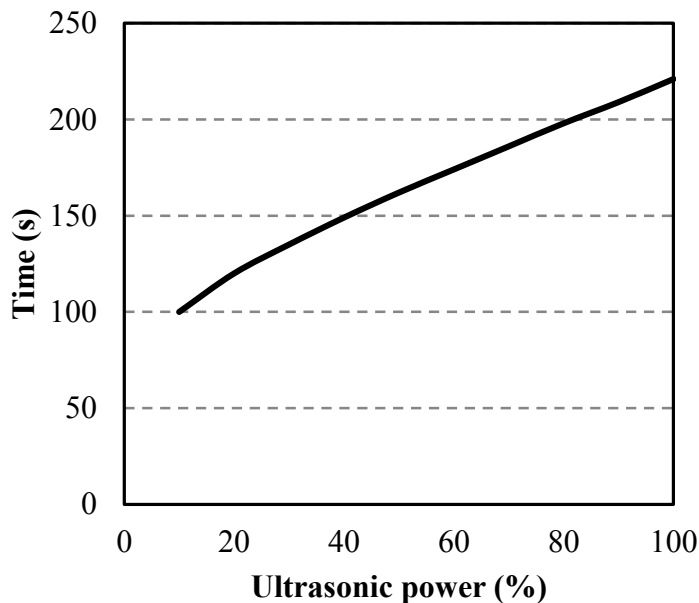
12.5 Pilot experimental validation and comparison

To verify the relations predicted by the temperature model, pelleting experiments were performed under ultrasonic power of six levels while other variables were kept as constants (as shown in Table 12-4). Experimental and predicted temperatures at the pellet center are compared in Figure 12-9. Temperature rise is proportional to the increase of ultrasonic power. It can be seen that the trend of predicted relation between ultrasonic power and temperature agrees well with that determined by experiments. The relation between temperature and pelleting duration are shown in Figure 12-10. It is noticed that the trends of simulation results agree well with the trends determined experimentally. It can be observed that, the value of T2 in experimental results is smaller than that in the simulation results. First, in the model, specific heat capacity of cellulosic biomass c is assumed to be constant. According to the reference in the literature [29], c is a function of temperature. As the temperature T increases, c will increases. For the same amount of heat Q, according to $Q = cm\Delta T$, the increase of c will result in the decrease of ΔT. Since the model does not consider the dependence of c on temperature, T2 in the experiments will be smaller than the simulation value. Second, when an ultrasonic wave passes through a medium, attenuation occurs due to reflection, scattering, and absorption. This model only considers effects of absorption, which is the conversion of ultrasound energy to heat. Effects of reflection and scattering have been neglected. So the heat amount in the model is larger than that in the experiments, causing smaller experimental value than simulation value. As seen in Figure 12-11, the model predicts that the equilibrium temperatures at T1 and T3 are the same. However, in the experiment, the temperature at T1 were slightly higher than that at T3. The reason is explained as, the model developed in Section 2 using an assumption that the temperatures at the boundaries are fixed as room temperature, which means the temperatures at the top and bottom surfaces are 300 K at any time. The k value at the top and bottom surfaces are infinity. However, it is not practical in the experiment. The top surface of the pellet is in contact with ultrasonic horn which is made of Ti. The bottom surface of the pellet is in contact with the mold which is made of Al. The k values of Ti and Al are not the same and not equals to infinity. In the following model, the differences between k values of Ti and Al will be considered.

Table 12-4 Conditions for pilot experimental verification.

Input variable	Value
Ultrasonic power (%)	20, 30, 40, 50, 60, 70
Pressure (psi)	40
Pelleting duration (s)	200
Pellet weight (g)	2

Figure 12-9 Comparison of equilibrium temperature between predicted results and experimental results at the pellet center
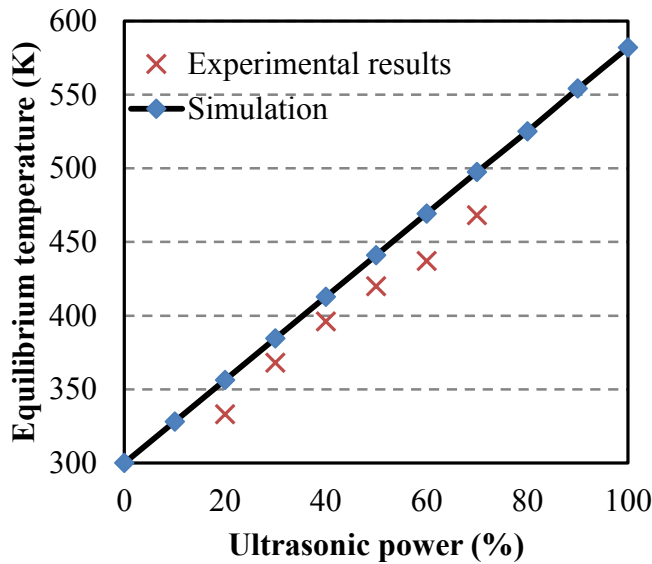
Figure 12-10 Comparison of experiment and simulation temperature vs. pelleting duration curves at the pellet center. (Ultrasonic power = 40%)
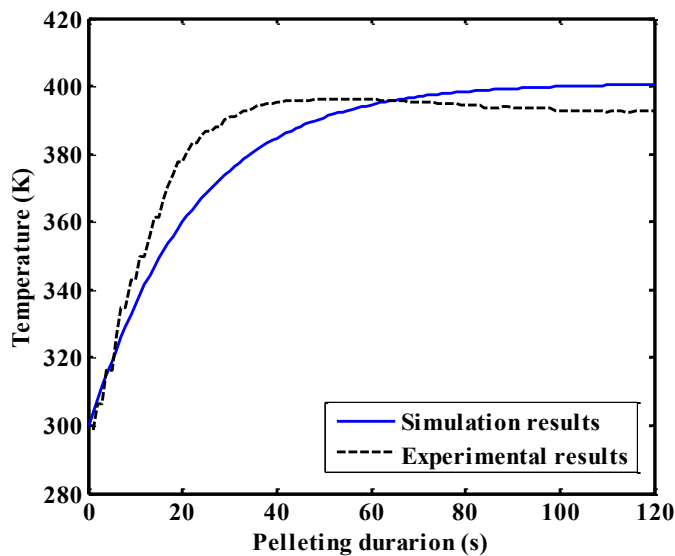
Figure 12-11 Comparison of equilibrium temperature between predicted results and experimental results at different locations. (Ultrasonic power = 40%).
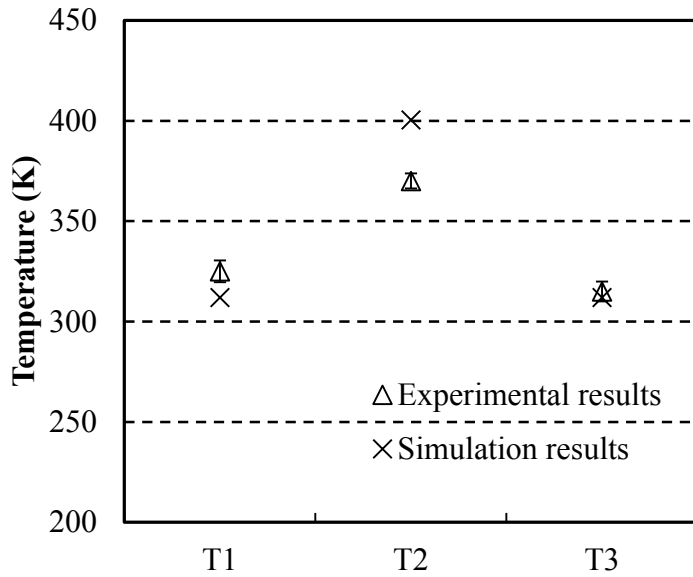
12.6 Improved model for second boundary conditions

In this section, a one dimensional temperature model will be developed in which the heat transfer will be considered in the boundaries.

12.6.1 Model assumptions

Development of the temperature model in this section is based on the following assumptions:

(1) Biomass uniformly fills the mold;

(2) Thermal conductivity of biomass is not a function of temperature [19-21];

(3) The ultrasound energy absorbed by the biomass all results in heat generation [22];

(4) Heat transfer takes place within the biomass by conduction only.

12.6.2 Derivation of model equations

The heat conduction differential equation for one dimensional becomes:

$$k\frac{\partial^2 T}{\partial x^2} + Q = \rho c \frac{\partial T}{\partial t} \tag{14}$$

The top surface of the pellet is in contact with ultrasonic horn which is made of Ti. The bottom surface of the pellet is contact with mold which is made of Al. There is heat transfer

happened at the boundaries. The temperatures at the boundaries are no longer fixed at room temperature. The heat flux q_x at the boundaries are the same. So the initial and boundary conditions become:

- Initial condition

$$T(0,x) = T_0 \tag{15}$$

- Boundary conditions

$$k_{Ti} \frac{\partial T_{Ti}}{\partial x_{Ti}} = k \frac{\partial T}{\partial x} \tag{16}$$

$$k \frac{\partial T}{\partial x} = k_{Al} \frac{\partial T_{Al}}{\partial x_{Al}} \tag{17}$$

12.6.3 Numerical scheme

Equations (14) - (17) were converted to finite difference equations where subscripts denote location and superscripts denote time ($T(x_i, t_j) = T_i^j$). Considering a cylindrical shaped pellet (shown in Figure 12-2) of radius r and height h. $i = 1$ represents the bottom surface of pellet, and $i = M$ locates the top surface of pellet. Then the approximation for the equation at $T(x_i, t_j)$ is

$$\frac{T_i^{n+1} - T_i^n}{\Delta t} = \frac{\alpha_{td}}{2} \left[\frac{T_{i+1}^{n+1} - 2T_i^{n+1} + T_{i-1}^{n+1}}{(\Delta x)^2} + \frac{T_{i+1}^n - 2T_i^n + T_{i-1}^n}{(\Delta x)^2} + Q \right] \tag{18}$$

The above equation utilizes an implicit (Crank-Nicolson) finite difference method scheme. Equation (18) is now rearranged in the form

$$-rT_{i+1}^{n+1} + (2+2r)T_i^{n+1} - rT_{i-1}^{n+1} = rT_{i+1}^n + (2-2r)T_i^n + rT_{i-1}^n + \alpha_{td} \Delta t Q \tag{19}$$

where $\qquad r = \frac{\alpha_{td} \Delta t}{(\Delta x)^2} \tag{20}$

At each time level n, equation (19) provide *M-1* simultaneous algebraic equations for the determination of *M-1* unknown internal node temperatures for the next time level *n+1*.

181

12.7 Predicted effects of input variables on temperature

Figure 12-12 shows the temperature distribution along biomass height (z) direction of a pellet at 400s. The highest equilibrium temperature still locates at the pellet center, but the temperature distribution is no longer symmetrical to the pellet center (4 mm). As seen in Figure 12-13, the equilibrium temperature at 2 mm is slightly higher than that at 6 mm. The equilibrium temperature at the top surface (0.2 mm) is slightly higher than that at the bottom surface (7.8 mm).

Figure 12-12 Temperature distribution along biomass height (z) direction. (Ultrasonic power = 40%)
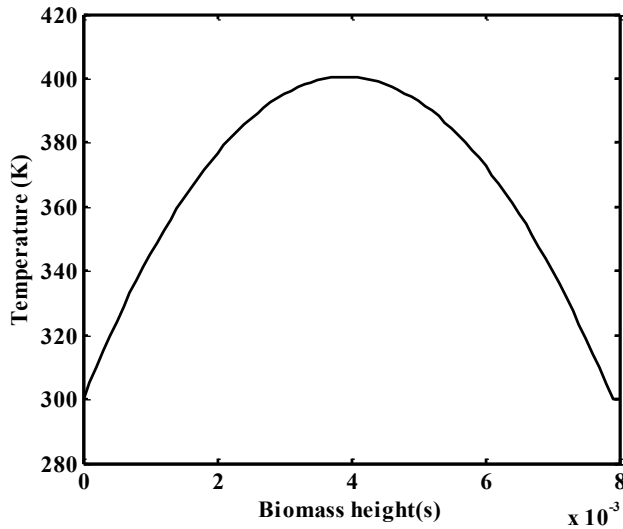
Figure 12-13 Temperature vs. pelleting duration for different locations.
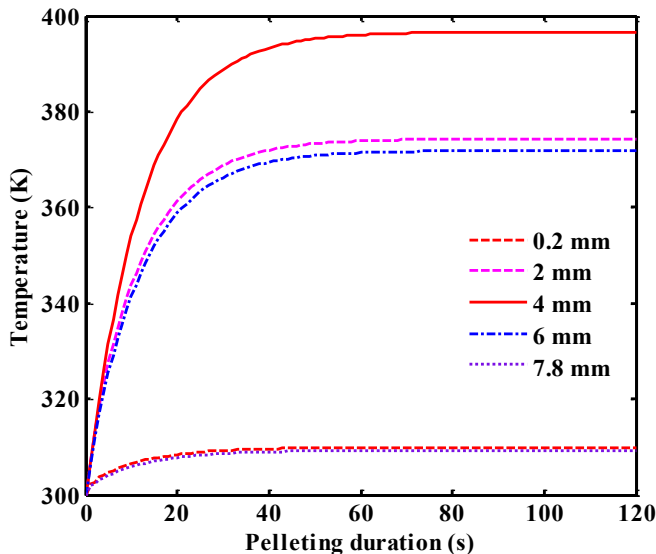
12.8 Conclusions

For the first time, a physics-based temperature model on UV-A pelleting of cellulosic biomass has been developed. The model was used to predict effects of input variables on pelleting temperature. Comparison was made between effects predicted by model and those determined by experiments. Trends of predicted effects of input variables on temperature agreed well with those determined by experiments. These predicted trends are (1) In UV-A pelleting, the temperature of cellulosic biomass increases with the increase of pelleting duration until reaches equivalent temperature. (2) Equilibrium temperature at the pellet center increases as ultrasonic power increases. (3) Time needed to reach the equilibrium temperature increases as ultrasonic power increases.

Differences between models developed in Section 2 (Model I) and in Section 6 (Model II) is the assumption that the temperatures at the boundaries are fixed as room temperature in Model I, while there is no such assumption in Model II. In Model I, the k value at the boundaries is infinity, and the temperature distribution is symmetric along the biomass height direction. However, the real experimental conditions are: the top boundary is made of Ti, the bottom boundary is made of Al, and the surrounding is made of Al as well. In this situation the k values of Ti and Al are different. So the temperature distribution should not be symmetric. The difference in the thermal prosperities of two materials was considered in Model II. Due to the k value of Ti is smaller than that of Al, the temperature distribution is no longer symmetric. The temperature at top surface is higher than that at the bottom surface. This differences has been found in the experiments as well.

Acknowledgements

References

[1]   Fargione, J., Hill, J., Tilman, D., Polasky, S., and Hawthorne, P., 2008, "Land clearing and the biofuel carbon debt," Science, 319(5867), pp. 1235-1238.

[2] Wyman, C. E., 1999, "Biomass ethanol: technical progress, opportunities, and commercial challenges," Annual Review of Energy and the Environment, 24(1), pp. 189-226.

[3] Perlack, R. D., Wright, L. L., Turhollow, A. F., Graham, R. L., Stokes, B. J., and Erbach, D. C., 2005, "Biomass as feedstock for a bioenergy and bioproducts industry: the technical feasibility of a billion-ton annual supply," DTIC Document.

[4] Huber, G. W., 2008, Breaking the chemical and engineering barriers to lignocellulosic biofuels: next generation hydrocarbon biorefineries, Citeseer.

[5] Falk, D., 1985, Pelleting cost center, American Feed Industry Association, Arlington, VA.

[6] Hess, J. R., Wright, C. T., and Kenney, K. L., 2007, "Cellulosic biomass feedstocks and logistics for ethanol production," Biofuels, Bioproducts and biorefining, 1(3), pp. 181-190.

[7] Sokhansanj, S., and Turhollow, A., 2004, "Biomass densification-cubing operations and costs for corn stover," Applied Engineering in Agriculture, 20(4), pp. 495-502.

[8] Song, X. X., Zhang, M., Pei, Z. J., and Deines, T., 2010, "Ultrasonic-Vibration-Assisted Pelleting of Cellulosic Biomass: Effects of Moisture Content," Proceedings of the ASME 2010 International Manufacturing Science and Engineering Conference (MSEC)Erie, PA, USA.

[9] Song, X. X., Zhang, M., Pei, Z. J., and Deines, T., 2010, "Ultrasonic-Vibration-Assisted Pelleting of Cellulosic Biomass: Effects of Moisture Content," Proceedings of the IIE Annual Conference and ExpoCancun, Mexico.

[10] Faborode, M., 1990, "Analysis of extrusion compaction of fibrous agricultural residues for fuel applications," Biomass, 21(2), pp. 115-128.

[11] Reece, F., 1966, "Temperature, pressure and time relationships in forming dense hay wafers," Trans, ASAE, 9, p. 749.

[12] Smith, I. E., Probert, S. D., Stokes, R. E., and Hansford, R. J., 1977, "The briquetting of wheat straw," Journal of Agricultural Engineering Research, 22(2), pp. 105-111.

[13] Tabil, L., and Sokhansanj, S., 1996, "Process Conditions Affecting the Physical Quality of Alfalfa Pellets," Applied Engineering in Agriculture, 12(3), pp. 345-350.

[14]   Hill, B. a. D. A. P., 1988, "A study of factors affecting pellet durability and pelleing efficiency in the production of dehydrated alfalfa pellets. ," Saskatchewan Dehydrators Association, Tisdale, SK, Canada.

[15]   Van Dam, J. E. G., van den Oever, M. J. A., Teunissen, W., Keijsers, E. R. P., and Peralta, A. G., 2004, "Process for production of high density/high performance binderless boards from whole coconut husk: Part 1: Lignin as intrinsic thermosetting binder resin," Industrial Crops and Products, 19(3), pp. 207-216.

[16]   Tang, Y. J., Chen, C. M., and Wang, G., 2012, "Temperature On-Line Measured in Ultrasonic Vibration-Assisted Pelleting Cellulosic Biomass," Applied Mechanics and Materials, 151, pp. 245-249.

[17]   Feng, Q., Cong, W. L., Zhang, M., Pei, Z. J., and Ren, C. Z., 2010, "An Experimental Study on Temperature in Ultrasonic Vibration-Assisted Pelleting of Cellulosic Biomass," Proceedings of the ASME 2010 International Manufacturing Science and Engineering Conference (MSEC)Erie, PA, USA.

[18]   Theerarattananoon, K., Xu, F., Wilson, J., Staggenborg, S., McKinney, L., Vadlani, P., Pei, Z., and Wang, D., 2012, "Effects of the Pelleting Conditions on Chemical Composition and Sugar Yield of Corn Stover, Big Bluestem, Wheat Straw, and Sorghum Stalk Pellets," Bioprocess and Biosystems Engineering, 35(4), pp. 615-623.

[19]   Kersten, S. R. A., Wang, X., Prins, W., and van Swaaij, W. P. M., 2005, "Biomass Pyrolysis in a Fluidized Bed Reactor. Part 1: Literature Review and Model Simulations," Industrial & Engineering Chemistry Research, 44(23), pp. 8773-8785.

[20]   Saastamoinen, J. J., 2006, "Simplified model for calculation of devolatilization in fluidized beds," Fuel, 85(17–18), pp. 2388-2395.

[21]   Sand, U., Sandberg, J., Larfeldt, J., and Bel Fdhila, R., 2008, "Numerical prediction of the transport and pyrolysis in the interior and surrounding of dry and wet wood log," Applied Energy, 85(12), pp. 1208-1224.

[22]   Bhargava, S. K., 2010, Step by Step Ultrasound, Jaypee Brothers, Medical Publishers.

[23]   Ozisik, N., 2013, Boundary Value Problems of Heat Conduction, Dover Publications.

[24]   Jaluria, Y., 2002, Computational Heat Transfer, Taylor & Francis.

[25]   Lestina, T., and Serth, R. W., 2010, Process Heat Transfer: Principles, Applications and Rules of Thumb, Elsevier Science.

[26]   Jiji, L. M., 2009, Heat Conduction, Springer-Verlag Berlin Heidelberg.

[27]   Som, S., and Ghosh, A., 2008, Introduction to Heat Transfer.

[28]   Love, L., and Kremkau, F., 1980, "Intracellular temperature distribution produced by ultrasound," The Journal of the Acoustical Society of America, 67, p. 1045.

[29]   Koufopanos, C. A., 1991, "Modelling of the pyrolysis of biomass particles. Studies on kinetics, thermal and heat transfer effects," The Canadian journal of chemical engineering, 69(4), p. 907.

[30]   Dinwiddie, R. B., White, M. A., Instruments, M., and McElroy, D. L., 2006, Thermal Conductivity 28: Thermal Expansion 16 : Joint Conferences : June 26-29, 2005, St. Andrews-by-the -Sea, New Brunswick, Canada, Destech Publications Incorporated.

Chapter 13 - A Constitutive Pellet Density Model For Ultrasonic Vibration-Assisted Pelleting for Cellulosic Biomass

Paper title:

Ultrasonic vibration-assisted (UV-A) pelleting of wheat straw: a constitutive model for pellet density

Published in:

Authors' names:

Xiaoxu Song[a], Meng Zhang[a], Z.J. Pei[a], and Donghai Wang[b]

Authors' affiliation:

[a]Department of Industrial and Manufacturing Systems Engineering, Kansas State University, Manhattan KS 66506 USA

[b]Department of Biological and Agricultural Engineering, Kansas State University, Manhattan, KS 66506, USA

Abstract

Ultrasonic vibration-assisted (UV-A) pelleting can increase cellulosic biomass density and reduce biomass handling and transportation costs in cellulosic biofuel manufacturing. Effects of input variables on pellet density in UV-A pelleting have been studied experimentally. However, there are no reports on modeling of pellet density in UV-A pelleting. Furthermore, in the literature, most reported density models in other pelleting methods of biomass are empirical. This paper presents a constitutive model to predict pellet density in UV-A pelleting. With the predictive model, relations between input variables (ultrasonic power and pelleting pressure) and pellet density are predicted. The predicted relations are compared with those determined experimentally in the literature. Model predictions agree well with reported experimental results.

Keywords

Biofuel, cellulosic biomass, density, constitutive model, ultrasonic power, ultrasonic vibration-assisted pelleting

13.1 Introduction

Cellulosic biofuels are produced from cellulosic biomass (including wood, agricultural residues, and herbaceous energy crops). Unlike other type of feedstocks (e.g. corn, sugar cane, and soybean) for biofuels, cellulosic biomass does not compete with food production for the limited agriculture land [1, 2].

However, raw cellulosic biomass feedstocks have low density, resulting in high costs in their transportation and handling. One strategy to overcome this barrier is the densification of raw cellulosic biomass feedstocks. Densification of cellulosic biomass into pellets [3] can increase the density from 40 - 250 kg/m^3 for raw cellulosic feedstocks to as high as 1200 kg/m^3 for pellets [4]. Improvements in density through pelleting can greatly reduce the feedstocks' transportation and handling costs.

Densification of biomass through pelleting is an useful pre-processing step considered in cellulosic biofuel manufacturing [5]. Traditional pelleting methods (e.g. using a screw extruder, a briquetting press, or a rolling machine [6] generally involve high-temperature steam and high pressure, and often use binder materials, making it difficult to realize cost-effective pelleting on or near the field where cellulosic biomass is available. Ultrasonic vibration-assisted (UV-A)

pelleting is a new pelleting method [7-9]. UV-A pelleting, without using binder materials or high-temperature steam, can produce biomass pellets whose densities are comparable to that processed by traditional pelleting methods [6].

13.1.1 Densification mechanism

In UV-A pelleting, biomass particles are densified in a closed-end mold. Initially, air is expelled from the die, and the biomass particles rearrange themselves due to inertial forces. This stage of compression was called the inertial deformation stage [10]. As pelleting pressure applies to biomass particles, biomass particles are forced against each other while undergoing elastic and plastic deformations. This increases interparticle contact area and, as a result, bonding forces like van der Waal's forces become effective [11-13]. In the meanwhile, the heat generated from ultrasonic vibration can lead to local melting of biomass materials. Once cooled, the molten biomass material forms very strong solid bridges [14]. Biomass contains components such as cellulose, hemicellulose, and lignin. Among these chemical components, lignin has a low melting point of about 140°C [15]. When ultrasonic vibration being applied to biomass in UV-A pelleting, the temperature of biomass will increased by the heat generated. When the temperature reaches the melting point of lignin, lignin will become soft and begin to melt, exhibiting thermosetting properties [16]. These properties will make lignin become permanently rigid and likely to bond together with other components such as cellulose and hemicellulose in the biomass. A similar compaction mechanism was identified in the alfalfa pelleting process [17]. When alfalfa is pelleted in a circular die pellet mill, the temperature of alfalfa reaches more than 90°C due to the heat generated from friction between the die and alfalfa [18].

13.1.2 Constitutive models

In general terms, constitutive models describe the relationships between the force and movement of the internal structures of force, temperature and deformation. Constitutive model includes a variety of factors: time, temperature, force, deformation, velocity, acceleration. Constitutive models are required as input to computer simulations of mechanical processes such as densification of cellulosic biomass [10]. One of the constitutive models is rheological models.

13.1.3 Rheological models

In rheology, ideal materials deform in three different ways: elastic, plastic, or viscous [19, 20]. In an ideal elastic body, deformation (or strain) occurs instantly when stress is applied. It is directly proportional to stress. Elastic deformation also recovers after stress is removed [10]. In an ideal plastic body, deformation does not begin until yield stress is reached. Plastic deformation is permanent and no recovery occurs after stress is removed [10]. In an ideal viscous body, deformation occurs instantly when stress is applied, and the stress is proportional to the rate of strain. Viscous deformation is not recovered after stress is removed [10]. These three types of deformation are denoted in rheological models as mechanical analogues as spring, friction, and dashpot elements [19, 20]. Developing rational models using rheological principles involves the use of combinations of discrete spring, friction, and dashpot elements [19-23].

The rheological models are expressed as a function of stress, strain, and time. It can be used to describe the mechanical behavior of the biomass material under different stress conditions. The mechanical behavior of biomass materials has been found to depend on stress, strain, strain rate, moisture content, temperature, and size and shape of the biomass materials [22, 23]. Biomass materials behave in complex ways when stress being applied. They also exhibit time-dependent, force-deformation characteristics. Therefore, rheological models have been used to simulate stress relaxation, elastic recovery, and creep in materials such as forage (alfalfa, clover, timothy, and corn) stalks [22]. Currently, lots of experimental investigations on pellet density in UV-A pelleting have been conducted. It has been commonly observed that pellet density increases, with increase of pelleting pressure and ultrasonic power. However, there is no pellet density model in UV-A pelleting. It is necessary to develop such a model to help explaining the mechanism in UV-A pelleting and predict how input variables affect pellet density. To fill this gap in the literature, this paper presents the first constitutive model of cellulosic biomass in UV-A pelleting.

13.2 Model development

13.2.1 Model assumptions

Biomass pellet was divided into M-1 small elements in the axial direction (as denoted by 1, 2, … M in Figure 13-1). Development of the model started with an analysis of an individual element of biomass pellet. The biomass height *h* for an individual element was obtained first.

Then the total biomass height H was derived by summing up the biomass heights of all the elements.

Figure 13-1 Pellet explicit scheme
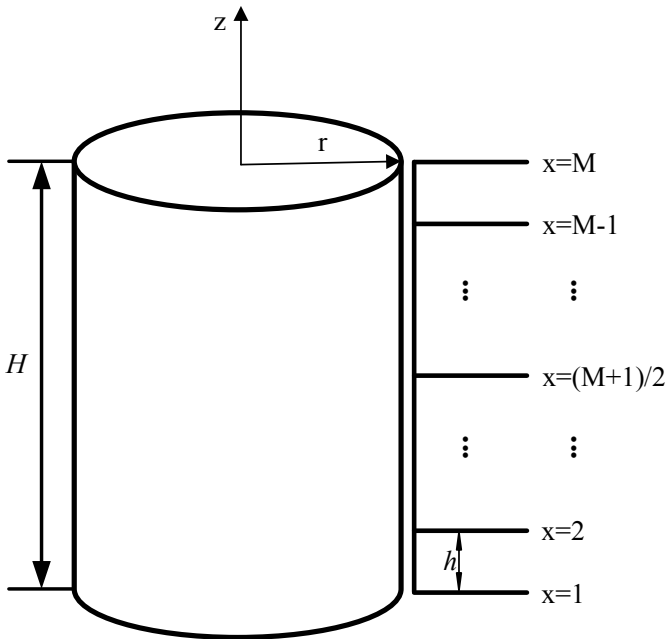
The model is based on the following assumptions:

(1) Biomass particles uniformly fill the mold.

(2) Biomass particles act as a continuum material during compression.

(3) Deformation of biomass particles occurs only along the axial direction of a pellet during compression. The lateral spreading of biomass particles during compression is not considered due to the lack of Poisson's ratio values for biomass particles in the literature. Therefore, a one-dimensional rheological model can be used to predict the compression behavior of biomass pellets.

(4) Only the normal compressive stress acts perpendicular to the horizontal plane of biomass pellet during compression. Shear stresses induced in the biomass pellet during compression are not considered.

(5) The coefficient of friction at any contacting point between biomass particles and mold is constant.

The compression of biomass particles is considered to occur due to a combination of two distinct deformation processes/stages: inertial deformation (this stage is not described by this

model) and elasto-visco-plastic deformation. The impact of bond formation and curing of bonds between particles during compression are not considered in the present model. Therefore, following the inertial deformation stage, the total deformation of the biomass particles is the simultaneous cumulative action of elastic deformation, plastic deformation, viscous dissipation, and frictional loss. At any point in time, the total stress is the sum of the stresses involved for elastic deformation, plastic deformation, viscous dissipation, and frictional loss. Thus, this stage of compression is called elasto-visco-plastic deformation stage. To depict the simultaneous action of these individual deformation mechanisms, an elasto-visco-plastic solid mechanical analogue is created to model the deformation of biomass particles at this stage.

The elasto-visco-plastic solid mechanical analogue is created by connecting in parallel a spring element, a dashpot element, and a Coulomb friction element (Figure 13-2). The spring element (E) represents the elastic and plastic deformation of biomass particles, the dashpot element (η) represents the viscous dissipation, and the Coulomb friction element (σ_f) represents the frictional loss. The derivation of the constitutive model for the elasto-visco-plastic deformation stage of compression is given below.

Figure 13-2 Mechanical analogy of the biomass pellet for the development of constitutive model for the compression process.
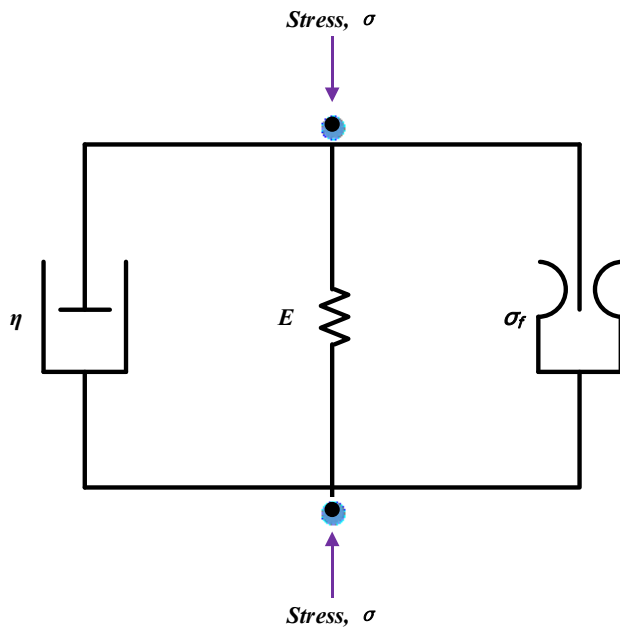
13.2.2 Relation between pellet density ρ and strain ε

$$\rho = \frac{m}{V} = \frac{m}{A \times H} \tag{1}$$

$$\varepsilon = \frac{\Delta h}{h} \tag{2}$$

where, ρ = pellet density, m = pellet weight, V = pellet volume, A = pellet cross section area, H = pellet height, h = a pellet element height, Δh = change of a pellet element height, ε = strain.

13.2.3 Relation between pellet pressure σ and strain ε

The constitutive behavior of the spring element was modelled as [20, 24]:

$$\sigma_1 = E\varepsilon \tag{3}$$

where, σ_1 = stress in the spring element, E = elastic modulus, ε = strain.

The constitutive behavior of the dashpot element was modelled as [19, 20, 24]:

$$\sigma_2 = \eta \frac{d\varepsilon}{dt} \tag{4}$$

where, σ_2 = stress in the dashpot element, η = viscous coefficient, and $d\varepsilon/dt$ = strain rate.

The constitutive behavior of the Coulomb friction element was taken as a constant [20, 24]:

$$\sigma_3 = \sigma_f \tag{5}$$

where, σ_3 = stress in the Coulomb friction element, and σ_f = frictional loss factor. According to Coulomb's law of friction, the shear stress due to friction at the mold-wall is equal to the multiplication of the coefficient of friction between the biomass particles and the mold-wall, radial pressure transmission coefficient (Janssen constant), and the axial stress applied to the biomass particles [10, 25]. This shows that the shear stress at the mold-wall is a constant for a given axial stress. Thus, the constitutive behavior of the Coulomb friction element was modeled as a constant.

The total stress (σ) in the elasto-visco-plastic solid mechanical analogue material (Figure 2) is the sum of the stress in the spring element (σ_1), dashpot element (σ_2), and the Coulomb friction element (σ_3):

$$\sigma = E\varepsilon + \eta \frac{d\varepsilon}{dt} + \sigma_f \tag{6}$$

Eq. (6) is a non-linear elasto-visco-plastic solid model.

13.2.4 Relation between Elastic Modulus E and temperature T

The elasticity of biomass depends its temperature. According to published data [26], the relationship between elastic modulus and the temperature of biomass can be represented as

$$\log E = f_1 \times e^{-f_2 \times (T-273)} \tag{7}$$

where E is elastic modulus in MPa and T is temperature in Kelvin. f_1 and f_2 are the mechanistic parameters. These parameters have to be determined experimentally for a specific material. The procedure to obtain f_1 and f_2 for wheat straw will be described in Section 13.3.

13.2.5 Relation between ultrasonic power U and temperature T

Ultrasonic power U in UV-A pelleting represents the power provided by a power supply. It determines the vibration amplitude. A larger ultrasonic power would result in larger vibration amplitude. Ultrasonic power is expressed as a percentage of the maximum ultrasonic power for the power supply.

It has been shown that temperature T is determined by ultrasonic power U. A model has been developed to establish the relationship between ultrasonic power and temperature in UV-A pelleting and results are published in a separate paper [27].

13.2.6 Numerical scheme

Equations (2), (6), and (7) are converted to finite difference equations where subscripts denote location and superscripts denote time ($h(x_i, t_j) = h_i^j$). Considering a cylindrical shaped pellet (shown in Figure 13-1) of radius r, biomass height H. $i = 1$ represents the pellet bottom surface, and $i = M$ locates the pellet top surface. Then the approximations for Eq. (2), Eq. (6), and Eq. (7) at $h(x_i, t_j)$ are

$$h_i^j = dy - \varepsilon_i^j \times dy \tag{8}$$

$$\varepsilon_i^j = \frac{\sigma - \sigma_f - \eta \dfrac{d\varepsilon}{dt}}{E_i^j} \tag{9}$$

$$E_i^j = 10^{\wedge}(f_1 \times e^{\wedge}(-f_2 \times (T_i^j - 273))) \tag{10}$$

h_i^j was solved by Equations (8) - (10), then the biomass height $H = \sum h_i^j$. Pellet density ρ could be obtained by Eq. (1).

13.3 Determination of mechanistic parameters f_1 and f_2 using experiments

13.3.1. Cellulosic biomass preparation

The cellulosic biomass used in this investigation is wheat straw. Wheat straw is processed by a knife mill (Model SM 2000 from Retsch, Inc., Haan, Germany). The sieve with sieve size 1 mm is used to control biomass particle size.

13.3.2 Experimental setup and procedure

Figure 13-3 is a schematic illustration of the experimental set-up for UV-A pelleting. UV-A pelleting experiments were performed on a modified ultrasonic machine (Model AP-1000, Sonic-Mill, Albuquerque, NM, USA). The machine included a power supply (which converts 60 Hz electrical power into 20,000 Hz electrical power), a converter (which converts high frequency electrical energy into mechanical motion), and a horn. The tip of the horn was a solid cylinder with a flat end (17.4 mm in diameter).

Before each pelleting test, the weight of wheat straw particles was measured by a scale. This weight was referred to as pellet weight. Then wheat straw was loaded into an aluminum mold. The mold was consisted of three parts. The upper two parts formed a cylindrical cavity (18.6 mm in diameter) and the bottom part was a square disk, serving as a base. They were assembled together with pins.

The pneumatic cylinder was driven by compressed air provided by a 1.6-HP, 33-Gal. air compressor (Sears, Roebuck and Co., Hoffman Estates, IL, USA). The air pressure in the pneumatic cylinder was controlled by a pressure regulator. A higher air pressure in the cylinder meant a higher pressure applied on the biomass in the mold by the tool.

Pelleting duration (t_d) was the entire period of a pelleting test, during which the horn was in contact with wheat straw particles inside the mold. Pelleting time (t) referred to the time between the beginning of a pelleting test till a point in time of interest. Pelleting time could have any value between 0 and pelleting duration (t_d).

In each pelleting test, pelleting duration was 120 s. After 120 s, the tool was retracted and the mold was disassembled to unload the pellet.

Figure 13-3 A schematic illustration of the experimental set-up for UV-A pelleting.
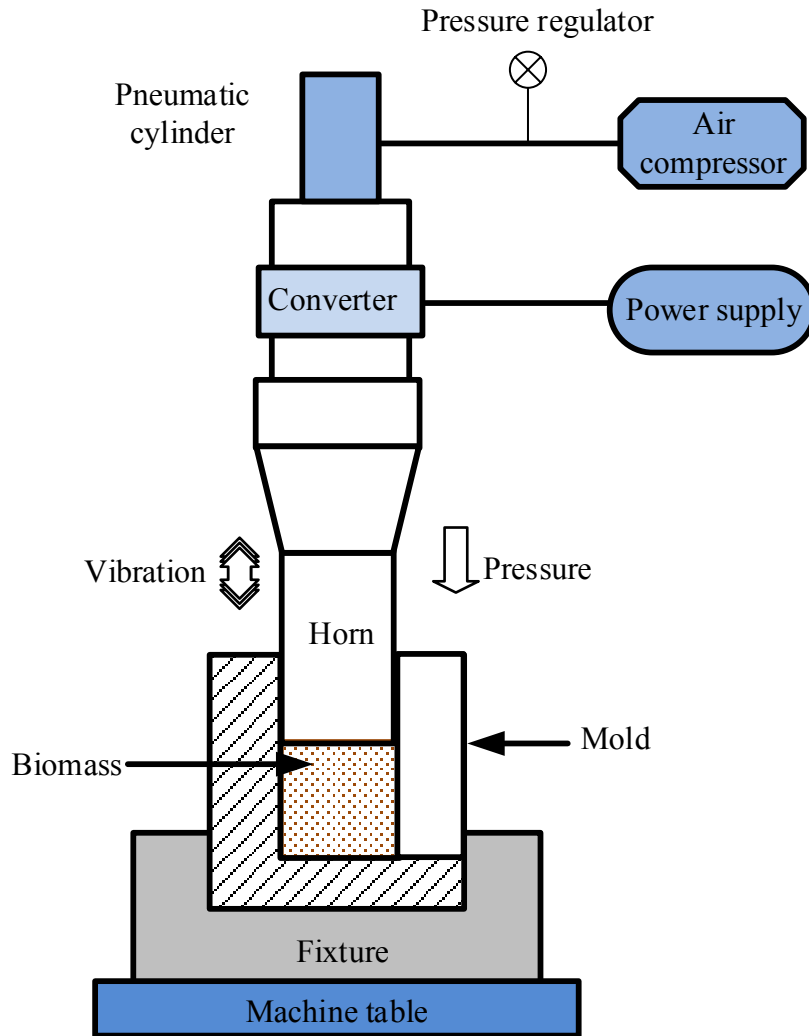
13.3.3 Measurement procedures

Pellet density is determined by dividing pellet weight by its volume. The weight of the sample pellets was measured on a high accuracy scale (Model TAJ 602, Ohaus Corp., Pine Brook, NJ, USA). The volume of the cylinder-shaped pellets was determined by $V = \dfrac{\pi d^2 H}{4}$.

Here d is the diameter of the pellet, and H is the height of the pellet. Diameters and heights of the pellets were measured using a digital caliper (Model IP-65, Mitutoyo Corp., Kawasaki, Japan).

The details of measurement procedure for pelleting temperature is described in a previous publication [27].

13.3.4 Design of experiments

A 2^2 (two variables, two levels) full factorial design was employed. Table 13-1 shows the values of low and high levels of the two variables. There were four different combinations and two replicated tests for each combination, bringing the total number of tests to 8, as shown in Table 13-2. Commercial software Minitab 16 (Minitab, Inc., State College, PA, USA) was used to generate a random order for these tests as well as to assist in analyzing experimental results.

Table 13-1 Low level and high level of input variables

Variable	Unit	Low level	High level
Ultrasonic power	%	40	60
Pelleting pressure	Psi	631	1578

Table 13-2 Experimental results on pellet density ρ and mechanistic parameters f_1 and f_2

Order	Ultrasonic power (%)	Pelleting pressure (Psi)	Pellet density (Kg/m³)	f_1	f_2
1	40	1578	1047.21	2	0.0037
2	60	631	710.06	2	0.0030
3	40	631	655.77	2	0.0037
4	60	1578	1174.70	2	0.0037
5	40	1578	1039.16	2	0.0037
6	60	631	727.27	2	0.0031
7	40	631	641.76	2	0.0037
8	60	1578	1211.57	2	0.0037

13.3.5 Experimental results

The purpose of this section is to estimate the values of f_1 and f_2 for a given biomass material using the data obtained from experiments. For each test, the values of f_1 and f_2 are obtained using temperature measurement data, pellet density measurement data, and equations described in Section 13.2. Experimental results on pellet density are presented in Table 13-2. Table 13-2 also includes values of mechanistic parameters f_1 and f_2 for each test. It shows that f_1 and f_2 are dependent on neither ultrasonic power nor pelleting pressure. The estimates of f_1 and f_2 were found to be 2 and 0.0037, respectively.

13.4 Influences of input variables on pellet density

13.4.1 Ultrasonic power U

Predicted relationships between pellet density ρ and ultrasonic power U at pelleting time of 60 s are plotted in Figure 13-4. As ultrasonic power U increases, pellet density ρ increases dramatically.

Figure 13-4 Relationship between ultrasonic power and pellet density
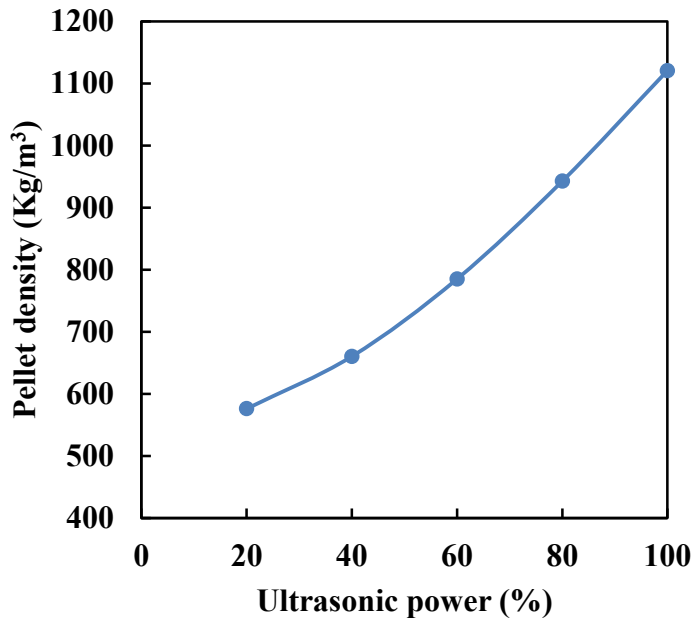
(Biomass weight = 1.5 g, pelleting pressure = 631 psi, pelleting time = 60 s)

13.4.2 Pelleting pressure σ

Predicted relationship between pellet density ρ and pelleting pressure σ at pelleting time of 60 s are plotted in Figure 13-5. As pelleting pressure σ increases, pellet density ρ increases dramatically.

13.4.3 Pelleting duration t_d

Predicted relationship between pellet density ρ and pelleting duration t_d are plotted in Figure 13-6. As pelleting duration t_d increases, pellet density ρ increases.

Figure 13-5 Relationship between pelleting pressure and pellet density
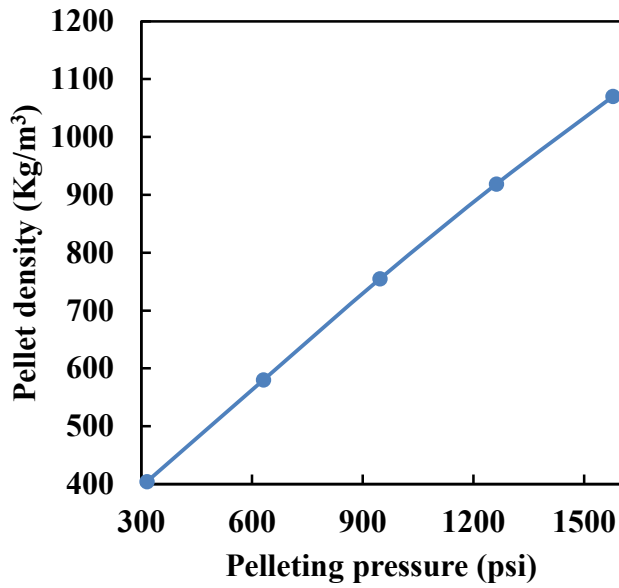
(Biomass weight = 1.5 g, ultrasonic power = 40%, pelleting time = 60 s)

Figure 13-6 Relationship between pelleting duration and pellet density
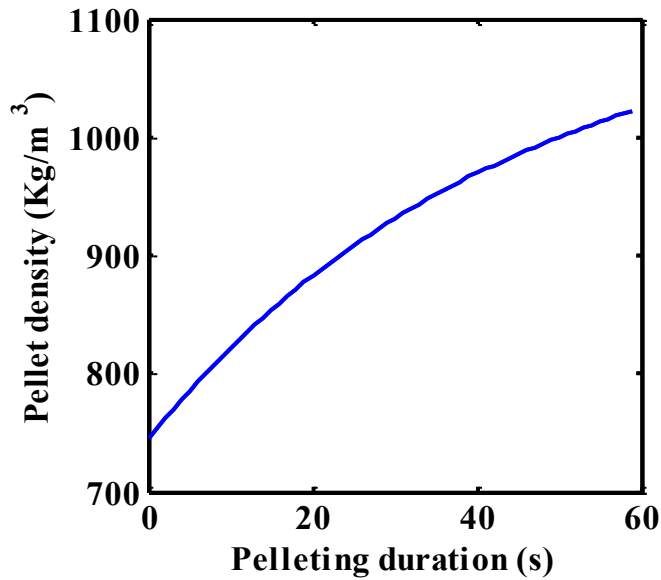
(Biomass weight = 1.5 g, ultrasonic power = 40%, pelleting pressure = 1578 psi)

13.4.4 Interaction effects of input variables

Figure 13-7 shows changes of intermediate variables of an element at pellet center with ultrasonic power U and pelleting duration t_d. As ultrasonic power U increases from 30% to 50%,

temperature T increases. According to Eq. (7), the increase in temperature T will result in a decrease in elastic modulus E. Pelleting pressure σ keeps constant, so strain ε increases as pelleting duration t_d increases, according to Eq. (6). For one element, change of biomass height $\triangle h$ is kept constant, so according to Eq. (2), biomass height h will decrease.

Figure 13-8 shows changes of biomass height H and pellet density ρ of a pellet with ultrasonic power U and pelleting duration t_d. Biomass height H decreases as ultrasonic power U and pelleting duration t_d increase. Pellet density ρ increases as ultrasonic power U and pelleting duration t_d increase.

Figure 13-9 shows changes of intermediate variables of an element at pellet center with pelleting pressure σ and pelleting duration t_d. As pelleting pressure σ increases from 947 psi to 1548 psi, temperature T decreases, elastic modulus E increases, strain ε increases, biomass height h decreases. So as pelleting pressure σ increases, pellet density ρ increases.

Figure 13-10 shows changes of biomass height H and pellet density ρ of a pellet with pelleting pressure σ and pelleting duration t_d. Biomass height H decreases as pelleting pressure σ and pelleting duration t_d increase. Pellet density ρ increases as pelleting pressure σ and pelleting duration t_d increase.

Figure 13-7 Interaction influences of ultrasonic power and pelleting duration on an element at pellet center
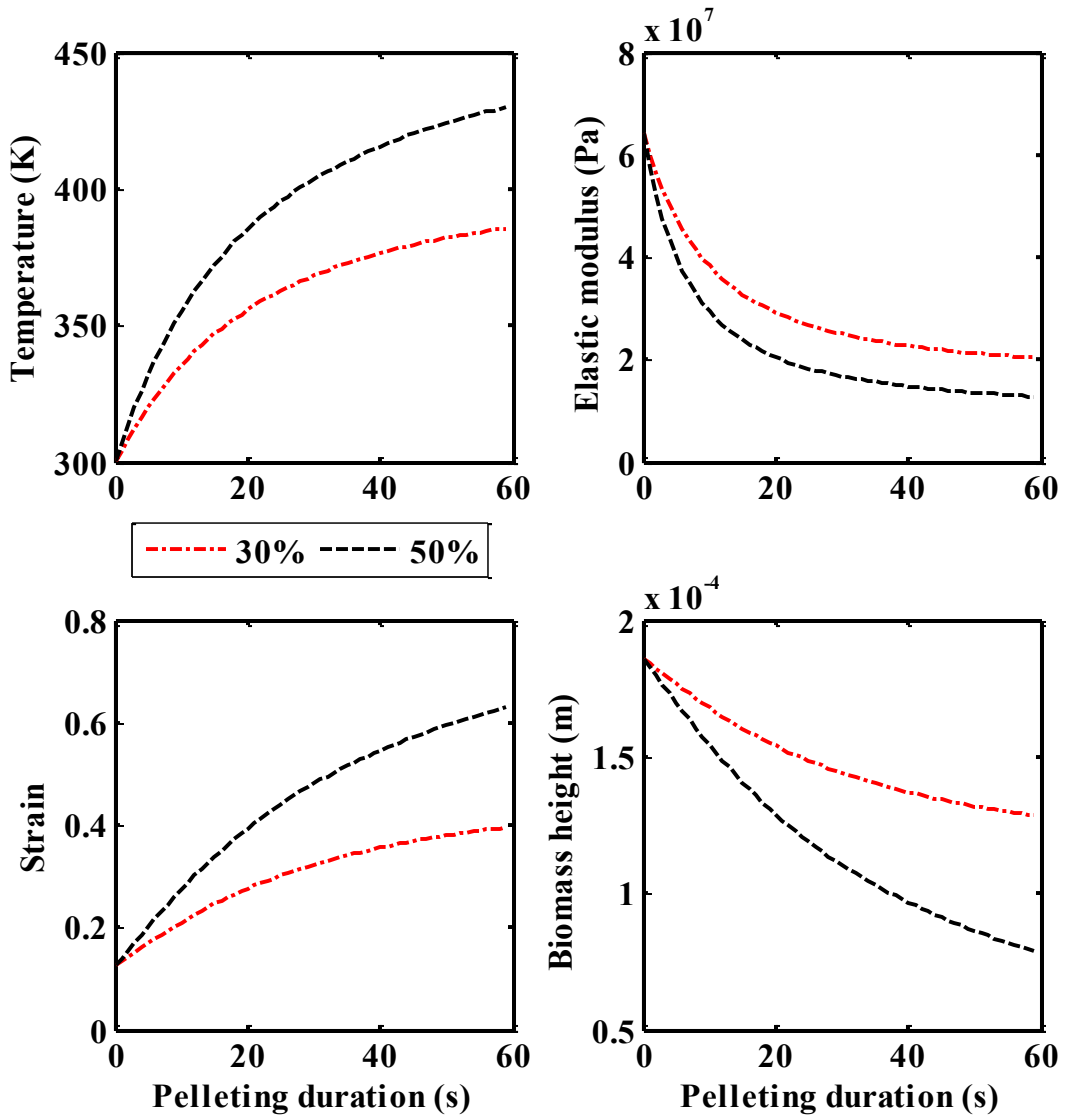
(Biomass weight = 1.5 g, pelleting pressure = 1578 psi)

Figure 13-8 Interaction influences of ultrasonic power and pelleting duration on a pellet
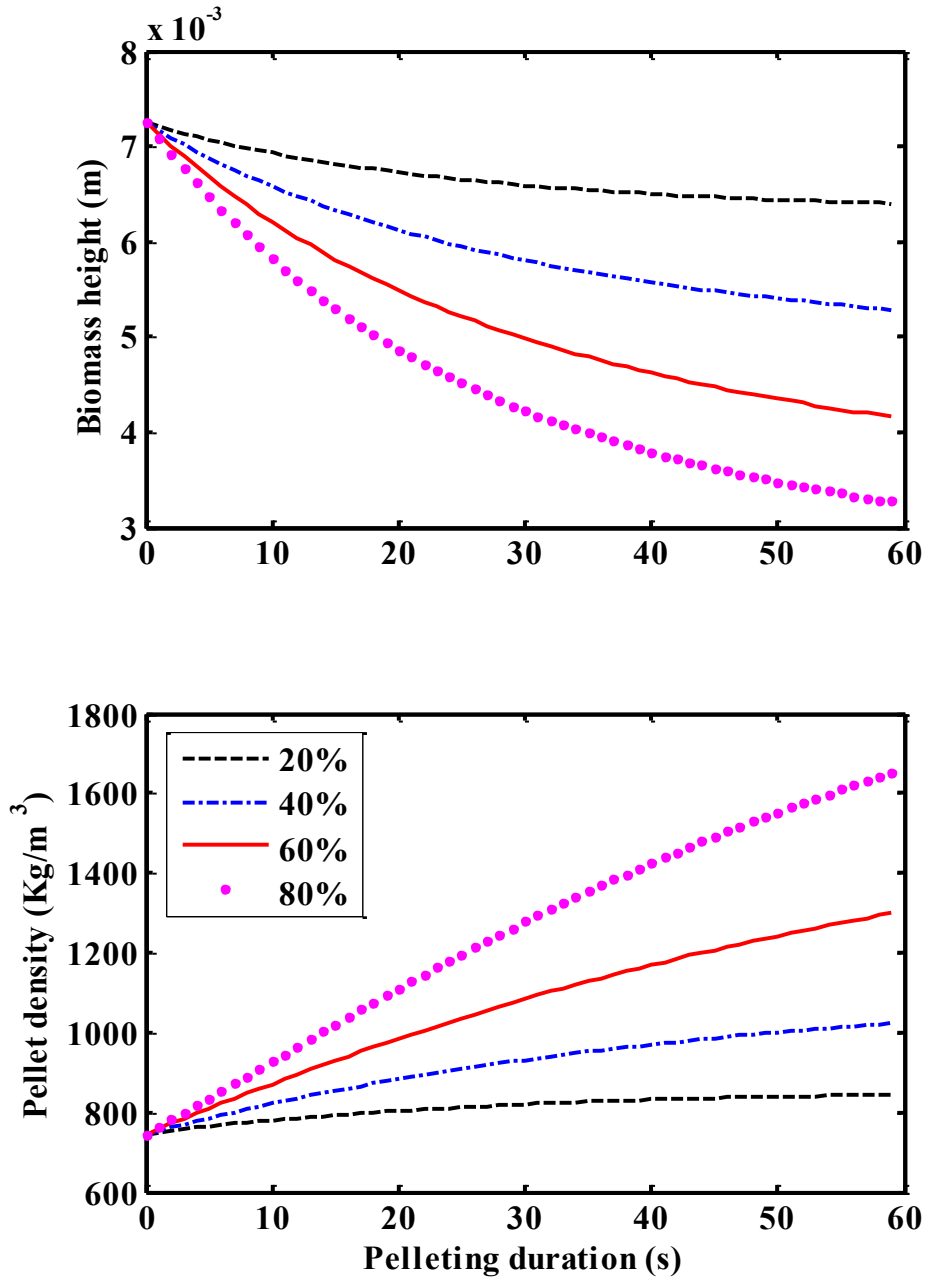
(Biomass weight = 1.5 g, pelleting pressure = 1578 psi)

Figure 13-9 Interaction influences of pelleting pressure and pelleting duration on an element at pellet center
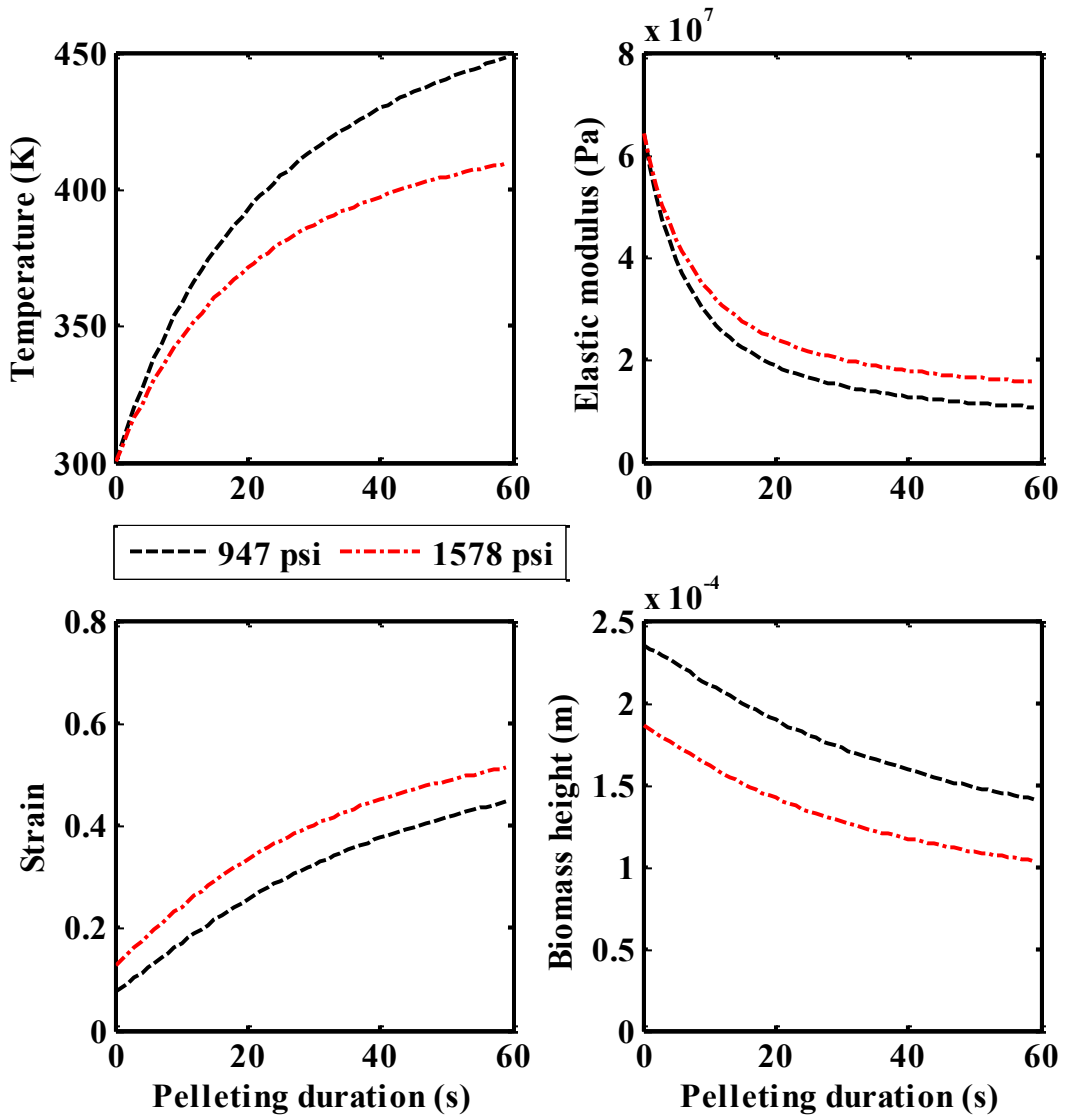
(Biomass weight = 1.5 g, ultrasonic power = 40%, pelleting time = 60 s)

Figure 13-10 Interaction influences of pelleting pressure and pelleting duration on a pellet
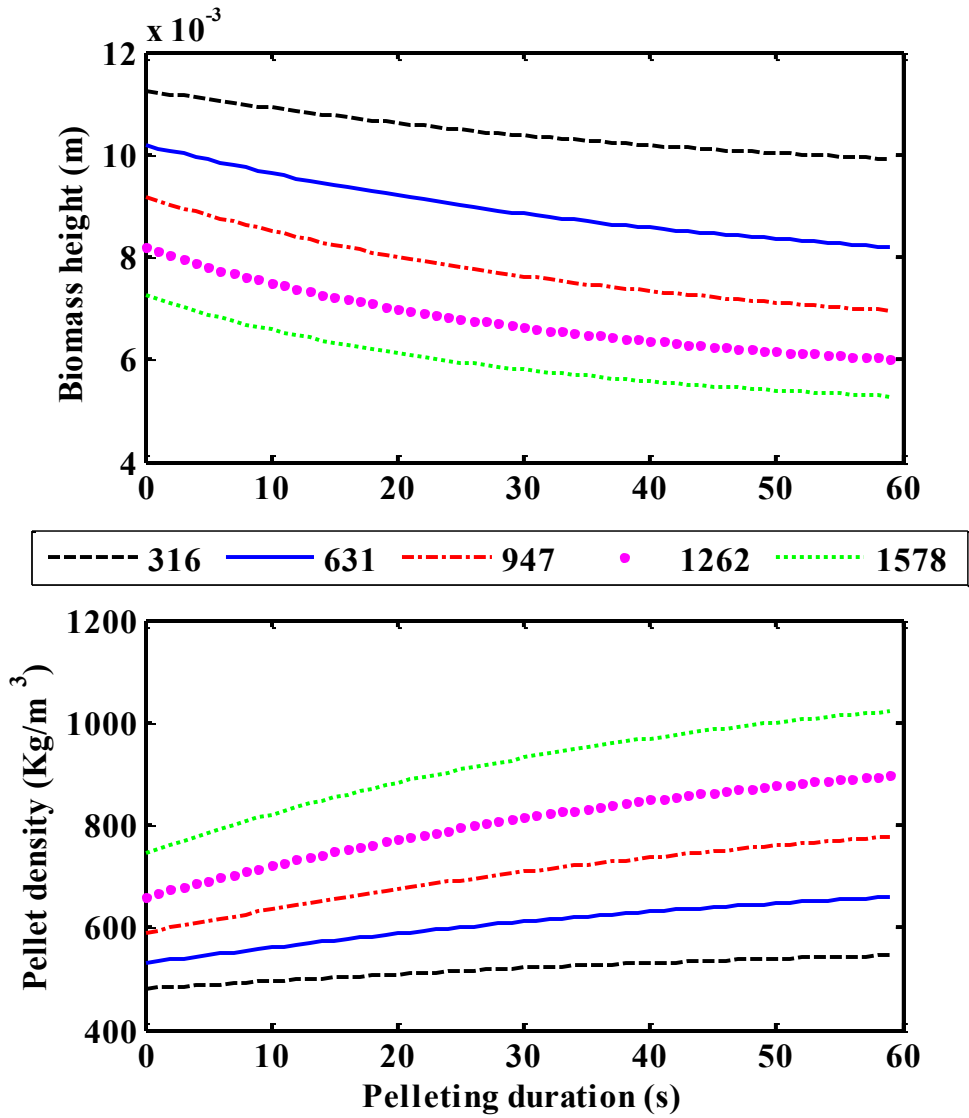
(Biomass weight = 1.5 g, ultrasonic power = 40%)

Figure 13-11 Experimental relations between ultrasonic power and pellet density
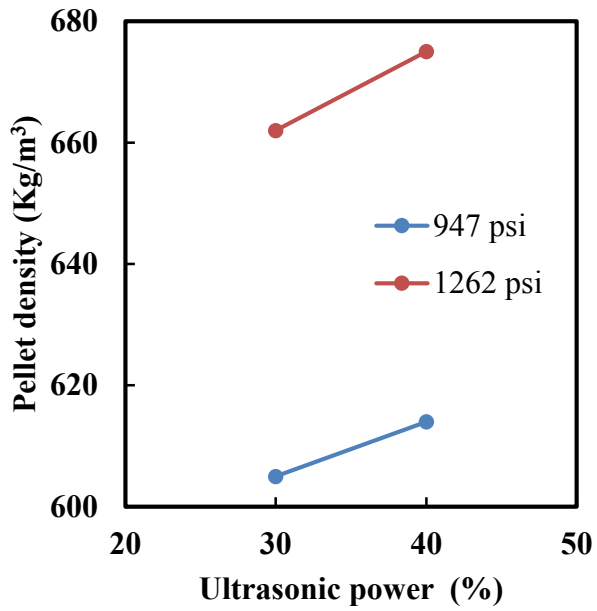
(a) Wheat straw (after [28])
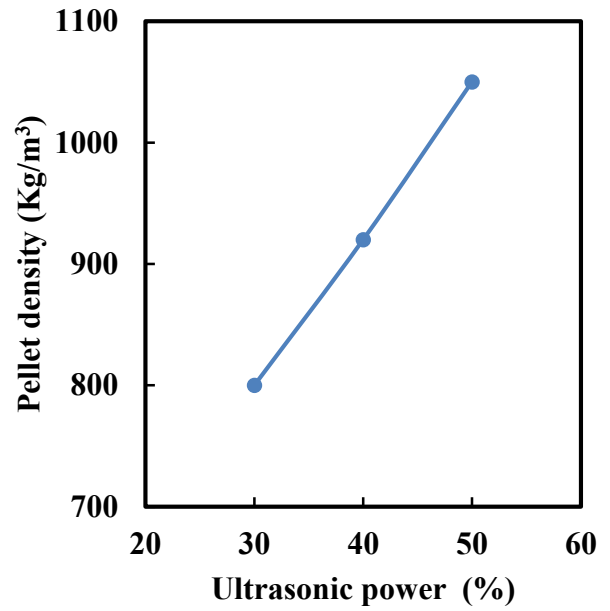
(b) Sorghum stalks (after [29])

Figure 13-12 Experimental relations between pelleting pressure and pellet density
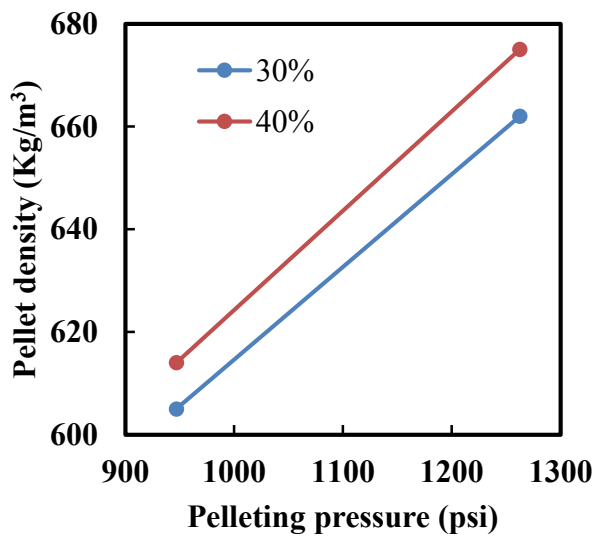
(a) Wheat straw (after [28])
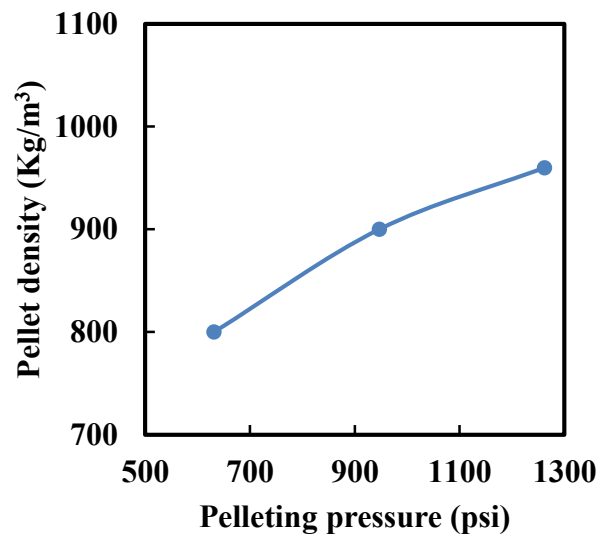
(b) Sorghum stalks (after [29])

13.5 Comparison with experimental results

In this section, predicted relations between input variables and pellet density are compared with experimental results from reported studies in the literature on UV-A pelleting.

The model predictes that pellet density will increase as ultrasonic power increases (Figure 13-4). This predicted trend agrees well with the experimental results on wheat straw as shown in Figure 13-11 (a), and those on sorghum stalks in Figure 13-11 (b).

The predicted trend of pelleting pressure's influence on pellet density (as shown in Figure 13-5) is consistent with the experimental results (as shown in Figure 13-12) on wheat straw and on sorghum stalks reported in the literature.

13.6 Conclusions

A constitutive model for pellet density in UV-A pelleting of cellulosic biomass has been developed using wheat straw as an example. The model can be used to predict the influences of input variables on pellet density. These predicted influences were compared with those determined by experiments in the literature. The trends of predicted effects of input variables on pellet density agreed well with the trends determined by experiments. Based on the model predictions, pellet density of the cellulosic biomass will increases as ultrasonic power and pelleting pressure increase.

Acknowledgements

References

[1]   K.A. Gray, L. Zhao, M. Emptage, Bioethanol, Current Opinion in Chemical Biology, 10 (2006) 141-146.

[2]   L.R. Brown, Why Ethanol Production Will Drive World Food Prices Even Higher in 2008, in, 2008.

[3]   R.H. Leaver, The Pelleting Process, Sprout-Waldron, Muncy, PA, USA., 1984.

[4]   S. Mani, S. Sokhansanj, X. Bi, A. Turhollow, Economics of Producing Fuel Pellets from Biomass, Applied Engineering in Agriculture, 22 (2006) 421-426.

[5]   T. Lope, A. Phani, K. Mahdi, Biomass Feedstock Pre-Processing – Part 2: Densification, 2011.

[6]   S. Mani, L.G. Tabil, S. Sokhansanj, An Overview of Compaction of Biomass Grinds, Powder Handling Processing, 15 (2003) 160-168.

[7]   X.X. Song, M. Zhang, Z.J. Pei, T. Deines, Ultrasonic-Vibration-Assisted Pelleting of Cellulosic Biomass: Effects of Moisture Content, in: Proceedings of the ASME 2010 International Manufacturing Science and Engineering Conference (MSEC), Erie, PA, USA, 2010.

[8]   X. Song, M. Zhang, Z. Pei, Effects of ultrasonic vibration-assisted pelleting of cellulosic biomass on sugar yield for biofuel manufacturing, Biomass Conversion and Biorefinery, 3 (2013) 231-238.

[9]   X. Song, M. Zhang, Z. Pei, D. Wang, Ultrasonic Vibration-assisted Pelleting of Wheat Straw: A Predictive Model for Energy Consumption Using Response Surface Methodology, Ultrasonics, 54 (2014) 305-311.

[10]   N. Kaliyan, R.V. Morey, Constitutive model for densification of corn stover and switchgrass, Biosystems Engineering, 104 (2009) 47-63.

[11]   W. Pietsch, Size enlargement by agglomeration, in: Handbook of Powder Science & Technology, Springer, 1997, pp. 202-377.

[12]   H. Rumpf, The strength of granules and agglomerates, in: Knepper，W.A. (Ed.) Agglomeration, John Wiley and Sons, New York,NY, 1962, pp. 379-419.

[13]   K.V.S. Sastry, D.W. Fuerstenau, Mechanisms of agglomerate growth in green pelletization, Powder Technology, 7 (1973) 97-105.

[14]   G. Sellassie, Mechanism of pellet formation and growth, in: G. Sellassie (Ed.) Pharmaceutical Pelletization Technology, Marcel Dekker, Inc., New York, NY, 1989, pp. 123- 143.

[15]   S. Mani, L. Tabil, S. Sokhansanj, Evaluation of compaction equations applied to four biomass species, Canadian Biosystems Engineering, 46 (2004) 55-61.

[16]   J.E.G. van Dam, M.J.A. van den Oever, W. Teunissen, E.R.P. Keijsers, A.G. Peralta, Process for production of high density/high performance binderless boards from whole coconut husk: Part 1: Lignin as intrinsic thermosetting binder resin, Industrial Crops and Products, 19 (2004) 207-216.

[17] L.G. Tabil, S. Sokhansanj, Compression and compaction behavior of alfalfa grinds - Part 1: Compression behavior, Powder Handling and Processing, 8 (1996) 7-23.

[18] L.G. Tabil, Pelleting and Binding Characteristics of Alfalfa, in: Department of Agricultural and Bioresource Engineering, University of Saskatchewan, Saskatoon, SK, 1996.

[19] C.W. Macosko, Rheology: principles, measurements, and applications, VCH, 1994.

[20] K. Peleg, RHEOLOGICAL MODEL OF NONLINEAR VISCOPLASTIC SOLIDS, Journal of Rheology, 27 (1983) 411-431.

[21] Y.M. Haddad, Viscoelasticity of Engineering Materials, Chapman & Hall, 1995.

[22] N.N. Mohsenin, Physical Properties of Plant and Animal Materials: Structure, Physical Characteristics, and Mechanical Properties, Gordon and Breach, 1986.

[23] G. Sitkei, Mechanics of Agricultural Materials, Elsevier Science, 1987.

[24] M.O. Faborode, J.R. O'Callaghan, A rheological model for the compaction of fibrous agricultural materials, Journal of Agricultural Engineering Research, 42 (1989) 165-178.

[25] J.C. Cunningham, I.C. Sinka, A. Zavaliangos, Analysis of tablet compaction. I. Characterization of mechanical behavior of powder and powder/tooling friction, Journal of Pharmaceutical Sciences, 93 (2004) 2022-2039.

[26] H.P.S.A. Khalil, M. Jawaid, A. Hassan, M.T. Paridah, A. Zaidon, Oil Palm Biomass Fibres and Recent Advancement in Oil Palm Biomass Fibres Based Hybrid Biocomposites, 2012.

[27] X. Song, X. Yu, M. Zhang, Z. Pei, D. Wang, A physics-based temperature model for ultrasonic vibration-assisted pelleting of cellulosic biomass, Accepted by Ultrasonics, (2014).

[28] P.F. Zhang, T.W. Deines, D. Nottingham, Z.J. Pei, D. Wang, X. Wu, Ultrasonic Vibration-Assisted Pelleting of Biomass: A Designed Experimental Investigation on Pellet Quality and Sugar Yield, in: Proceedings of the ASME 2010 International Manufacturing Science and Engineering Conference (MSEC), Erie, PA, USA, 2010.

[29] Q. Zhang, P.F. Zhang, T. Deines, Z.J. Pei, D. Wang, X. Wu, G. Pritchett, Ultrasonic Vibration-Assisted Pelleting of Sorghum Stalks: Effects of Pressure and Ultrasonic Power, in: Proceedings of the ASME 2010 International Manufacturing Science and Engineering Conference (MSEC), Erie, PA, USA, 2010.

Chapter 14 - Summaries and Conclusions

14.1 Summaries of this research

In this dissertation, ultrasonic vibration-assisted (UV-A) pelleting and dilute acid pretreatment of cellulosic biomass for biofuel manufacturing are investigated. Effects of input variables (such as biomass moisture content, biomass type, binder material, pelleting pressure, and ultrasonic vibration power) in UV-A pelleting on pellet quality (such as density, durability, and stability), pelleting force, energy consumption, and sugar yield are studied. Effects of input variables (such as pretreatment time, pretreatment temperature, acid concentration, and ultrasonic vibration) in dilute acid pretreatment on sugar yield, water usage, energy consumption, and pretreatment energy efficiency are studied. Predictive models in UV-A pelleting and dilute acid pretreatment on energy consumption are developed, respectively. Mechanisms through which UV-A pelleting increases density and sugar yield are investigated. A physics-based model is developed to predict temperature in UV-A pelleting. A constitutive model is developed to predict pellet density in UV-A pelleting. The studies presented in this dissertation are highlighted in Figure 14-1 and Figure 14-2.

Below are the main conclusions drawn from this dissertation:

(1) A physics-based predictive temperature model is developed for UV-A pelleting of cellulosic biomass. Predicted influences of input variables on temperature are compared with those determined experimentally. The trends of predicted influences agree well with experimental results. Pelleting temperature increases as pelleting time and ultrasonic power increase.

(2) A constitutive model for pellet density in UV-A pelleting of cellulosic biomass has been developed using wheat straw as an example. The model is used to predict effects of input variables on pellet density. Predicted effects are compared with those determined by experiments in the literature. Trends of predicted effects of input variables on pellet density agree well with those determined by experiments. Based on model predictions, pellet density of cellulosic biomass increases as ultrasonic power and pelleting pressure increase.

Figure 14-1 Studies on ultrasonic vibration-assisted pelleting

Ultrasonic vibration-assisted pelleting

Experimental investigations

Theoretical studies

Input

Moisture content
Biomass type
Binder material
Ultrasonic vibration
Pellet weight
Pellet duration

Output

Pellet density
Pellet durability
Pellet temperature
Pelleting fore
Energy consumption
Sugar yield

Physics-based model
for pellet temperature
Constitutive model for
pellet density
Predictive model for
energy consumption

Methodology: Single factor, Design of Experiments (DOE), Response surface methodology (RSM), Finite difference method (FDM)

Figure 14-2 Studies on dilute acid pretreatment

Dilute acid pretreatment

Experimental investigations

Theoretical study

Input
Pretreatment time
Pretreatment
temperature
Ultrasonic vibration
Acid concentration

Output
Sugar yield
Water usage
Pretreatment energy
efficiency
Energy consumption

Predictive model
for energy
consumption

Methodology: Single factor, Response surface methodology
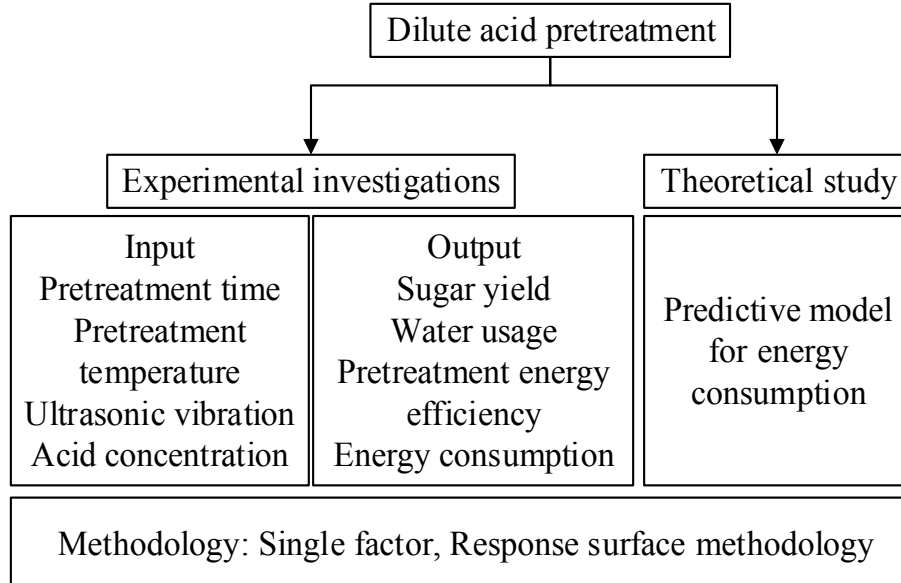
(3)   Effect of moisture content (MC) in UV-A pelleting of three types of biomass materials have been studied. MC has significant effects on pellet density and stability. The highest density (1043 kg/m^3) is found with sorghum of 20% MC. The lowest density (446 kg/m^3) is found with wheat straw of 25% MC. Sorghum has the

highest density among these three types of biomass materials. Furthermore, the pellets processed with a lower MC are more stable.

(4)   Effects of corn starch serving as binder material in UV-A pelleting of switchgrass have been studied. Pellet density, stability, and durability are evaluated. Results shows that no general trends are observed in density, stability, and durability as the binder content increased. The highest binder content (10%) did not help to improve the finished pellet quality in UV-A pelleting.

(5)   Effects of ultrasonic vibration on pelleting of wheat straw have been studied. Pellet density, durability, and pelleting force are evaluated. The average density of the pellets processed with ultrasonic vibration is 65% higher than that of the pellets processed without ultrasonic vibration. Durability is also increased with the assistance of ultrasonic vibration. The pelleting forces under the same compressed air pressure with ultrasonic vibration and without ultrasonic vibration are very close (2,760 N and 2,758 N). However, due to the high frequency mechanical vibration of the tool in UV-A pelleting, a certain degree of variations in pelleting force can be observed when pelleting with ultrasonic vibration.

(6)   Energy consumption in UV-A pelleting increases as sieve size, ultrasonic power, and pellet weight increase, and as pelleting pressure decrease. Machine type used in the size reduction process has a significant effect on energy consumption in UV-A pelleting of wheat straw. Energy consumption in UV-A pelleting of wheat straw particles milled by knife milling is roughly 12% higher than that in UV-A pelleting of wheat straw particles milled by hammer milling.

(7)   A predictive model for energy consumption in UV-A pelleting of wheat straw has been developed. The model can predict effects of ultrasonic power, sieve size, and pellet weight on energy consumption in UV-A pelleting of wheat straw. It is found that all these three parameters significantly affect energy consumption in UV-A pelleting. Energy consumption decreases with a decrease in ultrasonic power, sieve size, and pellet weight. Effect of pelleting pressure has no significant effect on energy consumption in UV-A pelleting. In addition, two of the predicted two-factor

interaction effects (between ultrasonic power and pellet weight, and between sieve size and pellet weight) are significant. Effect of pellet weight on energy consumption are stronger at the higher level of ultrasonic power and at the higher level of sieve size.

(8) Effects of operating variables (pretreatment time, pretreatment temperature, and acid concentration) in dilute acid pretreatment of poplar wood on energy consumption, water usage, sugar yield, and pretreatment energy efficiency are experimentally studied. As pretreatment time increases from 10 to 30 min, energy consumption, water usage, and sugar yield increase; but pretreatment energy efficiency first increases (when pretreatment time increases from 10 to 20 min) and then decreases slightly. As pretreatment temperature increases from 100oC to 180oC, energy consumption and water usage increase; sugar yield and pretreatment energy efficiency first increase (when pretreatment temperature increases from 100oC to 160oC) and then become constant or decrease slightly. As acid concentration increases (from 0.8% to 2%), energy consumption and water usage do not change noticeably; sugar yield and pretreatment energy efficiency first increase (when acid concentration first increases from 0.8% to 1.5%) and then decrease.

(9) A predictive model for energy consumption in dilute acid pretreatment has been developed. The model can predict effects of pretreatment time, pretreatment temperature, and solid content on energy consumption in dilute acid pretreatment of wheat straw. Main effects of pretreatment time and pretreatment temperature are significant at the significance level of $\alpha = 0.05$. Longer pretreatment time and higher pretreatment temperature result in higher power energy consumption. The optimal values of the process conditions are pretreatment time 14-21 min and pretreatment temperature 129-139°C.

(10) Effects of ultrasonic vibration-assisted (UV-A) pelleting on biomass sugar yield are studied in terms of total sugar yield (Y_p) and enzymatic hydrolysis sugar yield (Y_h). Considering both pretreatment and enzymatic hydrolysis processes, the total sugar yield (Y_p) of biomass processed with UV-A pelleting are 30% to 43% higher than

that of biomass not processed with UV-A pelleting. Considering enzymatic hydrolysis process alone, enzymatic hydrolysis sugar yield (Y_h) of biomass processed with UV-A pelleting are 6% to 22% higher than that of biomass not processed with UV-A pelleting. With UV-A pelleting, pretreatment weight recovery (R) is increased for all four types of biomass.

14.2 Contributions of this dissertation

The major contributions of this dissertation are:

(1) This research, for the first time, has developed a physics-based predictive temperature model in UV-A pelleting of cellulosic biomass and the predicted results are consistent with experiments results. This research has filled a gap in the literature on UV-A pelleting of cellulosic biomass.

(2) This research, for the first time, has developed a constitutive pellet density model in UV-A pelleting of cellulosic biomass and the predicted results are consistent with experiments results. This research has filled a gap in the literature on UV-A pelleting of cellulosic biomass.

(3) This research, for the first time, has developed an energy consumption model in UV-A pelleting of cellulosic biomass.

(4) This research, for the first time, has developed an energy consumption model in dilute acid pretreatment.

(5) The developed pellet density model can serve as a useful template for development of models to predict pellet durability, and stability in UV-A pelleting of cellulosic biomass.

(6) This research, for the first time, has studied effects of binder material in UV-A pelleting. Knowledge obtained in this research has filled a gap in the literature and provides guidance in manufacturing of cellulosic biofuels.

(7) For the first time, this research has studied effects of ultrasonic vibration on pelleting force in UV-A pelleting.

(8) This research reports the first study using pre-pretreatment sugar yield to investigate effects UV-A pelleting on biomass sugar yield when considering both pretreatment

and enzymatic hydrolysis steps. This result will add to the literature of enzymatic hydrolysis of cellulosic biomass.

Appendix A - Publications during PhD study

Journals and transactions

1. **Song, X.X.,** Zhang, M., Pei, Z.J., and Wang, D.H., 2015, "Ultrasonic vibration-assisted (UV-A) pelleting of wheat straw: a constitutive model for pellet density," Ultrasonics, Vol. 60, pp. 117－125.

2. **Song, X.X.,** Yu, X.M., Zhang, M., Pei, Z.J., and Wang, D.H., 2014, "A physics-based temperature model for ultrasonic vibration-assisted pelleting for cellulosic biomass," Ultrasonics, Vol. 54, No. 7, pp. 2042－2049.

3. **Song, X.X.,** Zhang, M., Pei, Z.J., and Wang, D.H., 2014, "Ultrasonic vibration-assisted pelleting of wheat straw: a predictive model for energy consumption using response surface methodology," Ultrasonics, Vol. 54, No. 1, pp. 305-311

4. **Song, X.X.**, Zhang, M., and Pei, Z.J., 2013, "Effects of ultrasonic vibration-assisted pelleting of cellulosic biomass on sugar yield for biofuel manufacturing," Biomass Conversion and Biorefinery, Vol. 3, No. 3, pp. 231-238.

5. **Song, X.X.**, Zhang, M., Deines, T.W., Zhang, P.F., and Pei, Z.J., 2013, "Energy consumption study in ultrasonic vibration-assisted pelleting of wheat straw for cellulosic biofuel manufacturing," International Journal of Manufacturing Research, Vol. 8, No. 2, pp. 135-149.

6. **Song, X.X.**, Zhang, M., Pei, Z.J., and Wang, D.H., 2012, "Preliminary study on pretreatment of poplar wood for biofuel production," Biofuels, Vol. 3, No. 5, pp. 525-533.

7. Zhang, M., **Song, X.X.**, Pei, Z.J., Deines, T.W., and Wang, D.H., 2014, "Size reduction of poplar wood using a lathe for biofuel manufacturing: effects of biomass crystallinity on sugar yield," Machining Science and Technology, Vol. 18, No. 1, pp. 1-14.

8. Zhang, M., **Song, X.X.**, Deines, T.W., Pei, Z.J., and Wang, D.H., 2014, "A consistency mapping for the effects on enzymatic hydrolysis sugar yield using two sugar yield definitions in cellulosic biofuel manufacturing," Renewable Energy, Vol. 62, pp. 243-248.

9. Zhang, M., **Song, X.X.**, Zhang, P.F., Pei, Z.J., Deines, T.W., and Wang, D.H., 2013, "Size reduction of cellulosic biomass in biofuel manufacturing: separating the confounding effects of particle size and biomass crystallinity," Journal of Manufacturing Science and Engineering, Vol. 135, No. 2, 021006.

10. Zhang, M., **Song, X.X.**, Deines, T.W., Pei, Z.J., and Wang, D.H., 2012, "Biofuel manufacturing from woody biomass: effects of sieve size used in biomass size reduction," Journal of Biomedicine and Biotechnology, Vol. 2012. http://dx.doi.org/10.1155/2012/581039.

11. Zhang, M., **Song, X.X.**, Zhang, P.F., Pei, Z.J., Deines, T.W., and Wang, D.H., 2012, "Size reduction of cellulosic biomass in biofuel manufacturing: a study on confounding effects of particle size and biomass crystallinity," Journal of Manufacturing Science and Engineering, Vol. 134, No. 1, pp. 011009-1 – 011009-9.

12. Zhang, M., **Song, X.X.**, Pei, Z.J., Deines, T.W., and Treadwell, C., 2012, "Ultrasonic-vibration-assisted pelleting of wheat straw: an experimental investigation," International Journal of Manufacturing Research, Vol. 7, No. 1, pp. 59-71.

Conference proceedings

13. **Song, X.X.**, Zhang, M., Pei, Z.J., and Wang, D.H., "Ultrasonic vibration-assisted (UV-A) dilute acid pretreatment of poplar wood for biofuel manufacturing: A preliminary study," Proceedings of the ASME 2015 International Manufacturing Science and Engineering Conference (MSEC), Charlotte, North Carolina, June 8-12, 2015, MSEC 2015-9340.

14. **Song, X.X.**, Zhang, M., Pei, Z.J., Nottingham, A., and Zhang, P.F., 2013, "Dilute acid pretreatment of wheat straw: a predictive model for energy consumption using response surface methodology," Proceedings of the ASME 2013 International Manufacturing Science and Engineering Conference (MSEC), Madison, Wisconsin, June 10-14, 2013, MSEC 2013-1043.

15. **Song, X.X.**, Zhang, M., Pei, Z.J., Deines, T., Zhang, Q., Zhang, P.F., and Wang, D.H., 2011, "Size reduction of poplar wood using a lathe for biofuel manufacturing: a preliminary experiment," Proceedings of the ASME 2011 International Mechanical Engineering Congress and Exposition, Denver, Colorado, November 11-17, 2011, IMECE 2011-63748.

16. **Song, X.X.**, Zhang, M., Pei, Z.J., and, Deines, T.W., 2010, "Ultrasonic-vibration-assisted pelleting of cellulosic biomass: effects of moisture content," Proceedings of the ASME 2010 International Manufacturing Science and Engineering Conference (MSEC), Erie, PA, October 12-15, 2010, MSEC 2010-34172.

17. **Song, X.X.**, Zhang, M., Deines, T.W., Zhang, P.F., Zhang, Q., and Pei, Z.J., 2010, "Ultrasonic-vibration-assisted pelleting of wheat straw: effects of moisture content," Proceedings of the IIE Annual Conference and Expo 2010 – Cancun, Mexico, June 5 – 9, 2010.

18. Hull, E., Grove, W., Zhang, M., **Song, X.X.**, Pei, Z.J., and Cong, W.L., 2015, "Effects of Process Variables on Extrusion of Carbon Fiber Reinforced ABS Filament for Additive Manufacturing," Proceedings of the ASME 2015 International

Manufacturing Science and Engineering Conference (MSEC), Charlotte, North Carolina, June 8-12, 2015, MSEC 2015-9396.

19. Fernando, P.K.S.C., Pei, Z.J., Zhang, M., **Song, X.X.**, and Cong, W.L., 2015, "Rotary Ultrasonic Machining of Carbon Fiber Reinforced Plastics: Design of Experiment," Proceedings of the ASME 2015 International Manufacturing Science and Engineering Conference (MSEC), Charlotte, North Carolina, June 8-12, 2015, MSEC 2015-9391.

20. Zhang, M., **Song, X.X.**, Zhang, P.F., and Pei, Z.J., 2013, "Diluted acid pretreatment and enzymatic hydrolysis of woody biomass for biofuel manufacturing: effects of particle size on sugar conversion," Proceedings of the ASME 2013 International Manufacturing Science and Engineering Conference (MSEC), Madison, Wisconsin, June 10-14, 2013, IMECE 2013-1050.

21. Zhang, Q., Zhang, P.F., Pritchett, G., Pei, Z.J., Zhang, M., **Song, X.X.**, and Deines, T.W., 2012, "Ultrasonic-vibration assisted pelleting for cellulosic ethanol manufacturing: effects of particle size and moisture content on power consumption," Proceedings of the ASME 2012 International Manufacturing Science and Engineering Conference (MSEC), Notre Dame, IN, June 4-8, 2012, MSEC 2012-7211.

22. Zhang, Q., Zhang, P.F., Pritchett, G., Pei, Z.J., Zhang, M., **Song, X.X.**, and Deines, T.W., 2012, "Ultrasonic-vibration assisted pelleting for cellulosic biofuel manufacturing: investigation on power consumption with design of experiment," Proceedings of the ASME 2012 International Manufacturing Science and Engineering Conference (MSEC), Notre Dame, IN, June 4-8, 2012, MSEC 2012-7212.

23. Zhang, Q., Zhang, P.F., Zhang, M., **Song, X.X.**, Pei, Z.J., and Siddiqui, O., 2012, "Sugar yield comparison of wheat straw processed by two pelleting methods for cellulosic biofuel manufacturing," Proceedings of the ASME 2012 International Manufacturing Science and Engineering Conference (MSEC), Notre Dame, IN, June 4-8, 2012, MSEC 2012-7228.

24. Zhang, M., **Song, X.X.**, Pei, Z.J., and Deines, 2011, "Size reduction of cellulosic biomass in biofuel manufacturing: effects of biomass crystallinity and particle size,"

Proceedings of the ASME 2011 International Mechanical Engineering Congress and Exposition, Denver, Colorado, November 11-17, 2011, IMECE 2011- 64059.

25. Zhang, M., **Song, X.X.**, Zhang, P.F., Zhang, Q., Pei, Z.J., Deines, T.W., and Wang, D.H., 2011, "Size reduction of cellulosic biomass in biofuel manufacturing: effects of milling orientation on sugar yield," Proceedings of the ASME 2011 International Manufacturing Science and Engineering Conference (MSEC), Corvallis, OR, June 13-17, 2011, MSEC2011-50117.

26. Zhang, Q., Zhang, P.F., **Song, X.X.**, Zhang, M., Pei, Z.J., and Deines, T.W., 2011, "A study on amount of biomass pellets used in durability testing," Proceedings of the ASME 2011 International Manufacturing Science and Engineering Conference (MSEC), Corvallis, OR, June 13-17, 2011, MSEC2011-50025.

27. Zhang, P.F., Zhang, M., **Song, X.X.**, Zhang, Q., Cong, W.L., Qin, N., Pei, Z.J., Deines, T.W., and Wang, D.H., 2011, "Ultrasonic vibration-assisted pelleting of cellulosic biomass for biofuel manufacturing," CD-ROM Proceedings of 2011 NSF CMMI Research and Innovation Conference; Atlanta, GA, January 4-7.

28. Zhang, M., **Song, X.X.**, Pei, Z.J., and Wang, D.H., 2010, "Effects of mechanical comminution on enzymatic conversion of cellulosic biomass in biofuel manufacturing: a review," Proceedings of the ASME 2010 International Manufacturing Science and Engineering Conference (MSEC), Erie, PA, October 12-15, 2010, MSEC 2010-34082.

29. Zhang, M., **Song, X.X.**, Deines, T.W., Zhang, P.F., Zhang, Q., Cong, W.L., Qin, N., and Pei, Z.J., 2010, "Ultrasonic-vibration-assisted pelleting of switchgrass: effects of binder material," Proceedings of the IIE Annual Conference and Expo 2010 – Cancun, Mexico, June 5 – 9, 2010.

30. Zhang, Q., Zhang, P.F., Deines, T.W., Zhang, M., **Song, X.X.**, and Pei, Z.J., 2010, "Ultrasonic vibration assisted pelleting of wheat straw: effects of particle size", Proceedings of the 20th International Conference on Flexible Automation and

Intelligent Manufacturing (FAIM 2010), California State University, CA, July 12-14, 2010.

Book chapter

31. Zhang, M., **Song, X.X.,** Pei, Z.J., and Wang, D.H., 2015, "Ultrasonic vibration-assisted pelleting of cellulosic biomass for biofuel production," in Production of biofuels and chemicals: ultrasound, Eds: Fang, Z., Smith, R.L. Jr., and Qi, X.H., Springer, New York, NY, USA, Vol. 4, pp. 243-267.

Posters

32. Zhang, M., **Song, X.X.**, Zhang, P.F., Zhang, Q., Jones, E., Deines, T.W., Pei, Z.J., and Wang, D.H., 2010, "Fundamental study on size reduction of poplar for biofuel manufacturing," Poster presentation at the ASME 2010 International Manufacturing Science and Engineering Conference (MSEC), Erie, PA, October 12-15, 2010, MSEC 2010-34352.

33. Zhang, P.F., Feng, Q., Zinke, E., Cong, W.L., Zhang, M., **Song, X.X.**, Zhang, Q., Deines, T.W., Pei, Z.J., and Wang, D.H., 2010, "Ultrasonic vibration-assisted pelleting of cellulosic biomass for bioethanol manufacturing," Poster presentation at the ASME 2010 International Manufacturing Science and Engineering Conference (MSEC), Erie, PA, October 12-15, 2010, MSEC 2010-34342.

34. Cong, W.L., Zhang, P.F., Qin, N., Zhang, M., **Song, X.X.**, Zhang, Q., Nottingham, N., Clark, R., Deines, T.W., Pei, Z.J., and Wang, D.H., 2009, "Ultrasonic vibration-assisted pelleting of cellulosic biomass for biofuel manufacturing," Poster presentation at the ASME 2009 International Manufacturing Science and Engineering Conference (MSEC), MSEC2009-84432, West Lafayette, IN, USA, October 4-7.

Working papers

35. Zhang, M., **Song, X.X.,** Zhang, K., Pei, Z.J., and Wang, D.H., 2015, "Effects of Sieve Size on Biochemical Conversion of Big Bluestem Biomass for Biofuel Production," submitted to Advances in Materials Science and Engineering.